

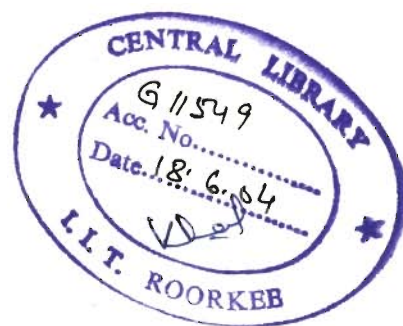
SIMULATION OF FLOW IN MULTILAYERED AQUIFER SYSTEM WITH AND WITHOUT DISCONTINUITY

A THESIS

*Submitted in fulfilment of the
requirements for the award of the degree
of
DOCTOR OF PHILOSOPHY
in
EARTH SCIENCES*

By

MATHEW KUTTY JOSE



**DEPARTMENT OF EARTH SCIENCES
INDIAN INSTITUTE OF TECHNOLOGY ROORKEE
ROORKEE-247 667 (INDIA)**

NOVEMBER, 2001

CANDIDATE'S DECLARATION

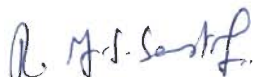
I hereby certify that the work which is being presented in the thesis entitled "**SIMULATION OF FLOW IN MULTILAYERED AQUIFER SYSTEM WITH AND WITHOUT DISCONTINUITY**" in fulfilment of the requirement for the award of the **Degree of Doctor of Philosophy** and submitted in the Department of Earth Sciences of the Indian Institute of Technology Roorkee is an authentic record of my own work carried out during a period from February, 1995 to November, 2001 under the supervision of Dr. R.G.S. Sastry, Dr. P.V. Seethapathi and Dr. Bhishm Kumar.

The matter presented in this thesis has not been submitted by me for the award of any other degree of this or any other Institute/ University.




(**MATHEW KUTTY JOSE**)

This is to certify that the above statement made by the candidate is correct to the best of our knowledge.


(**Dr. R.G.S. Sastry**)

Associate Professor
Department of Earth Sciences
IIT Roorkee


(**Dr. P.V. Seethapathi**)

Professor and Director
NEERIWALM
Tezpur


(**Dr. Bhishm Kumar**)

Scientist-E and Head (NH Div.)
National Institute of Hydrology
Roorkee

Date: 29-11-2001

The Ph.D. Viva-Voce examination of Mr. Mathew Kutty Jose, Research Scholar, has been held on 26/8/02



Signature of Supervisor(s)



Signature of H.O.D.


26/8/02

Signature of External Examiner

ABSTRACT

Ever-increasing dependence on groundwater for various uses has not only triggered environmental hazards but depletion of many aquifers too. This necessitates rejuvenation of the aquifer systems through artificial recharge methods. Recharging is influenced by hydrogeology of the aquifer, the hydraulic properties, ^{flow} parameters of the porous medium and flux boundaries of the aquifer system. Therefore, efficiency of recharging schemes vis-a-vis hydraulic response of the aquifer system needs to be investigated. Nevertheless, quantitative results on flow regimes and hydraulic responses of aquifer systems recharged by surface water sources are still evasive especially in complex aquifer systems. In this context, analytical as well as numerical groundwater models can be of ~~great use.~~ ^{Significant value from a practical point of view}

A critical review of the literature relevant to surface water - groundwater interaction, artificial recharge practices, analytical as well as numerical groundwater flow modelling and geophysical aspects of porous media has been carried out. Based on the review, it has been perceived that there is a possibility of developing ^{better} new analytical approaches for aquifer simulation in multilayered aquifer systems by considering the analogy between groundwater flow and electrical flow in the context of advances made in exploration geophysics. Unlike numerical models, analytical models ^{do not} render faster techniques ^{computationally faster} to simulate flow/ hydraulic potentials in aquifer systems with fewer data sets. Further, they offer qualitative insights that may not be revealed through the quantitative results obtained by numerical simulations. However, analytical models developed for idealised conditions are not effective for detailed investigations on the flow characteristics in complex aquifer systems with discontinuities (like distributed clay lenses in alluvial aquifer systems). Alternately, numerical modelling is desirable in such cases. Thus, analytical and numerical methods can be complementary to each other for conducting effective flow simulation studies in isotropic/ anisotropic layered aquifer systems with or without discontinuities.

In view of the above, the major objectives of the present thesis are set as: (i) development of analytical models for simulation of hydraulic potentials and streamlines due to recharging by surface water sources in multilayered aquifer systems, (ii) development of analytical models for aquifer simulation in a homogeneous anisotropic aquifer system with recharging sources kept on the

earth surface, (iii) validation of the generated analytical models in several numerical experiments and (iv) numerical simulation studies in an aquifer-aquitard-aquifer system with continuous as well as discontinuous aquitard in the medium. The analytical solutions have been derived by invoking the advances made in the realm of exploration geophysics. The numerical simulation studies in an aquifer-aquitard-aquifer system brought forth many results on the recharging characteristics of such a system.

Steady state analytical expressions for hydraulic potentials and streamlines due to recharging by a point source have been derived for the case of a layered aquifer system with a maximum of three layers. By applying appropriate convolution techniques the solutions have been modified to suit recharge by finite-length line sources and areal sources. Subsequently, by devising an alternate methodology, analytical expressions have been developed for the case of multilayered aquifer systems with large number of layers (say, n layers). A recurrence relationship has been developed to achieve this in an iterative manner. Several computational algorithms using these analytical expressions have been coded in FORTRAN77. For a three-layered aquifer system the computational algorithms developed are: (i) 3LPNT- for a point source, (ii) 3LLIN- for a finite length line source and (iii) 3LARL- for an areal source. Whereas, NLPNT is the computational algorithm for the case of a multilayered aquifer system. A number of numerical examples pertaining to the recharge of the multilayered aquifer systems have been presented and discussed with illustrations. Also, the comparison of corresponding results obtained from analytical models and that obtained from the numerical flow model, MODFLOW is undertaken. The results match extremely well, confirming the validity of the developed analytical models. Besides, aquifer simulations using these analytical models are found to be highly efficient compared to an identical simulation by the numerical model MODFLOW in terms of data requirement and computational speed.

Further, by making use of analogies from geophysical vertical electric sounding methods and applying relevant domain transformation techniques, analytical expressions have been developed for simulating hydraulic potentials due to recharging by a point source in a homogeneous (transverse) anisotropic aquifer system with dipping beds. Based on the analytical solutions, an effective computational algorithm (HANI-P) has been devised to enable simulation of the anisotropic aquifer system. Illustrations with numerical examples have been provided for several coefficients of anisotropy and angles of dip of the soil strata in the anisotropic medium. Also, analytical

solutions for hydraulic potentials have been developed for the case of recharging of a homogeneous anisotropic aquifer system due to a finite-length line source. The corresponding computational algorithm, HANI-L is used to demonstrate numerical examples. Also, the validity of these analytical expressions have been verified for homogeneous isotropic conditions.

In order to gain further insight into the recharging characteristics of a three-layered aquifer-aquitard-aquifer system, elaborate numerical simulation studies have been carried out. An aquifer-aquitard-aquifer system having a surface water recharging source has been conceptualised with a provision to keep the aquitard continuous or discontinuous (as the case may be) in the model discretisation. The analyses performed pertain to: (i) Effect of the dimension as well as the positioning of a continuous aquitard on the recharging of the aquifer system; (ii) Effect of the dimension of the aquitard discontinuity in a centrally positioned aquitard on the recharging of the aquifer system; (iii) Effect of the location of the discontinuity in the aquitard with respect to the source on the recharging of the aquifer system; (iv) Effect of depth-wise positioning of the discontinuous aquitard in the aquifer system on the recharging of the aquifer system. Using several dimensionless parameters, analyses of the simulation results have been carried out to infer useful conclusions that are presented with illustrations.

ACKNOWLEDGEMENTS

I wish to express my sincere thanks to Prof. P.V. Seethapathi, Director, NEERIWALM, Tezpur, Dr. R.G.S. Sastry, Assoc. Professor, Department of Earth Sciences, IIT Roorkee and Dr. Bhishm Kumar, Scientist-E, National Institute of Hydrology, Roorkee for their efficient guidance throughout the span of the research work. Their constant inspiration and support was instrumental in accomplishing the task. I also thankfully acknowledge Prof. G.C. Mishra, Professor, WRDTC, IIT Roorkee for useful discussions and especially, for proposing the study on anisotropic aquifer systems. The helpful review-comments rendered by Prof. H.M. Haitjema, Indiana University, USA, Prof. D. Kashyap, IIT Roorkee, Prof. P. Gupta, IIT Roorkee and the anonymous reviewers of *Water Resources Research* and *Journal of Hydrology* are gratefully appreciated.

I thank Prof. A.K. Awasthi, HOD, Department of Earth Sciences, IIT Roorkee for extending all help. Besides, I acknowledge Dr. K.S. Ramasastry, Director, National Institute of Hydrology, Roorkee for his encouragement. Thanks are also due to Mr. R.D. Singh, Scientist-F, National Institute of Hydrology, Roorkee for his support. Further, I would like to record my profound gratitude to my relatives and friends for their good services. Messrs. Jayagopalan Nair, T.P. Panicker, M.P. Jai Singh, Q.A. Ansari, Dayal Singh, R P Nachiappan, C.P. Kumar, P.K. Majumdar, P.R. Pujari, T.Chandramohan, B.K. Purandara, S.K. Verma, Senthilkumar, B. Venkatesh and A.K. Lohani have all enthused and helped me in many possible ways. My heartfelt thanks are also due to Rev. Fr. Devasya, Vicar, Sacred Heart Church, Roorkee, who has been of great inspiration to me through his prayers and solace.

Lastly, I am extremely grateful to my mother Mrs. Chinnamma Joseph, wife Mrs. Jenny Maria Mani and daughter Ms. Anusha Jane Mathew for their reassurances as well as their gesture of patience and understanding by way of forfeiting many a pleasures during the tenure of the work. Further, I am thankful to my brother Mr. Joshy Jose for all his wholehearted help. Above all, I say Hallelujah! for the Divine Blessings bestowed upon us during all these times.



Mathew Kutty Jose

CONTENTS

Page No.

ABSTRACT	i
ACKNOWLEDGEMENTS	iv
LIST OF TABLES	ix
LIST OF FIGURES	x
LIST OF NOTATIONS	xix

CHAPTER 1: INTRODUCTION 1-6

1.1	GENERAL	1
1.2	BACKDROP OF THE THESIS	1
1.2.1	ROLE OF ANALYTICAL AND NUMERICAL METHODS	2
1.3	SCOPE OF THE PRESENT WORK	4
1.4	LAY OUT OF THE THESIS	5

CHAPTER 2: REVIEW OF LITERATURE 7-22

2.1	GENERAL	7
2.2	STUDIES ON SURFACE WATER-GROUNDWATER INTERACTION .	8
2.3	GROUNDWATER MODELLING- ANALYTICAL METHODS	10
2.4	GROUNDWATER MODELLING- NUMERICAL METHODS	13
2.5	FLOW IN ANISOTROPIC AQUIFER SYSTEMS	16
2.6	FORMULATION OF STREAM FUNCTIONS	17
2.7	GEOPHYSICAL ASPECTS OF AQUIFER SIMULATION	19
2.8	SUMMING UP	21

CHAPTER 3: ANALYTICAL SOLUTIONS FOR HYDRAULIC POTENTIAL AND STREAMLINES IN MULTILAYERED AQUIFER SYSTEMS 23-63

3.1	GENERAL	23
3.2	BASIC THEORETICAL FRAMEWORK	25
3.3	HYDRAULIC POTENTIAL AND STREAM FUNCTION: TWO/ THREE- LAYERED AQUIFER SYSTEMS	28
3.3.1	HYDRAULIC POTENTIAL	30
3.3.2	STREAM FUNCTION	33

3.3.3	COMPUTATIONAL ALGORITHMS	35
3.3.3.1	Model Description	35
3.3.3.2	Convergence Test	36
3.3.3.3	Validation Test	36
3.3.4	NUMERICAL EXPERIMENTS	37
3.3.4.1	Hydraulic Potential Due to a Point Source	37
3.3.4.2	Hydraulic Potential Due to a Line Source	38
3.3.4.3	Hydraulic Potential Due to an Areal Source	43
3.4	HYDRAULIC POTENTIAL AND STREAM FUNCTION: MULTILAYERED AQUIFER SYSTEM	46
3.4.1	RECURRENCE RELATIONS FOR $A_i(\lambda)$ AND $B_i(\lambda)$	48
3.4.2	HYDRAULIC POTENTIAL IN MULTILAYERED AQUIFER SYSTEMS	50
3.4.2.1	Determination of Coefficients f_j and g_j	51
3.4.3	STREAM FUNCTION IN MULTILAYERED AQUIFER SYSTEMS	53
3.4.4	COMPUTATIONAL ALGORITHM FOR MULTILAYERED AQUIFER SYSTEM	53
3.4.4.1	Description of the Model	54
3.4.5	NUMERICAL EXPERIMENTS	55
3.5	RESULTS AND DISCUSSION	58
3.5.1	THREE-LAYERED AQUIFER SYSTEMS	62
3.5.2	MULTILAYERED AQUIFER SYSTEMS	62
 CHAPTER 4: ANALYTICAL SOLUTIONS FOR HYDRAULIC POTENTIAL IN HOMOGENEOUS ANISOTROPIC AQUIFER SYSTEMS 64-93		
4.1	GENERAL	64
4.2	THEORETICAL FRAMEWORK	65
4.2.1	HYDRAULIC CONDUCTIVITY TENSOR	66
4.3	HYDRAULIC POTENTIALS DUE TO A POINT SOURCE	70
4.4	HYDRAULIC POTENTIALS DUE TO A FINITE-LENGTH LINE SOURCE	74
4.4.1	SOLUTION FOR HOMOGENEOUS, ISOTROPIC AQUIFER	76
4.4.2	SOLUTION FOR HOMOGENEOUS, ANISOTROPIC AQUIFER	77
4.5	NUMERICAL SIMULATION ALGORITHMS	79
4.5.1	AQUIFER SIMULATIONS WITH POINT SOURCE	80

4.5.2	AQUIFER SIMULATIONS WITH FINITE-LENGTH LINE SOURCE	88
4.6	RESULTS AND DISCUSSION	92
CHAPTER 5:	RECHARGING IN AN AQUIFER-AQUITARD- AQUIFER SYSTEM: INFLUENCE OF A CONTINUOUS AQUITARD	94-111
5.1	GENERAL	94
5.2	SCOPE OF THE ANALYSIS	94
5.3	METHODOLOGY	95
5.3.1	GOVERNING EQUATION	95
5.3.2	MODEL DESCRIPTION	96
5.3.3	BOUNDARY CONDITIONS	98
5.3.4	SOLUTION PROCEDURE	98
5.4	MODEL CONCEPTUALISATION	98
5.4.1	DISCRETISATION	100
5.5	ANALYSIS AND DISCUSSION	101
5.5.1	TERMINOLOGY	104
5.5.2	EFFECT OF DEPTH-WISE POSITIONING OF THE AQUITARD ON RECHARGING	104
5.5.3	EFFECT OF AQUITARD THICKNESS ON RECHARGING	106
5.6	RESULTS	110
CHAPTER 6:	RECHARGING IN AN AQUIFER-AQUITARD- AQUIFER SYSTEM: INFLUENCE OF A DISCONTINUOUS AQUITARD	112-168
6.1	GENERAL	112
6.2	SCOPE OF THE ANALYSIS	112
6.3	METHODOLOGY	113
6.4	CONCEPTUALISATION	113
6.5	TERMINOLOGY	115
6.6	ANALYSIS AND DISCUSSION	116
6.6.1	EFFECT OF DIMENSION OF THE AQUITARD DISCONTINUITY ON RECHARGING	117
6.6.2	EFFECT OF LOCATION OF THE DISCONTINUITY IN THE AQUITARD ON RECHARGING	136

6.6.2.1	Effect of Shifting of the Discontinuity on Recharge for a Specified Value of S/T Ratio and Several Percentage Openings	137
6.6.2.2	Effect of Shifting of the Discontinuity on Recharge for a Specified Discontinuity of the Aquitard and Several Values of the S/T Ratio	147
6.6.2.3	Effect of Shifting of the Discontinuity on Recharge for a Specified Position of the Aquitard and Several Values of the S/T Ratio	148
6.6.2.4	Effect of Shifting of the Discontinuity to Several X/L Points on Recharge for a Specific Position of the Aquitard	154
6.6.3	EFFECT OF DEPTH-WISE POSITIONING OF THE DISCONTINUOUS AQUITARD ON RECHARGING	159
6.6.3.1	Effect of Positioning of the Aquitard on the Recharge for Several Depth-wise Positions and Values of S/T Ratio	159
6.7	RESULTS	167
6.7.1	DIMENSION OF THE AQUITARD DISCONTINUITY	167
6.7.2	HORIZONTAL LOCATION OF THE AQUITARD DISCONTINUITY	168
6.7.3	POSITIONING DEPTH OF THE DISCONTINUOUS AQUITARD	168
CHAPTER 7: SUMMARY AND CONCLUSIONS		169-171
7.1	GENERAL	169
7.2	SUMMARY OF RESULTS AND CONCLUSIONS	169
7.3	FURTHER PERSPECTIVES	171
REFERENCES		172-185
APPENDIX: LIST OF PUBLICATIONS RELEVANT TO THE THESIS		

LIST OF TABLES

Table No.	Title	Page No.
Table 3.1	Types of aquifer systems (based on layer conductivities) for which simulations are performed with 3LPNT.	37
Table 3.2	Types of aquifer systems (based on layer conductivities) for which simulations are performed with 3LLIN.	43
Table 3.3	Types of aquifer systems (based on layer conductivities) in which simulations are performed with 3LARL.	46
Table 3.4	Types of aquifer systems (3-layer, 4-layer and 5-layer) with patterns of respective layer conductivities simulated using NLPNT.	55
Table 4.1	Aquifer Parameter values used for the numerical simulations of hydraulic potentials due to a point source.	80
Table 4.2	Set of cases where hydraulic potentials due to a point source have been simulated with different combinations of angle of dip, α and coefficients of anisotropy, β .	80
Table 4.3	Aquifer Parameter values used for the numerical simulations of hydraulic potentials due to a finite-length line source.	88
Table 4.4	Set of cases where hydraulic potentials due to a finite-length line source have been simulated with different combinations of the angle of dip, α and the coefficients of anisotropy, β .	92
Table 5.1	Aquitard Depth Ratios (ATDR) and Aquifer Thickness Ratios (AFTR).	105
Table 5.2	Discharge Ratios (DISR) for different Aquifer Thickness Ratios (AFTR) for a fixed Aquitard Depth Ratio, ATDR=2.15 while changing the aquitard thickness.	110
Table 6.1	Matrix table of parameter combinations used in different cases.	119
Table 6.2	Matrix table of various cases with position of the aquitard at $P_d=0.53$ and $S/T = 0.1081$.	137
Table 6.3	Matrix table of various cases simulated with position of the aquitard at $P_d=0.53$ and Percentage Opening, $O_p=5\%$.	147
Table 6.4	Matrix table of various cases studied with position of the aquitard at $P_d=0.53$ and Percentage Opening, $O_p=117\%$.	148
Table 6.5	Matrix table of various cases studied with position of the aquitard at $P_d=0.53$ and Percentage Opening, $O_p=100\%$.	154
Table 6.6	Matrix table of various cases studied with different positions of the aquitard for Percentage Opening, $O_p=5\%$.	159

LIST OF FIGURES

Figure No.	Title	Page No.
Fig. 3.1	Schematic diagram of the multilayered aquifer system with reference to the cylindrical coordinate system. A point-source is located at A; hydraulic potential (ϕ_1) and stream function (ψ_1) are computed at any arbitrary point $P(r,z)$ within the aquifer system.	26
Fig. 3.2	Schematic diagram of the three-layered aquifer system with a point-source located at A, on air-earth interface; $P(r,z)$ is an arbitrary point in the cylindrical coordinate system.	29
Fig. 3.3	Convergence of the series terms in the expression for hydraulic potential; computed by 3LPNT with 100 terms (dotted lines), 200 terms (dashed lines) and 300 terms (solid lines) of the series expression in the analytical solution. The aquifer layer setup with respect to hydraulic conductivities shown is of the type: $K_1 > K_2 > K_3$.	36
Fig. 3.4a	Contour plot of equipotentials in the vertical section of the homogeneous aquifer system ($K_1 = K_2 = K_3$) computed by 3LPNT (solid contours) and MODFLOW (dashed contours). Dotted contours are the streamlines computed by 3LPNT.	39
Fig. 3.4b	Vertical distribution of hydraulic potential obtained from 3LPNT (solid line) and MODFLOW (dashed line) at the centre and at a distance 200m from the source for the case where $K_1 = K_2 = K_3$	39
Fig. 3.5a	Contour plot of equipotentials in the vertical section of the layered aquifer system ($K_1 > K_2 > K_3$) computed by 3LPNT (solid contours) and MODFLOW (dashed contours). Dotted contours are the streamlines computed by 3LPNT.	40
Fig. 3.5b	Vertical distribution of hydraulic potentials obtained from 3LPNT (solid line) and MODFLOW (dashed line) at the centre and at a distance 200m from the source for the case where $K_1 > K_2 > K_3$.	40
Fig. 3.6a	Contour plot of equipotentials in the vertical section of the aquifer system with ($K_1 < K_2 > K_3$) computed by 3LPNT (solid contours) and MODFLOW (dashed contours). Dotted contours are the streamlines computed by 3LPNT.	41
Fig. 3.6b	Vertical distribution of hydraulic potentials obtained from 3LPNT (solid line) and MODFLOW (dashed line) at the centre and at a distance 200m from the source for the case where $K_1 < K_2 > K_3$.	41
Fig. 3.7a	Contour plot of equipotentials in the vertical section of the layered aquifer system ($K_1 > K_2 < K_3$) computed by 3LPNT (solid contours) and MODFLOW (dashed contours). Dotted contours are the streamlines computed by 3LPNT.	42

Fig. 3.7b	Vertical distribution of hydraulic potentials obtained from 3LPNT (solid line) and MODFLOW (dashed line) at the centre and at a distance 200m from the source for the case where $K_1 > K_2 < K_3$.	42
Fig. 3.8	Contour plot of equipotential in the vertical section of a layered aquifer system ($K_1 > K_2 > K_3$) due to a finite-length line source along its strike (computed by 3LLIN); a solid line section on top shows the position of the line source. Dashed horizontal lines represent the layer interfaces.	44
Fig. 3.9	Contour plot of equipotentials in the vertical section of a layered aquifer system ($K_1 > K_2 < K_3$) due to a finite-length line source along its strike (computed by 3LLIN); a solid line section on top shows the position of the line source. Dashed horizontal lines represent the layer interfaces.	44
Fig. 3.10	Equipotential contours in the vertical section of a layered aquifer system ($K_1 < K_2 > K_3$) due to a finite-length line source along its strike (computed by 3LLIN); a solid line section on top shows the position of the line source. Dashed horizontal lines represent the layer interfaces.	45
Fig. 3.11	Contour plot of equipotentials in the vertical section of a layered aquifer system ($K_1 > K_2 > K_3$) due to an areal source (computed by 3ARL); a dashed rectangle on top of the aquifer system shows the position of the areal source. Dashed horizontal lines represent the layer interfaces.	45
Fig. 3.12	Contour plot of equipotential in the vertical section of a layered aquifer system ($K_1 > K_2 < K_3$) due to an areal source (computed by 3ARL); a dashed rectangle on top of the aquifer system shows the position of the areal source. Dashed horizontal lines represent the layer interfaces.	47
Fig. 3.13	Contour plot of equipotential in the vertical section of a layered aquifer system ($K_1 < K_2 > K_3$) due to an areal source (computed by 3ARL); a dashed rectangle on top of the aquifer system shows the position of the areal source. Dashed horizontal lines represent the layer interfaces.	47
Fig. 3.14	Equipotential contours in the vertical section of a layered aquifer system with three layers ($K_1 > K_2 < K_3$) computed by NLPNT (solid contours) and MODFLOW (dashed contours); the dashed horizontal lines represent the layer interfaces.	56
Fig. 3.15	Equipotential contours (solid contours) and streamlines (dotted contours) in the vertical section of a layered aquifer system with three layers ($K_1 > K_2 < K_3$) computed by NLPNT; the dashed horizontal lines represent the layer interfaces.	56
Fig. 3.16	Equipotential contours in the vertical section of a layered aquifer system with four layers ($K_1 > K_2 < K_3 > K_4$) computed by NLPNT (solid contours) and MODFLOW (dashed contours); the dashed horizontal lines represent the layer interfaces.	57

Fig. 3.17	Equipotential contours (solid contours) and streamlines (dotted contours) in the vertical section of a layered aquifer system with four layers ($K_1 > K_2 < K_3 > K_4$) computed by NLPNT; the dashed horizontal lines represent the layer interfaces.	57
Fig. 3.18	Equipotential contours in the vertical section of a layered aquifer system with five layers ($K_1 > K_2 > K_3 > K_4 > K_5$) computed by NLPNT (solid contours) and MODFLOW (dashed contours); the dashed horizontal lines represent the layer interfaces.	59
Fig. 3.19	Vertical distribution of hydraulic potential obtained from NLPNT (solid line) and MODFLOW (dashed line) at the centre and at a distance 200m from the source for the 5-layered aquifer system where $K_1 > K_2 > K_3 > K_4 > K_5$.	59
Fig. 3.20	Equipotential contours (solid contours) and streamlines (dotted contours) in the vertical section of a layered aquifer system with five layers ($K_1 > K_2 > K_3 > K_4 > K_5$) computed by NLPNT; the dashed horizontal lines represent the layer interfaces.	60
Fig. 3.21	Equipotential contours (solid contours) and streamlines (dotted contours) in the vertical section of a layered aquifer system with five layers ($K_1 > K_2 < K_3 > K_4 < K_5$) computed by NLPNT; the dashed horizontal lines represent the layer interfaces.	60
Fig. 3.22	Mean error between the hydraulic potentials computed by NLPNT and MODFLOW (for the 3, 4 and 5 layered cases), expressed as a percentage of the MODFLOW-hydraulic potential at the central node in the first layer.	61
Fig. 3.23	Maximum error between the hydraulic potentials computed by NLPNT and MODFLOW (for the 3, 4 and 5 layered cases).	61
Fig. 4.1	Scheme of the homogeneous anisotropic aquifer system (YZ-plane) of infinite extent with a point source, Q located centrally on the surface. Dotted lines represent bedding planes of soil strata with angle of dip, α .	67
Fig. 4.2	A finite line-source of strength Q_L (m^2/s) is centrally placed at air-earth interface along the strike of the bedding plane in: [a] the reference coordinate plane (R); [b] the transformed domain (T) to facilitate the analytical solution.	75
Fig. 4.3	Selected equipotential contours (for a point source, $Q=0.1m^3/s$) in: [a] an isotropic aquifer where inclination of bedding planes, $\alpha = 0$ and coefficient of anisotropy, $\beta = 1$; [b] in an anisotropic aquifer where inclination of bedding planes, $\alpha = 0$ and coefficient of anisotropy, $\beta = 10$.	82
Fig. 4.4	Equipotential contours (dotted lines) in a stratified anisotropic aquifer system due to a point source, $Q=0.1m^3/s$ for different inclinations (α) of the bedding planes (solid lines) when the coefficient of anisotropy, $\beta=2$. For [a] $\alpha=0$; [b] $\alpha=\pi/12$; [c] $\alpha=\pi/4$; [d] $\alpha=\pi/2$.	83

Fig. 4.5	Hydraulic potential distribution in an anisotropic aquifer system due to a point source, $Q=0.1\text{m}^3/\text{s}$ for different coefficients of anisotropy (β) when the angle of dip, $\alpha=0$. For [a] $\beta=2$; [b] $\beta=4$; [c] $\beta=7$; [d] $\beta=10$.	84
Fig. 4.6	Hydraulic potential distribution in an anisotropic aquifer system due to a point source, $Q=0.1\text{m}^3/\text{s}$ for different coefficients of anisotropy (β) when the angle of dip, $\alpha=\pi/4$. For [a] $\beta=2$; [b] $\beta=4$; [c] $\beta=7$; [d] $\beta=10$.	85
Fig. 4.7	Hydraulic potential distribution in an anisotropic aquifer system due to a point source, $Q=0.1\text{m}^3/\text{s}$ for different coefficients of anisotropy (β) when the angle of dip, $\alpha=\pi/2$. For [a] $\beta=2$; [b] $\beta=4$; [c] $\beta=7$; [d] $\beta=10$.	86
Fig. 4.8	Distribution of hydraulic potentials due to a point source, $Q=0.1\text{m}^3/\text{s}$ in the vertical section of the anisotropic aquifer system for $\alpha=\pi/4$ and $\beta=10$.	87
Fig. 4.9	Equipotential distribution (dotted lines) in a homogeneous anisotropic aquifer system due to a finite-length line source for different inclinations (α) of the beds when the coefficient of anisotropy, $\beta=4$. For [a] $\alpha=0$; [b] $\alpha=\pi/12$; [c] $\alpha=\pi/4$; [d] $\alpha=\pi/2$.	89
Fig. 4.10	Hydraulic potentials in an anisotropic aquifer system due to a finite-length line source of strength, $Q_L=0.01\text{ m}^2/\text{s}$ for different coefficients of anisotropy (β) when the angle of dip, $\alpha=0$. For [a] $\beta=2$; [b] $\beta=4$; [c] $\beta=7$; [d] $\beta=10$.	90
Fig. 4.11	Hydraulic potentials in an anisotropic aquifer system due to a finite-length line source of strength, $Q_L=0.01\text{ m}^2/\text{s}$ for different coefficients of anisotropy (β) when the angle of dip, $\alpha=\pi/4$. For [a] $\beta=2$; [b] $\beta=4$; [c] $\beta=7$; [d] $\beta=10$.	91
Fig. 5.1	Plan-view of the aquifer-aquitard-aquifer system with recharging-source.	99
Fig. 5.2	Vertical cross-section (through AA' of Fig. 5.1) of the aquifer-aquitard-aquifer system with the recharging-source.	99
Fig. 5.3	Cumulative discharge from the aquifer system for various time steps.	102
Fig. 5.4	Progress of transient simulations with length of the stress period, eventually approaching steady-state condition.	102
Fig. 5.5	Absolute values of hydraulic head approaching steady state with progress of time-steps at two sections in the aquifer system.	103
Fig. 5.6	Effect of the aquitard at different depths: Aquitard Depth Ratio (ATDR) versus Aquifer Head Ratio (AFHR) at different Normalised Distances (X/L)	103
Fig. 5.7	Aquitard Depth Ratio (ATDR) versus Aquitard Head Ratio (ATHR) for different Normalised Distances (X/L).	107

Fig. 5.8	Normalised Distance (X/L) versus Aquifer Head Ratio (AFHR) for different Aquitard Depth Ratios (ATDR).	107
Fig. 5.9a	Normalised Distance (X/L) versus Aquitard Head Ratio (ATHR) as well as Aquifer Head Ratio (AFHR) for a given Aquifer Thickness Ratio, AFTR=0.40.	108
Fig. 5.9b	Normalised Distance (X/L) versus Aquitard Head Ratio (ATHR) as well as Aquifer Head Ratio (AFHR) for a given Aquifer Thickness Ratio, AFTR=1.10.	108
Fig. 5.9c	Normalised Distance (X/L) versus Aquitard Head Ratio (ATHR) as well as Aquifer Head Ratio (AFHR) for a given Aquifer Thickness Ratio, AFTR=3.0.	109
Fig. 5.10	Aquifer Thickness Ratio (AFTR) versus Average Discharge (DISR) in the top aquifer and bottom aquifer for a given Aquitard Depth Ratio, ATDR=2.15.	109
Fig. 6.1	Vertical section of the aquifer system with a discontinuous aquitard in the middle of it.	114
Fig. 6.2	Storage Coefficient (S) versus Seepage per unit depth in the aquifer system for a given value of Hydraulic Conductivity, $K=0.000125\text{m/s}$.	114
Fig. 6.3	Hydraulic Conductivity (K) versus Seepage per unit depth in the aquifer system for a given value of Storage Coefficient, $S=0.001$.	118
Fig. 6.4	Percentage Openings, O_p versus Fractional Seepage, F_{sb} , for two different Transmissivity values (T) while S/T ratio being kept constant.	118
Fig. 6.5	Distribution of Hydraulic Potential (h) in the aquifer system when $S/T = 0.0540$ for Percentage Openings, $O_p = 0.2\%$, 1% , 30% and 100% .	120
Fig. 6.6	Distribution of Hydraulic Potential (h) in the aquifer system when $S/T = 0.2162$ for Percentage Openings, $O_p = 0.2\%$, 1% , 30% and 100% .	121
Fig. 6.7	Distribution of Hydraulic Potential (h) in the aquifer system when $S/T = 0.4000$ for Percentage Openings, $O_p = 0.2\%$, 1% , 30% and 100% .	122
Fig. 6.8	Distribution of Hydraulic Potential (h) in the aquifer system when $S/T = 0.5045$ for Percentage Openings, $O_p = 0.2\%$, 1% , 30% and 100% .	123
Fig. 6.9	Distribution of Hydraulic Potential (h) in the aquifer system when Percentage Opening, $O_p = 30\%$ for $S/T = 0.0540$, 0.2162 , 0.4000 and 0.5045 .	125
Fig. 6.10	Distribution of Hydraulic Potential (h) in the aquifer system when Percentage Opening, $O_p = 100\%$ for $S/T = 0.0540$, 0.2162 , 0.4000 and 0.5045 .	126

Fig. 6.11	Distribution of Normalised Hydraulic Potentials (h_n) between the Centre and the Boundary of the aquifer system (vertical section) when Percentage Opening, $O_p=0.2\%$ and $S/T=0.0540$.	127
Fig. 6.12	Distribution of Normalised Hydraulic Potentials (h_n) between the Centre and the Boundary of the aquifer system (vertical section) when Percentage Opening, $O_p=1\%$ and $S/T=0.0540$.	127
Fig. 6.13	Distribution of Normalised Hydraulic Potentials (h_n) between the Centre and the Boundary of the aquifer system (vertical section) when Percentage Opening, $O_p=30\%$ and $S/T=0.0540$.	128
Fig. 6.14	Distribution of Normalised Hydraulic Potentials (h_n) between the Centre and the Boundary of the aquifer system (vertical section) when Percentage Opening, $O_p=100\%$ and $S/T=0.0540$.	128
Fig. 6.15	Distribution of Normalised Hydraulic Potentials (h_n) between the Centre and the Boundary of the aquifer system (vertical section) when Percentage Opening, $O_p=0.2\%$ and $S/T=0.5045$.	129
Fig. 6.16	Distribution of Normalised Hydraulic Potentials (h_n) between the Centre and the Boundary of the aquifer system (vertical section) when Percentage Opening, $O_p=1\%$ and $S/T=0.5045$.	129
Fig. 6.17	Distribution of Normalised Hydraulic Potentials (h_n) between the Centre and the Boundary of the aquifer system (vertical section) when Percentage Opening, $O_p=30\%$ and $S/T=0.5045$.	130
Fig. 6.18	Distribution of Normalised Hydraulic Potentials (h_n) between the Centre and the Boundary of the aquifer system (vertical section) when Percentage Opening, $O_p=100\%$ and $S/T=0.5045$.	130
Fig. 6.19	Distribution of Normalised Hydraulic Potentials (h_n) in the top aquifer between the Centre and the Boundary of the aquifer system (vertical section) for different Percentage Openings (O_p) and S/T ratios.	131
Fig. 6.20	Distribution of Normalised Hydraulic Potentials (h_n) in the bottom aquifer between the Centre and the Boundary of the aquifer system (vertical section) for $S/T=0.0540$ and Percentage Openings, $O_p = 0.2\%$, 1% , 30% and 100% .	131
Fig. 6.21	Distribution of Normalised Hydraulic Potentials (h_n) in the bottom aquifer between the Centre and the Boundary of the aquifer system (vertical section) for $S/T=0.5045$ and Percentage Openings, $O_p = 0.2\%$, 1% , 30% and 100% .	132
Fig. 6.22	Distribution of Normalised Hydraulic Potentials (h_n) in the bottom aquifer between the Centre and the Boundary of the aquifer system (vertical section) for several Percentage Openings (O_p) and S/T ratios.	132

Fig. 6.23	Percentage Opening (O_p) versus Reversal Points (X_R) of hydraulic potentials (expressed in terms of Normalised Distance, X/L) for $S/T=0.1081$ and 0.5045 .	134
Fig. 6.24	Difference curve of Reversal Points (X_R) of hydraulic potentials (expressed as percentage variance) corresponding to $S/T = 0.0540$ and 0.5045 plotted against Percentage Opening (O_p)	134
Fig. 6.25	Percentage Opening (O_p) versus specific seepage to the top as well as the bottom aquifer, respectively for several values of S/T ratio.	135
Fig. 6.26	S/T ratio versus Fractional Seepage, F_{sb} to the bottom aquifer for Percentage Openings, $O_p = 0.2\%$, 1% , 30% and 100% .	135
Fig. 6.27	Distribution of hydraulic potentials (h) in the aquifer system for three locations (Shift, $M_p=0\%$, 50% and 100%) with Percentage Opening, $O_p=5\%$ when the discontinuous Aquitard Position, $P_d=0.53$.	139
Fig. 6.28	Distribution of hydraulic potentials (h) in the aquifer system for several Percentage Openings (O_p) with the aquitard discontinuity located mid-way between the centre and the fringe of the source (Shift, $M_p=50\%$) when the discontinuous Aquitard Position, $P_d=0.53$.	140
Fig. 6.29	Normalised Distance (X/L) versus Normalised Hydraulic Potentials (h_n) in the bottom aquifer for three locations (M_p) of the aquitard discontinuity (Percentage Opening, $O_p=5\%$) below the source.	141
Fig. 6.30	Normalised Distance (X/L) versus Normalised Hydraulic Potentials (h_n) in the bottom aquifer for two locations (M_p) of the aquitard discontinuity (Percentage Opening, $O_p=25\%$) below the source.	141
Fig. 6.31	Normalised Distance (X/L) versus Normalised Hydraulic Potentials (h_n) in the bottom aquifer for two locations (M_p) of the aquitard discontinuity (Percentage Opening, $O_p=45\%$) below the source.	142
Fig. 6.32	Normalised Distance (X/L) versus Normalised Hydraulic Potentials (h_n) in the bottom aquifer for different Percentage Openings (O_p) with a Shift, $M_p=0\%$ and $S/T = 0.1081$.	142
Fig. 6.33	Normalised Distance (X/L) versus Normalised Hydraulic Potentials (h_n) in the bottom aquifer for different Percentage Openings (O_p) with a Shift, $M_p=50\%$ and $S/T = 0.1081$.	144
Fig. 6.34	Location (M_p) of the aquitard discontinuity below the source versus maximum values of Normalised Hydraulic Potentials (h_n -max) in the bottom aquifer for several Percentage Openings (O_p).	144
Fig. 6.35	Percentage Opening (O_p) versus maximum values of Normalised Hydraulic Potentials (h_n -max) in the bottom aquifer for several locations (M_p) of the aquitard discontinuity below the source.	145

Fig. 6.36	Location (M_p) of the aquitard discontinuity below the source versus Normalised Hydraulic Potentials (h_n) in the bottom aquifer for two Percentage Openings (O_p); hydraulic potentials at the centre (solid line) and that at the discontinuity (dashed line) are compared.	145
Fig. 6.37	Location (M_p) of the aquitard discontinuity below the source versus Fractional Seepage (F_{sb}) to the bottom aquifer for several Percentage Openings (O_p) when $S/T=0.1081$.	146
Fig. 6.38	Location (M_p) of the aquitard discontinuity below the source versus maximum values of Normalised Hydraulic Potentials (h_n -max) in the bottom aquifer for two S/T ratios with Percentage Opening, $O_p=5\%$.	146
Fig. 6.39	S/T ratio versus Fractional Seepage (F_{sb}) to the bottom aquifer for two locations (Shift, $M_p=0\%$ and 100%) of the aquitard discontinuity with $O_p=5\%$.	149
Fig. 6.40	Distribution of hydraulic potentials (h) in the aquifer system with the aquitard discontinuity located at $X/L=0$ and $X/L=0.43$ in the aquitard for $S/T=0.1081$ and $S/T=0.5045$ when the discontinuous Aquitard Position, $P_d=0.53$.	151
Fig. 6.41	Normalised Distance (X/L) versus Normalised Hydraulic Potentials (h_n) in the bottom aquifer for different S/T ratios when the aquitard discontinuity ($O_p=117\%$) is located at $X/L=0$.	152
Fig. 6.42	Normalised Distance (X/L) versus Normalised Hydraulic Potentials (h_n) in the bottom aquifer for different S/T ratios when the aquitard discontinuity ($O_p=117\%$) is located at $X/L=0.43$.	152
Fig. 6.43	Normalised Distance (X/L) versus Normalised Hydraulic Potentials (h_n) in the bottom aquifer for two S/T ratios when the aquitard discontinuity ($O_p=117\%$) is located at $X/L=0$ and $X/L=0.43$.	153
Fig. 6.44	S/T ratio versus Fractional Seepage (F_{sb}) to the bottom aquifer when the aquitard discontinuity ($O_p=117\%$) is located at $X/L=0$ and $X/L=0.43$, respectively.	153
Fig. 6.45	S/T ratio versus maximum values of Normalised Hydraulic Potentials (h_n -max) in the bottom aquifer when the aquitard discontinuity ($O_p=117\%$) is located at $X/L=0$ and $X/L=0.43$.	155
Fig. 6.46	Distribution of hydraulic potentials (h) in the aquifer system for three locations (at $X/L=0, 0.15$ and 0.30) of the aquitard discontinuity ($O_p=100\%$) when the discontinuous Aquitard Position, $P_d=0.53$.	155
Fig. 6.47	Normalised Distance (X/L) versus Normalised Hydraulic Heads (h_n) in the top aquifer when the aquitard discontinuity ($O_p=100\%$) is located at different X/L points.	157

Fig. 6.48	Normalised Distance (X/L) versus Normalised Hydraulic Potentials (h_n) in the bottom aquifer when the aquitard discontinuity ($O_p=100\%$) is located at different X/L points.	157
Fig. 6.49	Location (M_p) of the aquitard discontinuity (in terms of Normalised Distance, X/L) versus maximum values of Normalised Hydraulic Potentials (h_n) in the bottom aquifer when % Opening, $O_p=100\%$.	158
Fig. 6.50	Location (M_p) of the aquitard discontinuity (in terms of Normalised Distance, X/L) versus Fractional Seepage (F_{sb}) to the bottom aquifer when Percentage Opening, $O_p=100\%$.	158
Fig. 6.51	Distribution of hydraulic potentials (h) in the aquifer system for several S/T ratios for a Percentage Opening, $O_p=5\%$ when the discontinuous Aquitard Position, $P_d=0.53$.	160
Fig. 6.52	Distribution of hydraulic potentials (h) for several Aquitard Positions (P_d) when $S/T=0.1081$ and Percentage Opening, $O_p=5\%$.	161
Fig. 6.53	Normalised Distance (X/L) versus Normalised Hydraulic Heads (h_n) in the top aquifer for different Aquitard Positions (P_d) when $S/T=0.1081$ and Percentage Opening, $O_p=5\%$.	163
Fig. 6.54	Normalised Distance (X/L) versus Normalised Hydraulic Potentials (h_n) in the bottom aquifer for different Aquitard Positions (P_d) when $S/T=0.1081$ and Percentage Opening, $O_p=5\%$.	163
Fig. 6.55	Normalised Distance (X/L) versus Normalised Hydraulic Heads (h_n) in the top aquifer for several S/T ratios when the Aquitard Position, $P_d=0.53$ and Percentage Opening, $O_p=5\%$.	164
Fig. 6.56	Normalised Distance (X/L) versus Normalised Hydraulic Potentials (h_n) in the bottom aquifer for different S/T ratios when the Aquitard Position, $P_d=0.53$ and Percentage Opening, $O_p=5\%$.	164
Fig. 6.57	Aquitard Position (P_d) versus max. values of Normalised Hydraulic Potentials (h_n -max) in the bottom aquifer for a % Opening, $O_p=5\%$.	165
Fig. 6.58	Aquitard Position (P_d) versus Fractional Seepage (F_{sb}) to the bottom aquifer for a Percentage Opening, $O_p=5\%$.	165
Fig. 6.59	S/T ratio versus Fractional Seepage (F_{sb}) to the bottom aquifer for the Aquitard Position, $P_d=0.53$ and a Percentage Opening, $O_p=5\%$.	166

LIST OF NOTATIONS

CHAPTER 3

$A_i(\lambda)$	First unknown function for i^{th} layer in the equation for hydraulic potential
$B_i(\lambda)$	Second unknown function for i^{th} layer in the equation for hydraulic potential
h_0	Some constant, [L]
h_i	Depth to i^{th} interface, [L]
$J_0(\lambda r)$	Bessel function of order zero
K_i	Hydraulic Conductivity of i^{th} layer, [LT^{-1}]
n	Number of layers
q	Strength of the point source, [L^3T^{-1}]
R	Radial axis of the cylindrical coordinate system, [L]
$P(r, z)$	Cylindrical coordinate of any point P in the medium
R_m	Denotes a coefficient a_m , b_m , d_m or f_m of the rational function g^m
s_i	Integer multipliers for the layers, $i=1$ and 2
Z	Vertical axis of the cylindrical coordinate system, [L]
λ	Variable of integration, [L^{-1}]
$\phi_i(r, z)$	Hydraulic head at arbitrary point P(r,z) in i^{th} layer, [L]
$\psi_i(r, z)$	Stream function in the i^{th} layer of the aquifer system, [L^2T^{-1}]

CHAPTER 4

b	Half-length of the line source, [L]
g	Acceleration due to gravity, [LT^{-2}]
k	Intrinsic permeability of the porous medium, [L^2]
K_1, K_2	Hydraulic conductivities in the principal directions of anisotropy, [LT^{-1}]
K_m	Equivalent isotropic hydraulic conductivity, [LT^{-1}]
Q	Strength of the point source, [L^3T^{-1}]
Q_L	Strength of the line source per unit length, [L^2T^{-1}]
q_x	Specific discharge in the X- direction, [LT^{-1}]
q_y	Specific discharge in the Y- direction, [LT^{-1}]
q_y^*	Specific discharge in the Y*- direction, [LT^{-1}]
q_z	Specific discharge in the Z- direction, [LT^{-1}]
q_z^*	Specific discharge in the Z*- direction, [LT^{-1}]
α	Angle of dip of the soil strata, [$^\circ$]
β	Coefficient of anisotropy
(γ, η, ζ)	Coordinate transformation parameters
$\Delta Y, \Delta Z$	Discretisation in the vertical plane, along the Y and Z- axes
μ	Dynamic viscosity of the fluid, [$ML^{-1}T^{-1}$]
ϕ	Hydraulic potential, [L]
ρ	Fluid density, [ML^{-3}]
Ω	Angle between Y_1^* and Y_1 -axes in the fictitious domain, [$^\circ$]

CHAPTER 5

AFHR	Aquifer Head Ratio
AFTR	Aquifer Thickness Ratio
ATDR	Aquitard Depth Ratio
ATHR	Aquitard Head Ratio
$CC_{i-\frac{1}{2},j,k}$	Conductance in column j and layer k between modes $i-1,j,k$ and i,j,k
$CR_{i,j-\frac{1}{2},k}$	Conductance in row i and layer k between nodes $i,j-1,k$ and i,j,k
$CV_{i,j,k-\frac{1}{2}}$	Conductance in row i and column j between modes $i,j,k-1$ and i,j,k
D	Depth of the aquifer system, [L]
DISR	Discharge Ratio
h	Potentiometric head/ hydraulic potential, [L]
H_b	Head in the sink, [L]
$h_{i,j,k}$	Hydraulic head in cell i,j,k
K_{xx}, K_{yy}, K_{zz}	Hydraulic conductivities along the major axes of anisotropy
L	Half width of the aquifer system
$P_{i,j,k}$	Certain constant for cell i,j,k
$Q_{i,j,k}$	Groundwater flow rate into cell i,j,k
S_s	Specific storage of the aquifer
$SS_{i,j,k}$	Specific storage of cell i,j,k
t	Time
W	Volumetric flux per unit volume
w	Half width of the water body
X/L	Normalised Distance
ΔH	Head causing-flow
$\Delta r_j \Delta c_i \Delta v_k$	Volume of cell i,j,k
Δt	Increment in time

CHAPTER 6

F_{sb}	Fractional Seepage
H_b	Head in the Boundary, [L]
h	Hydraulic Head/ Potential, [L]
h_n	Normalised Hydraulic Potential
M_p	Percentage Shift/ Shift
O_p	Percentage Opening
P_d	Positioning Depth [L]
S	Storage coefficient
T	Transmissivity, [L^2T^{-1}]
X/L	Normalised Distance
X_R	Reversal Point, [L]
ΔH	Head Causing Flow, [L]

INTRODUCTION

1.1 GENERAL

Of the total volume of fresh water available on Earth, only a quarter of it is either in vapour or liquid phase; the major portion being in the form of ice, and does not participate in the water cycle on short time-scales [Seiler and Lindner 1995]. Among liquid fresh water, groundwater predominates. Certain regions of the world depend solely on the availability of groundwater for their domestic, agricultural and various other activities. Even so, growth in industrial, agricultural, and municipal sectors has resulted in increasing utilisation of water, which has caused considerable pressure on the development and sustenance of ground-water reservoirs. Ever-increasing dependence on groundwater for various uses has not only triggered environmental hazards like land subsidence and sea water intrusion in coastal aquifers but depletion of many aquifers too. Hence, sustainable management and utilisation of groundwater in such regions is essential and that requires good knowledge of the flow dynamics [Prasad and Romkens 1986] in the underlying aquifers.

1.2 BACKDROP OF THE THESIS

Artificial recharge methods [Brown and Signor 1972, Nutbrown 1976, Warner et al. 1989, Allam et al. 1998, Bouwer et al. 1999], which are eco-friendly means to revive fragile hydrologic regimes, are being proposed and implemented in order to rejuvenate depleting groundwater aquifers in many countries, including India. There has been a continuing interest in artificial recharge practices apparently due to reasons of escalating demands, recurring drought events, depletion of aquifers due to reduced recharge/ increased pumping rates, safe disposal of waste water as well as losing popularity of dams due to social and environmental reasons. Methods of recharging [Brown and Signor 1972] include spreading basins, over-irrigation, stream impoundment, percolation tanks,

recharge ponds, injection wells and hydraulic connectors. ^A among these, percolation tanks and recharge ponds are common in India.

The important issues associated with artificial recharge can be identified as the nature of the rechargeable water source, the system of recharge to be used, ~~the~~ expected recharging rates, the hydraulic response of the system to recharging and the long-term management of the total water resources system. Planning systems for the artificial recharge of ground water requires investigations on infiltration rates to assess the ability of the porous medium to transmit water to the underlying aquifer [Rastogi and Pandey 1998, Ranganna et al. 1991, Bouwer et al. 1999, Balek 1989]. Recharging can be influenced by hydrogeology of the aquifer, the hydraulic properties and flow parameters of the porous medium as well as flux boundaries of the aquifer system. Knowledge of the flow regime and hydraulic responses of a recharging aquifer system may facilitate effective planning and implementation of recharge schemes. Moreover, there are issues pertaining to storage, extraction/ recovery and possibility of waterlogging need to be addressed in the long-term effect of recharge on ground water. Geohydrological aspects deserve special attention in the planning, locating and designing of an artificial recharge scheme. Nevertheless, investigations leading to quantitative results on flow regimes are still evasive especially in the case of multiaquifer systems characterised by stratifications, discontinuities (like distributed clay lenses) and inhomogeneities. Both analytical and numerical groundwater models can be used to simulate effects of regional recharge inputs and extractions ^{from} for the aquifer systems. However, a quick concept concerning aquifer situation can be obtained from steady-state analytical models [Bouwer et al. 1999].]?

With this backdrop, it has been perceived that there is an imperative need for carrying out further investigations/ analyses on the hydraulic responses of recharging (from surface water sources) aquifer systems of layered/ anisotropic nature.

1.2.1 ROLE OF ANALYTICAL AND NUMERICAL METHODS

A critical review of the literature relevant to surface water - groundwater interaction, artificial recharging and groundwater flow modelling indicates that though there are many specific cases of

aquifer simulation studies; generalised methodologies ^{and discussion on} results on flow regimes are still lacking in the case of complex aquifer systems. ^{Therefore} it has been perceived that there is a possibility of developing new analytical approaches for aquifer simulation in multilayered/ anisotropic aquifer systems by considering the analogy between groundwater flow and electrical flow ^{involving the} in the context of advances made in exploration geophysics.

Unlike numerical models, analytical models render handy techniques to simulate flow/ hydraulic potentials in aquifer systems with fewer data sets. Also, analytical models are quick simulators that are computationally more efficient than any numerical simulator. Further, ^{these models} they offer qualitative insights that may not be revealed through the quantitative results obtained by numerical simulations. Besides, formulation of analytical models can be advantageous for simulation of flow in anisotropic aquifer systems with dipping beds as numerical modelling in such cases can be often error-prone due to horizontal approximation of the model layers. When simple solutions are sought as part of initial investigations or field applications, analytical modelling results can be of great advantage. Besides, the relevance of analytical results are obvious in the context of analytic element method [Haitjema and Kraemer 1988, Haitjema 1995, Fitts and Strack 1996, Strack 1999] for groundwater flow problems. ^{Therefore} So, here attempts are made towards the development of analytical models for complex aquifer systems. Further, in the case of anisotropic porous media the directions of flow and of the hydraulic gradient are not parallel [Marcus 1962]. Hence, numerical modelling of anisotropic flow domains attempted through isotropic approximations may introduce error in the computation of flow. Therefore, it is desirable to develop analytical models for anisotropic aquifer conditions too.

However, analytical models developed for idealised conditions are not effective for detailed investigations on the flow characteristics in complex aquifer systems with discontinuities (like distributed clay lenses in alluvial aquifer systems). Therefore, numerical modelling is desirable for the simulation of groundwater flow in multilayered aquifer systems with discontinuities and complex boundary conditions as numerical models relax the idealised conditions of analytical methods. Examples of numerical modelling of groundwater flow/ solute transport, and seepage from surface water bodies may be found in the literature [Eldho and Rao 1996, Rabbani and Warner 1997,

Beckers and Frind 2000]. Among the numerical groundwater models, the MODFLOW [Mc Donald and Harbaugh 1984] is being applied extensively in investigations [Grundl and Delwiche 1992, Cheng and Anderson 1993, Swain 1994, Bradley 1996, Genereux and Bandopadhyay 2001] pertaining to groundwater flow.

Thus, analytical and numerical methods can be complementary to each other for conducting effective flow simulation studies in isotropic/ anisotropic layered aquifer systems with or without discontinuities. Consequently, formulation of analytical models in multilayered and anisotropic aquifer systems as well as numerical simulation studies in an aquifer-aquitard-aquifer system constitute the core of the thesis. While advancements made in the realm of exploration geophysics has been invoked for the development of analytical models, the USGS three-dimensional modular numerical model, MODFLOW has been employed for the aquifer simulations.

1.3 SCOPE OF THE PRESENT WORK

In view of the above, it has been proposed to carry out theoretical investigations/ analyses in a layered aquifer system ^{using} ~~by use of~~ analytical methods as well as numerical modelling techniques, ~~leading to valuable results~~. Thus, the current work constitutes derivation of analytical expressions for hydraulic potential (potential function) and streamlines (stream function) in multilayered/ anisotropic aquifer systems as well as application of a three-dimensional numerical groundwater flow model for simulations and analyses in a three layered aquifer-aquitard-aquifer system.

Steady state analytical solutions for hydraulic potentials and streamlines due to a surface water source (point source/ line source/ areal source) have been derived for the case of (i) a layered aquifer system with a maximum of three layers, and (ii) a multi-layered aquifer system with large number of layers (say, n - layers). Steady state analytical solutions for hydraulic potentials due to a point source and a finite length-line source in a homogeneous anisotropic aquifer system with inclined soil strata have also been derived. Besides, appropriate validation procedures for the developed analytical models have been done. Further, numerical simulation studies have been carried out in an aquifer-aquitard-aquifer system with and without aquitard discontinuity using the

three dimensional finite difference groundwater flow model, MODFLOW [Mc Donald and Harbaugh 1984]. These studies ^{include} covered: (i) the effect of depth-wise positioning of an aquitard on the flow regime, (ii) the impact of the degree of aquitard discontinuity on the recharging of the aquifer system, and (iii) the effect of location of the aquitard discontinuity on the recharging of the aquifer system.

1.4 LAY OUT OF THE THESIS

The thesis is organised in 7 chapters, each chapter ^{covers} being devoted to a particular aspect of the work.

Chapter 1: This chapter attempts to introduce the rationale of the present work by dwelling on the background of the work. The major objectives and a profile of methodologies are also provided.

Chapter 2: It contains an elaborate review of the literature on all pertinent aspects related to the current work. The review brings out the need and rationale for the studies.

Chapter 3: Here, analytical models have been presented for the computation of steady state hydraulic potentials and streamlines in a three-layer aquifer system as well as in a multilayered aquifer system with large number of layers. The application of these analytical models have been demonstrated with numerical examples. Further, performance comparison of the presented analytical models have been made with corresponding results from a standard numerical model.

Chapter 4: This chapter presents analytical solutions for hydraulic potential due to a point source as well as that due to a finite-length line source in a stratified homogeneous anisotropic aquifer system with dipping strata.

Chapter 5: It deals with a study on the recharging in an aquifer-aquitard-aquifer system vis-à-vis the influence of the dimension and depth-wise positioning of a continuous aquitard on the flow regime, based up on numerical simulations by MODFLOW.

Chapter 6: Recharge investigations on the recharging in an aquifer-aquitard-aquifer system with a discontinuous aquitard ^{is} presented. The influence of the following aspects on the flow regime has been studied using numerical modelling: (i) dimension of the aquitard discontinuity, (ii) location of

the discontinuity in the aquitard, and (iii) depth-wise position of the discontinuous aquitard in the aquifer system.

Chapter 7: A discussion on the summary of contributions and conclusions with a note on further perspectives for future investigations ~~in continuation to the present effort~~ are given in this chapter.

Finally, all the relevant references cited in the thesis have been listed in the end of the thesis.

Normally a narrative description is more readable

via

Chapter 1 deals with

2 looks into

3 examines

4 investigates et al.

however I leave it to the guides if they think the same way

REVIEW OF LITERATURE

2.1 GENERAL

Study of the interaction between surface water and groundwater is of great importance from a quantitative and qualitative point of view. However, this necessitates ^{an adequate} a sound background of theoretical and applied investigations. Understanding the dynamic nature of surface water - groundwater interaction aids in the interpretation of hydrologic and chemical relations between surface water bodies like lakes, recharge ponds etc. and the ground water [Sacks et al. 1992]. Again, it is of fundamental concern to those interested in sustainable development of water resources and implementation of artificial recharge schemes [Brown and Signor 1972, Rastogi and Pandey 1998, Bouwer et al. 1999] and is to be given a greater attention [James 1995].

Study of surface water - groundwater interaction can be carried out by means of numerical as well as analytical methods. A general mathematical description of interactions between surface water and ground water, as a complicated structural system, requires the use of hydrodynamic and water-balance equations [Popov and Sokolov 1986]. Availability of efficient numerical models offer promising opportunities to relax many assumptions of analytical solutions and interpret field data more generally. Besides, analytical solutions could be advantageous when groundwater flow is considered in complex aquifer systems of layered/ anisotropic nature as some parallels may be found in the geoelectric sounding principles [Bhattacharya and Patra 1968, Patra and Nath 1999]. However, this aspect deserves special attention. In numerical models the inverse method [Konikow and Mercer 1988, Konikow and Bredehoeft 1992, Finsterle and Pruess 1995] is used to achieve hydraulic characterisation of the aquifer, wherein hydraulic parameters are calibrated to best-match the observed water levels. Nevertheless, the hydraulic response of a subsurface flow system is governed by its geometric attributes, its forcing functions, and its material properties [Narasimhan 1998].

Analytical tools help in comprehending the physics behind the processes.

Understanding the interaction of surface water bodies with groundwater requires an understanding of the dynamic character of the distribution of hydraulic head in the groundwater system [Winter 1983]. This distribution of hydraulic head/ potential is controlled to a large extent by the distribution of groundwater recharge. There are a number of factors which affect the process of groundwater recharge. Among those, the hydraulic conductivity and porosity of soil have the most profound influence. Though recharge processes have been investigated using different forms of mathematical models, most of these models cannot elaborate the physics of groundwater recharge [Su 1994]. The surface water - groundwater interaction is controlled by the geologic framework through which the water flows [Winter and Pfannkuch 1984] and hydraulic behaviour like anisotropy of the porous media.

2.2 STUDIES ON SURFACE WATER - GROUNDWATER INTERACTION

There has been an increasing interest, in recent times, in modelling tools that integrate the surface and subsurface components of the hydrologic cycle [Beckers and Frind 2000] in a natural watershed that should take care of the interaction aspects too. Assessment of groundwater potential for conjunctive water use is essential in irrigation projects [Sondhi Rao and Sarma 1989]. Field studies of surface water-groundwater interaction are reported in the literature from various regions of the globe [Anderson and Cheng 1993, Cherkauer and Zvibleman 1981, Crowe and Schwarts 1981, Singh 1992, Munter and Anderson 1982, Eshleman et al. 1994, Pucci and Pope 1995, Isiorho et al. 1996, Lee 2000]. It has been shown using mathematical modelling, that the major mechanism of vertical flow through the zones of low hydraulic conductivity in alluvial aquifers of Gujarat (India) was causing rapid declines in the water table / piezometric heads [Rushton and Tiwari 1989]. Another investigation exposed the common understanding that inflow to a large water body like a lake is largest at the shoreline and decreases exponentially with distance offshore [McBride and Pfannkuch 1975, Pfannkuch and Winter 1984] need not be a norm [Cherkauer and Nader 1989].

The heterogeneities within the hydrogeologic system beneath surface-water bodies may modify the flow system. Further, the presence of clay layers between the ground and phreatic surface can limit the flow leading to water-logging at the ground surface and declining groundwater heads in the aquifer [Rushton 1986]. Generalised results on the recharge characteristics for aquifer systems having discontinuous flow barriers like clay lenses are required to be framed.

Previous research on interaction between surface water bodies and aquifers is focused generally on specific cases to understand the features of a particular type of flow system or alternatively to evaluate particular modelling techniques [Townley and Davidson 1988]. Though an elaborate study of two dimensional numerical modelling [Nield et al. 1994] attempts to provide a general framework for surface water-groundwater interaction, it is still limited by a number of simplifying assumptions. Despite the continuing interest in many aspects of surface water - groundwater interaction, a comprehensive classification [Townley and Trefry 2000] for groundwater flow patterns near surface water bodies is still lacking. Augmentation of an existing two dimensional flow classification scheme for lake aquifer systems [Nield et al. 1994] to three dimensions has been reported recently [Townley and Trefry 2000]. Nevertheless, assumptions of homogeneity and isotropy have been imposed in these idealised mathematical models. A compilation of hydrogeologic data for numerous lakes in North America with a preliminary classification framework for lakes based on hydrogeologic considerations is reported [Born et al. 1979]. However, existing results on surface water - groundwater interaction for those specified situations [Winter 1976, 1978, 1981, 1983, 1995, 1999, Wright 1980, Kacimov 2000] are not easily transferable to non-identical situations; their usefulness lies in the methodology rather than the general applicability.

Theoretical analyses of seepage from surface water bodies like canals, ponds, rivers etc. to the underlying aquifer system as well as two or three dimensional flow regimes using either analytical techniques or numerical methods are also reported [Nutbrown 1976, Winter 1978, Bruch 1979, Rushton and Redshaw 1979, Smiles and Knight 1979, Pfannkuch and Winter 1984, Sahuquillo 1986a, 1986b, Sophocleous and Perkins 1993, Meigs and Bahr 1995, Rai and Singh 1995]. An analytical solution is reported for the growth of groundwater mound in finite aquifers bounded by open water bodies, in response to recharge from rectangular areas [Rao and Sarma 1981].

Further, investigations of surface water-groundwater interaction in an interdisciplinary manner are also reported [Bobba et al. 1992, Pfannkuch and Winter 1984, Krabbenhoft et al. 1990b, Kacimov 2000, Nachiappan 2000]. The results of a field study in which stable isotopes and a numerical model were used independently to calculate groundwater flow rates indicate that taken together the two methods are complementary in establishing confidence in the results [Krabbenhoft et al. 1990a, 1990b]. Theoretical studies of steady groundwater flow near a hemispherical lake have been reported by utilising known solutions from electromagnetism [Kacimov 2000].

2.3 GROUNDWATER MODELLING: ANALYTICAL METHODS

The analytical approach is often the simplest and quickest way to obtain answers to questions posed by water-resource managers. Analytical models can also be instrumental in improving our understanding of physical processes occurring within a ground water flow system.

Unlike numerical models, the results from analytical models remain continuous functions of space and time. Thus, many of the difficulties and errors associated with the discrete-space and discrete-time numerical solutions are avoided [Hemker 1999a]. Besides, analytical solution techniques are often less computationally demanding and can give greater insight into the behaviour of the dependent variable [Connell et al. 1998]. Analytical solutions can be employed to test/ check results obtained through numerical models during their developmental phase or afterwards [Holder et al. 2000]. In general, analytical models are useful in aquifer-test analysis; evaluation of simple aquifer systems; design, calibration, or verification of numerical computer models; and understanding basic principles of groundwater flow and transport.

A large number of analytical models structured to solve partial differential equations governing the flow of groundwater to and from wells, and streams for isotropic or anisotropic conditions are available [Sridharan et al. 1990a, Walton 1979]. Analytical models are applied chiefly to relatively uniform aquifers with simple geometry. While numerical modelling may be required at advanced stages of groundwater flow problems, simple analytical solutions can be informative during the preliminary stages of investigations as evident from some of the recent investigations

[Marinelli and Niccoli 2000, Lei 1999]. Numerical models can be more realistic, but availability of abundant and accurate data is imperative. Cases where basic data are not sufficient to warrant numerical modelling, analytical models can be the alternative. Thus, the choice to select an analytical or a numerical technique mainly depends on the complexity of the type of problem at hand and the solution requirements.

Recognised departures from ideal conditions do not necessarily dictate that analytical models be rarely used as there are means for circumventing analytical difficulties posed by complicated field conditions, and many aquifer systems can be highly idealised with little sacrifice in accuracy of analysis [Walton 1970]. Further, this limitation can be overcome by superimposing many analytic solutions, allowing the total solution to meet irregular boundary conditions [Strack and Haitjema 1981a, 1981b, Strack 1989, Haitjema 1995, Strack 1999]. Irregular and diverse boundary conditions can be modeled using this approach and the resulting composite analytic solution satisfies the governing differential equation exactly except at singular points, curves, or surfaces associated with the analytic functions [Fitts 1991]. To remove singular behaviour of the flow near source/ sink zones, analytical techniques are available [Charbeneau and Street 1979].

The utility of analytic element method for groundwater flow problems [Haitjema and Kraemer 1988, Haitjema 1995, Fitts and Strack 1996, Strack 1999] by way of superposition of analytic functions underscores the continuing interest in analytical results. The literature is replete with analytical solutions for the interaction of confined, leaky, and water table aquifers with an adjoining streams or water bodies [Barlow and Moench 1998]. Although extensive research has been carried out on developing analytical solutions for surface water - groundwater interaction, no generalisation of the solution scheme for dealing with general initial and boundary conditions has been published [Ostfeld et al. 1999]. Analytical models are shown to be useful tools in the quantification of the interaction of surface water and groundwater [Moench and Barlow 2000]. A recharge relationship of groundwater profiles with constant groundwater tables was derived using the integral solution approach [Prasad and Romkens 1986]. Also, an explicit formula obtained through analytical inverse solution has been presented in the literature to compute recharge of groundwater [Su 1994].

There are many analytical solution techniques presented in the literature for two-dimensional ground water flow problems [Strack 1981a, 1981b, Boehmer and Boonstra 1987, Yates 1988, Van der Veer 1994, Fitts and Strack 1996, Bruker and Haitjema 1996, Connell et al. 1998, Verhoest and Torch 2000]. In one of the studies, analytical Dupuit solutions for multi-aquifer flow are compared to exact solutions for two-dimensional flow [Bakker 1999]. Procedures are presented for delineating capture zones of pumping wells [Bakker and Strack 1996]. Flow to a well in a multi-aquifer system is a problem that has great practical interest and importance in groundwater literature [Sokol 1963, Hunt 1985]. Solutions for groundwater flow are available for the case of layered aquifer systems using the differential equations of ground water motion and the pertinent initial and boundary conditions [Polubarinova-kochina 1962, Hantush 1967a, 1967b, Neuman and Witherspoon 1969b, Herrera 1970, Hemker and Maas 1987]. Solutions for radial flow in a confined infinite aquifer systems with the well represented by a line sink has been reported [Neuman and Witherspoon 1969a, Khader 1980]. Further, analytical solutions are found to be convenient to predict the rate of growth and shape of the recharge mounds in artificial recharge schemes [Warner et al. 1989]. The analyses are applicable to steady flow through a system of two/ many aquifers of infinite extent.

Flow in an extensive heterogeneous aquifer that is composed of a succession of horizontal homogeneous sublayers, is a type of problem that can be solved by an integration of both analytical and numerical techniques [Hemker 1999a]. Solutions for aquifer systems having a number of layers are reported [Hemker and Maas 1987, Gjerde and Tyvand 1987]. Some of these models treat every other layers as identical [Gjerde and Tyvand 1987]. Still, there are very few analytical solutions allowing some sort of vertical heterogeneity [Hemker 1999a, 1999b] within the aquifer.

Analytical description of determination of flow to a point sink in a perfectly layered subsurface has been published [Nieuwenhuizen et al. 1995]. The non-vertical well is constructed by a number of point sinks along a line or on a surface, and the flow solutions for each point sink are superimposed to find the full solution as the well can be composed of a number of point sinks. Each point sink causes a flow field and the total flow field is obtained by superposition of these fields. The restrictions in the above solution procedure are: the points sinks can not be located at the earth-surface, or at an the interface between layers, and assumption of isotropic subsurface. Flow driven

by a well (using a generalised Fourier transform technique) in a perfectly layered subsurface, where the permeability is a function of the depth only, has been described elsewhere [Maas 1987a, 1987b]. A general method has been reported for the analytical solution of steady flow problems in leaky multiple-aquifer systems of infinite extent, being pumped or recharged at a constant rate [Hemker 1984].

An analytical model to simulate stream-aquifer interactions, only using transmissivity, specific yield, and recharge as parameters, for alluvial conditions has been reported [Workman et al. 1997]. A general solution scheme [Ostfeld et al. 1999] for determining groundwater levels for groundwater systems with recharge exists. A grave limitation of the model is the selection of a 'representative flow depth' to facilitate the solution, which can only be determined given the numerical solution.

A perturbation solution with probabilistic approach to three dimensional radial flow in heterogeneous porous media is reported [Naff 1991]. Mean radial flow with stationarity of flow and relative potential in an infinite three dimensional medium is assumed to simplify the analysis. Analytical solution for the problem of abstraction from a well in a multilayered aquifer, each layer being independently homogeneous, isotropic and artesian, is obtained [Wikramaratna 1984].

Evidently, advances in analytical modelling virtually dominated groundwater literature until the invention of digital computers [Walton 1979], thereafter numerical modelling took over. Yet, significant progress in analytical modelling continues, especially in the case of complex aquifer systems, and the inventory of analytical models is impressive.

2.4 GROUNDWATER MODELLING: NUMERICAL METHODS

Numerical models commonly used to analyse or predict the response of groundwater systems have increasing capabilities for dealing with complex flow and transport processes. However, greater model sophistication is usually accompanied by an increasing number of hydrogeologic parameters, which enter the governing equations to describe the interaction between the fluids and the porous

media. Therefore, measurements [Dane and Molz 1991] needed to define the basic hydraulic properties of subsurface porous media constitute a fundamental problem, since these models make realistic predictions if the correct values for the hydraulic properties are used. Even so, the measured parameters may differ significantly from their model counterparts both conceptually and numerically, mainly because of scale effects [Finsterle and Pruess 1995, Narasimhan 1998]. The model-related formation parameters are obtained through calibration of the model using inverse modelling techniques [Konikow and Mercer 1988, Konikow and Bredhoeft 1992].

Because of inevitable errors and uncertainty in model parameters, all predictions need to be accompanied by some indication of their reliability or uncertainty [Konikow and Mercer 1988]. The numerical errors arising strictly from inaccuracies in the equation solving algorithm usually are much smaller than the errors associated with or produced by : theoretical misconceptions, or over-idealizations about the system that are incorporated in the model, uncertainty and error in the specification of system properties, boundary conditions, and initial conditions, and uncertainty in past and future stresses. It is possible to specify boundary conditions for the boundaries of an embedded microscale model using values from the embedding macro-scale model [Leake et al. 1998]. Literature relevant to flow and capture zone modelling of complex three-dimensional ground water flow systems, focuses on the importance of the geologic structure, the parameter estimation and model calibration, and techniques for the delineation of three-dimensional capture zones. It has been found that a three-dimensional conceptual model based on the geologic structure is essential for a valid definition of the flow field, and hence for creating a credible basis for delineating well capture zones [Martin and Frind 1998].

Recent years witnessed the application of analytic element method [Strack and Haitjema 1981a, 1981b, Strack 1989, Haitjema 1995, Strack 1999], a numerical method that gives an approximate solution to a problem, to groundwater modelling studies. The method is based upon the superposition of analytic functions [Haitjema and Kraemer 1988, Fitts and Strack 1996] and might be considered as an extension of classical models of regional flow based on the superposition of elementary functions such that each function is unaffected by the other functions in the solution. Methods are presented in the literature for finding approximate analytic solutions to three-

dimensional steady state ground water flow and for combining those solutions with regional two-dimensional models [Haitjema 1985, Luther and Haitjema 2000].

Numerical modelling of groundwater flow/ solute transport, and seepage from surface water bodies using various schemes can be found in the relevant literature [La Venue and Rama Rao 1989, Eldho and Rao 1996, Rabbani and Warner 1997, Beckers and Frind 2000]. Flow mechanisms in groundwater basins with a distinction between the behaviour of aquifers and aquitards are reported [Marsily et al. 1978, Sridharan et al. 1990b, Lopez and Smith 1995]. The application of Finite Element and Boundary Integral Equation methods are reported in deriving solutions for complex aquifers [Lafe et al. 1981, Yu and Singh 1994]. Among the available numerical groundwater models, the USGS three-dimensional modular numerical model, MODFLOW [Mc Donald and Harbaugh 1984] has been applied extensively (either the original codes, or modified ones with additional features) in investigations pertaining to groundwater flow as well as transport related problems [eg: Grundl and Delwiche 1992, Sophocleous and Perkins 1993, Cheng and Anderson 1993, Swain 1994, Reynolds and Spruill 1995, Anderman et al. 1996, Bradley 1996, Srinivas et al. 1996, 1999, Genereux and Bandopadhyay 2001]. Of late, an investigation using MODFLOW on the relative significance of several factors controlling lake bed seepage patterns [Genereux and Bandopadhyay 2001] is reported.

Numerical methods relax the idealised conditions of analytical models and yield approximate solutions to the governing equations [Konikow and Mercer 1988]; they require discretisation of space and time . Within the discretised format one approximates the internal variable properties, boundaries, and stresses of the system. However, in applying groundwater models to the field problems, errors arise from conceptual deficiencies, numerical errors, and inadequate parameter estimation [Konikow and Bredehoeft 1992]. A better quantitative insight into the relation between spatial scale and problem schematisation will provide better insight into the applicability and accuracy of numerical models. Methods aimed at understanding the relationships among spatial and temporal discretisations and numerical errors will enable evaluation of grid size and vertical dimension of a groundwater model [Stolwijk et al. 1996, Lal 2000].

Numerical models of any scale contain uncertainties because of inaccuracies in the inputs, parameters, and algorithms [Lal 2000]. Input uncertainty is due to inaccurate or inadequate spatial and temporal input data. Parameter uncertainty is mainly due to inaccurate values of spatially varying physical characteristics. Numerical errors are considered to be the source of algorithm. Most numerical flow models fail to simulate hydraulic heads in an anisotropic porous medium with inclined planes of stratification. The reason being the assumption of the principal axes of anisotropy coinciding with the reference coordinate axes, which is not true. Hence, numerical modelling of anisotropic flow domains attempted by isotropic approximations introduces error in the computation of hydraulic heads and thereby in the flow.

2.5 FLOW IN ANISOTROPIC AQUIFER SYSTEMS

Natural porous media are generally inhomogeneous and layered structures with anisotropy are very common. Anisotropic behaviour of a porous medium at one scale may be related to the presence of lower-scale directional structures [Ursino et al. 2000]. The effect of anisotropy on the flow of groundwater through geologic formations has been of particular interest to hydrologists. The theory of flow of fluids through anisotropic porous medium is presented in the literature [Scheiddegger 1957, Polubarinova-Kochina 1962, Harr 1962, Marcus 1962]. Further, theories on geoelectric sounding procedures [Bhattacharya and Patra 1968, Koefoed 1979, Niwas and Israil 1986, Patra and Nath 1999] provide insight into the computation of surface electric potentials in layered anisotropic earth medium. However, parallel results enabling computation of hydraulic heads in layered anisotropic medium are not available in the hydrological literature.

The direction of the flow and of the hydraulic gradient in an anisotropic porous medium are generally not parallel [Marcus 1962]. The directional permeability can be expressed either as a function of the properties of a porous medium or as a function of the properties and dimensions of the porous medium. The two definitions do not yield the same result; the difference is a function of the anisotropy of the material and of the directions of the gradient with respect to the principal permeabilities [Marcus and Evenson 1961]. The analysis of ground-water flow in a homogenous and anisotropic medium can be facilitated by appropriate transformation of the coordinate axes, thereby

the anisotropic medium can be transformed into a fictitious isotropic one [Mishra 1972, Strack 1989].

An investigation of the fundamentals of the two dimensional flow through anisotropic porous media was carried out, and general solutions reported [Marcus 1962]. A two dimensional linear theory of the decay of a disturbed free surface in an anisotropic porous layer has been presented [Tyvand 1984, 1986] with an arbitrary two-dimensional anisotropy assumed for the homogeneous porous medium. Methods for parameter estimation for an anisotropic leaky aquifer system has been reported [Sekhar et al. 1994]. Theoretical analyses for the steady state seepage of ponded water into drainage ditches in a homogenous and anisotropic soil are available [Barua and Tiwari 1995, 1996]. Laboratory experiments have also been reported to examine the combined effect of heterogeneity, anisotropy and saturation in porous media on steady flow/ transport [Ursino et al. 2001].

It is observed that there are not many analytical results reported in the literature for most of the types of flows in anisotropic porous media, particularly for the distribution of hydraulic heads in an anisotropic medium with inclined bedding planes.

2.6 FORMULATION OF STREAM FUNCTIONS

For two-dimensional groundwater flow governed by Laplace equation there exists both a discharge potential function and a stream function, which are conjugate harmonics of each other [Strack 1989]. The stream function is constant along a streamline, and the difference in its value for two streamlines represents the total flow between these streamlines. Basically, the importance of the stream function stems from its application to constant density flow problems in which hydraulic head is a potential function that completely describes the flow system. Under these circumstances equipotentials are everywhere normal to flow lines, and the stream function and hydraulic potential satisfy the Cauchy-Riemann conditions [Harr 1962], thereby lending themselves to solutions using the tools of complex variables.

Therefore, in modelling groundwater flow it is often useful to formulate the flow equation

in terms of the stream function [Polubarinov-Kochina 1962, Strack 1989, Evans and Raffensperger 1992]. The stream function enables accurate determination of streamlines leading to accurate results [Christian 1980, Fogg and Senger 1985, Frind and Matanga 1985, Senger and Fogg 1990]. Once the stream functions are calculated, simple contouring leads to a family of streamlines that can be superimposed on the equipotential contours to create an accurate flow net. The flow net provides the most intuitive means of visualizing the flow field. Computed streamlines are especially desirable in regional cross-sectional models where extreme vertical exaggeration of scale and anisotropic permeability give velocities that are not perpendicular to equipotential contours [Fogg and Senger 1985].

Analytical solutions for computing both equipotentials and streamlines of flow net were available for long in the literature [Polubarinov-Kochina 1962], but these are limited to relatively simple flow systems. Subsequently, application of stream functions in two-dimensional ground water flow systems has received much attention [Frind and Matanga 1985, Fogg and Senger 1985, Senger and Fogg 1990, Evans and Raffensperger 1992]. There are methods for generation of the streamlines based on numerical groundwater flow modelling algorithms also [Charbeneau and Street 1979, Christian 1980, Fogg and Senger 1985]. However, some of these methods are not applicable when sources or sinks occur within the flow region, and do not handle transient conditions too. The intricate issue of extending the stream function theory to three-dimensional flow systems has been discussed elsewhere [Bear 1972, Zijl 1986, Matanga 1993].

Accurate construction of flow nets can be difficult in heterogeneous, anisotropic porous media due to nonexistence of orthogonality between streamlines and equipotentials, or in regional cross sections where vertical exaggeration of scale is large. Usually, the nonexistence of the orthogonality can be circumvented by transformation of the anisotropic porous medium into an isotropic one [Mishra 1972, Strack 1989]. However, the flow domain transformation can be avoided by constructing flow nets with streamlines and pseudopotential lines [Matanga 1988]. Generation of individual streamlines in heterogeneous and anisotropic porous media with sources or sinks, and for steady state as well as transient conditions is reported [Charbeneau and Street 1979].

Since any solution of the flow field in terms of the stream function guarantees conservation of fluid mass, the stream function has significant numerical advantages in variable density groundwater flow modelling and the formulation of the mass flux-based stream function [Evans and Ruffensperger 1992]. Description of steady state variable density stream functions and their computation through minor modifications of conventional numerical modelling algorithms is available [Senger and Fogg 1990]. Besides, a technique has been proposed which allows the stream function to be used in models which include areal recharge leakage [Haitjema and Kelson 1996].

Finally, analytical expressions for stream functions enabling straight computation of stream lines are not known to exist in the case of multilayered aquifer systems with internal boundary interfaces.

2.7 GEOPHYSICAL ASPECTS OF AQUIFER SIMULATION

The mathematical analogy between electrical flow (Ohm's law) and groundwater flow (Darcy's law) has long been recognised [Hubbert 1940]. Steady-state flow of electricity or groundwater through a homogeneous and isotropic, conductive medium bounded by planes is described mathematically by the three-dimensional Laplace equation [Bhattacharya and Patra 1968, Freeze and Cherry 1979]. Analogous quantities between steady-state electrical flow and groundwater flow are well identified [Freeze and Cherry 1979]. In Ohm's law resistance of the conducting body is an integral evaluated over the whole body, whereas Darcy's law involves spatial derivative of potential. Thus, Darcy's law is compatible with the differential equation, while Ohm's law is well suited for integral equations [Narasimhan 1998].

More than any other geophysical technique, electrical and electromagnetic methods are directly affected by the presence of conductive pore fluids in the subsurface [Nobes 1994]. The utility of these methods in groundwater studies [Walton 1970, Zohdy et al. 1974, Prickett 1975] is in the similarity of current flow and fluid flow depending on the connectivity and geometry of the pores in soils. Also, the pore water quality influences the geophysical response.

A discussion on the factors influencing relations between electrical and hydraulic properties of aquifers and aquifer materials can be found elsewhere [Mazac et al. 1985]. Surface resistivity methods are used by engineers and geo-hydrologists to obtain aquifer information such as yield, hydraulic conductivity, and transmissivity. The layered earth model is a fundamental interpretation aid for direct current resistivity data [Daniels 1978]. However, interpretation procedures for vertical electrical sounding (VES) assuming a horizontally layered medium is only an approximation of reality due to the scale of the heterogeneities in aquifer systems.

Realisation of the direct analogy between ground water flow and the flow of electricity through conductive porous media aids in the interpretation of electrical potential data [Mazac et al. 1985, Osiensky and Donaldson 1995] derived by *mise-a-la-masse* method, which involves the measurement of electrical current flow through the earth materials under investigation [Parasnis 1967]. Techniques for utilising the three dimensional finite difference ground-water flow model MODFLOW [Mc Donald and Harbaugh 1984] to develop approximate solution for point source electrical flow through conductive porous media are reported [Osiensky and Williams 1996, Pujari 1998].

On the other hand, electrical analogue models have been used to analyse transient behaviour of groundwater systems. Electrical resistance being analogous to inverse of hydraulic conductivity and electrical capacitance being analogous to storage coefficient, resistor network models have been used to simulate the transient behaviour of wells [Skibitzke 1963], water column movements in wells subject to periodic loading [Bredehoeft et al. 1966] or to verify analytical solutions for the flow of water in aquifer systems [Papadopoulos 1965]. Flow net based on electric analogue models have been used for complex boundary conditions as well as for anisotropic and heterogeneous aquifers [Freeze and Cherry 1979]. Further, in order to evaluate the effect of distribution of seepage through lake beds electric-analogue models have been employed [Pfannkuch and Winter 1984].

In view of the above, it is pertinent to invoke relevant results in the realm of exploration geophysics to aid formulation of solution techniques for groundwater applications; such procedures for a complex aquifer system are yet to be cited in the literature of groundwater hydrology.

2.8 SUMMING UP

A critical review of the literature relevant to aquifer simulations using numerical as well as analytical techniques has been presented with an emphasis on the groundwater flow modelling aspects pertaining to surface water - groundwater interaction in multilayered and anisotropic aquifer systems. Also, the formulation of stream functions and their utility in aquifer simulations has been discussed. Besides, pertinent aspects related to the analogy between groundwater flow and electrical flow have also been examined with a view to carry out analytical studies making use of some of the advances in the area of exploration geophysics.

The review indicates that there are many investigative results existing in the literature for simple as well as complex aquifer systems. Yet, generalised methodologies/ results are lacking because of the fact that each aquifer system is unique in its set-up and characteristics, which eludes possibility of any universal solution technique. Even so, research investigations on aquifer systems ought to continue to address issues that are yet to be covered or attempted. Conception of new methodologies as well as improvements over the existing ones are also desirable.

The above critical review suggests a possibility of developing analytical (semi-analytical) approaches to meet specific hydrological modelling demands in an interdisciplinary manner by considering various advances made in exploration geophysics. Also, there is a need for numerical modelling studies for intricate hydrological situations yet important ones for e.g., role of distributed clay/ shale (aquitard) present in a stratified medium controlling water logging at the surface and declining heads in the aquifer. In view of the above the following constitute the major objectives of the present thesis:

1. To develop analytical expressions for the computation of hydraulic potentials and stream functions due to recharging by surface water sources in a stratified porous media .
2. To tackle the problem of defining hydraulic potentials analytically in an anisotropic medium due to a point source and a finite-length line source kept on the air-earth interface.

3. To generate computational algorithms based on the analytical results and validate them in several numerical experiments.
4. To carry out numerical modelling studies in an aquifer-aquitard-aquifer system with a continuous and a discontinuous aquitard (like distributed clay lenses) in the medium.

ANALYTICAL SOLUTIONS FOR HYDRAULIC POTENTIAL AND STREAMLINES IN MULTILAYERED AQUIFER SYSTEMS

3.1 GENERAL

Analytical methods are handy compared to numerical techniques when a steady state solution of hydraulic potential or stream function is sought in an aquifer system. Though numerical groundwater models are effective in simulating flow in aquifer systems, a good computing facility is necessary for model implementation. Therefore, the objective here is to develop easy-to-compute analytical solutions for steady-state hydraulic potential and streamlines in a stratified aquifer system with a surface water source of recharge at the centre.

With appropriate analytical solutions (functions) it is possible to model flow in stratified aquifer systems. In such aquifer systems, it is assumed that the hydraulic conductivity changes abruptly across the boundaries. However, at the boundaries, the conditions of continuity of flow and continuity of hydraulic potential must be satisfied. Laplace equation, the governing equation for the steady-state groundwater potential, can be solved along with appropriate boundary conditions to obtain the required solution in a stratified aquifer system. Since Laplace equation, the governing differential equation for steady groundwater flow [Fitts 1991], is a linear partial differential equation two or more solutions to it may be superimposed and their sum will also be a solution. Therefore, such analytical solutions can be used for simulating aquifer systems with line sources as well as areal sources also with suitable convolution algorithms. The functions can be implemented in a manner that provides continuity of flow across the boundaries.

Since the analogy between electrical flow and groundwater flow is well established [Hubbert 1940, Freeze and Cherry 1979], the methodology presented herein to derive analytical expressions for the hydraulic potential invokes the geoelectric sounding principles [Bhattacharya and Patra 1968, Kocfod 1979, Patra and Nath 1999]. Discussions of direct current electrical resistivity methods and electrical analogue models in groundwater applications under different contexts are available in the literature [Walton 1970, Zohdy et al. 1974, Prickett 1975]. On the other hand, groundwater flow models have even been used in simulating electrical flow through porous media [Osiensky and Williams 1996, Pujari 1998].

There are very few analytical solutions allowing some sort of vertical heterogeneity [Hemker and Maas 1987, Hemker 1984, Hemker 1999a] within an aquifer system. An analytical solution for flow of water in a saturated three layered aquitard-aquifer-aquitard system of finite length is cited in the literature [Yates 1988]. The solution obtained was for one-dimensional flow in the aquifer. Besides, the solution was limited by the condition that ratios of hydraulic conductivity between layers should approach zero. Analytical description of determination of flow to a point sink in a perfectly layered subsurface is also reported [Nieuwenhuizen et al. 1995]. However, there are limiting factors like, the inability to locate point sinks at the earth-surface (air-earth interface) or at the interface between layers, and the assumption of an isotropic subsurface.

However, in the present study analytical expressions for steady state hydraulic potential and streamlines due to a point-source have been derived for a multilayered aquifer system without any restrictions on the number of layers and layer conductivities. Here, the hydraulic conductivity can vary from layer to layer in any fashion and the flow is cylindrically symmetrical around the point-source of recharge. Further, the source is located at the earth-surface, signifying a surface water recharge source. Making use of the analytical expressions developed in this chapter, several computational algorithms have been devised to compute the required hydraulic heads/ potentials as well as streamlines in multilayered aquifer systems. Also, the solution procedure has been extended to the cases of line source (river, canal etc.) and areal source (lake, reservoir etc.) by devising appropriate convolution algorithms.

3.2 BASIC THEORETICAL FRAMEWORK

In geoelectrical prospecting, the depths and electrical resistivities of horizontal layers of earth are determined by using the electrical potential and electrical field at any point on the surface of the earth. As such, analytical solution for electrical potentials on the surface of a stratified earth medium exists in the geophysical literature [Bhattacharya and Patra 1968, Koefoed 1979, Patra and Nath 1999]. However, for geohydrological applications the hydraulic potential and flow need to be determined in the various layers below the earth-surface, and for which analytical solutions are non-existent. Therefore, the analysis followed is aimed at deriving a set of expressions for hydraulic potential and streamlines in a multilayered aquifer system.

Consider a horizontally stratified aquifer system with n layers in a cylindrical coordinate frame, (R, Z) with its origin at the point source, A [Fig. 3.1]. Let K_1, K_2, \dots, K_n be the hydraulic conductivities, and h_1, h_2, \dots, h_n be the depths to the bottom of respective layers [Fig. 3.1] from the surface. It is assumed that the last layer extends to infinite depth (half-space). Then, the Laplace equation to be satisfied at any point in Layer i (for $i = 1, 2, \dots, n$) by the steady state hydraulic potential $\phi_i(r, z)$, notated as ϕ_i for brevity, is:

$$\frac{\partial^2 \phi_i}{\partial r^2} + \frac{1}{r} \frac{\partial \phi_i}{\partial r} + \frac{\partial^2 \phi_i}{\partial z^2} = 0 \quad \left. \begin{array}{l} \text{axis radial} \\ \text{boundary conditions} \end{array} \right\} \quad (3.1)$$

The general solution of eqn. (3.1) can be written as [Bhattacharya and Patra 1968]:

$$\phi_i(r, z) = \frac{q}{2\pi K_1} \left\{ \frac{1}{(r^2 + z^2)^{1/2}} + \int_0^\infty [A_i(\lambda)e^{-\lambda z} + B_i(\lambda)e^{\lambda z}] J_0(\lambda r) d\lambda \right\} \quad (3.2)$$

where q (m^3/s) is the recharge by the point source; $A_i(\lambda)$ and $B_i(\lambda)$ are rational functions in which numerator and denominator are polynomials in $e^{-2\lambda}$; and $J_0(\lambda r)$ is the Bessel function of zeroth order.

The variable of integration λ [L^{-1}] ranges from 0 to ∞ .

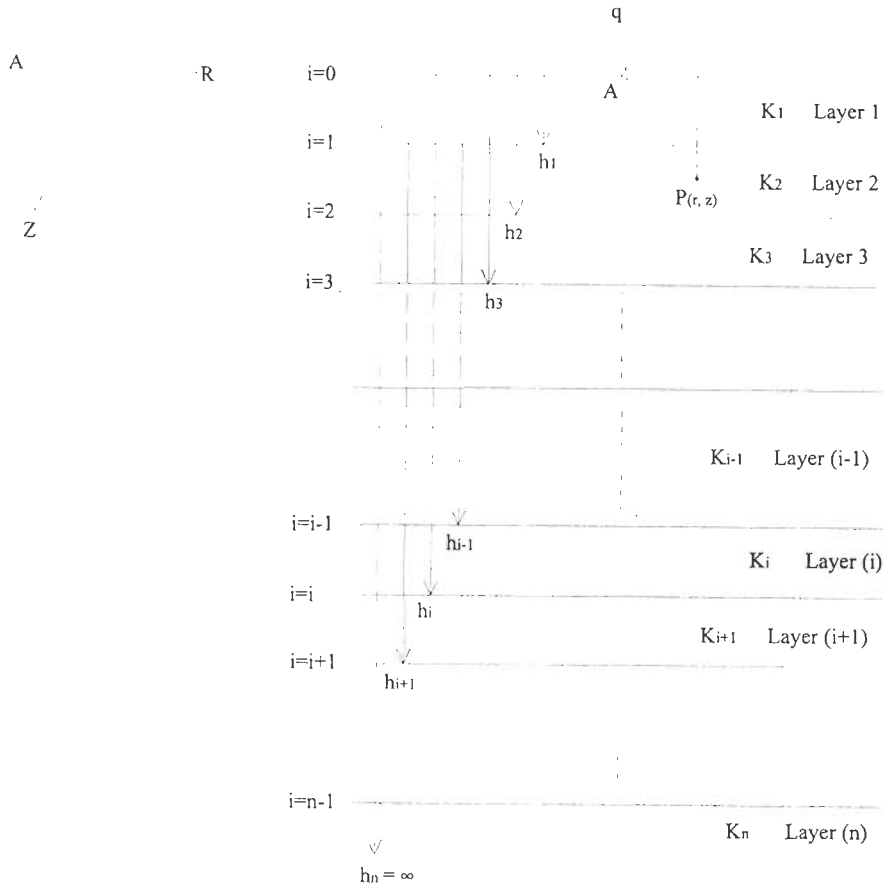


Fig. 3.1 Schematic diagram of the multilayered aquifer system with reference to the cylindrical coordinate system. A point-source is located at A; hydraulic potential (ϕ_i) and stream function (ψ_i) are computed at any arbitrary point P(r,z) in the aquifer system.

Invoking the Integral of Lipschitz from the theory of Bessel functions [Watson 1980], viz.,

$$\int_0^{\infty} e^{-\lambda z} J_0(\lambda r) d\lambda = \frac{1}{(r^2 + z^2)^{1/2}} \quad (3.3)$$

eqn. (3.2) may be re-written as:

$$\phi_i(r, z) = \frac{q}{2\pi K_1} \left\{ \int_0^{\infty} [e^{-\lambda z} + A_i(\lambda)e^{-\lambda z} + B_i(\lambda)e^{\lambda z}] J_0(\lambda r) d\lambda \right\} \quad (3.4)$$

Now, the unknown functions $A_i(\lambda)$ and $B_i(\lambda)$ in eqn. (3.4) need to be evaluated subject to certain boundary conditions [Koefoed 1979] given below:

- (i) At the air-earth interface (earth-surface) the vertical component of flow must be zero; i.e.,

$$K_1 \frac{\partial \phi_1}{\partial z} \Big|_{z=0} = 0 \quad (3.5a)$$

This implies that, in eqn. (3.4) the functions $A_i(\lambda)$ and $B_i(\lambda)$ must be identical so that,

$$A_1(\lambda) = B_1(\lambda) \quad (3.5b)$$

It can be noted, as a corollary, that the surface potential, $\phi_1(r, z=0)$ can be obtained by substitution of eqn. (3.5b) into (3.4) as:

$$\phi_1(r) = \frac{q}{2\pi K_1} \int_0^{\infty} P_1(\lambda) J_0(\lambda r) d\lambda \quad (3.6)$$

where,

$$P_1(\lambda) = 1 + 2A_1(\lambda) \quad (3.7)$$

$P_1(\lambda)$ is the kernel function determined by thicknesses and hydraulic conductivity of the layers. A solution for the surface potential due to eqn. (3.6) is being used [Koefoed 1979] in geophysical applications.

- (ii) At each of the boundary planes in the subsurface, the hydraulic potential as well as flow must

be continuous. So, at any i^{th} interface within the medium,

$$\phi_i = \phi_{i-1} \quad \text{and} \quad K_i \frac{\partial \phi_i}{\partial z} = K_{i-1} \frac{\partial \phi_{i-1}}{\partial z} \quad (3.8a)$$

Applying these conditions to eqn. (3.4), we obtain the following identities:

$$A_i(\lambda) e^{-\lambda h_i} + B_i(\lambda) e^{\lambda h_i} = A_{i-1}(\lambda) e^{-\lambda h_i} + B_{i-1}(\lambda) e^{\lambda h_i} \quad (3.8b)$$

$$K_i [1 + A_i(\lambda) e^{-\lambda h_i} - B_i(\lambda) e^{\lambda h_i}] = K_{i-1} [\{1 + A_{i-1}(\lambda)\} e^{-\lambda h_i} - B_{i-1}(\lambda) e^{\lambda h_i}] \quad (3.8c)$$

(iii) At infinite depth/ distance, the hydraulic potential must approximate to zero, i.e.,

$$\lim_{z \rightarrow \infty} \phi(r, z) = 0 \quad \text{and} \quad \lim_{r \rightarrow \infty} \phi(r, z) = 0 \quad (3.9a)$$

Eqn. (3.9a) necessitates $B_n(\lambda) e^{\lambda z}$ to vanish in eqn. (3.4). Therefore,

$$B_n(\lambda) = 0 \quad (3.9b)$$

3.3 HYDRAULIC POTENTIAL AND STREAM FUNCTION: TWO/ THREE-LAYERED AQUIFER SYSTEMS

As mentioned earlier, analytical solution for surface (electrical) potential for a stratified earth medium is available [Bhattacharya and Patra 1968] in the literature. However, for groundwater analyses the analytical expression of hydraulic potentials within the porous medium needs to be derived as it is non-existent. Hydrogeological investigations indicate that aquifer systems with single, two or three layers are most common. Therefore, the theoretical analysis presented in the current section attempts to develop analytical solutions for hydraulic potential as well as streamlines

in the case of aquifer systems with number of layers restricted to three or less [Fig. 3.2].

An alternate solution technique has been presented to compute the hydraulic potentials and streamlines in the case of a three-layered aquifer system. The methodology makes use of application of the matrix theory and the theory of analytical functions for the computations. Suitable convolution algorithms have also been developed to extend the analytical solutions for the point source to the case of a line-source and an areal-source.

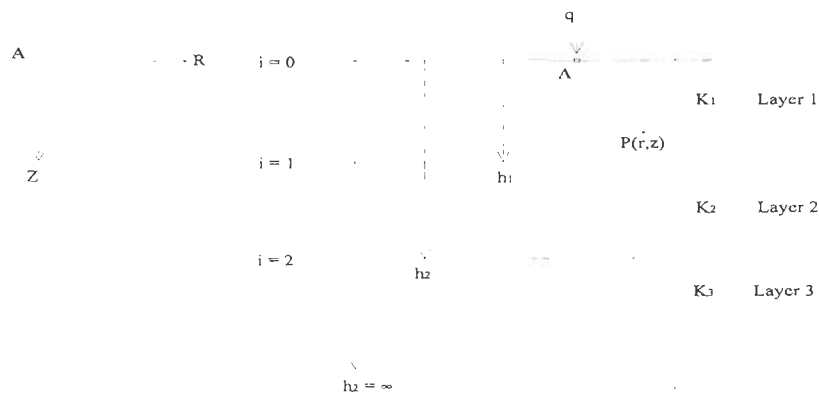


Fig. 3.2 Schematic diagram of the three-layered aquifer system with a point-source located at A, on air-earth interface; $P(r,z)$ is an arbitrary point in the cylindrical coordinate system.

By using the equations (3.5b), (3.8b), (3.8c) and (3.9b), a system of $2n$ equations in $2n$ unknown functions $A_i(\lambda)$ and $B_i(\lambda)$ can be formed. By introducing the following notations,

$$\begin{aligned}
 u_i &= e^{-\lambda h_i} \\
 v_i &= e^{-\lambda h_i} \\
 t_i &= K_{i-1}/K_i
 \end{aligned}
 \tag{3.10}$$

the corresponding system of equations in $A_i(\lambda)$ and $B_i(\lambda)$ can be written as [Koefoed 1979]:

and

$$B_3(\lambda) = 0 \quad (3.16)$$

where $c_1 = (1 - t_1)/(1 + t_1)$ and $c_2 = (1 - t_2)/(1 + t_2)$.

It may be noted that as $A_i(\lambda)$ and $B_i(\lambda)$ are functions in λ , it is necessary to express them in convenient mathematical forms to enable evaluation of integral in eqn. (3.4). Hence, the following procedure has been devised to express the hydraulic potential, $\phi_i(r, z)$ given by eqn.(3.4) in a suitable analytical form for computation. Now, the depths to layer interfaces shall be expressed in terms of multiples of a given depth, h_0 .

Thus, let $h_1 = s_1 h_0$ and $h_2 = s_2 h_0$ where s_1 and s_2 are integer multipliers, and h_0 is set to some fixed value. Also, let us denote $\exp(-2\lambda h_0) = g$ for the sake of brevity. Then, $A_i(\lambda)$ and $B_i(\lambda)$ for $i=1, 2$, and 3 can be rewritten in terms of s_1, s_2 and g . Also, since s_1 and s_2 are integers, $A_i(\lambda)$ and $B_i(\lambda)$ are rational functions of g . Thus, equations (3.12), (3.13), (3.14) and (3.15), respectively can be rewritten as,

$$A_1(\lambda) = \frac{c_1 g^{s_1} + c_2 g^{s_2}}{1 - c_1 g^{s_1} - c_2 g^{s_2} + c_1 c_2 g^{(s_2 - s_1)}} = \sum_{m=0}^{\infty} a_m g^m \quad (3.17)$$

$$A_2(\lambda) = \frac{c_1 + c_1 g^{s_1} + c_2 g^{s_2} - c_1 c_2 g^{(s_2 - s_1)}}{1 - c_1 g^{s_1} - c_2 g^{s_2} + c_1 c_2 g^{(s_2 - s_1)}} = \sum_{m=0}^{\infty} b_m g^m \quad (3.18)$$

$$B_2(\lambda) = \frac{c_2 g^{s_2} + c_1 c_2 g^{s_2}}{1 - c_1 g^{s_1} - c_2 g^{s_2} + c_1 c_2 g^{(s_2 - s_1)}} = \sum_{m=0}^{\infty} d_m g^m \quad (3.19)$$

$$A_3(\lambda) = \frac{\left(c_2 + \frac{2c_1K_2}{K_2+K_3} \right) + \left(\frac{2c_1K_2}{K_2+K_3} - c_1c_2 \right) g^{s_1} + c_2g^{s_2} - c_1c_2g^{(s_2-s_1)}}{1 - c_1g^{s_1} - c_2g^{s_2} + c_1c_2g^{(s_2-s_1)}} = \sum_{m=0}^{\infty} f_m g^m \quad (3.20)$$

where a_m , b_m , d_m , and f_m are the coefficients of the respective polynomial expansions.

Equating coefficients of various orders of g on both sides of the above equations will yield a_m , b_m , d_m , and f_m , when $m \leq s_2$ as the highest order of g on the left hand side is s_2 . However, the higher order coefficients of g (i.e. a_m , b_m , d_m , or f_m when $m > s_2$) on the right hand side of the above equations (eqns. 3.17 - 3.20) must be zero. This leads to the following recurrence formula for obtaining the coefficients a_m , b_m , d_m , or f_m , when $m > s_2$:

$$R_{s_2j} = c_1 R_{s_2-s_1, j} - c_2 R_j + c_1 c_2 R_{s_1, j}, \quad \text{for } j = 1, 2, 3, \dots \quad (3.21)$$

Thus, the unknown functions $A_i(\lambda)$ and $B_i(\lambda)$ in the equation for hydraulic potential were reduced to a set of rational functions in terms of $\exp(-2\lambda h_0)$ as:

$$A_1(\lambda) = B_1(\lambda) = \sum_{m=0}^{\infty} a_m e^{-2\lambda m h_0} \quad (3.22)$$

$$A_2(\lambda) = \sum_{m=0}^{\infty} b_m e^{-2\lambda m h_0} \quad (3.23)$$

$$B_2(\lambda) = \sum_{m=0}^{\infty} d_m e^{-2\lambda m h_0} \quad (3.24)$$

$$A_3(\lambda) = \sum_{m=0}^{\infty} f_m e^{-2\lambda m h_0} \quad (3.25)$$

$$B_3(\lambda) = 0 \quad (3.26)$$

Now, substituting the expressions given by equations eqn. (3.22), (3.23), (3.24), (3.25), (3.26), respectively for $A_i(\lambda)$ and $B_i(\lambda)$ for $i=1, 2$, and 3 in eqn. (3.4), followed by application of the integral formula of Lipschitz (eqn. 3.3) will provide the hydraulic potential function, $\phi_i(r, z)$ for the computation of hydraulic potential at any point in the i^{th} layer of the three layer aquifer system.

Thus, the hydraulic potential in Layer 1, Layer 2, and Layer 3, respectively are given by:

$$\phi_1(r, z) = \frac{q}{2\pi K_1} \left[\frac{1}{\sqrt{r^2 + z^2}} + \sum_{m=0}^{\infty} \frac{a_m}{\sqrt{r^2 + (2mh_0 - z)^2}} + \sum_{m=0}^{\infty} \frac{a_m}{\sqrt{r^2 + (2mh_0 + z)^2}} \right] \quad (3.27)$$

$$\phi_2(r, z) = \frac{q}{2\pi K_1} \left[\frac{1}{\sqrt{r^2 + z^2}} + \sum_{m=0}^{\infty} \frac{d_m}{\sqrt{r^2 + (2mh_0 - z)^2}} + \sum_{m=0}^{\infty} \frac{b_m}{\sqrt{r^2 + (2mh_0 + z)^2}} \right] \quad (3.28)$$

$$\phi_3(r, z) = \frac{q}{2\pi K_1} \left[\frac{1}{\sqrt{r^2 + z^2}} + \sum_{m=0}^{\infty} \frac{f_m}{\sqrt{r^2 + (2mh_0 + z)^2}} \right] \quad (3.29)$$

where h_0 is a chosen fixed value, and a_m , b_m , d_m , and f_m are the coefficients in polynomial expansions which can be determined using the procedure explained above.

3.3.2 STREAM FUNCTION

Generating streamlines in the stratified aquifer system enables visualising the groundwater flow regime. The stream function can be obtained from the hydraulic potential function [Harr 1962] by virtue of the Cauchy-Riemann equations. Let $\psi_i(r, z)$ be the stream function (written as ψ_i) for the i^{th} layer. Then,

$$-K_i \frac{\partial \phi_i}{\partial r} = \frac{\partial \psi_i}{\partial z} \quad (3.30)$$

$$-K_i \frac{\partial \phi_i}{\partial z} = -\frac{\partial \psi_i}{\partial r} \quad (3.31)$$

Integration of either eqn. (3.30) or eqn. (3.31) will yield the stream function for the i^{th} layer as:

$$\psi_i = -\int K_i \frac{\partial \phi_i}{\partial r} dz + C_1 \quad (3.32)$$

or

$$\psi_i = -\int K_i \frac{\partial \phi_i}{\partial z} dr + C_2 \quad (3.33)$$

In eqn. (3.32) and eqn. (3.33), the constants of integration C_1 and C_2 can be taken to be zero by virtue of the boundary conditions given by eqn. (3.9a).

Thus, the stream function for the i^{th} layer may be evaluated using,

$$\psi_i = -K_i \int \frac{\partial \phi_i}{\partial r} dz \quad (3.34)$$

The final expression for stream function in the i^{th} layer is obtained in two steps: (i) evaluate the derivatives $\partial \phi_i / \partial r$ for $i=1,2$, and 3 using eqn. (3.27), eqn. (3.28), and eqn. (3.29) and (ii) substitute those derivatives into equation (3.34), followed by integration. The evaluation of the resulting integral has been performed by using the identity [Dwight 1961] given by eqn. (3.35):

$$\int \frac{dx}{X^{3/2}} = \frac{4ax + 2b}{(4ac - b^2)X^{1/2}}, \quad \text{where } X^{1/2} = (ax^2 + bx + c)^{1/2} \quad (3.35)$$

Thus, we have, the required expressions for the stream functions as:

$$\psi_1(r, z) = \frac{q}{2\pi} \left[\frac{z}{r\sqrt{r^2+z^2}} + \sum_{m=0}^{\infty} \frac{a_m(z-2mh_0)}{r\sqrt{r^2+(2mh_0-z)^2}} + \sum_{m=0}^{\infty} \frac{a_m(z+2mh_0)}{r\sqrt{r^2+(2mh_0+z)^2}} \right] \quad (3.36)$$

$$\psi_2(r, z) = \frac{qK_2}{2\pi K_1} \left[\frac{z}{r\sqrt{r^2+z^2}} + \sum_{m=0}^{\infty} \frac{d_m(z-2mh_0)}{r\sqrt{r^2+(2mh_0-z)^2}} + \sum_{m=0}^{\infty} \frac{b_m(z+2mh_0)}{r\sqrt{r^2+(2mh_0+z)^2}} \right] \quad (3.37)$$

$$\psi_3(r, z) = \frac{qK_3}{2\pi K_1} \left[\frac{z}{r\sqrt{r^2+z^2}} + \sum_{m=0}^{\infty} \frac{f_m(z+2mh_0)}{r\sqrt{r^2+(2mh_0+z)^2}} \right] \quad (3.38)$$

3.3.3 COMPUTATIONAL ALGORITHMS

Using the derived analytical solutions [set of equations (3.27), (3.28), & (3.29) for hydraulic potentials and set of equations (3.36), (3.37), & (3.38) for streamlines] an algorithm, 3LPNT has been devised for computing the steady state hydraulic potentials and streamlines, respectively in a single, two layered or three layered aquifer systems.

3.3.3.1 Model Description

The hydraulic potential and streamlines have been computed in the case of three layered aquifer systems using 3LPNT, at the nodes of a rectangular grid of dimensions 1180 m by 580 m in the RZ-plane [vide Fig. 3.2] in order to illustrate the solution procedure. The vertical plane has been discretised into 59 columns and 29 layers (vertical discretisation) of dimension 20m each. The model parameters of the system are: $h_1=100\text{m}$, $h_2=200\text{m}$ and $h_3=\infty$ by letting $n=3$, $s_1=1$, $s_2=2$, and $h_0=100\text{m}$. A point source of strength, $q=0.01\text{ m}^3/\text{s}$ has been assigned to recharge the aquifer system. Hydraulic conductivities for the layers (K_1 , K_2 and K_3) have been so chosen as to form several types of layered aquifer systems viz., Type-I: $K_1=K_2=K_3$, Type-II: $K_1>K_2>K_3$, Type-III: $K_1<K_2>K_3$ and Type-IV: $K_1>K_2<K_3$.

$\approx 864 \frac{\text{m}^3}{\text{d}}$
OK

3.3.3.2 Convergence Test

It may be observed that the analytical solutions consist of Cauchy convergent sequences. Therefore, the number of terms required for convergence may be chosen based on some closure criterion. The convergence pattern is demonstrated by comparing equipotentials computed by 3LPNT with different number of terms in the sequences [see Fig. 3.3]. The closure criterion has been taken as 10^{-4} m. The difference in computed values with 200 and 300 terms of the sequences was found to be less than the closure criterion for all the cases. Hence, for the present computations only the first 200 terms of the sequences have been included.

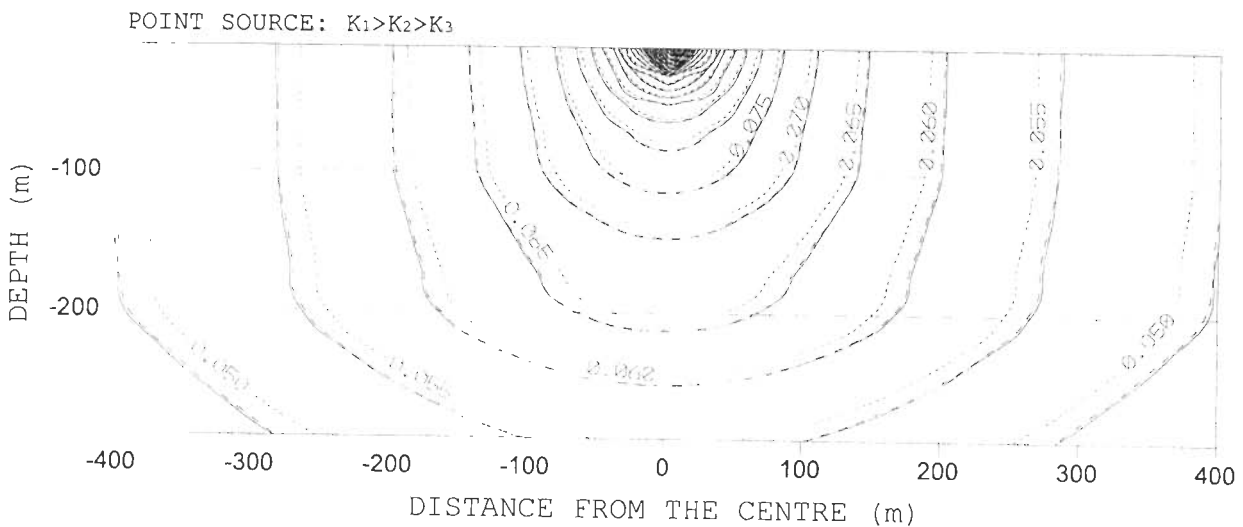


Fig. 3.3 Convergence of the series terms in the expression for hydraulic potential; computed by 3LPNT with 100 terms (dotted lines), 200 terms (dashed lines) and 300 terms (solid lines) of the series expression in the analytical solution. The aquifer layer setup with respect to hydraulic conductivities shown is of the type: $K_1 > K_2 > K_3$ (Table 3.1).

3.3.3.3 Validation Test

For validation purpose, steady state simulation of hydraulic potential has been performed by using a three dimensional finite difference groundwater flow model, MODFLOW [Mc Donald and Harbaugh 1984] with identical grid setup and boundary conditions as that of the semi-analytical solution procedure. Thus, the three dimensional model grid has been discretised into 59 rows, 59

It is desirable to give the governing flow equation and boundary condition and a small fig for this problem.

columns and 29 layers (vertical discretisation) of dimension 20m each. A recharge well (with $q=0.01\text{m}^3/\text{s}$) has been introduced at the central node (L1, R30, C30) of the top layer to act as the source. Constant head boundary condition has been assigned to the boundaries (at sufficiently large distance from the source) of the model grid with near-zero head values. Model parameters have been assigned cell-wise in the model. While MODFLOW uses an iterative procedure to compute hydraulic potential, computation by 3LPNT is direct.

3.3.4 NUMERICAL EXPERIMENTS

Based on the analytical solutions presented for the hydraulic potential and streamlines, the computational algorithms 3LPNT, 3LLIN and 3LARL for the cases of a point source, a finite-length line source and an areal source, respectively have been coded in FORTRAN77 for demonstrating the solution procedure with numerical examples. Comparison of respective results with that corresponding to MODFLOW simulations has also been given. Descriptions of these numerical experiments are given in the following sections:

3.3.4.1 Hydraulic Potential Due to a Point Source

The hydraulic potential and streamlines have been computed in several types of aquifer systems [see Table 3.1] using 3LPNT and MODFLOW. The contour plots of hydraulic potential and

Table 3.1 Types of aquifer systems (based on layer conductivities) in which simulations are performed with 3LPNT.

AQUIFER TYPE	K_1 (m^3/s)	K_2 (m^3/s)	K_3 (m^3/s)
$K_1 = K_2 = K_3$	1e-03	1e-03	1e-03
$K_1 > K_2 > K_3$	1e-03	1e-04	1e-05
$K_1 < K_2 > K_3$	1e-04	1e-03	1e-05
$K_1 > K_2 < K_3$	1e-03	1e-05	1e-04

$K \rightarrow \text{m/d}$

streamlines have been presented for the various cases [Fig. 3.4a, 3.5a, 3.6a and 3.7a]. The plots have been depicted in the vertical section, bound by (-400m, 400m) in the horizontal direction and (0, 300m) in the vertical. The dashed horizontal lines in the plots demarcate the interfaces between layers.

The intervals used for the equipotentials are: 0.002m for Fig. 3.4a, 0.005m for Fig. 3.5a, 0.01m for Fig. 3.6a and 0.005m for Fig. 3.7a. The equipotentials corresponding to MODFLOW simulations (dashed contours) have also been provided for comparison. Contour plots of hydraulic potentials computed by 3LPNT and MODFLOW have been merged in single plots to facilitate visual comparison. To avoid clustering, the streamlines have been plotted selectively. Apparently, the streamlines follow the tangent law of incidence and refraction [Hubbert 1940].

Figure 3.4a represents a homogeneous aquifer as $K_1=K_2=K_3$. Then, the coefficients a_m , b_m , d_m , and f_m are all zeroes and the summation terms of eqns. (3.27), (3.28), and (3.29) vanish. Then, the solution for hydraulic potential reduces to: $\phi = q/[2\pi K_1(r^2 + z^2)^{1/2}]$, which is nothing but the exact solution for steady state potential in a homogeneous aquifer. The depth-wise distribution of hydraulic potential at the centre (through the point source) and at a distance of 200 m away from the source is given in Fig. 3.4b. Similar kind of plots are presented for other types of layered aquifer systems also. A performance comparison of computed hydraulic potentials between the analytical and numerical methods can be made by visual inspection of Fig. 3.5a, Fig. 3.6a and Fig. 3.7a for the equipotentials, and Fig. 3.5b, Fig. 3.6b and Fig. 3.7b for the vertical distribution in the case of various types of aquifer systems. It is noticed that there is a fairly good agreement between the hydraulic potentials computed by 3LPNT and those computed by MODFLOW. In general, the percentage difference between MODFLOW results and 3LPNT results is less than 2%.

3.3.4.2 Hydraulic Potential Due to a Line Source

For practical applications, river sections and canals can be represented as line sources of finite length. Analytically, the integration of a point source along a finite length results in a finite-line source [Parasnis 1967]. A linear convolution of hydraulic potentials due to point sources along

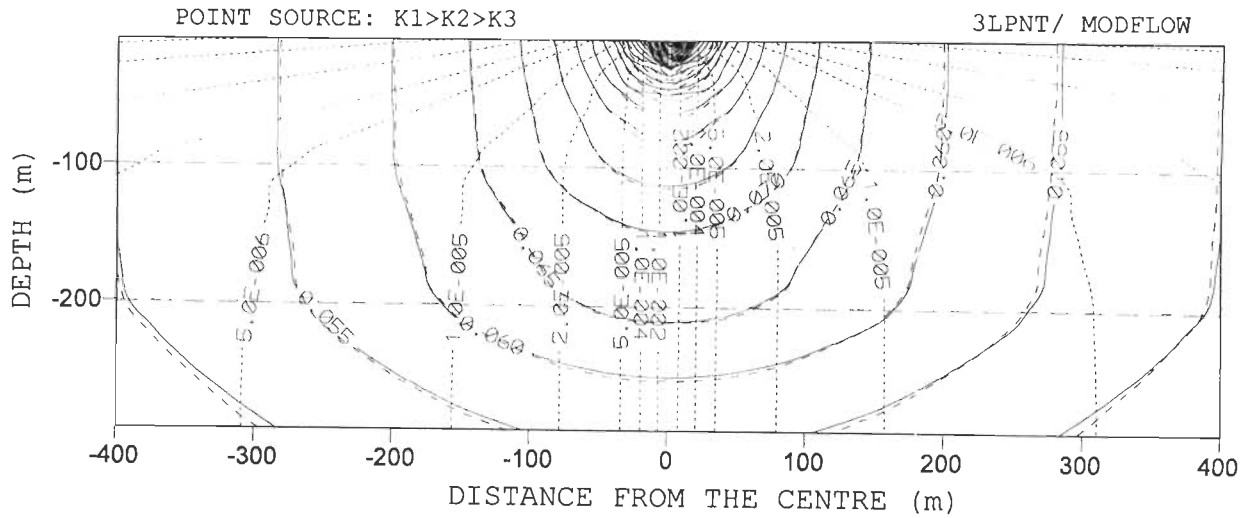


Fig. 3.5a Contour plot of equipotentials in the vertical section of the layered aquifer system ($K_1 > K_2 > K_3$) computed by 3LPNT (solid contours) and MODFLOW (dashed contours). Dotted contours are the streamlines computed by 3LPNT.

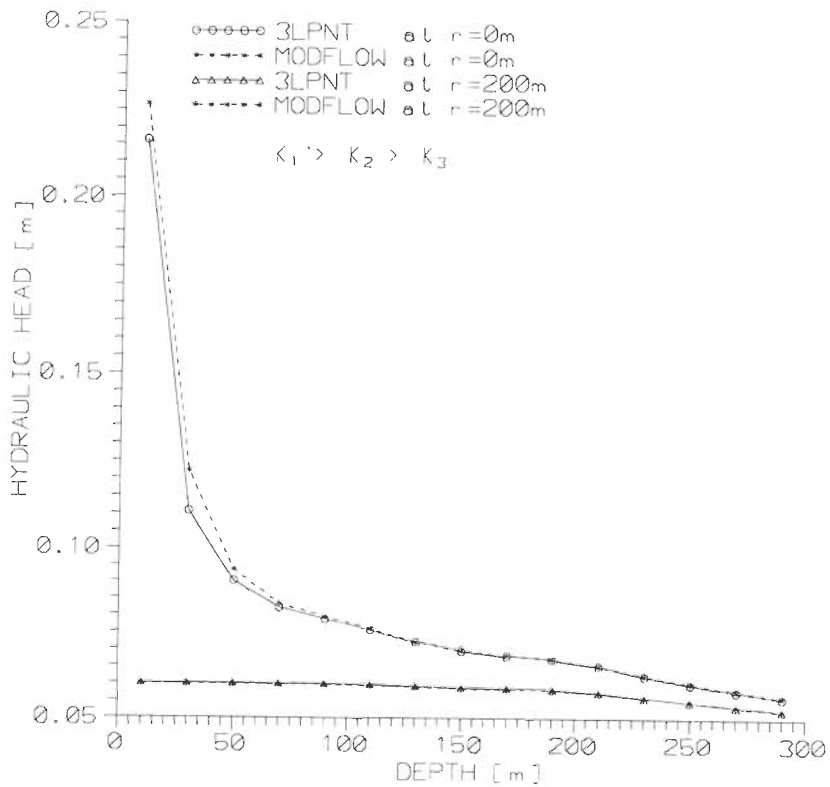


Fig. 3.5b Vertical distribution of hydraulic potentials obtained from 3LPNT (solid line) and MODFLOW (dashed line) at the centre and at a distance 200m from the source for the case where $K_1 > K_2 > K_3$.

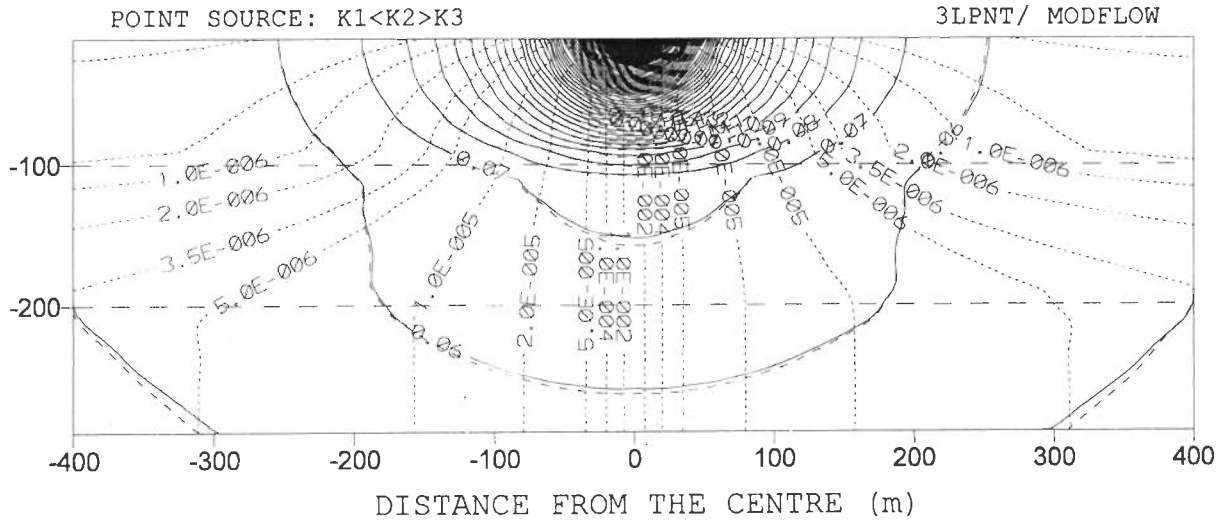


Fig. 3.6a Contour plot of equipotentials in the vertical section of the aquifer system with ($K_1 < K_2 > K_3$) computed by 3LPNT (solid contours) and MODFLOW (dashed contours). Dotted contours are the streamlines computed by 3LPNT.

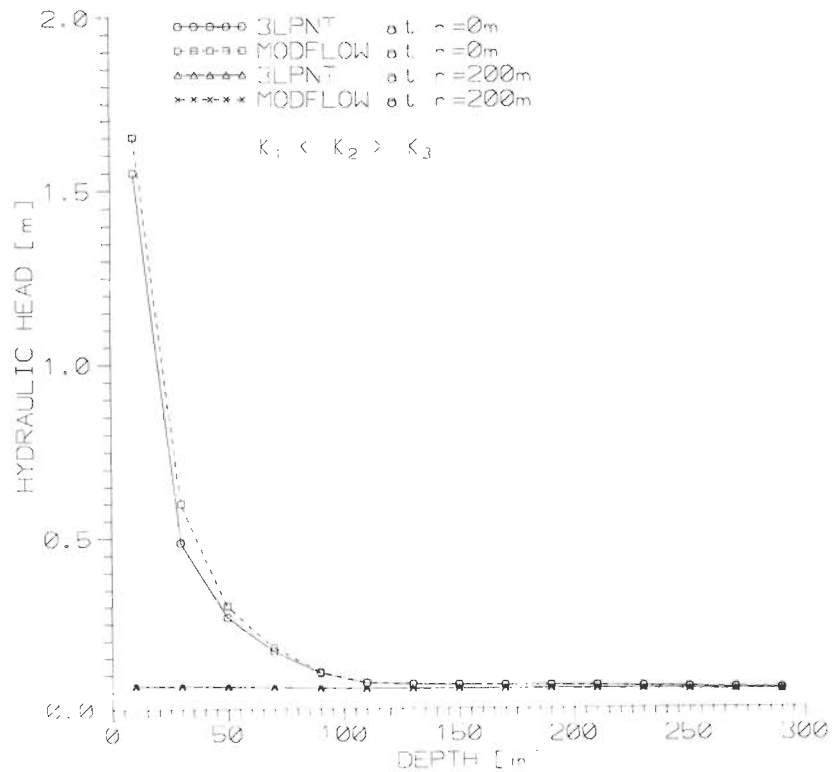


Fig. 3.6b Vertical distribution of hydraulic potentials obtained from 3LPNT (solid line) and MODFLOW (dashed line) at the centre and at a distance 200m from the source for the case where $K_1 < K_2 > K_3$.

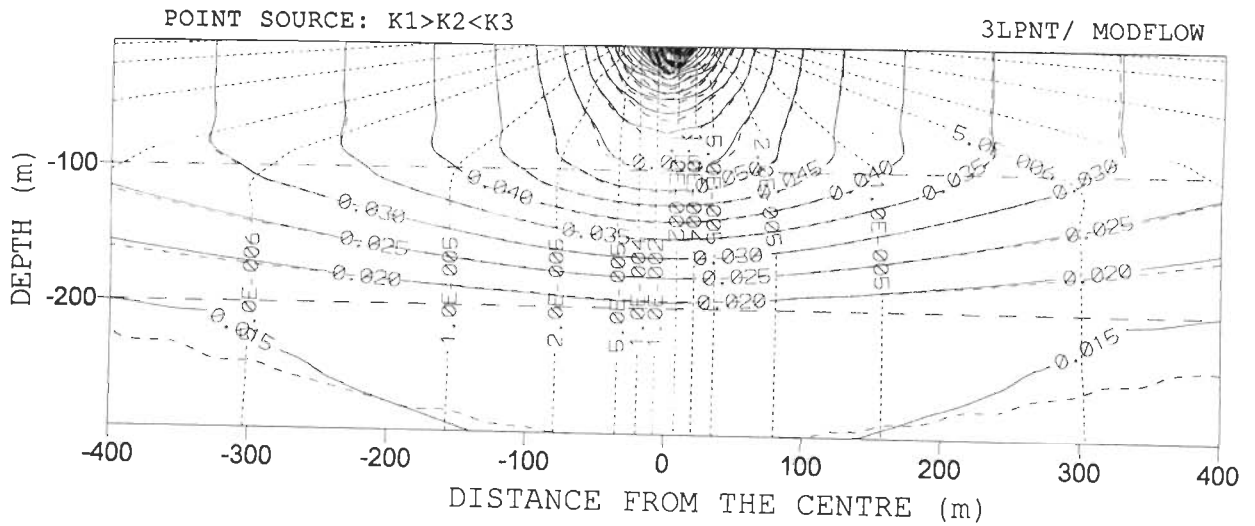


Fig. 3.7a Contour plot of equipotentials in the vertical section of the layered aquifer system ($K_1 > K_2 < K_3$) computed by 3LPNT (solid contours) and MODFLOW (dashed contours). Dotted contours are the streamlines computed by 3LPNT.

Why hydraulic head is slightly lower in small 2m cell

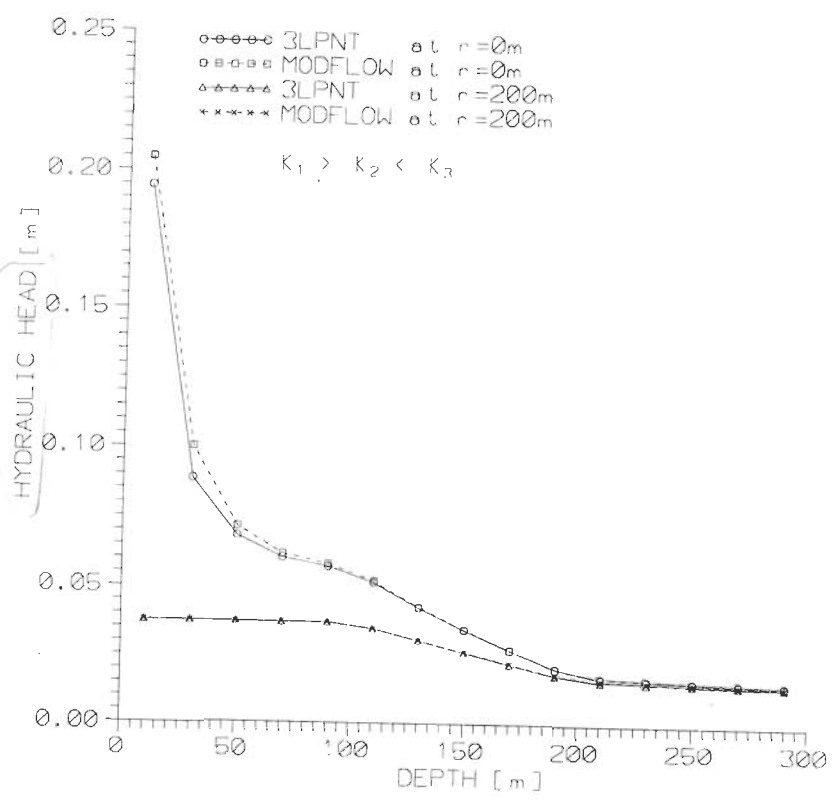


Fig. 3.7b Vertical distribution of hydraulic potentials obtained from 3LPNT (solid line) and MODFLOW (dashed line) at the centre and at a distance 200m from the source for the case where $K_1 > K_2 < K_3$.

a given length can therefore be considered as the hydraulic potentials due to a finite-line source of certain strength. As such, the algorithm for point source, 3LPNT has been modified by incorporating appropriate linear convolution techniques. The evolved algorithm, 3LLIN simulates the hydraulic potential in the porous medium due to a line source of finite length kept on the earth surface.

Table 3.2 Types of aquifer systems (based on layer conductivities) in which simulations are performed with 3LLIN.

AQUIFER TYPE	K_1 (m ² /s)	K_2 (m ² /s)	K_3 (m ² /s)	Source Length
$K_1 > K_2 > K_3$	1e-03	1e-04	1e-05	200 m
$K_1 > K_2 < K_3$	1e-03	1e-05	1e-04	200 m
$K_1 < K_2 > K_3$	1e-04	1e-03	1e-05	200 m

This is a fluid mechanics consideration of line source strength. In ge. wells hydraulics, how the intake determined is more important.

A line source of finite length, $2b=200\text{m}$ (discretised in 20 nodes) and strength, $q=0.1\text{m}^2/\text{s}$ is used to simulate the hydraulic potentials in three layered aquifer systems using the simulation algorithm, 3LLIN. The hydraulic conductivities of the various layers in different cases have been assigned as indicated in Table 3.2. The hydraulic potentials in the vertical section of the porous medium along the strike of finite-line source for the various cases are depicted as equipotential contour plots [Fig.3.8, Fig.3.9 and Fig.3.10]. Since such plots across the strike of the finite-line source are quite similar to that of the point source, those have been omitted here.

3.3.4.3 Hydraulic Potential Due to an Areal Source

Following a methodology similar to that for the line source, integration of a point source over a finite area results in an areal source. Lakes, ponds, recharge tanks etc. may be viewed as areal sources of recharge. The recharge intensity (indicated by the strength of the source) may be either uniform over the spread area of the source or varying from point to point. The algorithm for point source, 3LPNT can be modified by the introduction of a two-dimensional convolution technique to compute the hydraulic potentials due to such areal sources. The resulting algorithm 3LARL

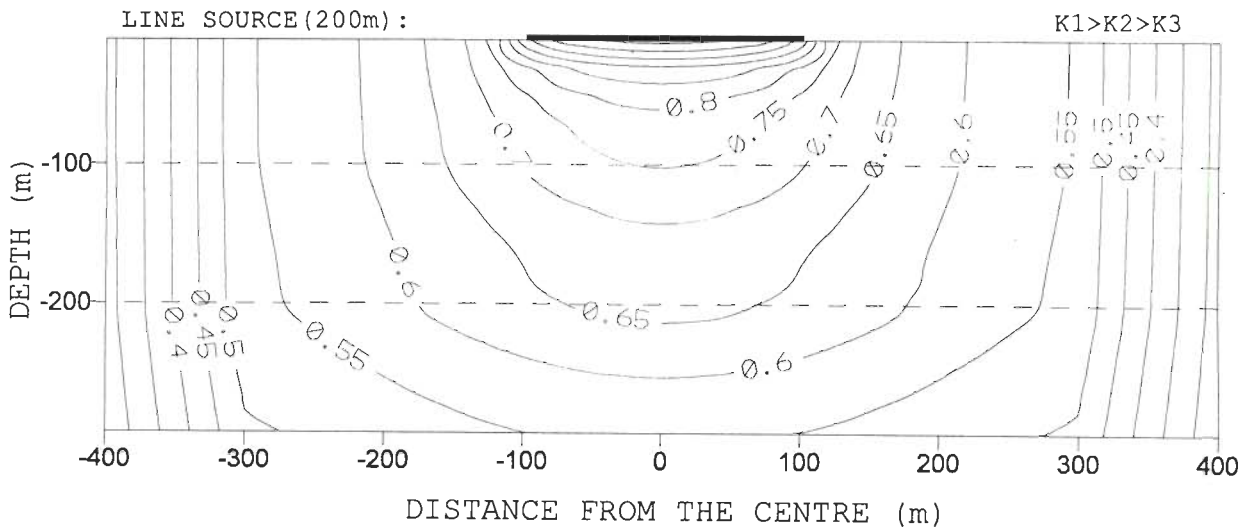


Fig. 3.8 Contour plot of equipotential in the vertical section of a layered aquifer system ($K_1 > K_2 > K_3$) due to a finite-length line source along its strike (computed by 3LLIN); a solid line section on top shows the position of the line source. Dashed horizontal lines represent the layer interfaces.

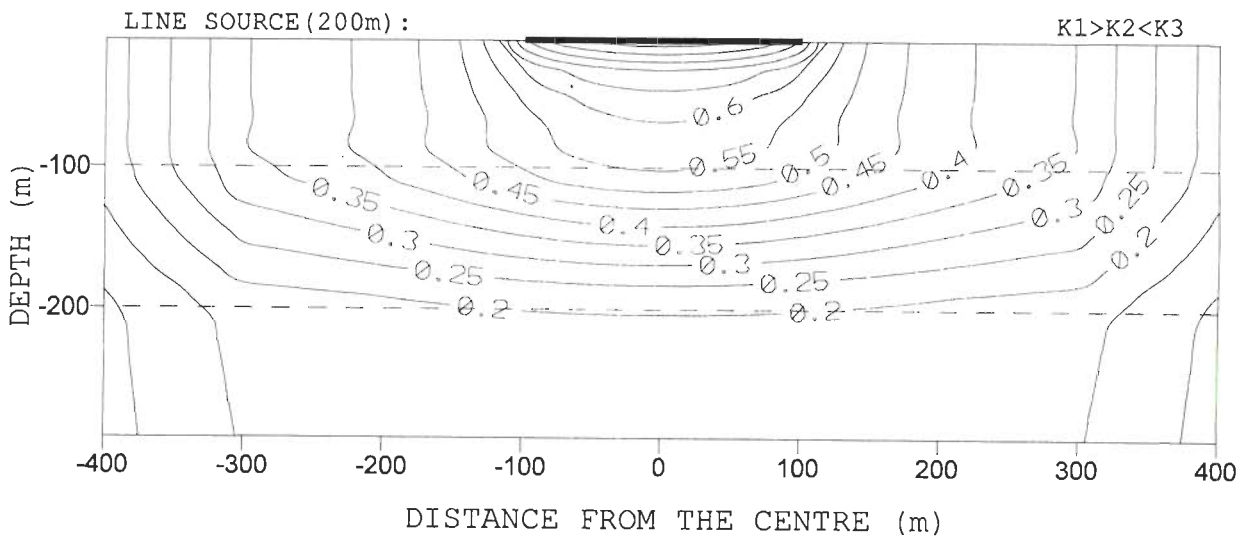


Fig. 3.9 Contour plot of equipotential in the vertical section of a layered aquifer system ($K_1 > K_2 < K_3$) due to a finite-length line source along its strike (computed by 3LLIN); a solid line section on top shows the position of the line source. Dashed horizontal lines represent the layer interfaces.

is it for unit width

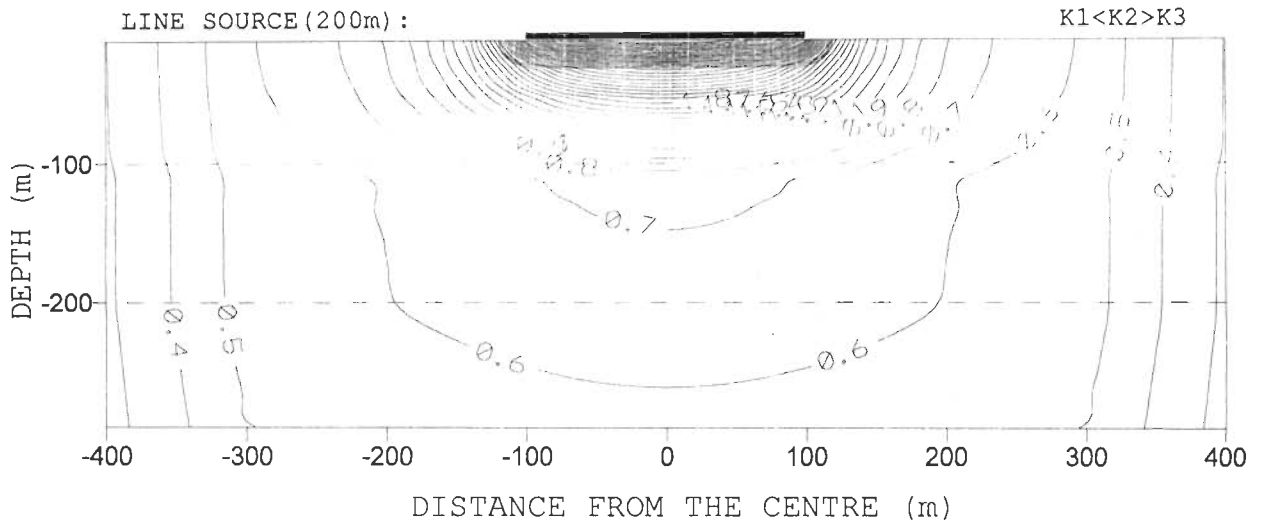


Fig. 3.10 Equipotential contours in the vertical section of a layered aquifer system ($K_1 < K_2 > K_3$) due to a finite-length line source along its strike (computed by 3LLIN); a solid line section on top shows the position of the line source. Dashed horizontal lines represent the layer interfaces.

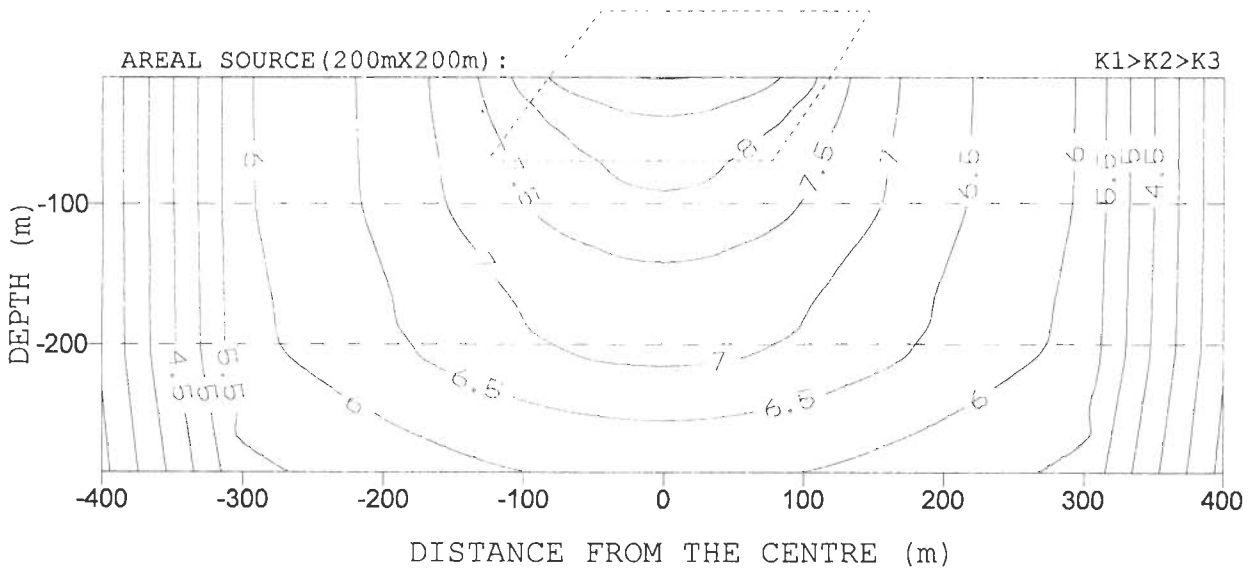


Fig. 3.11 Contour plot of equipotential in the vertical section of a layered aquifer system ($K_1 > K_2 > K_3$) due to an areal source (computed by 3ARL); a dashed rectangle on top of the aquifer system shows the position of the areal source. Dashed horizontal lines represent the layer interfaces.

simulates the hydraulic potentials in the porous medium due to an areal source of given strength.

Table 3.3 Types of aquifer systems (based on layer conductivities) in which simulations are performed with 3LARL.

AQUIFER TYPE	K_1 (m/s)	K_2 (m/s)	K_3 (m/s)	Source Area (m ²)
$K_1 > K_2 > K_3$	1e-03	1e-04	1e-05	40000
$K_1 > K_2 < K_3$	1e-03	1e-05	1e-04	40000
$K_1 < K_2 > K_3$	1e-04	1e-03	1e-05	40000

The hydraulic potentials due to an areal source (discretised in 20x20 nodes) of strength, $q=1.0\text{m/s}$ placed at the air-earth interface of layered aquifer systems have been computed using 3LARL. The type of aquifer systems and hydraulic conductivities of the layers are given in Table 3.3. Plots of equi-potential lines in the vertical section are shown in Fig. 3.11, Fig. 3.12 and Fig. 3.13 for different cases.

3.4 HYDRAULIC POTENTIAL AND STREAM FUNCTION: MULTILAYERED AQUIFER SYSTEM

It is appropriate to generalise the analytical solutions developed for the three-layered aquifer system in the preceding section for the case of a multilayered aquifer system with large number of layers. Though the methodology adopted to formulate the analytical solutions for the three-layered aquifer system has been tried for aquifer systems having more layers, it is found to be unwieldy as a result of bulky expressions for $A_i(\lambda)$ and $B_i(\lambda)$. Therefore, a different methodology has been framed (based on the theoretical aspects presented in section 3.2) to develop the required analytical solutions for a multilayered aquifer system with n layers. The analytical formulations and solution procedures have been described in subsequent sections.

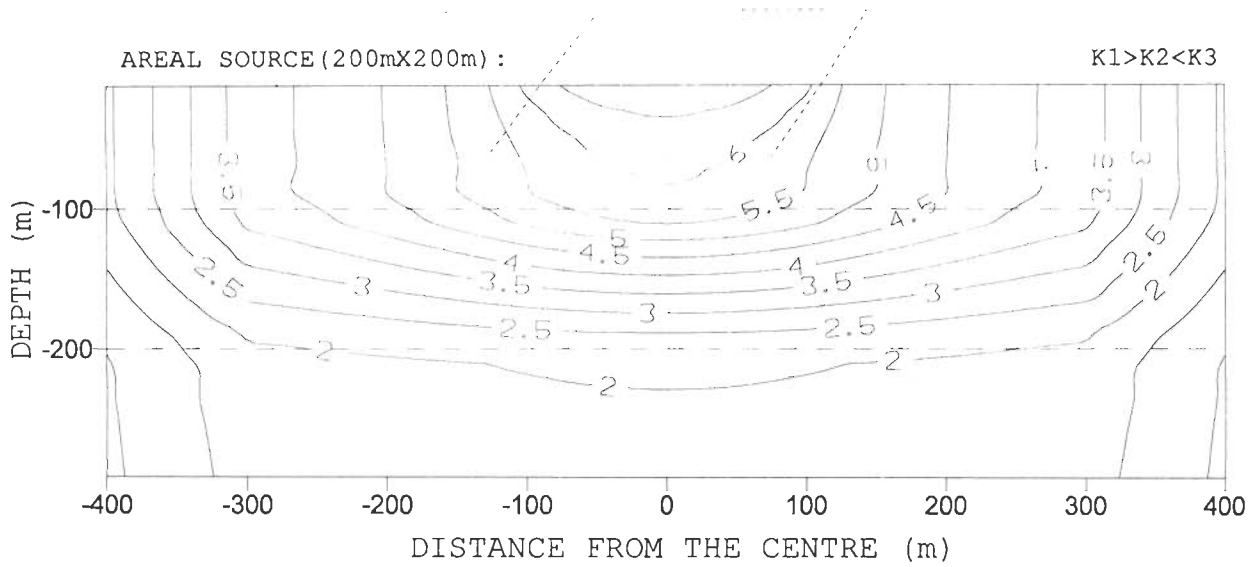


Fig. 3.12 Contour plot of equipotential in the vertical section of a layered aquifer system ($K_1 > K_2 < K_3$) due to an areal source (computed by 3ARL); a dashed rectangle on top of the aquifer system shows the position of the areal source. Dashed horizontal lines represent the layer interfaces.

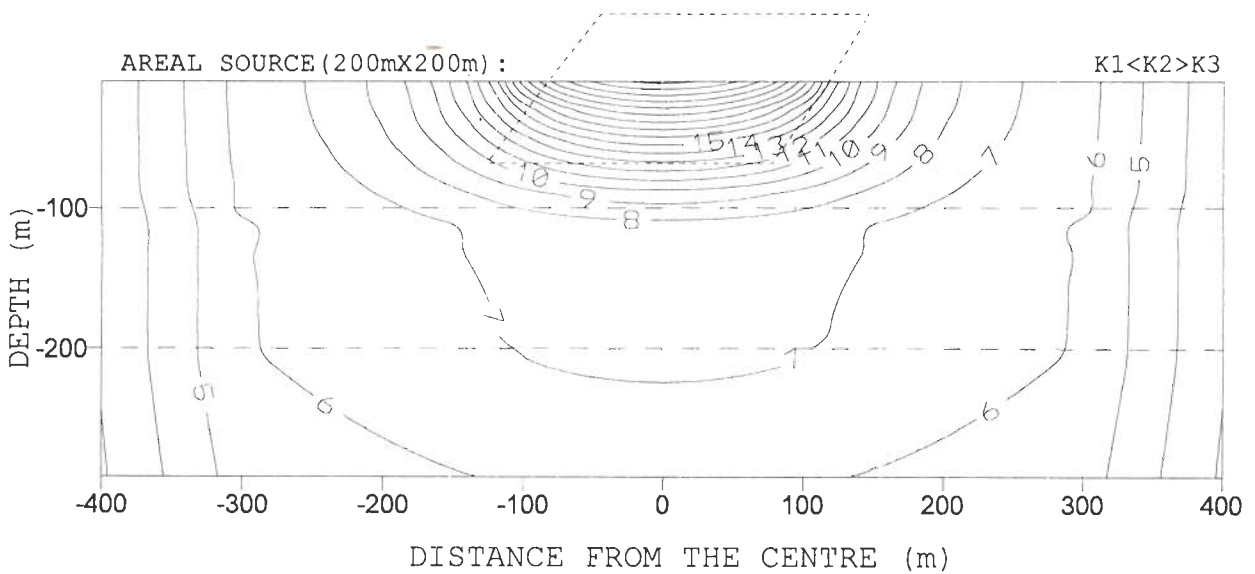


Fig. 3.13 Contour plot of equipotential in the vertical section of a layered aquifer system ($K_1 < K_2 > K_3$) due to an areal source (computed by 3ARL); a dashed rectangle on top of the aquifer system shows the position of the areal source. Dashed horizontal lines represent the layer interfaces.

3.4.1 RECURRENCE RELATIONS FOR $A_i(\lambda)$ AND $B_i(\lambda)$

As indicated earlier, in order to compute the hydraulic potentials at various points below the surface of the layered medium, the first requirement is to evaluate the rational functions $A_i(\lambda)$ and $B_i(\lambda)$ in eqn. (3.4) for various layers. Therefore, expressions have been developed by using eqn. (3.8b) and eqn. (3.8c) to evaluate $A_i(\lambda)$ and $B_i(\lambda)$ in a recursive manner. The procedure followed to derive the recurrence relations for $A_i(\lambda)$ and $B_i(\lambda)$ with $A_{i+1}(\lambda)$ and $B_{i+1}(\lambda)$, respectively is detailed below:

By letting,

$$\begin{aligned} u_i &= e^{-\lambda h_i} \\ v_i &= e^{+\lambda h_i} \\ t_i &= K_{i+1}/K_i \end{aligned} \quad (3.39)$$

equations (3.8b) and (3.8c) can be rewritten as:

$$u_i A_{i+1} = u_i A_i + v_i B_i - v_i B_{i+1} \quad (3.40)$$

$$t_i v_i B_{i+1} = t_i u_i A_{i+1} - u_i A_i + v_i B_i + t_i u_i - u_i \quad (3.41)$$

Substitution of eqn. (3.41) into eqn. (3.40) after multiplication by c_i yields:

$$A_{i+1} = \frac{1+t_i}{2t_i} A_i - \frac{(1-t_i)}{2t_i} v_i^2 B_i + \frac{(1-t_i)}{2t_i} \quad (3.42)$$

Similarly, substitution of eqn. (3.40) into eqn. (3.41) and re-arranging, we get

$$B_{i+1} = \frac{1+t_i}{2t_i} B_i - \frac{(1-t_i)}{2t_i} u_i^2 A_i - \frac{(1-t_i)}{2t_i} u^2 \quad (3.43)$$

Equations (3.42) and (3.43) are expressed in matrix form, after reverting back to the original

notations in eqn. (3.39), as follows:

$$\begin{bmatrix} A_{i+1} \\ B_{i+1} \end{bmatrix} = \begin{bmatrix} a_i & b_i e^{2\lambda h_i} \\ b_i e^{-2\lambda h_i} & a_i \end{bmatrix} \cdot \begin{bmatrix} A_i \\ B_i \end{bmatrix} + \begin{bmatrix} -b_i \\ b_i e^{-2\lambda h_i} \end{bmatrix} \quad (3.44)$$

where,

$$a_i = \frac{K_{i+1} + K_i}{2K_{i+1}} \quad (3.45)$$

$$b_i = \frac{K_{i+1} - K_i}{2K_{i+1}}$$

Eqn. (3.44), which is the required recurrence relation, can be used to evaluate $A_i(\lambda)$ and $B_i(\lambda)$ progressively for $i=1, 2, \dots, n$ provided $A_1(\lambda)$ and $B_1(\lambda)$ for the top layer are already known. In order to obtain $A_i(\lambda)$ or $B_i(\lambda)$, the Pekeris recurrence relation [Koefoed 1979] given by eqn. (3.46) can be employed:

$$P_i(\lambda) = \frac{P_{i+1}(\lambda) + (K_{i+1}/K_i) \tanh(\lambda d_i)}{(K_{i+1}/K_i) + P_{i+1}(\lambda) \tanh(\lambda d_i)} \quad (3.46)$$

where $P_i(\lambda)$ is defined as,

$$P_i(\lambda) = \frac{1 + A_i(\lambda) + B_i(\lambda) e^{2\lambda h_{i+1}}}{1 + A_i(\lambda) - B_i(\lambda) e^{2\lambda h_{i+1}}} \quad (3.47)$$

Applying the boundary condition for the n^{th} layer (eqn. 3.9b) in eqn. (3.47) we get,

$$P_n(\lambda) = 1 \quad (3.48)$$

Also, for the top layer $P_1(\lambda)$ and $A_1(\lambda)$ are related by virtue of eqn. (3.7), which can also be

deduced from eqn. (3.47) by application of boundary conditions for the top layer (eqn. 3.5b). Therefore, eqn. (3.46) in conjunction with eqn. (3.48) can be used to evaluate $P_1(\lambda)$ and, thereby, $A_1(\lambda)$ or $B_1(\lambda)$ in a recursive fashion.

3.4.2 HYDRAULIC POTENTIAL IN MULTILAYERED AQUIFER SYSTEMS

Since $A_i(\lambda)$ and $B_i(\lambda)$ are rational functions in which the numerator and the denominator are polynomials in $e^{-2\lambda}$, these functions can be expressed as approximate exponential series [Hamming 1962] with a finite number of terms, m as

$$A_i(\lambda) = \sum_{j=1}^m f_j e^{-\epsilon_j \lambda} \quad (3.49)$$

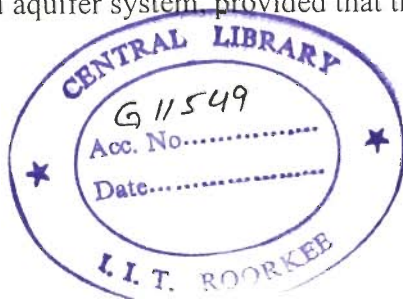
$$B_i(\lambda) = \sum_{j=1}^m g_j e^{-\epsilon_j \lambda} \quad (3.50)$$

where f_j and g_j are coefficients in the respective expansions and ϵ_j determines the position of approximating functions along the abscissa.

Now, substitution of $A_i(\lambda)$ and $B_i(\lambda)$ by equations (3.49) and (3.50) in eqn. (3.4) followed by application of the Integral of Lipschitz (eqn. 3.3) will facilitate solution of the integral equation for hydraulic potential. Thus, we get the expression for hydraulic potential in any layer, i as:

$$\phi_i(r, z) = \frac{q}{2\pi K_1} \left[\frac{1}{(r^2 + z^2)^{1/2}} + \sum_{j=1}^m \frac{f_j}{[r^2 + (z + \epsilon_j)^2]^{1/2}} + \sum_{j=1}^m \frac{g_j}{[r^2 + (z - \epsilon_j)^2]^{1/2}} \right] \quad (3.51)$$

Eqn. (3.51) may be used to compute the hydraulic potentials in the respective layers of the multilayered aquifer system, provided that the coefficients f_j and g_j are ascertained.



When the hydraulic conductivities of various layers in a multilayered aquifer system are the same, then it becomes a homogeneous aquifer. As a result, the coefficients f_j and g_j in eqn. (3.51) become zeroes. Then, the expression for hydraulic potential reduces to: $\phi_1 = q / \{2\pi K_1 (r^2 + z^2)^{1/2}\}$, which is nothing but the exact solution for steady state potential in a homogeneous aquifer.

3.4.2.1 Determination of Coefficients f_j and g_j

In the eqn. (3.51), the coefficients f_j and g_j need to be evaluated. The following procedure has been framed to determine the coefficients f_j and g_j :

If the rational functions $A_i(\lambda)$ and $B_i(\lambda)$ are known at discrete values λ_t ($t = 1, 2, \dots, s$ for $s > m$ or $s < m$), then eqns. (3.49) and (3.50) can be rewritten as:

$$A_i(\lambda_t) = \sum_{j=1}^m f_j e^{-\epsilon_j \lambda_t} \quad (3.52)$$

and

$$B_i(\lambda_t) = \sum_{j=1}^m g_j e^{-\epsilon_j \lambda_t} \quad (3.53)$$

Now, equations (3.52) and (3.53) form s equations each with $A_i(\lambda_t)$ and $B_i(\lambda_t)$ which can be used to evaluate $2m$ unknowns in each set, (f_j, ϵ_j) and (g_j, ϵ_j) . But, eqns. (3.52) and (3.53) are obviously nonlinear system of equations in ϵ_j , and solution is rather difficult. However, m values of ϵ_j can be assigned as per some criterion to convert those equations to over-determined linear system ($s > m$) of equations in f_j and g_j and to get a solution.

Therefore, let us consider eqn. (3.52) where (f_j, ϵ_j) are to be evaluated. Replacing the functions $A_i(\lambda)$ and f_j by vector quantities (column matrices) and the exponential term by an $(s \times m)$ matrix yields,

$$[A_i] = [A_i(\lambda_1), A_i(\lambda_2), \dots, A_i(\lambda_s)]^T \quad (3.54)$$

$$[E] = \left[e^{-\epsilon_j \lambda_r} \right] \quad \text{for } r = 1, s \text{ \& } j = 1, m; \quad s > m \quad (3.55)$$

$$[F] = \left[f_1, f_2, \dots, f_m \right]^T \quad (3.56)$$

Therefore, eqn. (3.52) can be rewritten as a matrix equation

$$\begin{matrix} [A_i] \\ (s \times 1) \end{matrix} = \begin{matrix} [E] \\ (s \times m) \end{matrix} \cdot \begin{matrix} [F] \\ (m \times 1) \end{matrix} \quad (3.57)$$

The least-square solution [Morrison 1969] of eqn. (3.57) is given by

$$[F] = [E_{ls}]^{-1} \cdot [A_i] \quad (3.58)$$

where $[E_{ls}]^{-1}$ is the least-square inverse of matrix $[E]$. It is established that

$$[E_{ls}]^{-1} = [E^T \cdot E]^{-1} [E^T] \quad (3.59)$$

Therefore, combining eqns. (3.58) and (3.59) we get,

$$[F] = [E^T \cdot E]^{-1} [E^T] [A_i] \quad (3.60)$$

Now, eqn. (3.60), consisting of a set of linear equations, can be solved by appropriate methods. An arithmetic progression has been chosen to assign values of ϵ_j in the solution procedure. The ϵ_j values are thus assigned by the expression

$$\epsilon_j = j \epsilon_0 \quad (3.61)$$

where ϵ_0 is a certain base value which is approximately equal to the total thickness of the first $(n-1)$ layers. The best set of coefficient for f_j can then be evaluated for a given set of corresponding ϵ_j values in order that the equations are satisfied within an accepted range of error.

3.4.3 STREAM FUNCTION IN MULTILAYERED AQUIFER SYSTEMS

The stream function, $\psi_i(r, z)$ for the i^{th} layer can be obtained from the hydraulic potential function [Harr 1962] by application of the Cauchy-Riemann equations given by eqn. (3.30) and eqn. (3.31) as:

$$\psi_i(r, z) = -K_i \int \frac{\partial \phi_i(r, z)}{\partial r} dz \quad (3.62)$$

Now, the expression for the stream function in any i^{th} -layer of the multilayered aquifer system can be obtained by following a procedure described in section 3.3.2 of this chapter, in two steps: the first being the evaluation of the derivative $\partial \phi_i / \partial r$ with eqn. (3.51) and then substitution of the derivative into eqn. (3.62), followed by integration. Thus, we obtain:

$$\psi_i(r, z) = \frac{qK_i}{2\pi K_1} \left[\frac{z}{r\sqrt{r^2+z^2}} + \sum_{j=1}^m \frac{(z+\epsilon_j)f_j}{r\sqrt{r^2+(z+\epsilon_j)^2}} + \sum_{j=1}^m \frac{(z-\epsilon_j)g_j}{r\sqrt{r^2+(z-\epsilon_j)^2}} \right] \quad (3.63)$$

Equation (3.63) is the required expression for the stream function that can be used to obtain streamlines in a multilayered aquifer system.

3.4.4 COMPUTATIONAL ALGORITHM FOR MULTILAYERED AQUIFER SYSTEM

A computational algorithm, NLPNT has been devised using the developed analytical solution procedure to simulate steady state hydraulic potentials and streamlines in a multilayered aquifer

system with infinite extent. Numerical examples of multilayered aquifer models of three, four, and five layers respectively have been designed to demonstrate simulations by NLPNT. The hydraulic potentials and streamlines computed using NLPNT have been reproduced in the form of contour plots, in vertical sections.

The corresponding results, for the chosen aquifer models, obtained by using the three-dimensional groundwater flow model MODFLOW [Mc Donald and Harbaugh 1984] have been utilised to compare the NLPNT results. Towards quantifying the comparison of analytical and numerical results, a *mean relative difference (mean error)* and a *maximum relative difference (maximum error)* between the corresponding values of hydraulic potentials have been calculated. The mean relative difference and the maximum relative difference, respectively between the analytical and numerical results are expressed as a percentage of the hydraulic potential at the central node (the base-value) of the respective MODFLOW solution.

3.4.4.1 Description of the Model

A point source of strength, $q=0.01 \text{ m}^3/\text{s}$ is placed at the centre of the aquifer surface to recharge the aquifer. The hydraulic potentials and streamlines have been computed in the central section of the aquifer system at the nodes of a rectangular grid with a lateral extent of 400 m each towards either side of the point source. At the boundaries of the aquifer system, the hydraulic potential tends to vanish. The thickness of each layer in these aquifer models has been taken as 100m.

To enable comparison, the steady state hydraulic potentials have also been simulated using MODFLOW with identical grid set-up and boundaries. Near-zero values for the hydraulic potential have been assigned as boundary conditions at large distances in the MODFLOW domain to conform with the assumptions in the NLPNT solution procedure. A recharge well (with $q=0.01 \text{ m}^3/\text{s}$) has been introduced at the central node for the point source. All the required parameters are assigned cell-wise in the model. MODFLOW simulations employed an iterative solution procedure, SIP to compute hydraulic potentials.

3.4.5 NUMERICAL EXPERIMENTS

Different hydraulic conductivity values have been assigned to the aquifer layers in several cases, to design different types of aquifer systems. The types of aquifer systems with relevant details where simulation experiments have been performed is presented in Table 3.4. For all the cases, the layer thickness is 100m each. The aquifer model with three layers is of the type $K_1 > K_2 > K_3$ with a depth of 300m. The hydraulic potentials obtained from NLPNT as well as MODFLOW are plotted as equipotential lines in Fig. 3.14. The equipotentials are spaced uniformly with 0.004m. The dashed-horizontal lines in the plots represent the interfaces between aquifer layers. It may be noticed that the analytical (NLPNT) and numerical (MODFLOW) solutions are in good agreement. The streamlines for the three layered case is shown in Fig. 3.15.

Table 3.4 Types of aquifer systems (3-layer, 4-layer and 5-layer) with patterns of respective layer conductivities simulated using NLPNT.

AQUIFER TYPE	K_1 (m ³ /s)	K_2 (m ³ /s)	K_3 (m ³ /s)	K_4 (m ³ /s)	K_5 (m ³ /s)
$K_1 > K_2 < K_3$	1e-03	1e-05	1e-04	--	--
$K_1 > K_2 < K_3 > K_4$	1e-03	1e-05	1e-03	1e-05	--
$K_1 > K_2 < K_3 > K_4 < K_5$	1e-03	5e-04	1e-03	5e-04	1e-03
$K_1 > K_2 > K_3 > K_4 > K_5$	1e-03	5e-04	1e-04	5e-05	1e-05

The four-layered aquifer system is 400 m deep with a repetitive layer design such that $K_1 > K_2 < K_3 > K_4$. The equipotentials for this aquifer model is depicted in Fig. 3.16. The corresponding equipotentials (dashed-contours) obtained from MODFLOW have been superimposed on to the plot to enable visual comparison. A very good match between the results obtained from the analytical model and the MODFLOW can be noticed. The streamlines have also been computed by NLPNT for the four-layered case and presented in Fig. 3.17.

Hydraulic potentials and streamlines have been computed in a five-layered aquifer system also. The aquifer depth is 500 m with layers of 100 m thickness each. The hydraulic conductivity values for the layers have been assigned in a diminishing pattern, starting with the top layer to form

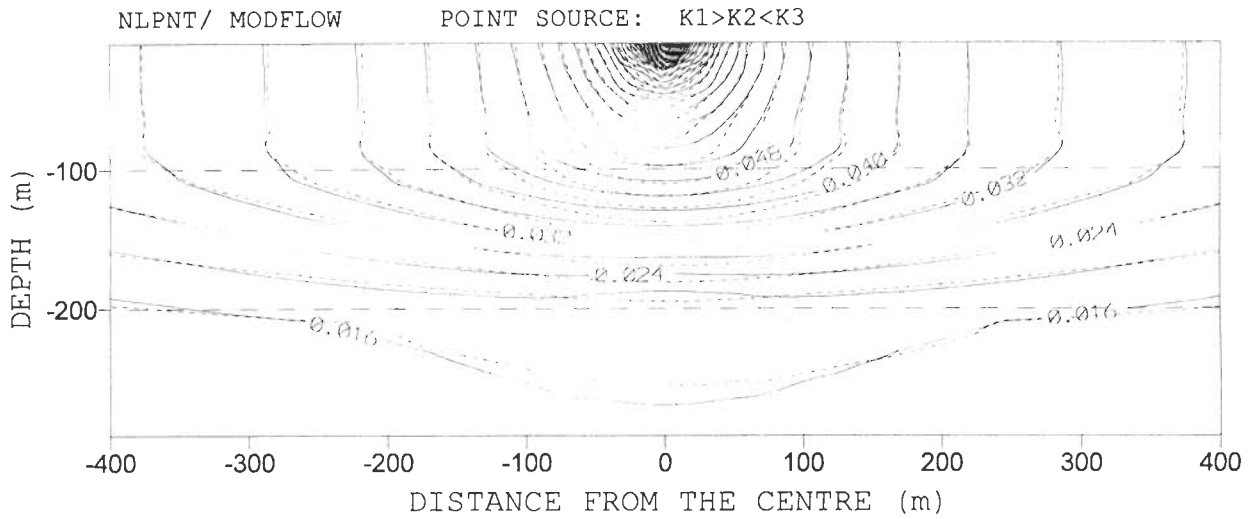


Fig. 3.14 Equipotential contours in the vertical section of a layered aquifer system with three layers ($K_1 > K_2 < K_3$) computed by NLPNT (solid contours) and MODFLOW (dashed contours); the dashed horizontal lines represent the layer interfaces.

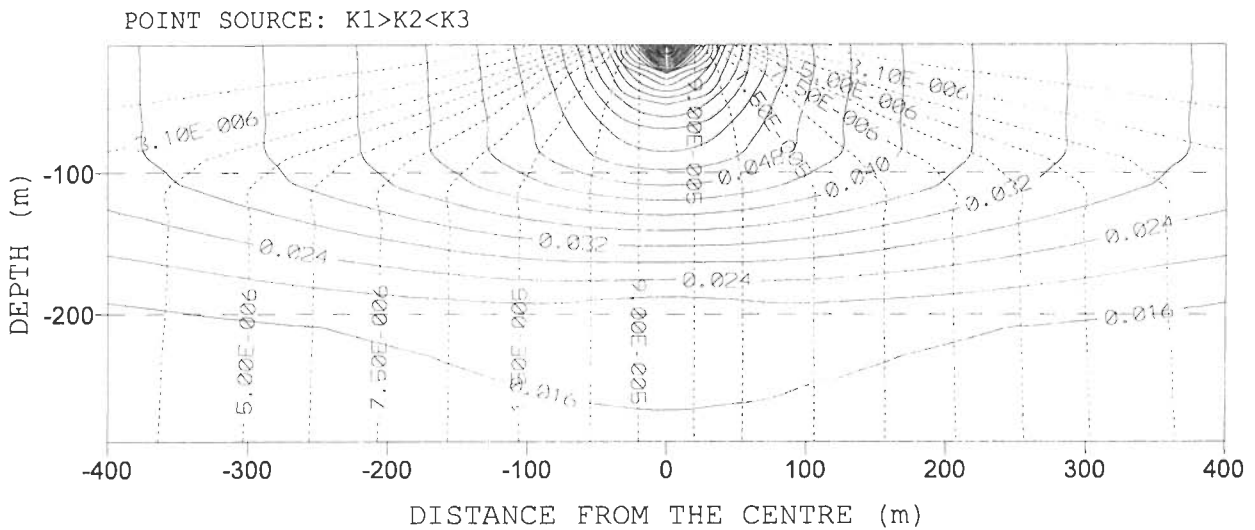


Fig. 3.15 Equipotential contours (solid contours) and streamlines (dotted contours) in the vertical section of a layered aquifer system with three layers ($K_1 > K_2 < K_3$) computed by NLPNT; the dashed horizontal lines represent the layer interfaces.

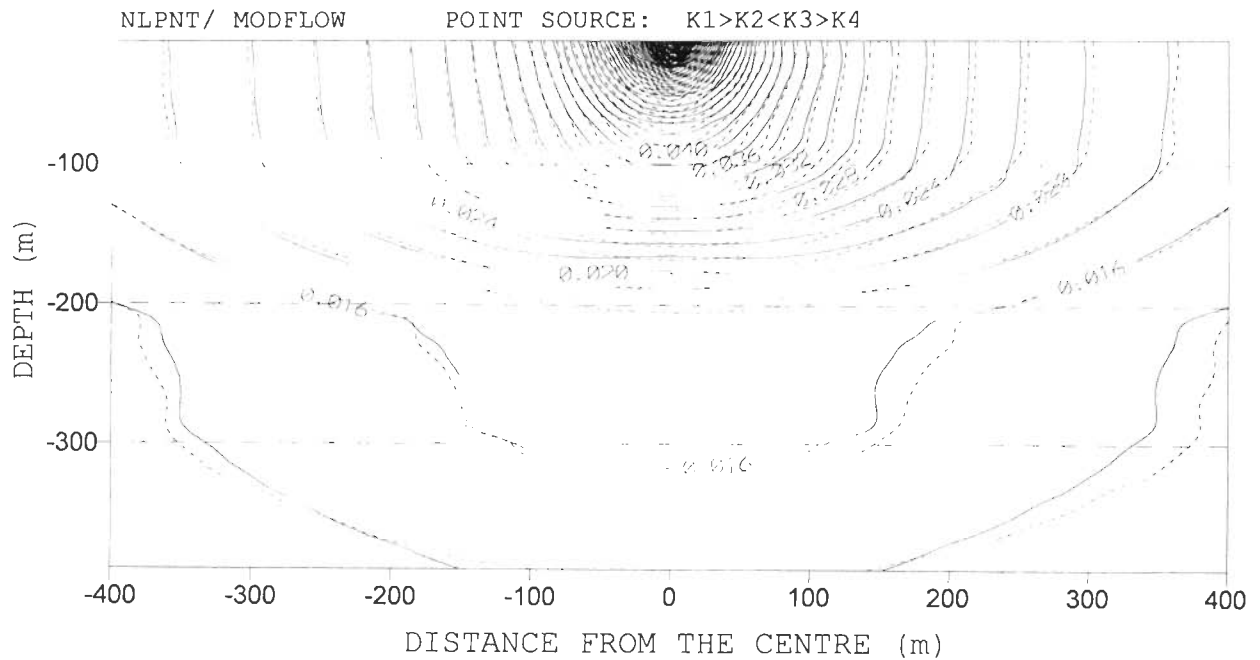


Fig. 3.16 Equipotential contours in the vertical section of a layered aquifer system with four layers ($K_1 > K_2 < K_3 > K_4$) computed by NLPNT (solid contours) and MODFLOW (dashed contours); the dashed horizontal lines represent the layer interfaces.

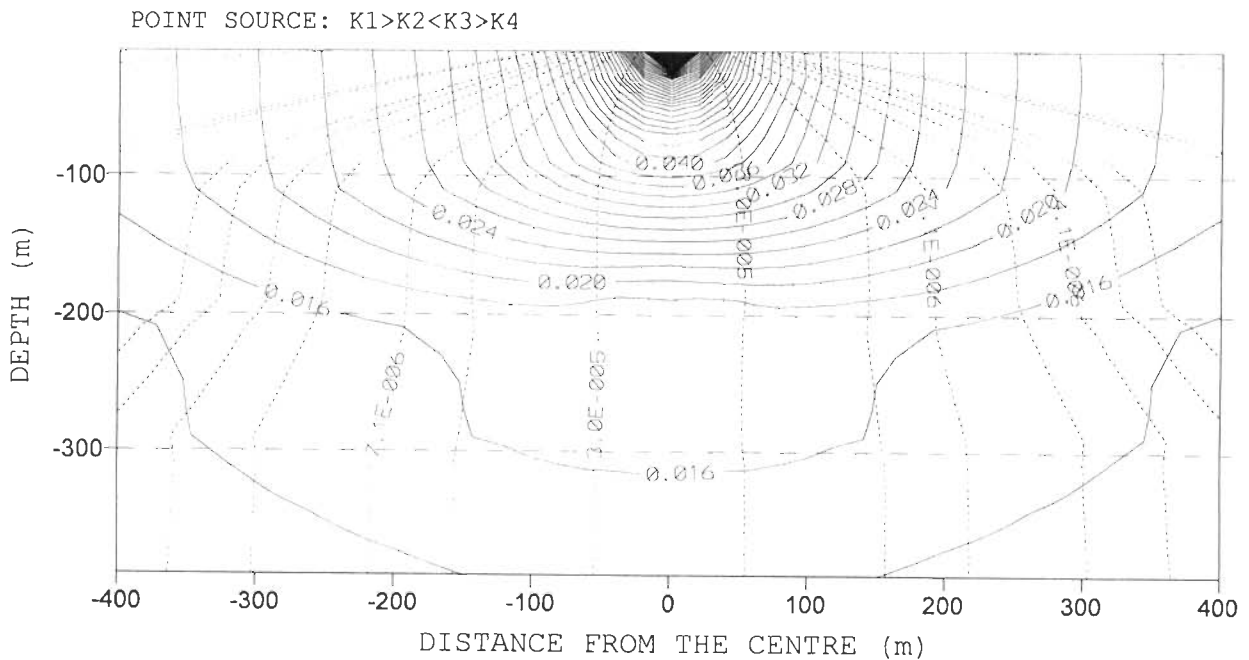


Fig. 3.17 Equipotential contours (solid contours) and streamlines (dotted contours) in the vertical section of a layered aquifer system with four layers ($K_1 > K_2 < K_3 > K_4$) computed by NLPNT; the dashed horizontal lines represent the layer interfaces.

the aquifer type $K_1 > K_2 > K_3 > K_4 > K_5$. Equipotentials for the five-layered aquifer model obtained by both analytical and numerical methods are plotted in Fig. 3.18. The analytical results compare well with the MODFLOW results. To elaborate further, the depth-wise plots of hydraulic potentials have been given in Fig. 3.19. The distributions of the hydraulic potentials (for analytical and numerical) are compared at two sections in the vertical plane, one at the centre and the other at a distance of 200m away from the point source. Also, the corresponding streamlines are shown in Fig. 3.20.

Finally, the equipotential lines and streamlines in another five-layered aquifer model of the type $K_1 > K_2 < K_3 > K_4 < K_5$ is plotted in Fig. 3.21.

The mean and maximum relative differences (*mean error* and *maximum error*) between the analytical simulations and MODFLOW simulations have been estimated to assess the closeness of these results. Figure 3.22 indicates that the mean error is less than 2%. Similarly, the maximum error between NLPNT and MODFLOW solutions can be discerned from Fig. 3.23. The maximum error is less than 2% in most of the aquifer domain, barring the points near the source where it is around 6%. The slightly larger deviation near the point source can be attributed to singularity effects. The comparisons of NLPNT results with that of MODFLOW validate the correctness of the analytical solution procedure for multilayered aquifer systems.

3.5 RESULTS AND DISCUSSION

Based on the geoelectrical sounding theory, analytical expressions for the solution of steady-state hydraulic potentials and streamlines have been derived for multilayered aquifer systems. An alternate solution procedure has also been developed when the number of layers in a stratified aquifer system are less than or equal to three. The analytical solutions assume that the stratified aquifer is of infinite extent. Also, there is cylindrical symmetry around the source kept on the air-earth interface.

The analytical simulations have been found to be very fast compared to the corresponding MODFLOW simulations in terms of computing time. In terms of CPU time, the analytical model

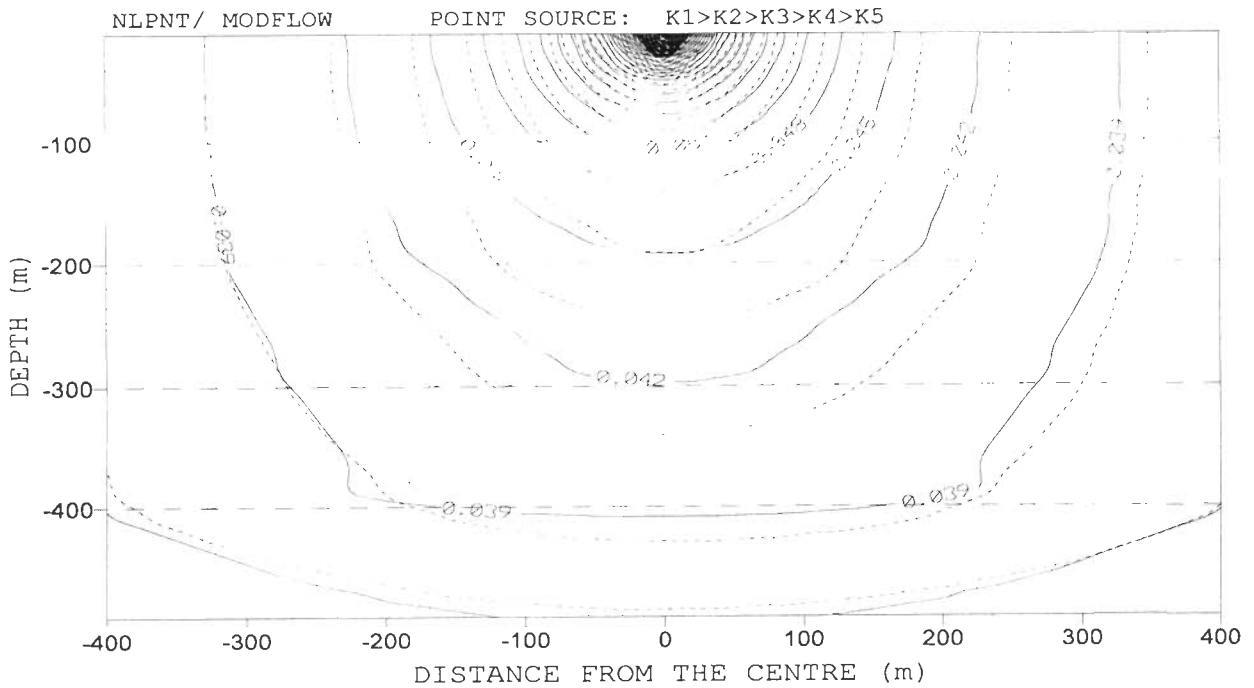


Fig. 3.18 Equipotential contours in the vertical section of a layered aquifer system with five layers ($K_1 > K_2 > K_3 > K_4 > K_5$) computed by NLPNT (solid contours) and MODFLOW (dashed contours); the dashed horizontal lines represent the layer interfaces.

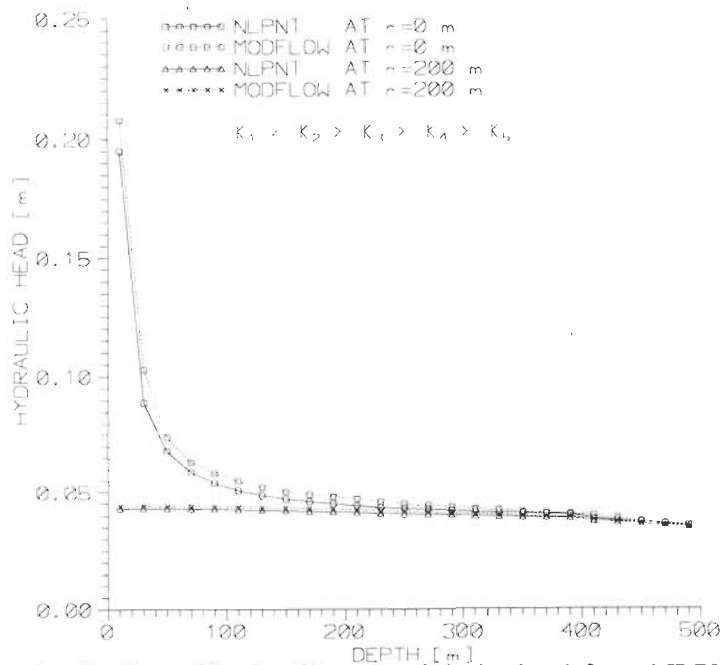
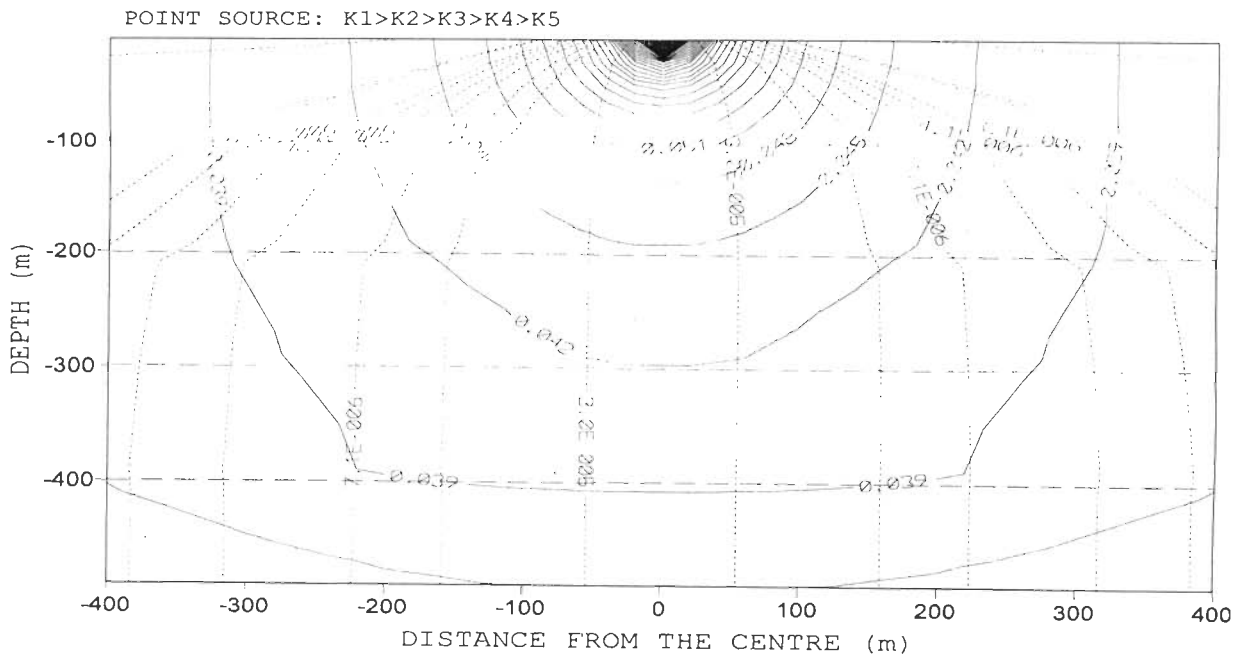


Fig. 3.19 Vertical distribution of hydraulic potential obtained from NLPNT (solid line) and MODFLOW (dashed line) at the centre and at a distance 200m from the source for the 5-layered aquifer system where $K_1 > K_2 > K_3 > K_4 > K_5$.



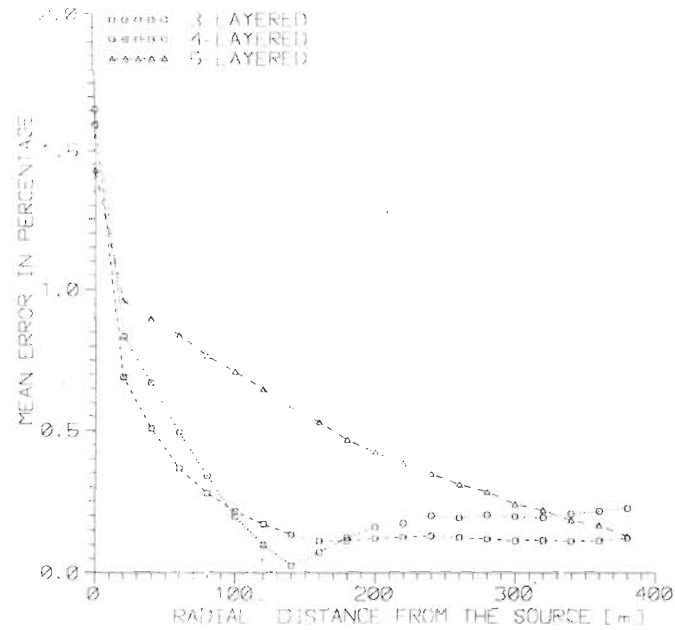


Fig. 3.22 Mean error between the hydraulic potentials computed by NLPNT and MODFLOW (for the 3, 4 and 5 layered cases), expressed as a percentage of the MODFLOW-hydraulic potential at the central node in the first layer.

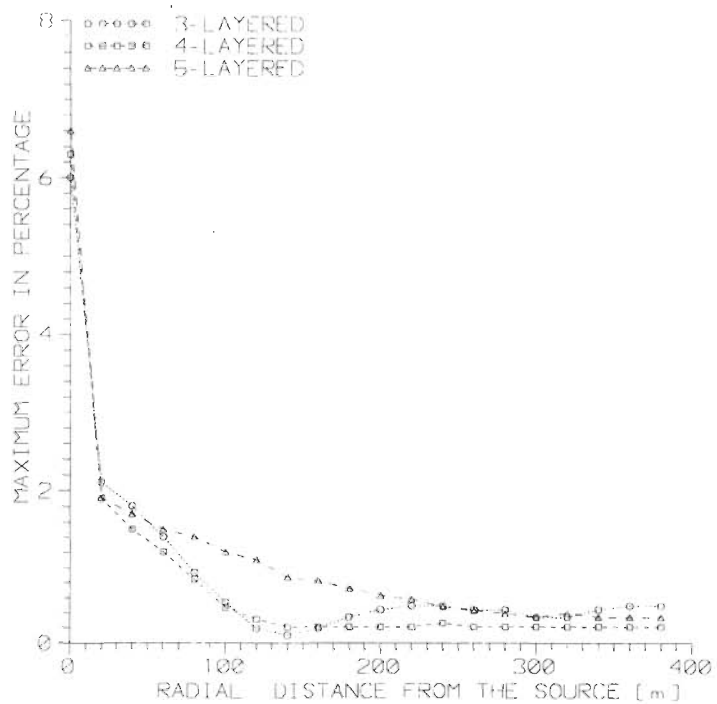


Fig. 3.23 Maximum error between the hydraulic potentials computed by NLPNT and MODFLOW (for the 3, 4 and 5 layered cases).

is found to be about twenty five times faster than MODFLOW simulations when executed in a 32-bit Pentium Pro personal computer. Besides, the analytical methods require only very few input parameters, whereas for the MODFLOW simulations detailed data preparations are necessary.

Further, comparison was made between the analytical solutions and a finite-difference solution using MODFLOW to check the veracity of the developed solution techniques. The equipotentials obtained through 3LPNT and MODFLOW matched well, there by establishing the computational effectiveness of the analytical solution. It has been observed that the streamlines follow the tangent law of incidence and refraction [Hubbert 1940], in all the cases. However, the small deviations exhibited between the results of the analytical models and that of the MODFLOW can be attributed to inaccuracies arising out of assigning finite boundaries with non-zero values for the hydraulic potentials in the MODFLOW simulations. It may be recalled that the analytical solutions, in the strict sense, are applicable to an infinite aquifer system with hydraulic potentials equal to zero at infinity. Further, there may be some rounding-off errors in MODFLOW simulations because of the iterative solution procedures.

3.5.1 THREE-LAYERED AQUIFER SYSTEMS

The simulation algorithm, 3LPNT requires only a few input parameters such as source strength, layer conductivities, layer thicknesses and grid information for computation. Therefore, when steady state hydraulic potential/ stream function is to be determined in a layered aquifer like the one described, these analytical solutions provide a means for easier computation. An added advantage lies in the straight computation of streamlines using the analytical expressions, unlike many numerical flow models. Further, the solution procedure has been extended to the cases of a line source and an areal source by incorporating appropriate convolution techniques.

3.5.2 MULTILAYERED AQUIFER SYSTEMS

Based on the analytical solution, an analytical computational procedure (NLPNT) has been developed and demonstrated with numerical examples in selected multilayered aquifer systems.

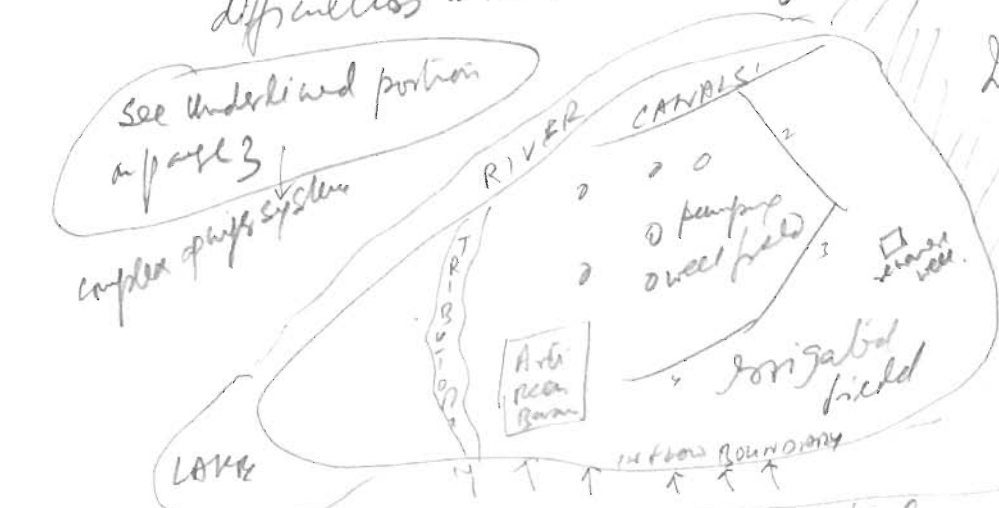
Since the proposed procedure requires only a few input parameters, it provides a means for easier and fast computation when steady state hydraulic potentials and streamlines are to be determined in a multilayered aquifer system. An added advantage is the straight computation of streamlines using the analytical expressions, unlike many numerical flow models. Further, it is possible to extend the given solution procedure for multilayered aquifer systems with a point source of recharge using the convolution procedure to the cases when a finite-line source or a an areal source acts as the recharging source.

1. Some where a ^{physical} problem description is required where the applicability of this numerical concept can be discussed.

2. A paragraph is required as to the limitations of the method for solving the real systems and prove importantly, the difficulties in the simulation of such models.

I want author to think about it, though he may not respond to it

See underlined portion in page 3
complex phys system



Implications

- A real system involves
 - ① rainfall recharge
 - ② irrigation return flow (canal + tube wells)
 - ③ canal (lined + unlined) seepage losses
 - ④ well with drawdown
 - ⑤ Reverse structures
 - ⑥ out flows to boundary
 - ⑦ Evaporation percolation losses
 - ⑧ Net storage or decline in the domain
- And all these are TIME VARIANT

In the light of these applicability of the analytical method should be considered, and its limitations stated.

ANALYTICAL SOLUTIONS FOR HYDRAULIC POTENTIAL IN HOMOGENEOUS ANISOTROPIC AQUIFER SYSTEMS

4.1 GENERAL

Anisotropy is the property by virtue of which the hydraulic conductivity values exhibit variations with the direction of measurement at a given point whereas variations through space within a geologic formation is termed heterogeneity. Generally, theoretical analyses of groundwater flow problems assume the porous medium to be isotropic and homogeneous with respect to hydraulic conductivity. But, field experience indicates that most aquifer systems are anisotropic to some degree. Layered earth formations like sedimentary rocks and loess exhibit anisotropic behaviour. Stratification, due to particle orientation, in such rock formations causes anisotropy. = loamy deposit

Two attributes of the hydraulic conductivity viz., *heterogeneity* and *anisotropy*, are required to define the nature of an aquifer. The directions in space at which the hydraulic conductivity, K attains its maximum and minimum values are termed as the *principal directions of anisotropy* and they are always orthogonal to one another [Freeze and Cherry 1979]. The effect of anisotropy on groundwater flow through such geologic formations has been of concern to groundwater hydrologists as the directions of flow and of the hydraulic gradient in an anisotropic porous medium are not parallel [Marcus 1962].

Generally, numerical groundwater flow models have been designed with the assumption that principal axes of anisotropy coincide with the reference coordinate axes. As such, popular groundwater flow models like the MODFLOW [McDonald and Harbaugh 1984] may not be able to simulate hydraulic potentials in an anisotropic porous medium with the planes of stratification of

the rock bedding are inclined with the ground surface. Alternately, in numerical groundwater modelling practices, coordinate rotations are effected so that the off diagonal components of the hydraulic conductivity tensor go to zero within grid elements or cells. This is accomplished by defining a global coordinate system for the entire problem domain and local coordinate systems for each cell in the grid [Anderson and Woessner 1991]. It is possible to derive equations relating the principal components of hydraulic conductivity defined in the local coordinate system to the components of hydraulic conductivity tensor defined in the global coordinate system [Bear 1972]. Sometimes, for simplicity, approximate answers for an equivalent isotropic situation are sought in the case of an anisotropic aquifer system. However, in approximating an anisotropic porous medium with an isotropic one introduces some degree of error in the computation of hydraulic potentials, and thereby in the flow. Therefore, alternate solution techniques may be desirable in the computation of hydraulic potentials/ flow in an anisotropic porous medium with inclined soil strata.

In this context, the possibility of translating some of the analytical formulations available in the theory of exploration geophysics for modelling hydraulic potentials in a stratified anisotropic porous medium has been explored. Therefore, the study presented herein considers homogeneous anisotropic aquifer simulations with different levels of stratification and dipping of bedding planes. The recharging of a stratified anisotropic aquifer system due to a point source and also, due to a finite-length line source of known strength has been contemplated. Analytical solutions for the hydraulic potential in the respective aquifer systems have been developed for the purpose. Suitable computational algorithms have also been formulated to facilitate demonstration of the developed techniques in several hypothetical homogeneous anisotropic aquifer systems, using numerical examples.

4.2 THEORETICAL FRAMEWORK

The theory of flow of fluids through anisotropic porous medium can be found in the literature [Scheiddegger 1957, Polubarinova-Kochina 1962, Harr 1962, and Marcus 1962]. Further, methodologies exist for the transformation of an anisotropic medium into an equivalent isotropic domain [Mishra 1972, and Strack 1989]. Further, principles of the geoelectrical sounding render

analytical methods for the computation of electric potentials at the earth surface (surface potentials) in layered earth medium [Parasnis 1965, and Bhattacharya and Patra 1968].

In groundwater problems soil body is considered to be a continuous medium of many interconnected openings which serve as the fluid carrier. Fluid flow in such porous media is governed by the Darcy's law which is represented as [Harr 1962]:

$$q_x = -K_x \frac{\partial \phi}{\partial x} \quad \text{K is the hyd. cond. in the direction where gradient is } \frac{\partial \phi}{\partial x} \text{ } \rightarrow \text{ distance is } \Delta x \quad (4.1)$$

where q_x [LT^{-1}] is the specific discharge, $\partial\phi/\partial x$ is the hydraulic gradient ^{that causes the flow} due to change in hydraulic potential, ϕ [L] over a distance, x [L], and K [LT^{-1}] is the hydraulic conductivity. It is a function of the intrinsic permeability of the medium k [L^2], fluid density ρ [ML^{-3}], dynamic viscosity of the fluid μ [$ML^{-1}T^{-1}$], and acceleration due to gravity g [LT^{-2}] and is related by [Freeze and Cherry 1979]:

$$K = \frac{k \rho g}{\mu} \quad (4.2)$$

4.2.1 HYDRAULIC CONDUCTIVITY TENSOR

In a homogeneous aquifer the hydraulic conductivity, K [LT^{-1}] is same in all directions. However, homogeneous aquifers in the true sense are rare and in practice, the soil often is layered with the hydraulic conductivity being different in the directions parallel and normal to the layers as illustrated in Fig. 4.1. The hydraulic conductivity parallel to the layer, K_1 (parallel to the X^*Y^* -plane) being larger in magnitude than that perpendicular to the bedding plane, K_2 (in the direction of Z^* -axis). Let, α be the angle of dip of the soil bedding plane in the rectangular Cartesian coordinate system. Let, also, (y, z) and (y^*, z^*) be the Cartesian coordinates of an arbitrary point, P in the actual plane, and in the rotated (through an angle α) plane, respectively.

Referring to Fig. 4.1, the following relationship holds good:

$$y = y^* \cos \alpha - z^* \sin \alpha \quad (4.3)$$

$$z = y^* \sin \alpha + z^* \cos \alpha$$

Let q_y , q_z and q_y^* , q_z^* be the corresponding specific discharge vectors in the actual and the rotated planes. Then, the expressions for q_y and q_z in terms of q_y^* and q_z^* are similar to eqn. (4.3):

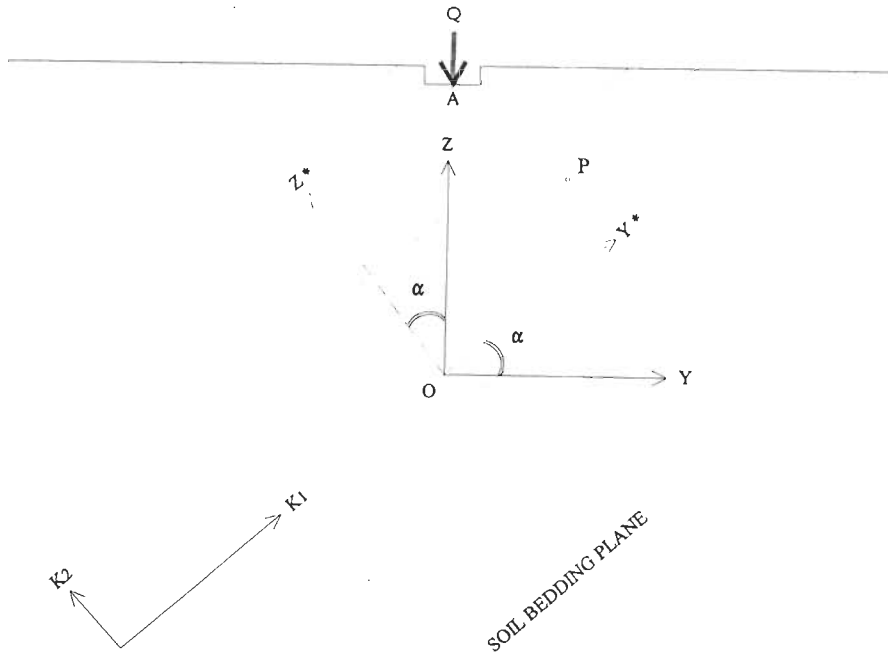


Fig. 4.1 Scheme of the homogeneous anisotropic aquifer system (YZ-plane) of infinite extent with a point source, Q located centrally on the surface. Dotted lines represent bedding planes of soil strata with angle of dip, α .

$$\begin{aligned}
 q_y &= q_y^* \cos \alpha - q_z^* \sin \alpha \\
 q_z &= q_y^* \sin \alpha + q_z^* \cos \alpha
 \end{aligned}
 \tag{4.4}$$

Now, application of Darcy's law in terms of Y^*Z^* coordinate system yields:

$$q_y = -K_1 \frac{\partial \phi}{\partial y'} \quad (4.5)$$

$$q_z = -K_2 \frac{\partial \phi}{\partial z'}$$

where K_1 and K_2 are the principal values of the hydraulic conductivity.

Using eqn.(4.5) in eqn.(4.4), we get:

$$q_y = -K_1 \frac{\partial \phi}{\partial y'} \cos \alpha + K_2 \frac{\partial \phi}{\partial z'} \sin \alpha \quad (4.6)$$

$$q_z = -K_1 \frac{\partial \phi}{\partial y'} \sin \alpha - K_2 \frac{\partial \phi}{\partial z'} \cos \alpha$$

By application of the chain rule with eqn.(4.3) yields:

$$\frac{\partial \phi}{\partial y'} = \frac{\partial \phi}{\partial y} \frac{\partial y}{\partial y'} + \frac{\partial \phi}{\partial z} \frac{\partial z}{\partial y'} = \frac{\partial \phi}{\partial y} \cos \alpha + \frac{\partial \phi}{\partial z} \sin \alpha \quad (4.7)$$

$$\frac{\partial \phi}{\partial z'} = \frac{\partial \phi}{\partial y} \frac{\partial y}{\partial z'} + \frac{\partial \phi}{\partial z} \frac{\partial z}{\partial z'} = -\frac{\partial \phi}{\partial y} \sin \alpha + \frac{\partial \phi}{\partial z} \cos \alpha$$

Combining eqn.(4.6) and eqn.(4.7), the Darcy's law for anisotropic hydraulic conductivity for two-dimensional flow is obtained [Strack 1989]:

$$q_y = -K_{yy} \frac{\partial \phi}{\partial y} - K_{yz} \frac{\partial \phi}{\partial z} \quad (4.8)$$

$$q_z = -K_{zy} \frac{\partial \phi}{\partial y} - K_{zz} \frac{\partial \phi}{\partial z}$$

where,

$$\begin{aligned}
 K_{yy} &= K_1 \cos^2 \alpha + K_2 \sin^2 \alpha \\
 K_{yz} &= K_{zy} = (K_1 - K_2) \sin \alpha \cos \alpha \\
 K_{zz} &= K_1 \sin^2 \alpha + K_2 \cos^2 \alpha
 \end{aligned} \tag{4.9}$$

In a similar fashion, for the general case of three-dimensional flow in (x,y,z) coordinate system, it can be shown that Darcy's law takes the form [Strack 1989]:

$$\begin{aligned}
 q_x &= -K_{xx} \frac{\partial \phi}{\partial x} - K_{xy} \frac{\partial \phi}{\partial y} - K_{xz} \frac{\partial \phi}{\partial z} \\
 q_y &= -K_{yx} \frac{\partial \phi}{\partial x} - K_{yy} \frac{\partial \phi}{\partial y} - K_{yz} \frac{\partial \phi}{\partial z} \\
 q_z &= -K_{zx} \frac{\partial \phi}{\partial x} - K_{zy} \frac{\partial \phi}{\partial y} - K_{zz} \frac{\partial \phi}{\partial z}
 \end{aligned} \tag{4.10}$$

The coefficients K_{ij} ($i = x, y, z; j = x, y, z$) in eqn. (4.10) are known as the coefficients of the hydraulic conductivity tensor, represented by:

$$\bar{K} = \begin{bmatrix} K_{xx} & K_{xy} & K_{xz} \\ K_{yx} & K_{yy} & K_{yz} \\ K_{zx} & K_{zy} & K_{zz} \end{bmatrix} \tag{4.11}$$

Eqn. (4.11) is a symmetric matrix with the diagonal elements K_{xx} , K_{yy} and K_{zz} and $K_{ij} = K_{ji}$ for $i = x, y, z; j = x, y, z$. Thus, in an anisotropic medium the hydraulic conductivity tensor is, in fact, characterised by six components.

4.3 HYDRAULIC POTENTIALS DUE TO A POINT SOURCE

The computation of hydraulic potentials in a homogeneous anisotropic aquifer system due to a point source of strength Q [L^3T^{-1}] is presented. The plane of stratification of the soil bedding can either be parallel to the ground surface or be inclined with an angle of dip, α . It is assumed that the dimensions of the aquifer system extend to infinity. A procedure has been devised based on analytical results translated from the geoelectrical sounding theory [Bhattacharya and Patra 1968] to compute hydraulic potentials. It is assumed that the major principal direction of anisotropy is along the plane of the soil strata while the other is perpendicular to it.

It is possible to orient the coordinate axes along the principal axes of anisotropy such that $K_{xy} = K_{yz} = K_{zx} = 0$. If (x^*, y^*, z^*) is the rotated (through an angle, α) coordinate system, then the resulting governing equation for steady state groundwater flow in a homogeneous anisotropic porous medium reduces to:

$$K_{xx} \frac{\partial^2 \phi}{\partial x^{*2}} + K_{yy} \frac{\partial^2 \phi}{\partial y^{*2}} + K_{zz} \frac{\partial^2 \phi}{\partial z^{*2}} = 0 \quad (4.12)$$

Now, if we choose a new system of coordinates with the transformation relationships,

$$\begin{aligned} x^* &= \gamma \sqrt{K_{xx}} \\ y^* &= \eta \sqrt{K_{yy}} \\ z^* &= \zeta \sqrt{K_{zz}} \end{aligned} \quad (4.13)$$

then eqn. (4.12) transforms to the Laplace's form:

$$\frac{\partial^2 \phi}{\partial \gamma^2} + \frac{\partial^2 \phi}{\partial \eta^2} + \frac{\partial^2 \phi}{\partial \zeta^2} = 0 \quad (4.14)$$

The solution of which can be obtained in a manner similar to that reported in the literature relevant to the geoelectrical sounding principles [Bhattacharya and Patra 1968]. Thus, we have:

$$\phi = \frac{C}{\sqrt{\gamma^2 + \eta^2 + \zeta^2}} = \frac{C}{\sqrt{\frac{x^2}{K_{xx}} + \frac{y^2}{K_{yy}} + \frac{z^2}{K_{zz}}}} \quad (4.15)$$

Now, consider the plane of stratification as the X*Y*-plane in the homogeneous anisotropic porous medium. Being very small, in most practical cases, the anisotropy in the plane of stratification can be neglected. Thus, let the longitudinal hydraulic conductivity be: $K_{xx} = K_{yy} = K_1$ (parallel to the plane of stratification) and the transverse hydraulic conductivity be: $K_{zz} = K_2$ (normal to the plane of stratification). Therefore, eqn. (4.15) can be rewritten as:

$$\phi = \frac{C}{\sqrt{\frac{x^2}{K_1} + \frac{y^2}{K_1} + \frac{z^2}{K_2}}} \quad (4.16)$$

Let, the coefficient of anisotropy (β) and the equivalent isotropic hydraulic conductivity (K_m) be two parameters of the anisotropic medium, defined such that:

$$\beta = \sqrt{\frac{K_1}{K_2}} \quad (4.17)$$

$$K_m = \sqrt{K_1 K_2}$$

By virtue of eqn. (4.17), eqn. (4.16) takes the form:

$$\phi = \frac{C \sqrt{K_1}}{\sqrt{x^2 + y^2 + (\beta z)^2}} \quad (4.18)$$

By comparison with eqn. (4.15), it can be shown that the hydraulic potential given by eqn. (4.18) also satisfies the Laplace's equation in terms of the variables x^* , y^* , and βz^* . Therefore, the specific discharge components can be obtained by taking the respective derivatives of eqn. (4.18) as:

$$q_x^* = \frac{K_1^{3/2} C x^*}{[x^{*2} + y^{*2} + (\beta z^*)^2]^{3/2}} \quad (4.19)$$

$$q_y^* = \frac{K_1^{3/2} C y^*}{[x^{*2} + y^{*2} + (\beta z^*)^2]^{3/2}} \quad (4.20)$$

$$q_z^* = \frac{K_1^{3/2} C z^*}{[x^{*2} + y^{*2} + (\beta z^*)^2]^{3/2}} \quad (4.21)$$

Therefore, the resultant specific discharge, q can be given by:

$$q = \sqrt{q_x^{*2} + q_y^{*2} + q_z^{*2}} = \frac{K_1^{3/2} C [x^{*2} + y^{*2} + z^{*2}]^{1/2}}{[x^{*2} + y^{*2} + \beta^2 z^{*2}]^{3/2}} \quad (4.22)$$

In order to evaluate the constant of integration C , let us consider the total flow through a hemisphere of radius R below the surface with the source as the centre (point A in Fig. 4.1). Obviously, this total outflow should be equal to the total input, Q (the strength of the recharging point source). Therefore, with reference to the spherical coordinate system (R, θ, ω) , we have:

$$Q = \int_s q ds = \int_0^{2\pi} \int_0^{\pi/2} q R^2 \sin\theta d\theta d\omega$$

*An explanatory figure
may be useful here.* (4.23)

Since,

$$x^2 + y^2 = R^2 \sin^2 \theta \quad (4.24)$$

and

$$z^2 = R^2 \cos^2 \theta \quad (4.25)$$

eqn. (4.22) becomes,

$$q = \frac{K_1^{3/2} C}{R^2 [1 + (\beta^2 - 1) \cos^2 \theta]^{3/2}} \quad (4.26)$$

and

$$Q = C K_1^{3/2} \int_0^{2\pi} d\omega \int_0^{\pi/2} \frac{\sin \theta d\theta}{[1 + (\beta^2 - 1) \cos^2 \theta]^{3/2}} = \frac{2\pi C K_1^{3/2}}{\beta} \quad (4.27)$$

Therefore,

$$C = \frac{Q\beta}{2\pi K_1^{3/2}} \quad (4.28)$$

Replacing the constant C in eqn. (4.18) with eqn. (4.28), we get:

$$\phi = \frac{Q}{2\pi K_m \sqrt{x^2 + y^2 + \beta^2 z^2}} \quad (4.29)$$

Now, eqn. (4.29) is the expression for the hydraulic potential due to a point source (of strength, Q) at any point in a horizontally stratified (that is the plane of stratification is parallel to

the ground surface) porous medium.

If the planes of stratification makes an angle of dip α , then the above expression for hydraulic potential can be generalised by considering a rotation of the coordinate axes (x,y,z) through an angle α . Let the rotated coordinate axes be (x^*,y^*, z^*) . Let the strike of the bed x be along x^* of the new (rotated) coordinate system. Then, it follows from simple trigonometric considerations that:

$$\begin{aligned} x^* &= x \\ y^* &= y \cos \alpha + z \sin \alpha \\ z^* &= -y \sin \alpha + z \cos \alpha \end{aligned} \quad (4.30)$$

Incorporating the relationship given by eqn. (4.30) into equation (4.29) yields the required solution for hydraulic potentials in a homogeneous anisotropic medium with inclined planes of stratification as:

$$\phi = \frac{Q}{2 \pi K_m \sqrt{x^2 + (y \cos \alpha + z \sin \alpha)^2 + \beta^2 (-y \sin \alpha + z \cos \alpha)^2}} \quad (4.31)$$

4.4 HYDRAULIC POTENTIALS DUE TO A FINITE-LENGTH LINE SOURCE

If a line source of finite length is used [Fig. 4.2] instead of the point source to recharge the homogeneous anisotropic aquifer system, then the analytical solution for hydraulic potentials can be developed by applying appropriate domain transformation techniques. In order to develop the required analytical expression for the hydraulic potential, we start from an expression for the case of a homogeneous isotropic medium. Subsequently, by application of suitable domain transformation techniques the equivalent analytical solution for the anisotropic medium can be formulated.

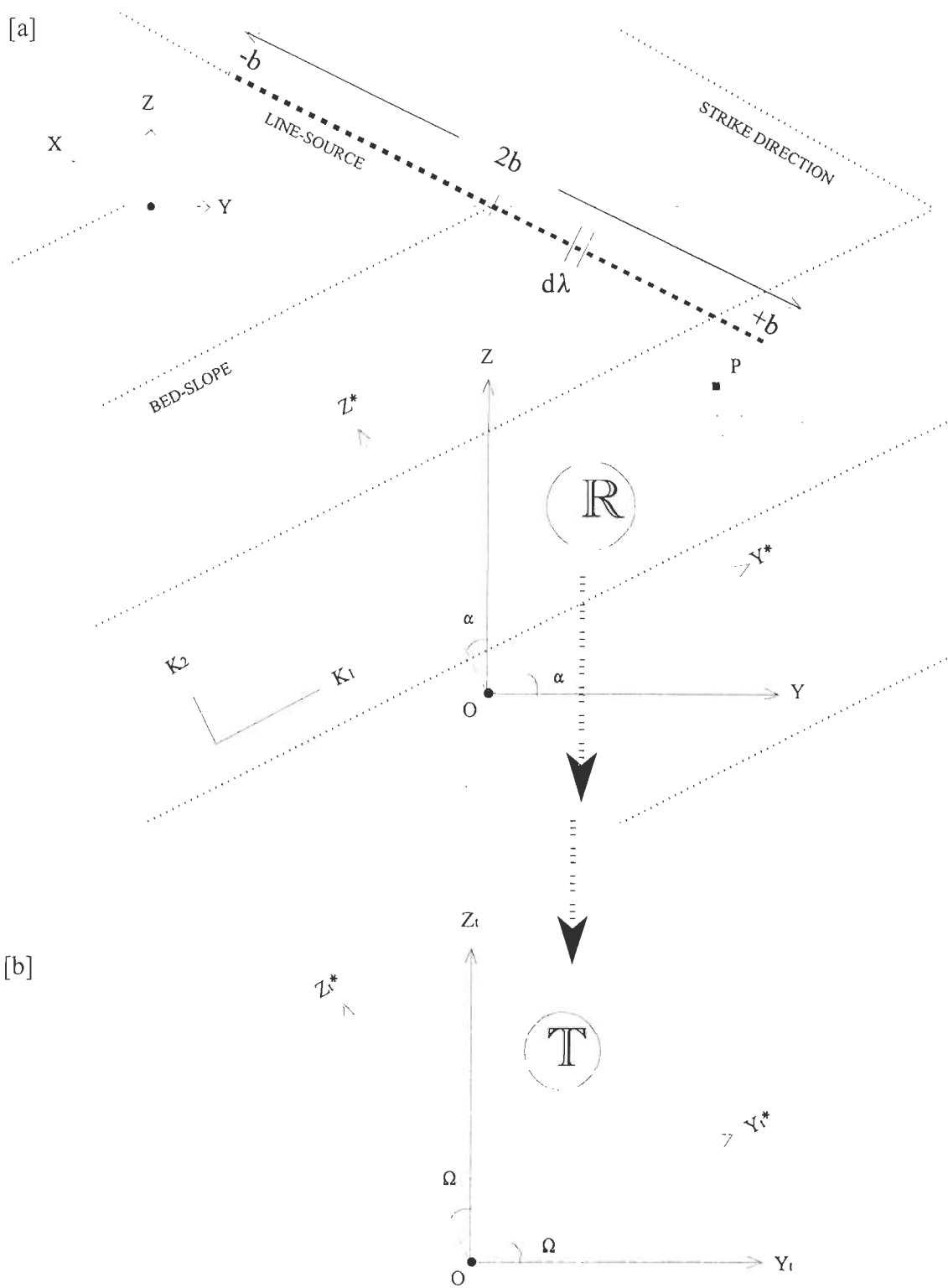


Fig 4.2 A finite line-source of strength Q_L (m^2/s) is centrally placed at air-earth interface along the strike of the bedding plane in: [a] the reference coordinate plane (R); [b] the transformed domain (T) to facilitate the analytical solution.

4.4.1 SOLUTION FOR HOMOGENEOUS, ISOTROPIC AQUIFER

In the case of an infinite homogeneous, isotropic porous medium recharged with a point source of strength Q , the expression for the steady state hydraulic potential (ϕ) in the porous medium at a distance, r from the source in the YZ -plane can be given as [Parasnis 1965, and Bhattacharya and Patra 1968]:

$$\phi = \frac{Q}{2\pi K\sqrt{y^2 + z^2}} \quad (4.32)$$

where K (m/s) is the isotropic hydraulic conductivity.

Now, let us consider the hydraulic potential in a homogeneous porous medium due to a line source of finite length, $2b$ and strength, Q_L (m^2/s) per unit length [a set up similar to Fig. 4.2]. The finite-length line source can be thought to be consisting of a number of infinitesimal point sources. The line source is located along the Y -axis symmetrically with the origin of the coordinate system. It is required to find the hydraulic potential at an arbitrary point P in the YZ -plane.

Let $d\lambda$ be an infinitesimally small element of the finite-length line source at a distance λ from the centre. Without loss of generality, $d\lambda$ may be deemed to be a point source of strength $Q_L d\lambda$ (m^3/s). If the porous medium be homogeneous and isotropic, then from eqn. (4.32), it follows that the steady state hydraulic potential at any point P in the YZ -plane would be:

$$d\phi = \frac{Q_L d\lambda}{2\pi K\sqrt{x^2 + (\lambda - z)^2}} \quad (4.33)$$

Integrating Eqn. (4.33) between the limits of the line source, $(-b, +b)$ yields the hydraulic potential due to the line source of length, $2b$ and strength, Q_L (m^2/s) in the homogeneous, isotropic porous medium:

$$\phi = \frac{Q_L}{2\pi K} \left[\sinh^{-1} \left(\frac{b-y}{z} \right) + \sinh^{-1} \left(\frac{b+y}{z} \right) \right] \quad (4.34)$$

4.4.2 SOLUTION FOR HOMOGENEOUS, ANISOTROPIC AQUIFER

An existing methodology [Strack 1989] has been adapted with some modifications to develop the analytical solution for the hydraulic potential in the vertical section of the homogeneous anisotropic aquifer system. The procedure involves three steps viz., (i) a transformation of the anisotropic medium into an isotropic domain, (ii) computation of the hydraulic potentials in the fictitious (isotropic) domain and (iii) finally, transformation of the fictitious hydraulic potentials back to the actual physical domain, yielding the required anisotropic hydraulic potentials.

Referring to Fig. 4.2a, let us consider a stratified anisotropic porous medium with principal directions of anisotropy oriented along the Y^* and Z^* axes with hydraulic conductivities K_1 (parallel to the plane of stratification) and K_2 (normal to the plane of stratification). Let the Cartesian coordinates in the physical plane be (Y, Z) . The major principal direction of the hydraulic conductivity tensor makes an angle α with the Y -axis. Also, let the Cartesian coordinates of a rotated plane be (Y^*, Z^*) , such that the Y^* -axis is inclined at an angle α with the Y -axis. Now, the Cartesian coordinates (Y_1^*, Z_1^*) in a transformed domain [Fig. 4.2b] are chosen such that they correspond to the coordinates (Y^*, Z^*) in the physical plane. Finally, the Cartesian coordinate system (Y_1, Z_1) is introduced in the transformed domain such that the Y_1 -axis corresponds to the Y -axis. Let K_m , as given in eqn. (4.17), denotes the equivalent isotropic hydraulic conductivity of the medium in the transformed domain, (Y_1, Z_1) . Further, in the fictitious domain, let the angle between the Y_1^* and Y_1 -axes be Ω .

It can be shown that the angle of dip, α in the physical domain and that in the transformed domain, Ω are related by:

$$\tan \Omega = \beta \tan \alpha \quad (4.35)$$

The hydraulic potential due to the finite-length line source would be isotropic with reference to the transformed domain, (Y_t, Z_t) and can be expressed by virtue of eqn. (4.34) as:

$$\phi(y_t, z_t) = \frac{Q_L}{2\pi K_m} \left[\sinh^{-1} \left(\frac{b-y_t}{z_t} \right) + \sinh^{-1} \left(\frac{b+y_t}{z_t} \right) \right] \quad (4.36)$$

Based on the theoretical aspects already presented in the case of hydraulic potentials due to a point source, the following transformation relations have been applied between the two domains:

$$\begin{aligned} Y_t &= Y \\ Z_t &= \beta Z, \quad \text{where} \quad \beta = \sqrt{K_1/K_2} \end{aligned} \quad (4.37)$$

Now, from trigonometric considerations, the relationship between the physical domain (Y, Z) and the transformed domain (Y_t, Z_t) can be established as:

$$y_t = y \left[\sqrt{\cos^2 \alpha + \beta^2 \sin^2 \alpha} \right] + z \left[\frac{(1 - \beta^2) \sin \alpha \cos \alpha}{\sqrt{\cos^2 \alpha + \beta^2 \sin^2 \alpha}} \right] \quad (4.38)$$

and,

$$z_t = z \left[\frac{\beta}{\sqrt{\cos^2 \alpha + \beta^2 \sin^2 \alpha}} \right] \quad (4.39)$$

Substituting eqns. (4.38) and (4.39) for y_t and z_t , respectively in eqn. (4.36) results in the required analytical expression for the hydraulic potential, due to the line source of finite length, 2b

and strength Q_L , in the YZ -plane of the homogeneous anisotropic aquifer system as:

$$\phi(y, z) = \frac{Q_L}{2\pi K_m} \left[\sinh^{-1} \left(\frac{B_s - G_s}{\beta z} \right) + \left(\frac{B_s + G_s}{\beta z} \right) \right] \quad (4.40)$$

where,

$$B_s = b \sqrt{\cos^2 \alpha + \beta^2 \sin^2 \alpha} \quad (4.41)$$

$$G_s = y [\cos^2 \alpha + \beta^2 \sin^2 \alpha] + z (1 - \beta^2) \sin \alpha \cos \alpha$$

4.5 NUMERICAL SIMULATION ALGORITHMS

Two algorithms, HANI-P and HANI-L have been devised based on the analytical expressions developed in the preceding sections and coded in FORTRAN77 in order to simulate the hydraulic potentials due to a point source as well as a finite-length line source, respectively in hypothetical homogeneous anisotropic porous media with tilted strata. The input information for the computation of hydraulic potentials include source strength, hydraulic conductivity values in the principal directions, angle of dip of the strata, and grid-node details.

The bedding planes of the rock layers in the hypothetical aquifer system make an angle α with the horizontal (XY) surface. As indicated earlier, the major principal direction of anisotropy, K_1 is uniform in the bedding plane of the strata and the minor principal direction of anisotropy, K_2 is perpendicular to the plane of the strata. The recharging source (point source, $Q [L^3T^{-1}]$ or finite-length line source, $Q_L [L^2T^{-1}]$ as the case may be) is located centrally on the earth surface. The boundaries of the hypothetical aquifer system are assumed to be at large distances from the source (i.e., a homogeneous anisotropic aquifer system of infinite extent). Simulations of hydraulic potentials have been carried out with several levels of anisotropy of the aquifer system as well as for different orientations (α), varied between zero and $\pi/2$, of the strata.

4.5.1 AQUIFER SIMULATIONS WITH POINT SOURCE

The aquifer parameter values used for the simulation of hydraulic potentials due to point source and the various sets of simulations performed using the algorithm HANI-P are given in Table 4.1 and Table 4.2, respectively.

Table 4.1 Aquifer Parameter values used for the numerical simulations of hydraulic potentials due to a point source.

Model Parameters	Numerical Values
Source strength, Q	0.1 m ³ /s
Hydraulic conductivity in the major direction, K_1	0.001 m/s
Dip angle of the strata, α	0, $\pi/12$, $\pi/4$, $\pi/2$
Coefficient of anisotropy, β	1, 2, 4, 7, 10
Ratio of hydraulic conductivity values, K_1/K_2	1, 4, 16, 49, 100
Grid dimensions	$Y = (-500 \text{ m}, +500 \text{ m}), Z = (0, -250 \text{ m})$ $\Delta Y = 10 \text{ m}, \Delta Z = 10 \text{ m}$

Table 4.2 Set of cases where hydraulic potentials due to a point source have been simulated with different combinations of angle of dip, α and coefficients of anisotropy, β .

Hydraulic Potentials due to Point Source in Homogeneous Anisotropic Aquifer Systems				
Parameters	$\alpha=0$	$\alpha=\pi/12$	$\alpha=\pi/4$	$\alpha=\pi/2$
$\beta=1$	✓	-	-	-
$\beta=2$	✓	✓	✓	✓
$\beta=4$	✓	✓	✓	✓
$\beta=7$	✓	✓	✓	✓
$\beta=10$	✓	✓	✓	✓

Equipotential lines are drawn for the vertical section of the aquifer system. In Fig. 4.3 comparison of the hydraulic potentials in a homogeneous isotropic aquifer [Fig. 4.3a] with that in an anisotropic aquifer system [Fig. 4.3b] with horizontal stratification (shown as solid lines) is made. The horizontal hydraulic conductivity, $K_1 = 0.001$ m/s, in both the cases. The coefficient of anisotropy, $\beta = 1$ for the isotropic aquifer and $\beta = 10$ for the anisotropic case. Since K_1 and K_2 are equal for the isotropic case [Fig. 4.3a], the equipotentials assume semi-circular pattern in the vertical section with the source at its centre, and uniform radial flow occurs. However, the orthogonal hydraulic conductivity, K_2 is smaller than K_1 by two orders of magnitude in the case of the anisotropic medium. Consequently, the shape of equipotentials in the anisotropic case [Fig. 4.3b] is semi-elliptical, indicating the tendency for the flow to follow the least resistive path.

Fig. 4.4 depicts several plots of equipotentials in the anisotropic aquifer systems with different orientations (solid lines) of the strata when the coefficient of anisotropy, $\beta = 2$. The hydraulic conductivity values in the principal directions are common for all these plots. The changes in the pattern of hydraulic potentials and flow gradients with changing orientation of the strata are obvious from the plots.

Fig. 4.5 shows the equipotentials in the anisotropic aquifer system with different coefficients of anisotropy. The bedding planes of the strata have been kept horizontal, as indicated by the solid lines. The coefficient of anisotropy used are $\beta = 2$, $\beta = 4$, $\beta = 7$ and $\beta = 10$, respectively for the various cases in Fig. 4.5a, Fig. 4.5b, Fig. 4.5c and Fig. 4.5c. The shape of equipotentials flatten as the degree of anisotropy increases. Similar kinds of plots have also been presented for a few other cases with the dip of the soil bedding planes as, $\alpha = \pi/4$, and $\alpha = \pi/2$, respectively in Fig. 4.6 and Fig. 4.7. Again, the coefficient of anisotropy applicable to these cases are $\beta = 2$, $\beta = 4$, $\beta = 7$ and $\beta = 10$, respectively.

In Fig. 4.8, distribution of hydraulic potentials due to a point source in the vertical section of the anisotropic aquifer system with $\alpha = \pi/4$ and $\beta = 10$ is shown. The hydraulic potential declines with increasing distance from the source. It can be noticed that the distributions of hydraulic potentials at -500 m (notated by Δ , towards the left of the source) and $+500$ m (notated by

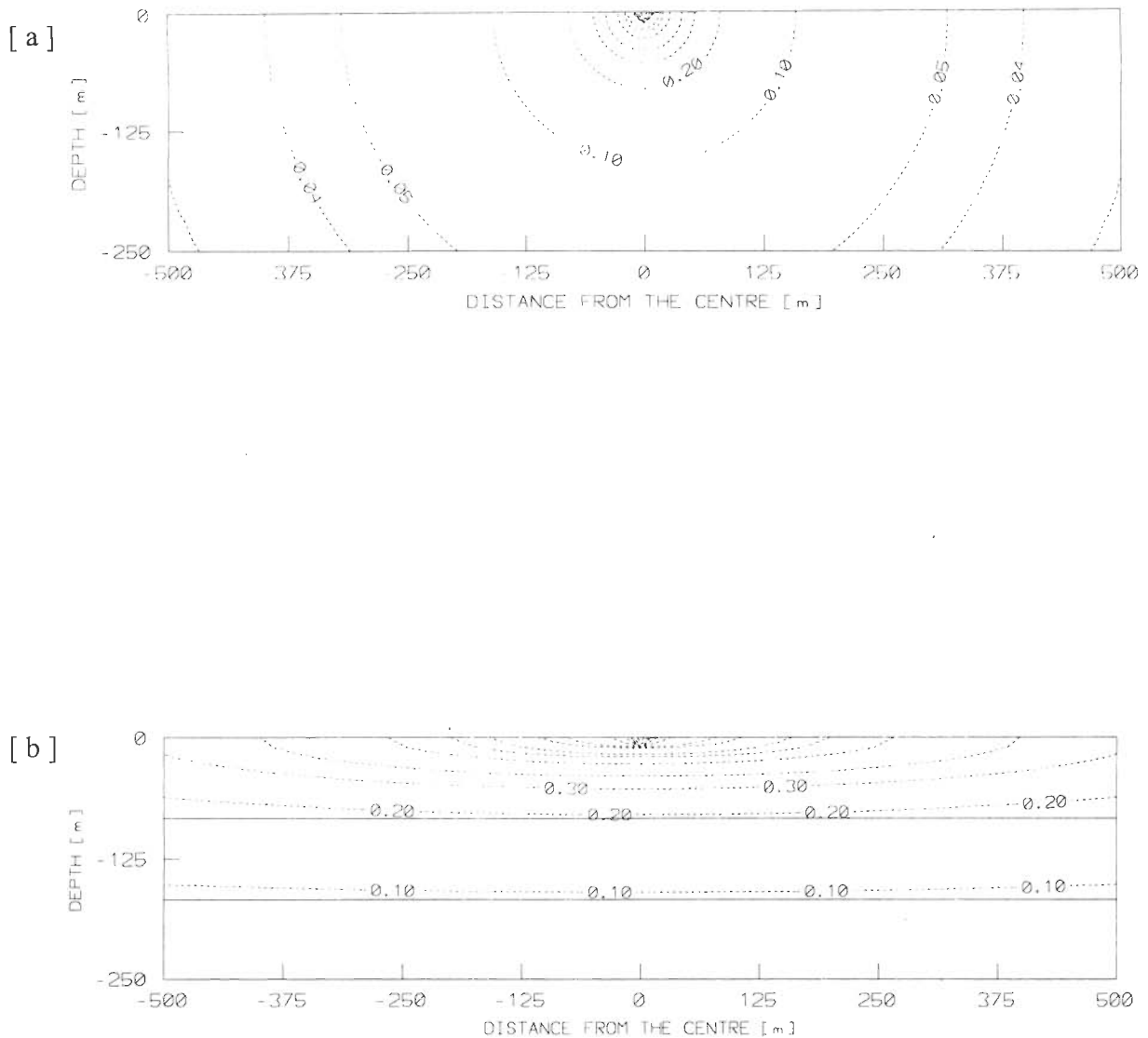


Fig. 4.3 Selected equipotential contours (for a point source, $Q=0.1\text{m}^3/\text{s}$) in: [a] an isotropic aquifer where inclination of bedding planes, $\alpha = 0$ and coefficient of anisotropy, $\beta = 1$; [b] in an anisotropic aquifer where inclination of bedding planes, $\alpha = 0$ and coefficient of anisotropy, $\beta = 10$.

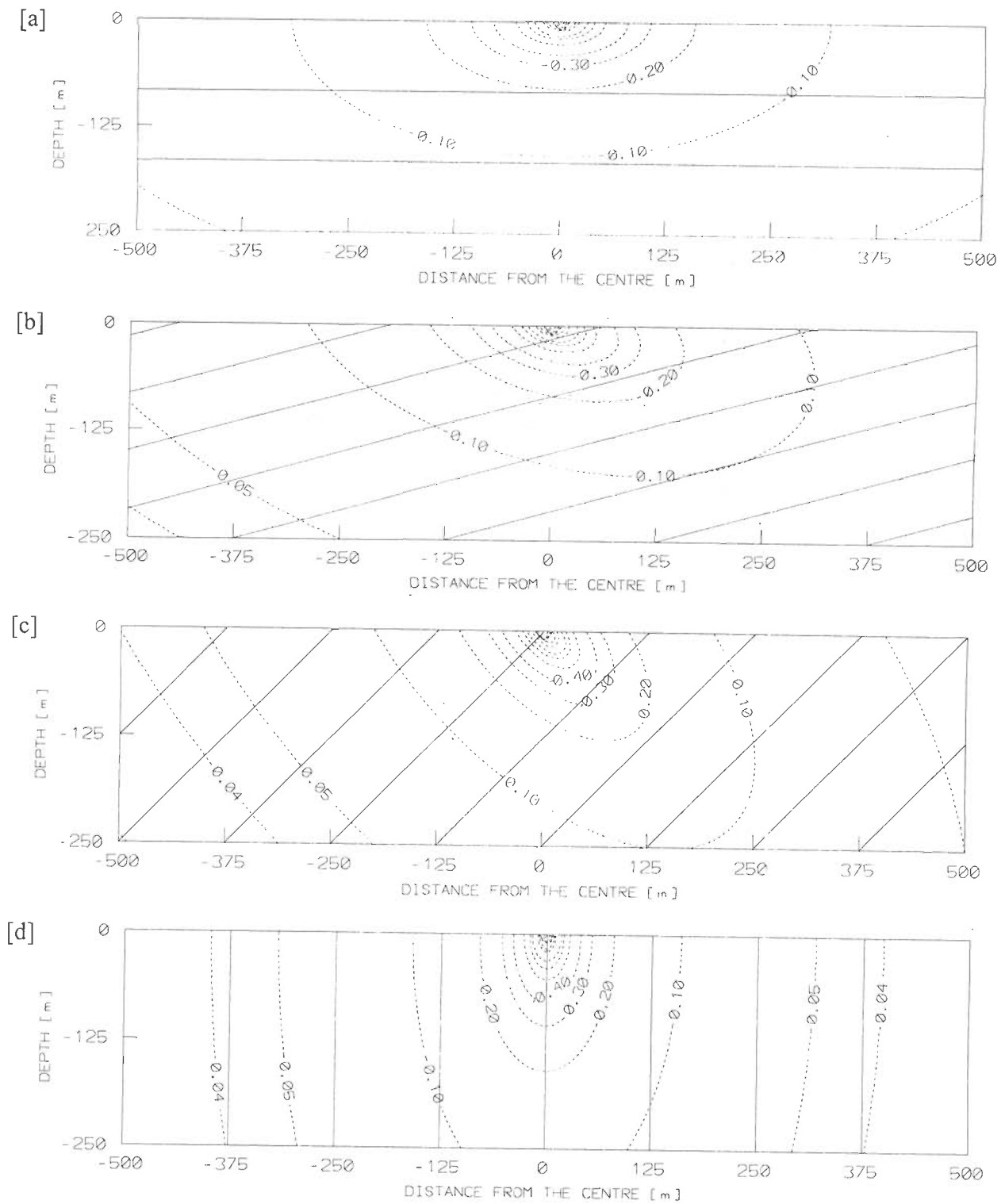


Fig. 4.4 Equipotential contours (dotted lines) in a stratified anisotropic aquifer system due to a point source, $Q=0.1\text{m}^3/\text{s}$ for different inclinations (α) of the bedding planes (solid lines) when the coefficient of anisotropy, $\beta=2$. For [a] $\alpha=0$; [b] $\alpha=\pi/12$; [c] $\alpha=\pi/4$; [d] $\alpha=\pi/2$.

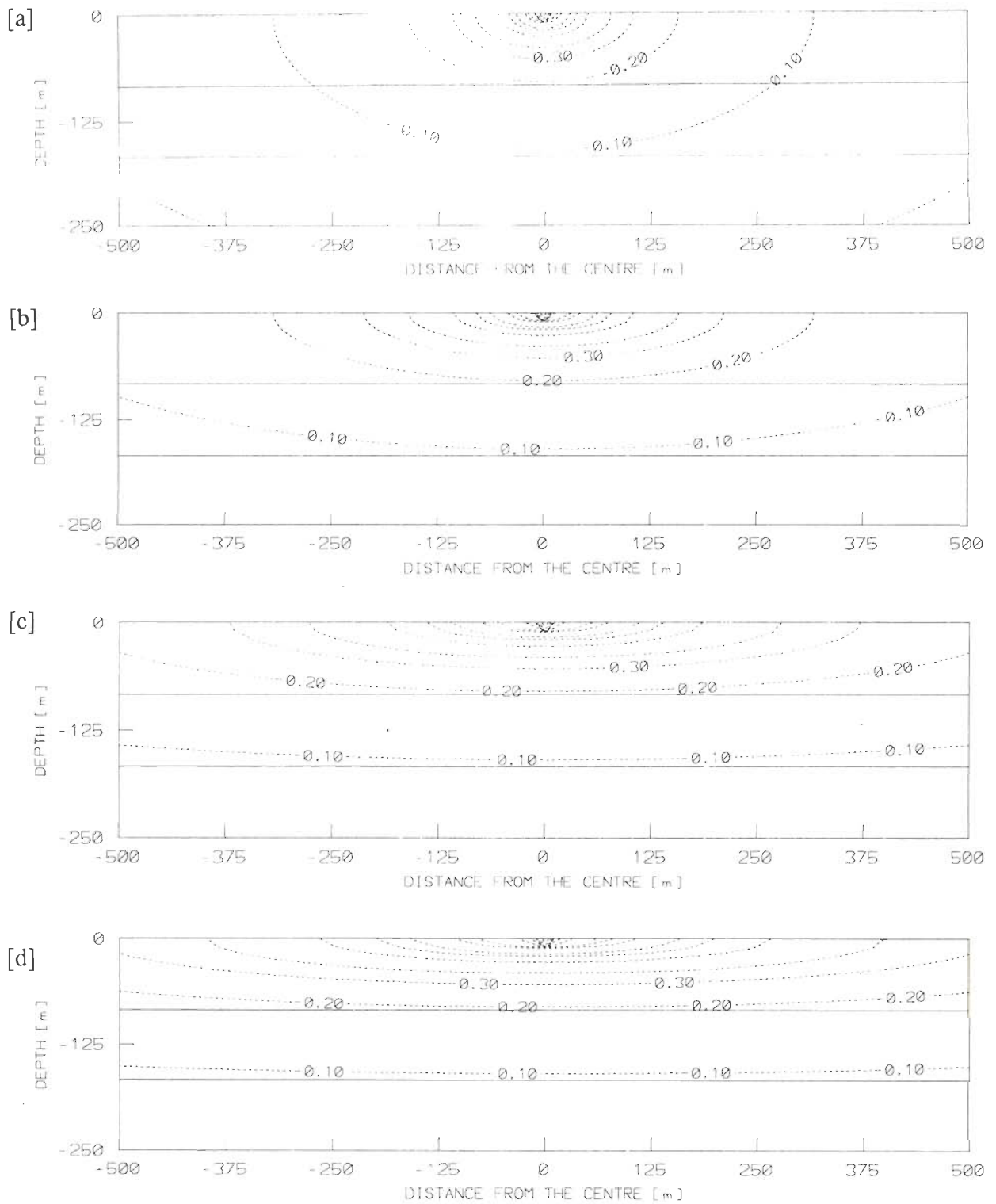


Fig. 4.5 Hydraulic potential distribution in an anisotropic aquifer system due to a point source, $Q=0.1\text{m}^3/\text{s}$ for different coefficients of anisotropy (β) when the angle of dip of the strata, $\alpha=0$. For [a] $\beta=2$; [b] $\beta=4$; [c] $\beta=7$; [d] $\beta=10$.

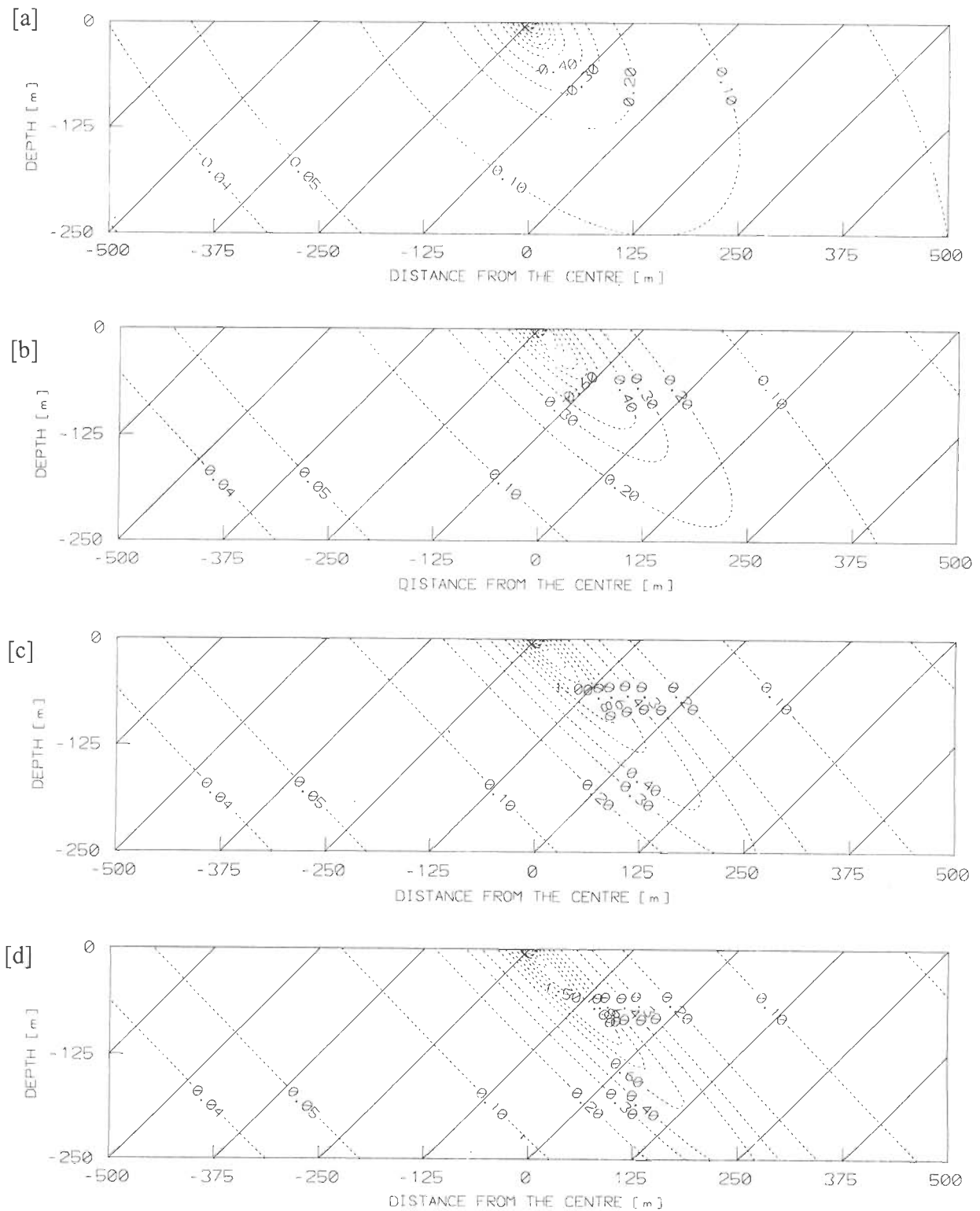


Fig. 4.6 Hydraulic potential distribution in an anisotropic aquifer system due to a point source, $Q=0.1\text{m}^3/\text{s}$ for different coefficients of anisotropy (β) when the angle of dip of the strata, $\alpha=\pi/4$. For [a] $\beta=2$; [b] $\beta=4$; [c] $\beta=7$; [d] $\beta=10$.

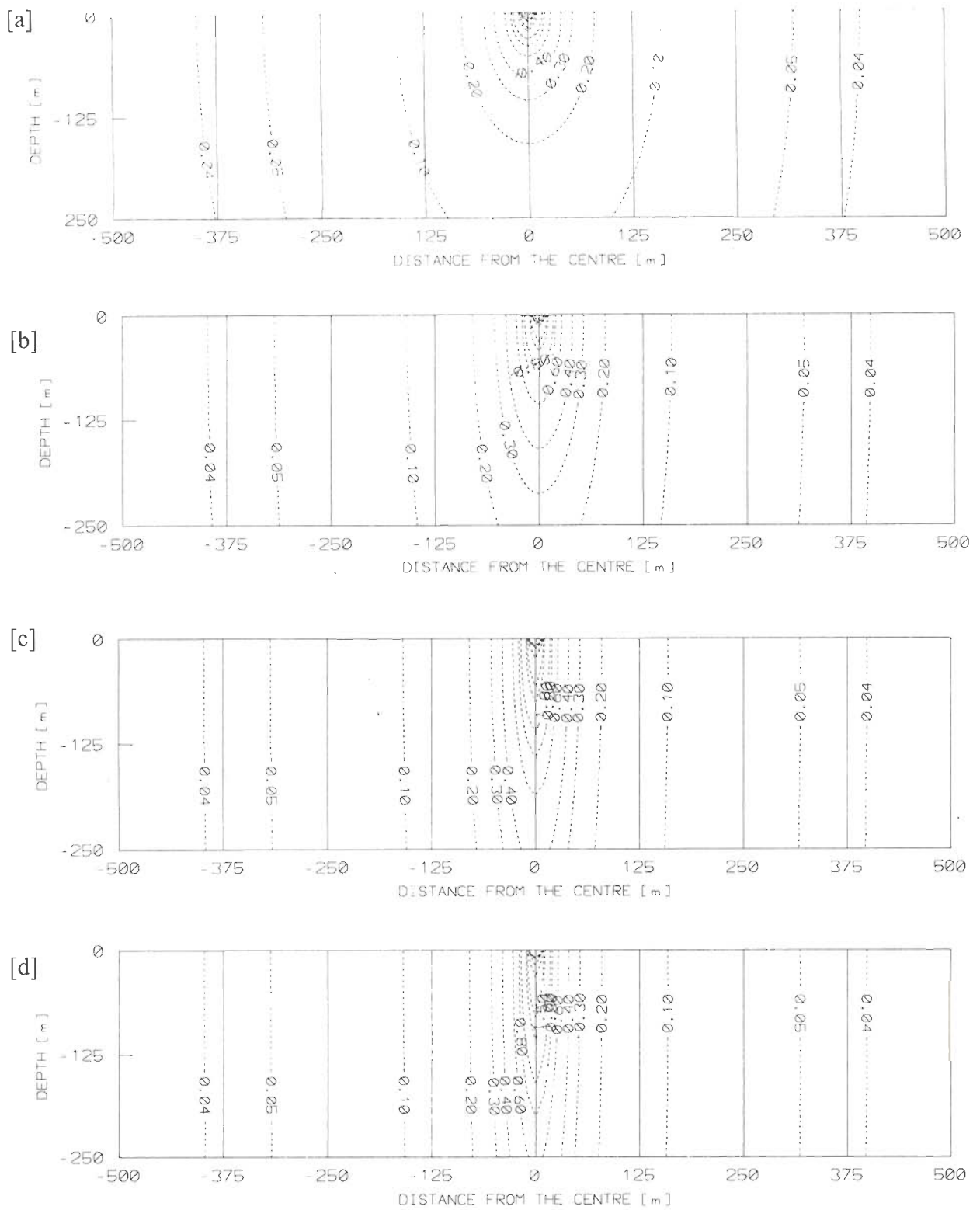


Fig. 4.7 Hydraulic potential distribution in an anisotropic aquifer system due to a point source, $Q=0.1\text{m}^3/\text{s}$ for different coefficients of anisotropy (β) when the angle of dip of the strata, $\alpha=\pi/2$. For [a] $\beta=2$; [b] $\beta=4$; [c] $\beta=7$; [d] $\beta=10$.

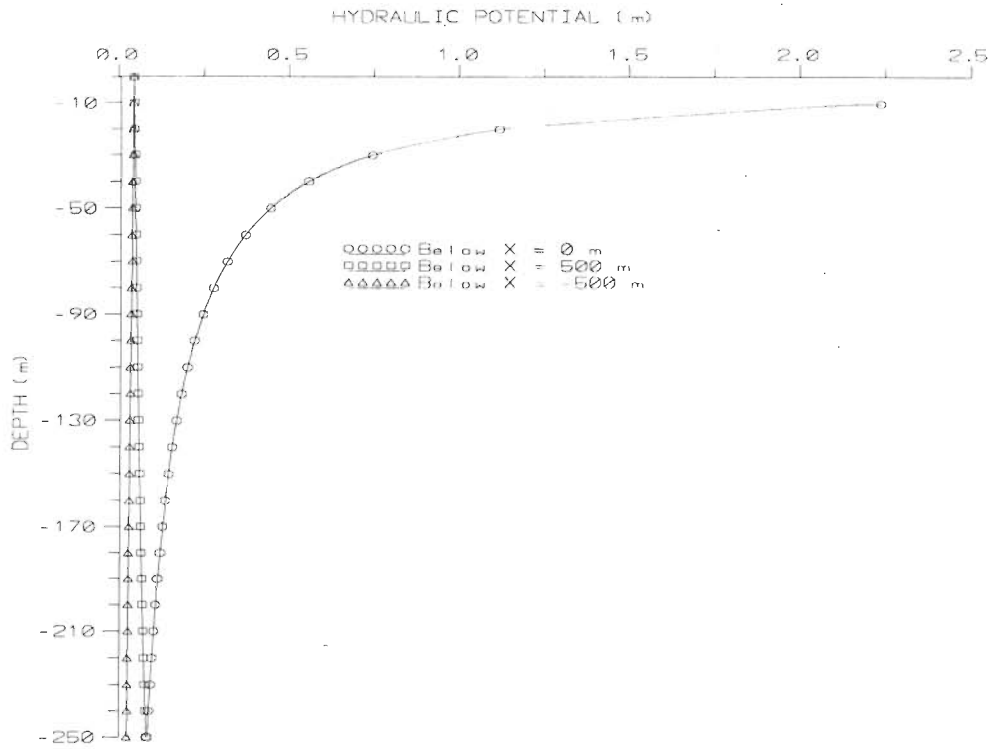


Fig. 4.8 Distribution of hydraulic potentials due to a point source, $Q=0.1\text{m}^3/\text{s}$ in the vertical section of the anisotropic aquifer system for $\alpha=\pi/4$ and $\beta=10$.

α , towards the right of the source) are different. Therefore, unlike the an isotropic aquifer, there is no symmetry of radial flow exhibited by the anisotropic aquifer system.

4.5.2 AQUIFER SIMULATIONS WITH FINITE-LENGTH LINE SOURCE

The aquifer parameter values used for the simulation of hydraulic potentials due to a finite-length line source and the various sets of simulations performed using the algorithm HANI-L are given in Table 4.3 and Table 4.4, respectively.

Table 4.3 Aquifer Parameter values used for the numerical simulations of hydraulic potentials due to a finite-length line source.

Model Parameters	Numerical Values
Source strength, Q_L	0.01 m ² /s
Length of the line source, $2b$	400 m
Hydraulic conductivity in the major direction, K_1	0.001 m/s
Dip angle of the strata, α	0, $\pi/12$, $\pi/4$, $\pi/2$
Coefficient of anisotropy, β	2, 4, 7, 10
Ratio of hydraulic conductivity values, K_1/K_2	4, 16, 49, 100
Grid dimensions	Y= (-500 m, +500 m), Z= (0, -250 m) $\Delta Y= 10$ m, $\Delta Z= 10$ m

The variation in the pattern of the hydraulic potentials due to the finite-length line source with different orientations of the strata are illustrated in Fig. 4.9. The equipotentials (dotted lines) are plotted for different angles of dip of the strata viz., $\alpha=0$, $\alpha=\pi/12$, $\alpha=\pi/4$ and $\alpha=\pi/2$, when the coefficient of anisotropy, $\beta=4$.

When the stratification is perfectly horizontal, the pattern of recharge due to a finite-length line source in the homogeneous anisotropic aquifer system with varying anisotropy levels can be inferred from Fig. 4.10. A similar set of plots are also given [Fig. 4.11] for the case when the aquifer

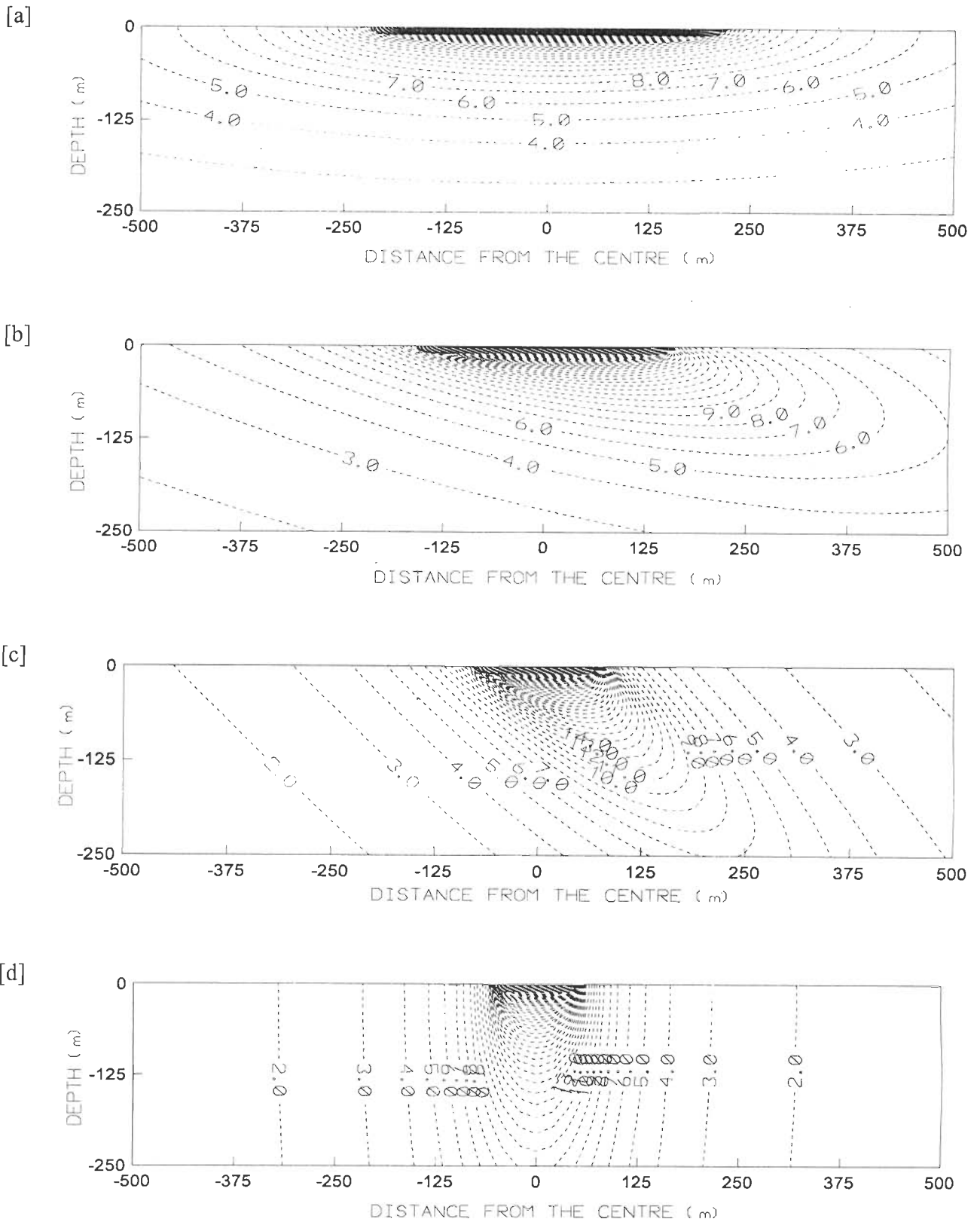


Fig. 4.9 Equipotential distribution (dotted lines) in a homogeneous anisotropic aquifer system due to a finite-length line source for different inclinations (α) of the beds when the coefficient of anisotropy, $\beta=4$. For [a] $\alpha=0$; [b] $\alpha=\pi/12$; [c] $\alpha=\pi/4$; [d] $\alpha=\pi/2$.

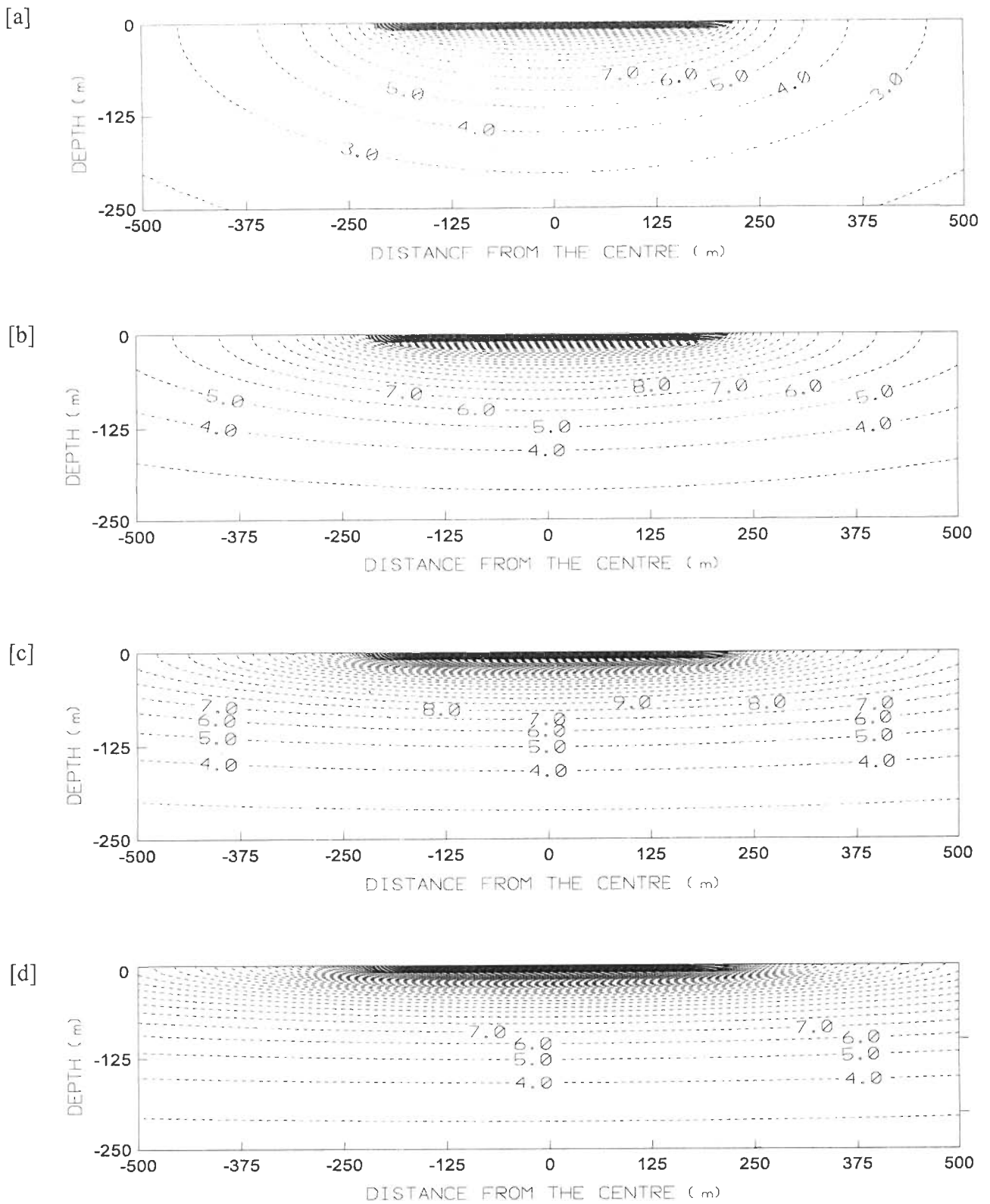


Fig. 4.10 Hydraulic potentials in an anisotropic aquifer system due to a finite-length line source of strength, $Q_L=0.01 \text{ m}^2/\text{s}$ for different coefficients of anisotropy (β) when the angle of dip, $\alpha=0$. For [a] $\beta=2$; [b] $\beta=4$; [c] $\beta=7$; [d] $\beta=10$.

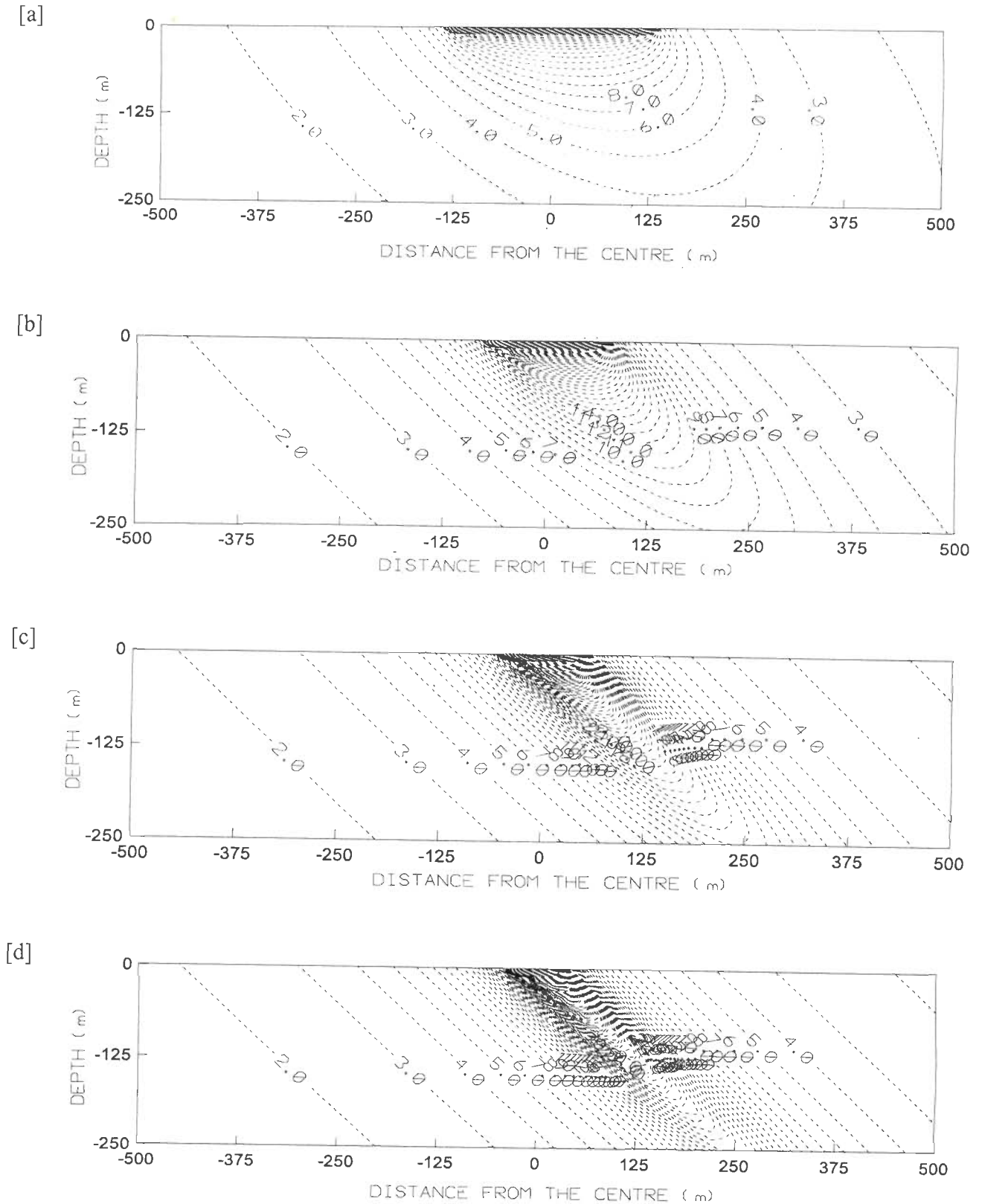


Fig. 4.11 Hydraulic potentials in an anisotropic aquifer system due to a finite-length line source of strength, $Q_L=0.01 \text{ m}^2/\text{s}$ for different coefficients of anisotropy (β) when the angle of dip, $\alpha=\pi/4$. For [a] $\beta=2$; [b] $\beta=4$; [c] $\beta=7$; [d] $\beta=10$.

Table 4.4 Set of cases where hydraulic potentials due to a finite-length line source have been simulated with different combinations of the angle of dip, α and the coefficients of anisotropy, β .

Hydraulic Potentials due to Line Source in Homogeneous Anisotropic Aquifer System				
Parameters	$\alpha=0$	$\alpha=\pi/12$	$\alpha=\pi/4$	$\alpha=\pi/2$
$\beta=2$	✓	-	✓	-
$\beta=4$	✓	✓	✓	✓
$\beta=7$	✓	-	✓	-
$\beta=10$	✓	-	✓	-

strata is sloping at an angle of 45° with the earth surface. The coefficients of anisotropy applicable to the cases presented in Fig. 4.10 and Fig. 4.11 are $\beta=2$, $\beta=4$, $\beta=7$ and $\beta=10$, respectively.

For all these simulations, the finite-length line source had been oriented along the strike of the bedding planes. Further, the plots have been depicted in a vertical plane through the length of the line source. The plots across the finite-length line source have not been shown as the pattern of those are similar to that of the point-source presented earlier, except for the magnitude of the potential.

4.6 RESULTS AND DISCUSSION

The study encapsulated in the present chapter renders a broad profile on the theory of anisotropic flow in porous media and provides analytical solutions, in the context of advancements made in the theory of exploration geophysics, for computing the hydraulic potentials. Numerical simulation procedures, HANI-P and HANI-L have been devised, using the analytical results developed, to compute the steady state hydraulic potentials in homogeneous anisotropic aquifer systems due to a point source as well as that due to a finite-length line source, respectively.

The hypothetical aquifer systems in which simulations have been carried out are presumably formed by numerous soil strata inclined with the surface. The input to the analytical simulation model includes the source strength, the length of the line source, the hydraulic conductivity values along the principal directions of anisotropy, the angle of dip of the strata and grid dimensions. The various plots presented are representative in nature from a spectrum of possible combinations of coefficient of anisotropy and orientation of bedding planes of the soil strata in homogeneous anisotropic aquifer systems. These illustrations enable to visualise the pattern of distribution of the respective hydraulic potentials (due to a point source or finite-length line source) and behaviour of groundwater flow in the aquifer systems.

RECHARGING IN AN AQUIFER-AQUITARD-AQUIFER SYSTEM: INFLUENCE OF A CONTINUOUS AQUITARD

5.1 GENERAL

The hydrogeological set-up of an aquifer system can influence the seepage from surface water bodies like lakes, recharge-ponds and percolation-tanks to the porous medium. Groundwater flow-barriers/ semi-flow barriers like clay lenses and sedimentary layers are known to exist in alluvial aquifer systems or sedimentary basins. Adept planning and implementation of artificial recharge schemes for such aquifer systems might require knowledge of seepage characteristics and role of hydrogeological controls on recharging. It is perceived that analyses and results based on studies formulated on the recharge in an aquifer-aquitard-aquifer system can be useful in getting insight in identical field situations.

5.2 SCOPE OF THE ANALYSIS

In view of the above, the numerical simulation-analyses have been carried out to bring about dimensionless relationships/ results pertaining to the hydraulic potential distributions and groundwater flow characteristics. The groundwater flow regime, characterised by the hydraulic head/ potential distribution and aquifer parameters, in the aquifer system beneath a recharging surface water body has been studied. Descriptions on the hydrogeological set-up of the layered aquifer system, source/ sink, the boundary set-up, discretisations, methodology as well as the groundwater flow model used are

provided subsequently.

Thus, the hydraulic head/ potential distribution and discharge characteristics for the aquifer-aquitard-aquifer system have been investigated in relation to:

- (i) the positioning of the aquitard at different depths in the aquifer-aquitard-aquifer system and
- (ii) the depth/ the vertical dimension (thickness) of the aquitard.

5.3 METHODOLOGY

The well-known USGS modular three dimensional finite difference groundwater flow model [Mc Donald and Harbaugh 1984] has been employed for simulating hydraulic heads/ groundwater flow. The dimensional matrix arrays have been augmented to accommodate the grid points in the system.

5.3.1 GOVERNING EQUATION

The three dimensional unsteady groundwater flow through heterogeneous and anisotropic porous earth material is given by the partial differential equation:

$$\frac{\partial}{\partial x} (K_{xx} \frac{\partial h}{\partial x}) + \frac{\partial}{\partial y} (K_{yy} \frac{\partial h}{\partial y}) + \frac{\partial}{\partial z} (K_{zz} \frac{\partial h}{\partial z}) - W = S_s \frac{\partial h}{\partial t} \quad (5.1)$$

where,

- K_{xx}, K_{yy}, K_{zz} : hydraulic conductivities along the major axes of anisotropy
- h : potentiometric head/ hydraulic potential
- W : volumetric flux per unit volume and represents sources and or sinks
- S_s : the specific storage of the aquifer
- t : time

In general, S_s , K_{xx} , K_{yy} and K_{zz} are functions of space, whereas h and W are functions of space and time. Thus, the above equation describes groundwater flow under non-equilibrium conditions in a heterogenous and anisotropic medium. Hence this equation together with specification of groundwater flow conditions at the boundaries of an aquifer system and specification of initial head conditions, constitutes a mathematical model of groundwater flow.

Generally, analytical solutions of the equation referred above are rarely possible. So various numerical methods may be used to arrive at approximate solutions. The well known finite difference method is one such approach. With this method, the continuous system is replaced by a system of simultaneous linear algebraic difference equations and their solution yields values of head at specific points and time. These constitute an approximation to the time varying head distribution that would be given by an analytical solution of the groundwater flow equation.

5.3.2 MODEL DESCRIPTION

white cell

Development of the groundwater flow equation in finite difference form follows from the application of the continuity equation: the sum of all flows into and out of a cell must be equal to the rate of change in storage within the cell. The finite difference approximation for any cell (i,j,k) in the grid may be obtained as:

$$\begin{aligned} & CR_{i,j-\frac{1}{2},k} (h_{i,j-1,k} - h_{i,j,k}) + CR_{i,j+\frac{1}{2},k} (h_{i,j+1,k} - h_{i,j,k}) + CC_{i-\frac{1}{2},j,k} (h_{i-1,j,k} - h_{i,j,k}) + CC_{i+\frac{1}{2},j,k} (h_{i+1,j,k} - h_{i,j,k}) \\ & + CV_{i,j,k-\frac{1}{2}} (h_{i,j,k-1} - h_{i,j,k}) + CV_{i,j,k+\frac{1}{2}} (h_{i,j,k+1} - h_{i,j,k}) + P_{i,j,k} h_{i,j,k} + Q_{i,j,k} \\ & = SS_{i,j,k} (\Delta r_j \Delta c_i \Delta v_k) \Delta h_{i,j,k} / \Delta t \end{aligned} \quad (5.2)$$

where,

$CR_{i,j-\frac{1}{2},k}$: the conductance in row i and layer k between nodes $i,j-1,k$ and i,j,k

$CC_{i-\frac{1}{2},j,k}$: the conductance in column j and layer k between modes $i-1,j,k$ and i,j,k

$h_{j,k}$: the head in cell i,j,k
$CV_{i,j,k-1/2}$: the conductance in row i and column j between nodes $i,j,k-1$ and i,j,k
$P_{i,j,k}$: certain constant for cell i,j,k
$SS_{i,j,k}$: specific storage of cell i,j,k
$Q_{i,j,k}$: groundwater flow rate into cell i,j,k
$\Delta r_j \Delta c_i \Delta v_k$: volume of cell i,j,k
Δt	: increment in time

The above equation can be rewritten in backward-difference form by specifying flow terms at t_m , end of the time interval, and approximating the time derivative of head over the interval t_{m-1} to t_m as:

$$\begin{aligned}
& CR_{i,j-1/2,k}(h_{i,j-1,k}^m - h_{i,j,k}^m) + CR_{i,j+1/2,k}(h_{i,j+1,k}^m - h_{i,j,k}^m) + CC_{i-1/2,j,k}(h_{i-1,j,k}^m - h_{i,j,k}^m) + CC_{i+1/2,j,k}(h_{i+1,j,k}^m - h_{i,j,k}^m) + \\
& CV_{i,j,k-1/2}(h_{i,j,k-1}^m - h_{i,j,k}^m) + CV_{i,j,k+1/2}(h_{i,j,k+1}^m - h_{i,j,k}^m) + P_{i,j,k}h_{i,j,k-1}^m + Q_{i,j,k} \\
& = SS_{i,j,k}(\Delta r_j \Delta c_i \Delta v_k) \{ (h_{i,j,k}^m - h_{i,j,k}^{m-1}) / (t_m - t_{m-1}) \}
\end{aligned} \tag{5.3}$$

If an equation of this type is formulated for each of the 'n' cells in the gridded system, then we are left with a system of 'n' equations in 'n' unknowns and the set of equations can be solved for obtaining the unknown head values for each of the cells. In the finite difference method, the continuous system described by the governing equation is replaced by a finite set of discrete points in space and time and the partial derivatives are replaced by differences between functional values at these points. This requires discretisation of the aquifer system into grids forming rows, columns and layers. To conform with computer array conventions an i, j, k , coordinate system is used where i is the row index j is the column index and k is the layer index. Nodes represent cell within which the hydraulic properties are constant. Hence, any value associated with a node is distributed over the extent of the cell. The width of the cells along row is designated as Δr_j for the j^{th} column and that along the column is Δc_i for the i^{th} row. Now, the volume of the grid cell located at (i,j,k) is $\Delta r_j \Delta c_i \Delta v_k$, where Δv_k is the thickness of the layer k .

The block-centred formulation is used for defining the configuration of cells for the present study, wherein the cells are formed by parallel lines and the mid-points are the nodes. For each block, the hydraulic properties are uniform over the extent of a cell.

5.3.3 BOUNDARY CONDITIONS

In the discretised aquifer system, the number of equations is equal to the number of 'variable-head' cells; variable-head cells are those in which head may vary with time. Cells that are not variable-head cells may be either 'constant head' or 'no-flow' cells. Constant head cells are those in which head remains constant with time and no-flow cells are those to which there is no flow from adjacent cells. Thus, the type of boundaries that may be imposed in the model include, constant head, no-flow, constant-flow and head-dependent flow.

5.3.4 SOLUTION PROCEDURE

An iterative method known as the Strongly Implicit Procedure (SIP) has been used to obtain the solutions. An interim solution is obtained and it becomes the new trial solution and the procedure is repeated until a specified 'closure criterion' is met. For the present simulations, a closure criterion is set so that the difference between two successive iterative solutions is less than 10^{-4} m.

5.4 MODEL CONCEPTUALISATION

The scheme of the layered aquifer system considered for the investigation is depicted in plan [Fig. 5.1] as well as cross-section [Fig. 5.2]. A rectangular-shaped water body (the source) of size, $2w \times 2w$ is located at the centre of the plan area of an isotropic aquifer system having dimensions, $2L \times 2L$. The bottom of the aquifer system conforms to an impermeable bed at depth, D . An aquitard, positioned within the aquifer system, partitions the porous medium into an unconfined top-aquifer and a semi-

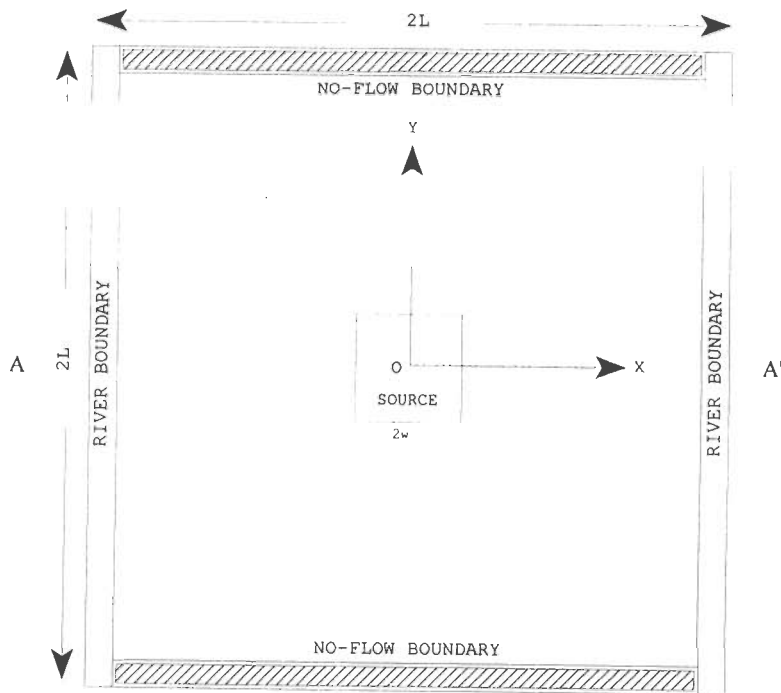


Fig. 5.1 Plan-view of the aquifer-aquitard-aquifer system with a recharging-source.

I would appreciate a line about the possibility of having unit recharge for 500 days from a source from practical point of view

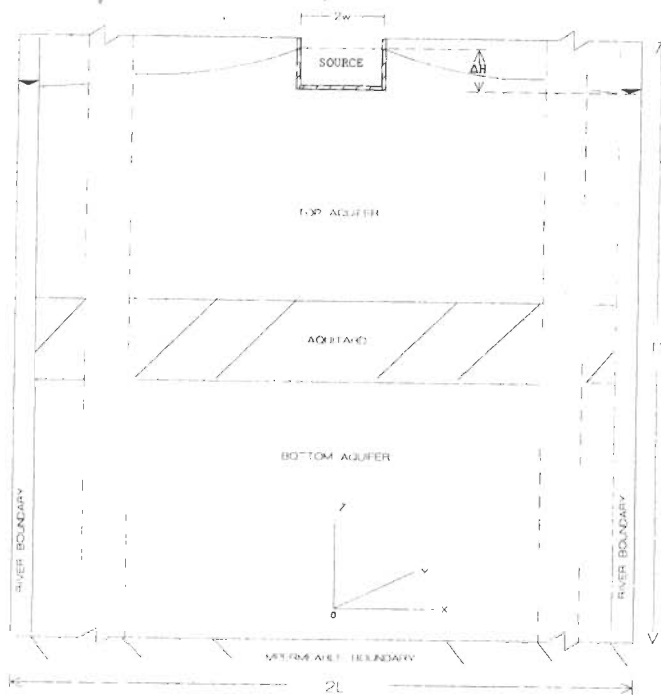


Fig. 5.2 Vertical cross-section (through AA' of Fig. 5.1) of the aquifer-aquitard-aquifer system with the recharging-source.

confined bottom-aquifer. The lateral boundaries of the aquifer system are fully penetrating constant head rivers (the sinks) on two sides while the other two sides are no-flow boundaries. These boundaries have been located at sufficiently large distance, L from the source. The sides and bottom of the water body are assumed to have a layer of sediments of low permeability. Difference between the head in the source and that in the sink (H_b), the head causing-flow (ΔH) is adequate to induce groundwater flow through the aquifer system. Appropriate parameter values have been assigned for the aquitard so as it to act like a groundwater flow barrier between the top and bottom aquifers.

5.4.1 DISCRETISATION

The domain discretisation has been done with the half-width, $L=4000\text{m}$ and the depth, $D=100\text{m}$ for the aquifer system. The water levels of the source and the constant head boundaries have been so maintained that a head-causing-flow, $\Delta H=9\text{m}$ is effected for the simulations. The area in plan [Fig. 5.1] is nearly 700 times that of the surface area of the water body. Thus, the respective ratio of their lateral sides is about 26. To facilitate the finite difference application of the groundwater flow equations of the model, the aquifer system has been discretised into 51 rows, 51 columns and 10 model layers, resulting in 26,010 rectangular grids. Variable grid spacing has been adopted appropriately to enable detailed information from finer grids beneath and surrounding the source.

Aquifer parameters that are well within the naturally permissible range [Freeze and Cherry 1979] have been assigned suitably for the aquifers and the aquitard. For simplicity, uniform hydraulic conductivities are assigned for both the horizontal and vertical directions in a layer. Aquifer parameters, however, may vary from one layer to another. For the simulations presented in this chapter, hydraulic conductivity for the aquitard and that for the aquifer differs by two orders of magnitude (0.0003m/s and 0.000003m/s respectively). A specific yield of 15% has been assigned for the unconfined layers above the aquitard. Storage coefficient values for the aquitard and the bottom aquifer are 0.001 and 0.000001 , respectively. The wetted-surface (sides and bottom) of the water body ^ppresumed to have a layer of

pl. well.

normally higher K and S go together
unless it is very special formation

without simulated by low k. new layer?

sediments of low permeability. The water levels in the source and the sinks are kept constant during the stress period of the simulation.

Transient simulation of groundwater flow has been carried out. A stress period of 500 days consisting of 50 time-steps ^($\Delta t = 10/191$) has been chosen for the simulations to attain steady-state. The hydraulic head/ potentials at the nodes of the medium and volumetric details have been obtained at the end of selected time steps during the stress period for further analysis. The cumulative volume of water discharged from the aquifer system at different time-steps during the stress period is found to be rising with increasing simulation time [Fig. 5.3]. It is noticed that rate of change in outflow tends to zero as the length of the simulation period approaches 500 days [Fig. 5.4], an indication of steady state condition. Further, the hydraulic heads tend to approach steady state as the time-step advances [Fig. 5.5].

5.5 ANALYSIS AND DISCUSSION

simulation The following general assumptions hold good ^{are considered for the conceptual model to compute the} for the simulation of hydraulic potentials and groundwater flow due to the recharging source in the aquifer-aquitard-aquifer system:

- (i) The layers are parallel to the ground surface and are continuous,
- (ii) The hydraulic parameters vary from layer to layer only, (i.e., distinct layers are homogeneous and isotropic in itself),
- (iii) Uniform horizontal and vertical hydraulic conductivities in distinct layers,
- (iv) Aquifer system is of finite dimensions with boundaries specified for all the sides,
- (v) Groundwater flow is predominantly towards the constant-head river boundaries,
- (vi) Uniform seepage from the source during simulations,
- (vii) No change in the properties of the fluid during simulations,
- (viii) Darcian flow of groundwater,
- (ix) Transient simulations for different time-steps until steady state condition,

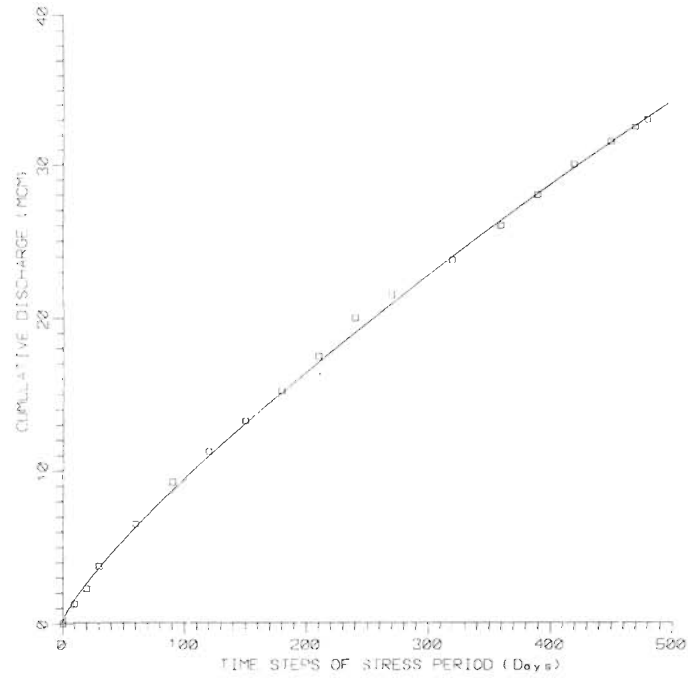


Fig. 5.3 Cumulative discharge from the aquifer system for various time steps.

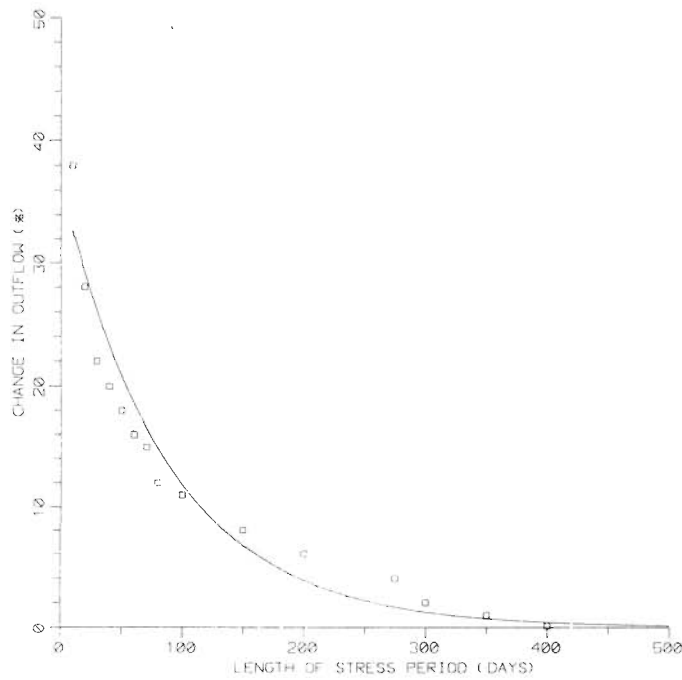


Fig. 5.4 Progress of transient simulations with length of the stress period, eventually approaching steady-state condition.

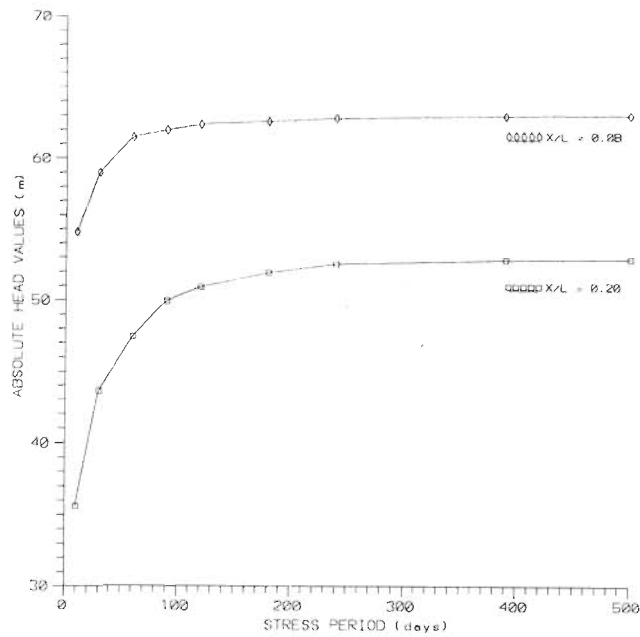


Fig. 5.5 Absolute values of hydraulic head approaching steady state with progress of time-steps at two sections in the aquifer system.

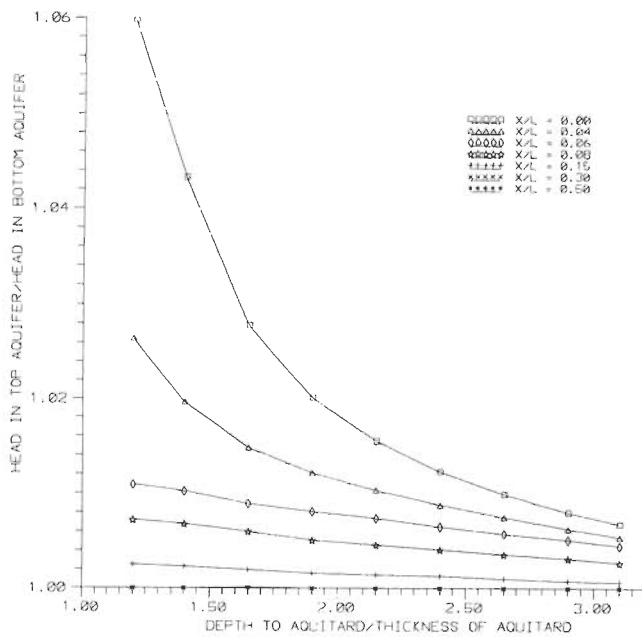


Fig. 5.6 Effect of the aquitard at different depths: Aquitard Depth Ratio (ATDR) versus Aquifer Head Ratio (AFHR) at different Normalised Distances (X/L)

5.5.1 TERMINOLOGY

The following dimensionless quantities have been defined to facilitate the analyses:

- For better clarity these should be shown by notations i.e. AFHR = $\frac{h_u}{h_b}$*
- (i) *Aquifer Head Ratio (AFHR)*: The ratio of hydraulic potential in the unconfined aquifer above the aquitard to that in the semi-confined aquifer below the aquitard (bottom aquifer).
 - (ii) *Aquifer Thickness Ratio (AFTR)*: The ratio of the thickness of the top aquifer to the thickness of the bottom aquifer. *AFTR =*
 - (iii) *Aquitard Depth Ratio (ATDR)*: The ratio of depth of the top surface of the aquitard to the thickness of the aquitard.
 - (iv) *Aquitard Head Ratio (ATHR)*: The ratio of hydraulic potential in the unconfined aquifer above the aquitard (top aquifer) to that in the aquitard.
 - (v) *Discharge Ratio (DISR)*: The ratio of average discharge per unit width of the top aquifer to that of the bottom aquifer.
 - (vi) *Normalised Distance (X/L)*: The distance from the centre of the source to any arbitrary point in the X-direction (X) normalised with respect to the half width (L) of the system.

5.5.2 EFFECT OF DEPTH-WISE POSITIONING OF THE AQUITARD ON RECHARGING

It has been observed that there is no significant change between hydraulic head values of consecutive nodes beyond a normalised distance, $X/L=0.5$. Thus, the groundwater flow regime under the present set-up is unaffected by any boundary effects. Table-5.1 lists the different cases for which simulation-analyses have been carried out. All diagrams are depicted in the vertical section through the source.

$$AFHR = \frac{h_u}{h_b}$$

$$AFTR =$$

Table 5.1 Aquitard Depth Ratios (ATDR) and Aquifer Thickness Ratios (AFTR) used.

Cases	1	2	3	4	5	6	7	8	9
ATDR	1.20	1.40	1.65	1.90	2.15	2.40	2.65	2.90	3.10
AFTR	0.40	0.50	0.70	0.80	1.10	1.40	1.80	2.30	3.00

Simulations are carried out with the aquitard positioned at various depths. This is facilitated by changing the thicknesses of the model layers in the top aquifer and/or thicknesses of the model layers in the bottom aquifer while preserving the original dimensions of the aquifer system.

Figure 5.6 depicts the variation of average values of hydraulic heads in the top aquifer and bottom aquifer as a result of locating the aquitard at different depths in the aquifer-aquitard-aquifer system. The ratio of average hydraulic potentials in the top and bottom aquifers are plotted against the aquitard depth ratios (ATDR) to visualise the influence of positioning of the aquitard in the system. The ratio of heads has also been plotted for various normalised distances (X/L) reflecting the behaviour with respect to distance from the centre of the system.

It may be observed that as the aquitard depth ratio (ATDR) increases the hydraulic potential in the top aquifer and that in the one below the aquitard steadily approaching the same value. Beyond ATDR=3.0, the difference is negligibly small. In fact, with increasing aquitard depth ratios (ATDR), the aquitard of constant thickness is being placed at deeper depths. In other words, when the aquitard is nearer to the source it transmits groundwater flow due to potential build-up above compared to that below the aquitard. At depth ratios higher than 3.0 the influence of the aquitard is apparently diminishing and no vertical flow is taking place as the hydraulic potentials stabilise throughout.

The maximum difference in the head values for all aquitard depth ratios (ATDR) have been plotted [Fig. 5.8] for different normalised distances (X/L). Further, difference of hydraulic potentials in the top and bottom aquifer is waning as one moves away from the centre ($X/L = 0$) and eventually

becomes insignificant beyond normalised distance, $X/L = 0.5$ [Fig. 5.8]. This behaviour has been verified by examining the ratio of heads in the top aquifer and aquitard also [Fig. 5.7].

Head ratios approach unity beyond aquitard depth ratio, $ATDR=3.0$ and also beyond normalised distance, $X/L=0.5$. Nonetheless, there is a marked reduction in the magnitude of the head ratios signifying higher potentials in the aquitard compared to the bottom aquifer. Accordingly, the hydraulic potential distribution in the vertical plane is one which is gradually decreasing from top aquifer to bottom aquifer through aquitard as well as from centre to boundaries when the aquitard is nearer to the source. This hydraulic potential difference results in a vertical gradient sustaining groundwater flow toward the bottom aquifer through the aquitard. Precisely, the hydraulic potentials tend to be uniform everywhere in the aquifer-aquitard system for aquitard depth ratios ($ATDR$) and normalised distances (X/L) larger than certain critical values, thereby nullifying the influence of aquitard present.

The aquifer head ratios ($AFHR$) and the aquitard head ratios ($ATHR$) have been traced [Figs. 5.9a - 5.9c] against the normalised distances (X/L) for different aquifer thickness ratios ($AFTR$). It may be noticed that the $AFHR$ and $ATHR$ are gradually decreasing when the aquifer thickness ratio ($AFTR$) increases. Also, the difference between these head ratios is diminishing and approaching unity for higher values of $AFTR$, marking uniform potentials everywhere in the system [Figs. 5.9b&5.9c].

Thus, if the top aquifer is deeper by three times or more the depth of the bottom aquifer, then the influence of the aquitard on seepage is not manifested in the system. The same is true when the aquitard is located at a depth greater than three times its thickness.

5.5.3 EFFECT OF AQUITARD THICKNESS ON RECHARGING

The effect of vertical dimension (thickness) of the aquitard on the groundwater flow has also been investigated. The aquitard depth ratio ($ATDR$) has been retained while changing the aquitard

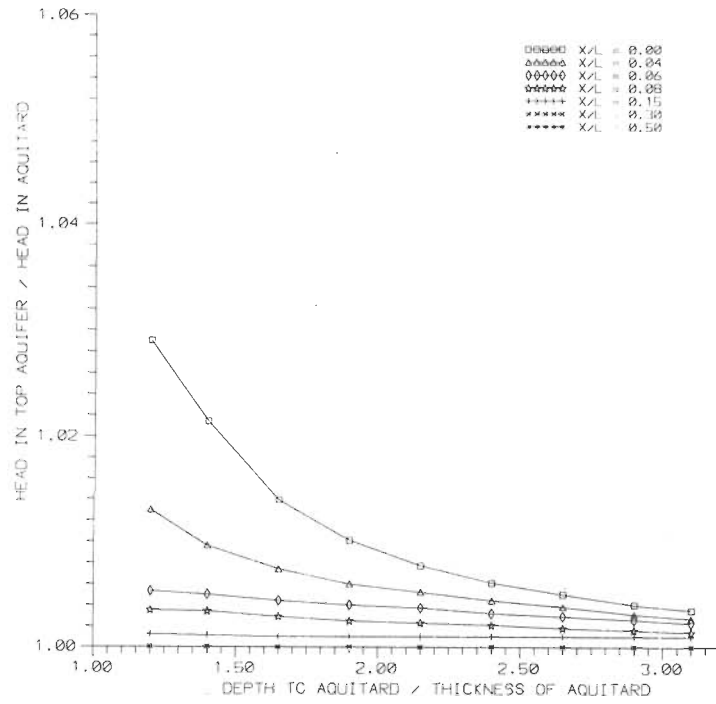


Fig. 5.7 Aquitard Depth Ratio (ATDR) versus Aquitard Head Ratio (ATHR) for different Normalised Distances (X/L).

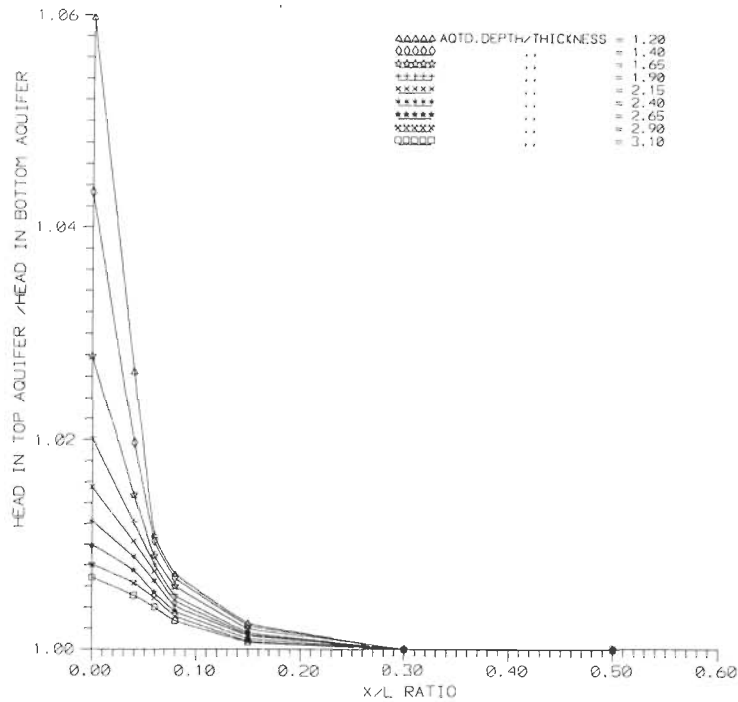


Fig. 5.8 Normalised Distance (X/L) versus Aquifer Head Ratio (AFHR) for different Aquitard Depth Ratios (ATDR).

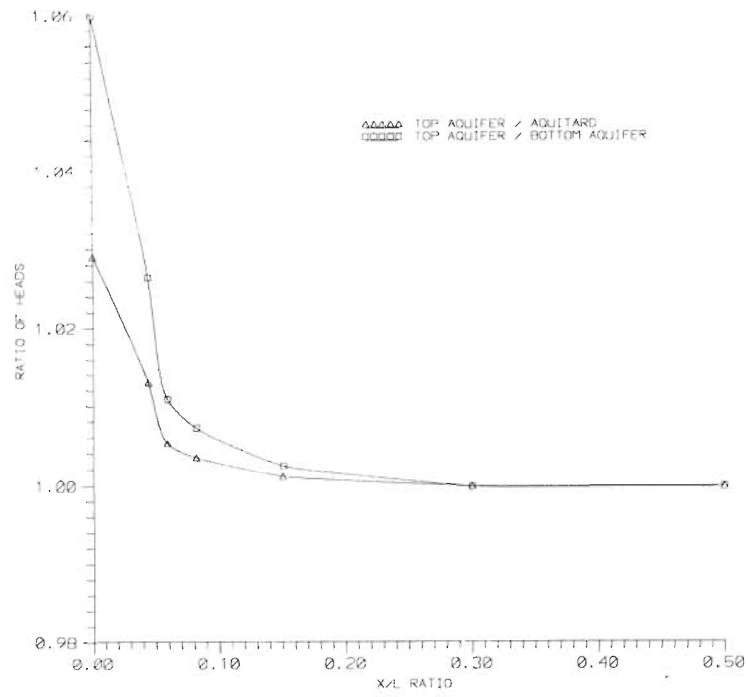


Fig. 5.9a Normalised Distance (X/L) versus Aquitard Head Ratio (ATHR) as well as Aquifer Head Ratio (AFHR) for a given Aquifer Thickness Ratio, AFTR=0.40.

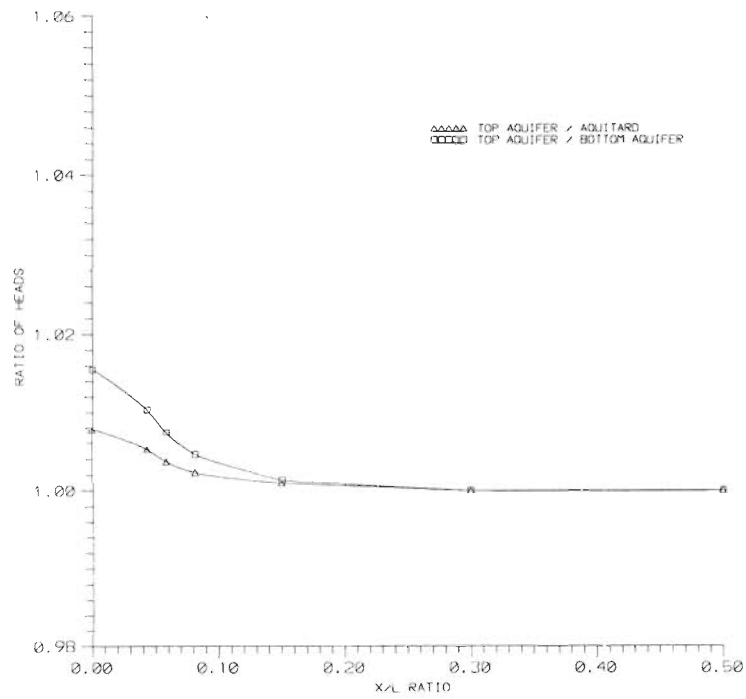


Fig. 5.9b Normalised Distance (X/L) versus Aquitard Head Ratio (ATHR) as well as Aquifer Head Ratio (AFHR) for a given Aquifer Thickness Ratio, AFTR=1.10.

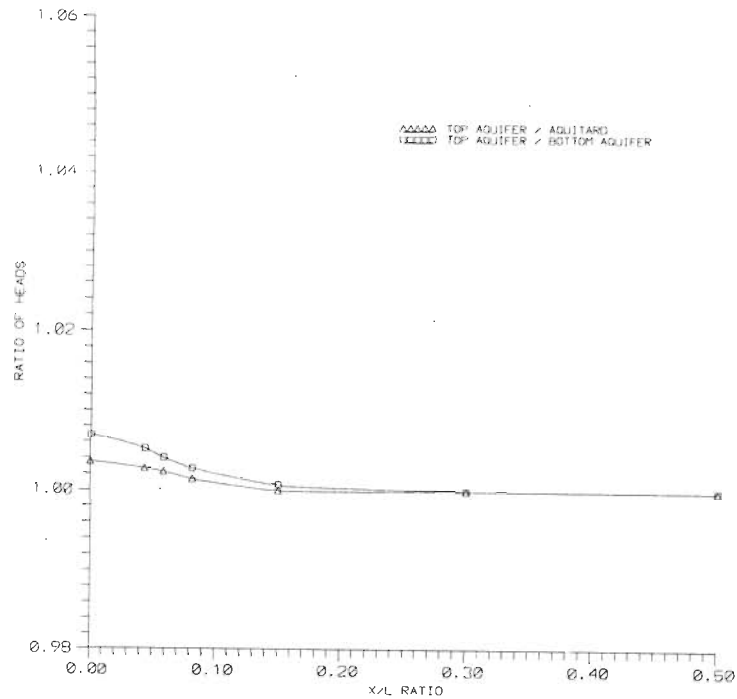


Fig. 5.9c Normalised Distance (X/L) versus Aquitard Head Ratio (ATHR) as well as Aquifer Head Ratio (AFHR) for a given Aquifer Thickness Ratio, $AFTR=3.0$.

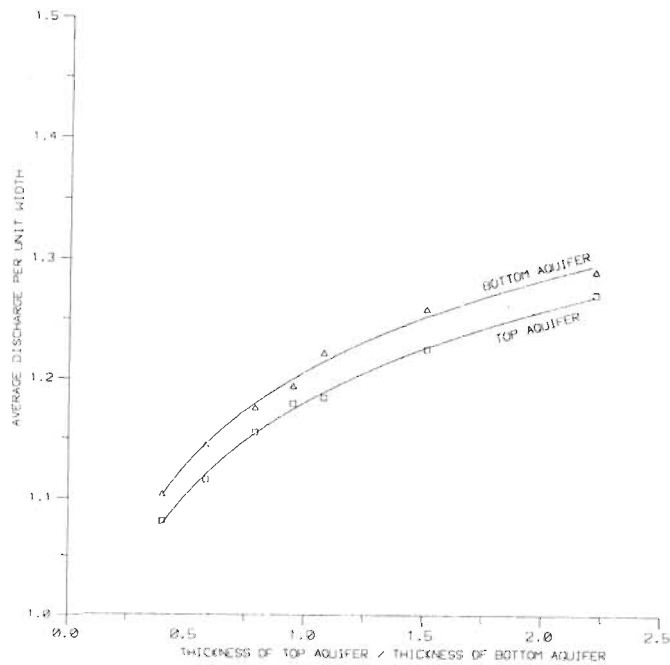


Fig. 5.10 Aquifer Thickness Ratio (AFTR) versus Average Discharge (DISR) in the top aquifer and bottom aquifer for a given Aquitard Depth Ratio, $ATDR=2.15$.

thickness.

Table 5.2 Discharge Ratios (DISR) for different Aquifer Thickness Ratios (AFTR) for a fixed Aquitard Depth Ratio, ATDR=2.15 while changing the aquitard thickness.

Cases	1	2	3	4	5	6	7
AFTR	0.40	0.58	0.79	0.95	1.08	1.51	2.22
DISR	0.98	0.97	0.98	0.98	0.97	0.97	0.98

In order to examine the effect of aquitard thickness on the groundwater flow, several cases have been simulated with different aquitard thicknesses [Table-5.2]. The aquitard depth ratio (ATDR) has been kept constant while changing the thickness of the aquitard. The average discharge per unit width for the top and the bottom aquifers have been computed.

The average discharge values are plotted against the aquifer thickness ratios (AFTR) in Fig. 5.10. The average discharge of the bottom aquifer is slightly more than that of the top aquifer for all the cases. However, the groundwater flow tends to stabilise in both the aquifers when the influence of the aquitard gradually diminishes at larger aquifer thickness ratios (AFTR).

5.6 RESULTS

An aquifer-aquitard-aquifer system recharged with a static water body has been subjected to investigation for different hydrogeological set-ups. The analysis leads to the following inferences:

- (i) The influence of the aquitard on the recharging of the aquifer system is not significant when the thickness of the top aquifer is more than three times that of the bottom aquifer. Also, the influence of the aquitard on the recharging is found to be negligible when the aquitard is positioned below a certain depth.

- (ii) The average discharge from the bottom aquifer is slightly more than that of the top aquifer for constant aquitard depth ratios (ATDR). *Why should be explained for fully application of the statement*
- (iii) The groundwater flow tends to become uniform in both the top and bottom aquifers when the influence of aquitard starts diminishing for larger aquifer thicknesses ratios (AFTR) and aquitard depth ratios (ATDR).

RECHARGING IN AN AQUIFER-AQUITARD-AQUIFER SYSTEM: INFLUENCE OF A DISCONTINUOUS AQUITARD

6.1 GENERAL

Existence of very low permeable layers within an aquifer system can influence the recharging of the aquifer system as they can act as partial barriers to groundwater flow. In continuance with the previous investigation (of Chapter 5), the present study aims at evaluating the influence of a discontinuous aquitard in a layered aquifer system on the seepage from a static recharge source. Here, the influence of location of an aquitard discontinuity (an opening in the aquitard which is presumed to be packed with the same porous material as that of the aquifer) as well as the depth-wise position of the discontinuous aquitard within the aquifer-aquitard-aquifer system on the recharging of the aquifer system are investigated. Often, the term *discontinuity* in the aquitard has been synonymously referred to as *opening* in the descriptions.

6.2 SCOPE OF THE ANALYSIS

The issue of heterogeneity pertaining to hydraulic conductivity has been in focus in research. However, the storage coefficient is an equally important parameter in transient groundwater flow systems. The time scale response of a groundwater system is dictated by its diffusivity (hydraulic conductivity divided by specific storage coefficient) and the dynamics of groundwater systems cannot be understood without paying attention to storage coefficient [Narasimhan 1998]. An attempt has been made to study the combined effect of storage coefficient and transmissivity on the hydraulic potential (h) distribution due to seepage from a recharge source in an aquifer-aquitard-aquifer system with a discontinuous aquitard. Hydrogeological conditions similar to the one

postulated in the present study can be found in parts of the basaltic terrain of India [Singh 1998]. As such, the studies contemplated in the present chapter are:

- (i) the effect of aquitard discontinuity (opening) of different dimensions on the seepage from the source (thereby recharging of the aquifer) for different aquifer parameter combinations,
- (ii) the influence of the location (with respect to the source) of the discontinuity in the aquitard on the recharging of the aquifer system, and
- (iii) the influence of positioning of the discontinuous aquitard at various depths in the aquifer system on the recharge characteristics of the aquifer system

6.3 METHODOLOGY

The USGS modular three dimensional finite difference groundwater flow model [Mc Donald and Harbaugh 1984] has been used for effecting the simulations. Descriptions on the governing equations, flow model, boundary conditions and solution procedure are already given in Chapter 5.

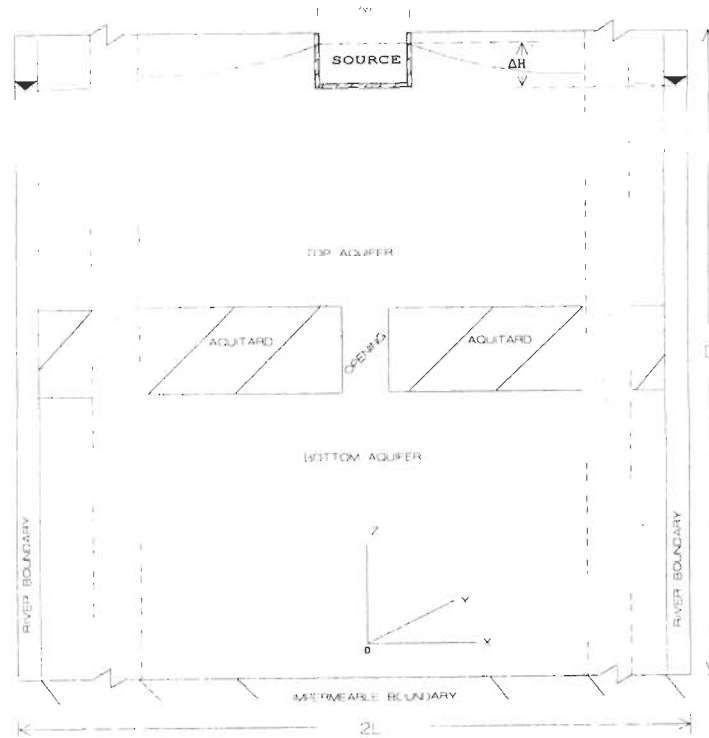
Also, the general assumptions applicable to the simulation studies are the same as that detailed in Chapter 5.

6.4 CONCEPTUALISATION

The conceptualisation of the aquifer domain is similar to that of the study reported in Chapter 5. However, different sets of aquifer parameter combinations have been used with very low aquitard permeability values. Further, provision is provided in the domain discretisation scheme to accommodate discontinuity (opening/ discontinuous-zone) at desired locations in the aquitard, and also to place the aquitard at different depths in the aquifer system. A cross-sectional scheme of the aquifer-aquitard-aquifer system with the discontinuous aquitard is shown in Fig. 6.1; a plan-view of the same is already depicted in Fig. 5.1 of Chapter 5. Simulation of hydraulic potential (h)/ groundwater flow in the aquifer system is carried out for different sets of parameter values and different dimensions of discontinuity in the aquitard.

At least for the first figure, the following no. must be specified

Initial condition of the system also needs to be specified.



PARAMETERS INDEX

K_1
K_M
K_L
L
D
W
q
HR
ΔH
etc.

Fig.6.1

Vertical section of the aquifer system with a discontinuous aquitard in the middle of it.

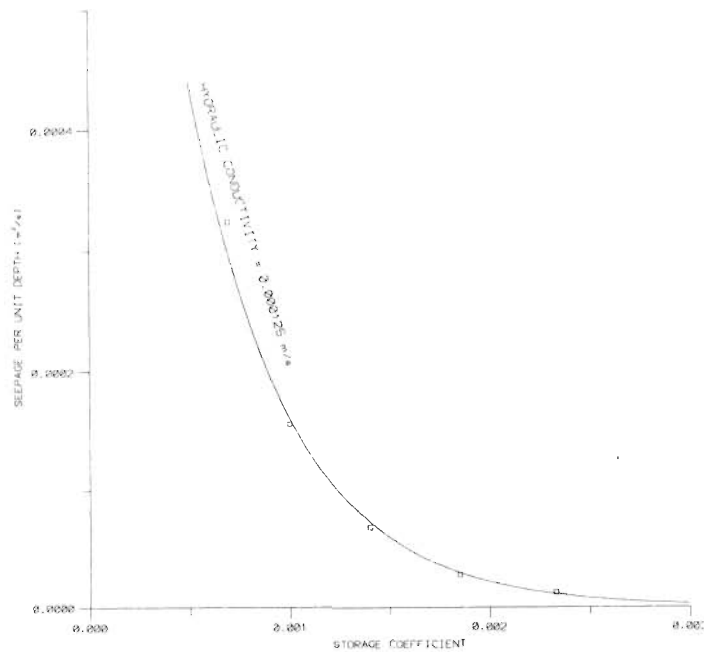


Fig.6.2

Storage Coefficient (S) versus Seepage per unit depth in the aquifer system for a given value of Hydraulic Conductivity, $K=0.000125\text{m/s}$.

The discontinuity in the flow barrier of the present set-up allows hydraulic connection between the aquifer above and below the barrier. Further, the discontinuity is assumed to be filled with the porous aquifer material so as to maintain continuity between the top and bottom aquifers at the discontinuity. The hydraulic conductivity and storage coefficient assigned for the model cells belonging to the opening portion of the aquitard are the same as that for the aquifer portion. Thus, Darcy's law would be applicable to the groundwater flow regime in the aquifer system with the discontinuous aquitard. Appropriate parameter values have been assigned for the discontinuous aquitard so as it to act like a total flow barrier between the top and bottom aquifers except at the discontinuity.

6.5 TERMINOLOGY

To facilitate the analysis of various cases investigated, certain terms have been used as per the following definitions: *use notation and express by notation* } *use schematic diagram for better clarity*

- $F_{sb} = \frac{\text{seepage to bottom aquifer}}{\text{total seepage}}$
- (i) *Fractional Seepage, F_{sb}* : The seepage contribution from the source to the bottom aquifer expressed as a fraction of the total seepage to the system.
 - (ii) *Head Causing Flow, ΔH* : The difference between the head in the source and that in the sink, which induces the seepage into the porous medium and sustains groundwater flow.
 - (iii) *Head in the Boundary, H_b* : Elevation of water column in the constant head river boundary.
 - (iv) *Hydraulic Head/ Potential, h* : The variable representing hydraulic head/ potential in the aquifer system.
 - (v) *Normalised Distance (X/L)*: The distance from the centre of the source to any arbitrary point in the X-direction (X) normalised with respect to the half width (L) of the system.
 - (vi) *Normalised Hydraulic Potential, $h_n = (h - H_b)/\Delta H$* : The ratio of difference between hydraulic potential at any point in the aquifer system and that in the boundary to the head causing flow.
 - (vii) *Percentage Opening, Op* : The dimension of the discontinuity in the aquitard expressed as a percentage of the dimension of the source water body in the X-direction.
 - (viii) *Percentage Shift/ Shift, M_p* : The location of the discontinuity expressed (as percentage) in terms of shifting/ movement from the centre of the aquifer system to the lateral edge of the

water body. Thus, $M_p=0\%$ when the discontinuity is placed below the centre of the water body (i.e., $X/L=0$) and $M_p=100\%$ when the discontinuity is placed below the lateral edge of the water body (i.e., at $X/L = 0.04$). Shift is also expressed in terms of X/L points when the discontinuity is moved beyond the source.

- (ix) *Positioning Depth/ Positioning, P_d* : The position of the discontinuous aquitard in the aquifer system expressed as a ratio between the depth to the aquitard and the total depth of the aquifer system.
- (x) *Reversal Point, X_R* : A point on the X axis between the source and the sink at which the hydraulic potentials are the same for both the top and the bottom aquifers.
- (xi) *S/T Ratio*: The ratio of storage coefficient to transmissivity value of the aquifer; (the reverse of this ratio namely, T/S is known as the *hydraulic diffusivity* of the medium).

6.6 ANALYSIS AND DISCUSSION

In conformity with the objectives, the analyses presented in this chapter deal with the effect of the following aspects on the recharging of the aquifer system:

- (i) different dimensions of the aquitard discontinuity (opening) in a centrally placed aquitard,
- (ii) different locations of the discontinuity in the aquitard, and
- (iii) different depth-wise positions of the discontinuous aquitard in the aquifer system.

An aquitard of very low permeability is positioned within the aquifer system. Had the aquitard been perfect without any discontinuities, essentially no flow would have passed through it. If a discontinuity (an opening) is introduced in the aquitard, groundwater flow can enter the bottom aquifer through it. The resulting detached space in the aquitard which defines the discontinuity is assumed to be filled with the same porous material as that of the top aquifer. The discontinuities have been quantified as percentage opening (O_p) with respect to the width of the source body.

Simulation of groundwater flow has been carried out in the aquifer-aquitard-aquifer system with different sets of parameter values, aquitard discontinuity dimensions and their locations. The

simulation of groundwater flow/ potentials in the aquifer system and the analyses are subjected to the assumptions stipulated in Chapter 5. The hydraulic heads/ potentials (h) in the aquifer system and volumetric details have been obtained at the end of each simulation period. The seepage from the source to the top and the bottom aquifers as well as the discharge to the constant head boundaries have been computed using the aquifer parameters and the hydraulic gradients.

Instead of hydraulic potential (h), its normalised value $[(h - H_b)/\Delta H]$ with respect to the head causing flow (ΔH) and head in the boundary (H_b) has been used in the analyses. Also, the seepage per unit width to the bottom aquifer has been normalised as a fraction of the total discharge from the aquifer system and this fractional seepage (F_{sb}) is found to be useful in the analyses followed.

6.6.1 EFFECT OF DIMENSION OF THE AQUITARD DISCONTINUITY ON RECHARGING

A discontinuity (quantified as percentage opening, O_p) symmetrical with respect to the source, has been provided in the aquitard through which seepage from the source enters the bottom aquifer. For this case, the aquitard exists at midway down in the aquifer system [Fig. 6.1] and the discontinuity is located at the centre of it (i.e., along the Y-axis). While maintaining the physical setup of the aquifer system unaltered, simulation of hydraulic potential (h)/ groundwater flow has been carried out for several cases of percentage opening (O_p) and aquifer parameter combinations [Table-6.1].

The seepage from the source to the top aquifer and that to the bottom aquifer has been computed. For a specified value of the storage coefficient (S), the seepage bears a direct proportionality with respect to hydraulic conductivity (K). However, for a given value of the hydraulic conductivity, there seems to be an inverse relationship between the seepage and the storage coefficient. Evidently, the seepage per unit width being steadily progressing with larger values of the hydraulic conductivity for a constant storage coefficient [Fig. 6.2]. Whereas, the seepage per unit width is receding with increasing values of the storage coefficient for a constant value of the hydraulic conductivity [Fig. 6.3]. Thus, the seepage into the aquifer system is regulated by the hydraulic conductivity (expressed in terms of the transmissivity, T for the vertically averaged

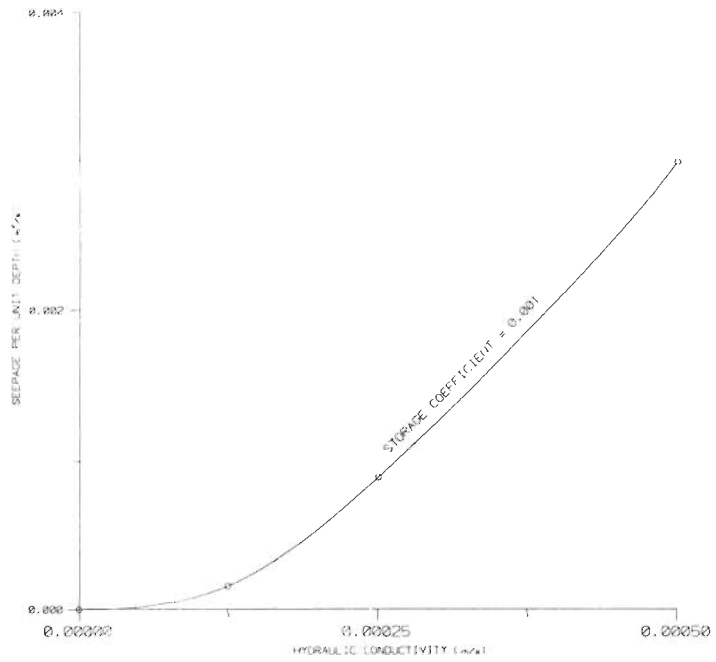


Fig. 6.3 Hydraulic Conductivity (K) versus Seepage per unit depth in the aquifer system for a given value of Storage Coefficient, $S=0.001$.

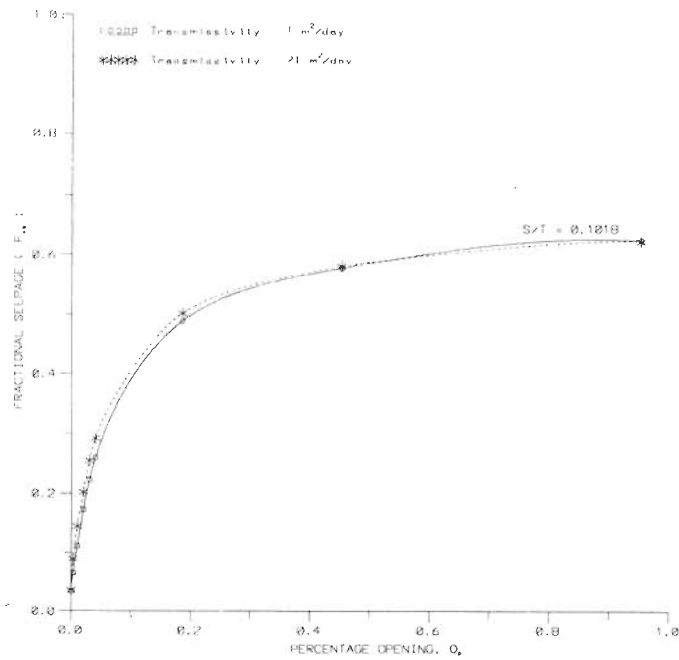


Fig. 6.4 Percentage Openings, O_p versus Fractional Seepage, F_{sb} for two different Transmissivity values (T) while S/T ratio being kept constant.

groundwater flow) and the storage coefficient (S).

Table 6.1 Matrix table of parameter combinations used in different cases.

S/T Ratio	Percentage Opening [O_p]												
	0.0	0.003	0.01	0.02	0.03	0.04	0.2	0.5	1.0	4.0	7.0	30.0	100.0
0.0540	✓	✓	✓	✓	✓	✓	✓	✓	✓	✓	✓	✓	✓
0.1081	✓	✓	✓	✓	✓	✓	✓	✓	✓	✓	✓	✓	✓
0.1500	✓	✓	✓	✓	✓	✓	✓	✓	✓	✓	✓	✓	✓
0.2162	✓	✓	✓	✓	✓	✓	✓	✓	✓	✓	✓	✓	✓
0.3027	✓	✓	✓	✓	✓	✓	✓	✓	✓	✓	✓	✓	✓
0.4000	✓	✓	✓	✓	✓	✓	✓	✓	✓	✓	✓	✓	✓
0.5045	✓	✓	✓	✓	✓	✓	✓	✓	✓	✓	✓	✓	✓
0.6000	✓	✓	✓	✓	✓	✓	✓	✓	✓	✓	✓	✓	✓

To facilitate further analyses, the seepage per unit width occurring in the top as well as the bottom aquifers respectively has been normalised as a fraction of the total. It has been noticed that this fraction, termed as the fractional seepage F_{sb} , bears certain relationship with the ratio of storage coefficient to transmissivity (S/T). Obviously, the quantity S/T represents the reverse of the process commonly known as the hydraulic diffusivity (T/S) of the aquifer system. Precisely, the fractional seepage, F_{sb} is found to be invariant with respect to the ratio, S/T even while specific values of the hydraulic conductivity and/or the storage coefficient vary [Fig. 6.4]. It is observed that the actual discharge from the aquifer system is sensitive to S/T ratio even while the fractional seepage (F_{sb}) is invariant. Thus, all physical parameters being the same and with a constant S/T value, the seepage from the source to the bottom aquifer expressed as a fraction of the total seepage to the system (F_{sb}) remained unaltered even when definite values of S and T are varied. Therefore, fractional seepage (F_{sb}) and S/T ratio are of value in the analyses in addition to the other parameters mentioned earlier.

The equipotential plots for the aquifer system have been drawn for several percentage openings (O_p) and for different values of S/T ratio. Fig. 6.5, Fig. 6.6, Fig. 6.7 and Fig. 6.8 depict the potential distribution in the central section for percentage openings, $O_p=0.2\%$, 1%, 30% and 100%

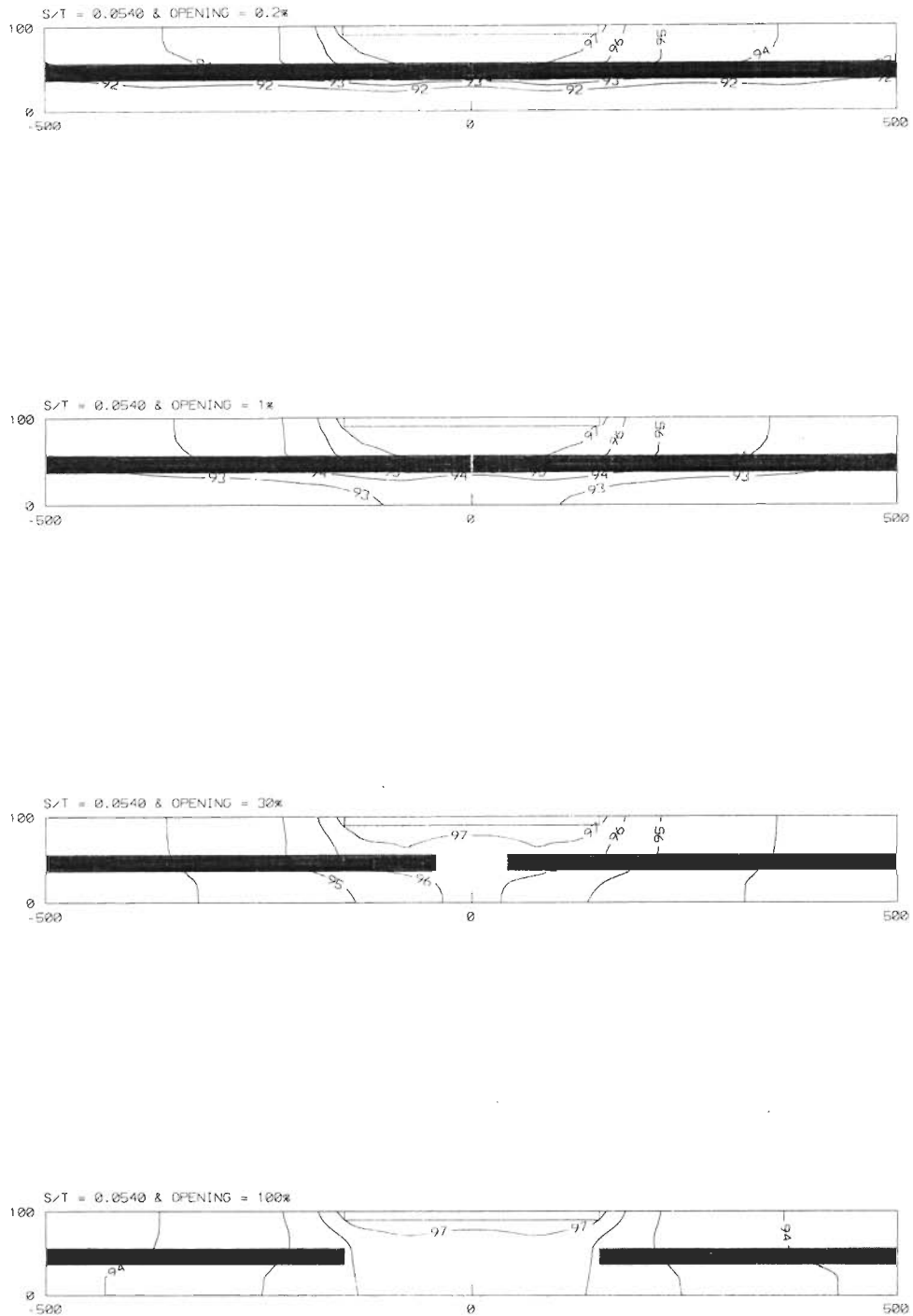


Fig. 6.5 Distribution of Hydraulic Potential (h) in the aquifer system when $S/T = 0.0540$ for Percentage Openings, $O_p = 0.2\%$, 1% , 30% and 100% .

SIMULATION OF FLOW IN MULTILAYERED AQUIFER SYSTEM WITH AND WITHOUT DISCONTINUITY

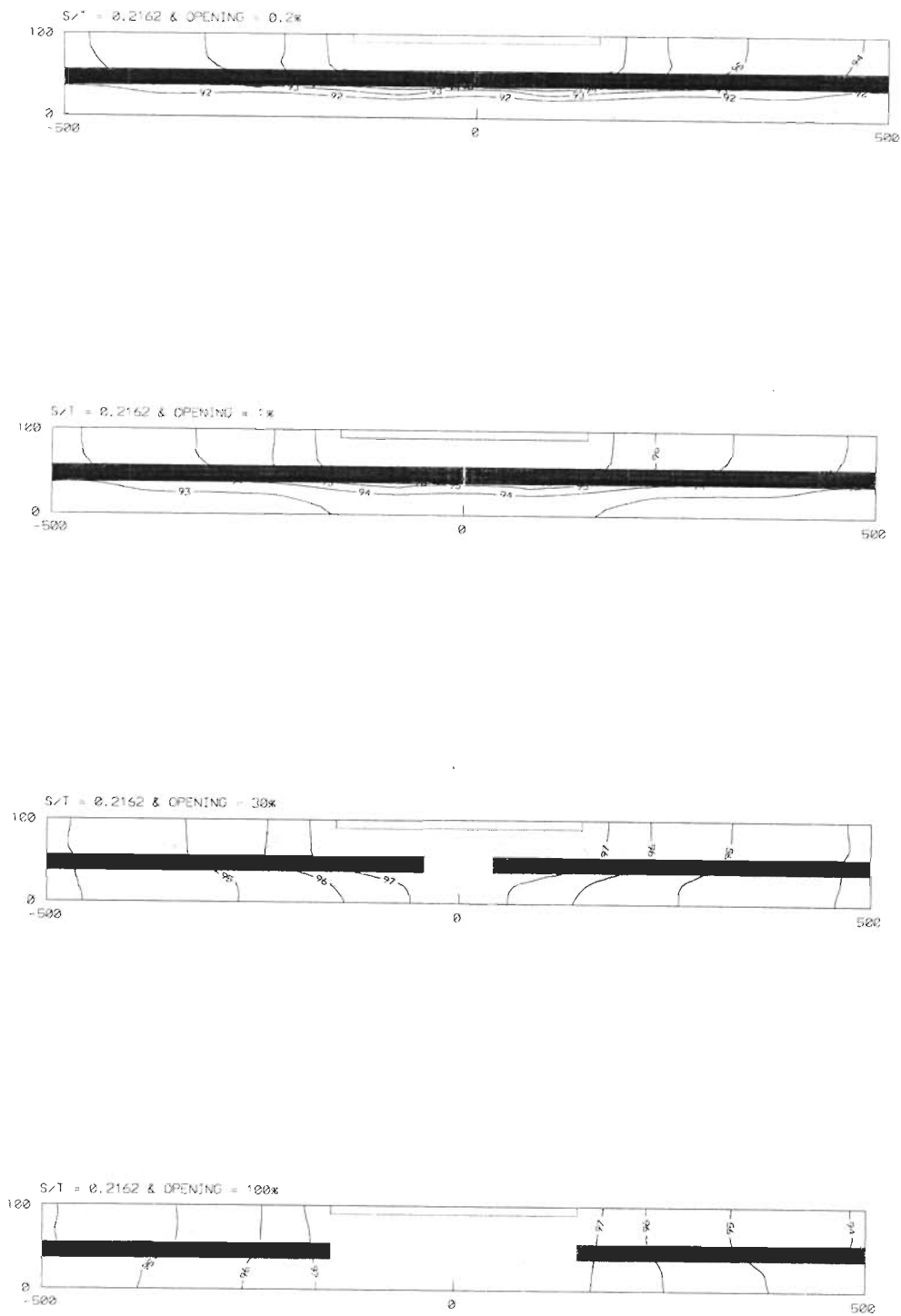


Fig. 6.6 Distribution of Hydraulic Potential (h) in the aquifer system when $S/T = 0.2162$ for Percentage Openings, $O_p = 0.2\%$, 1% , 30% and 100% .

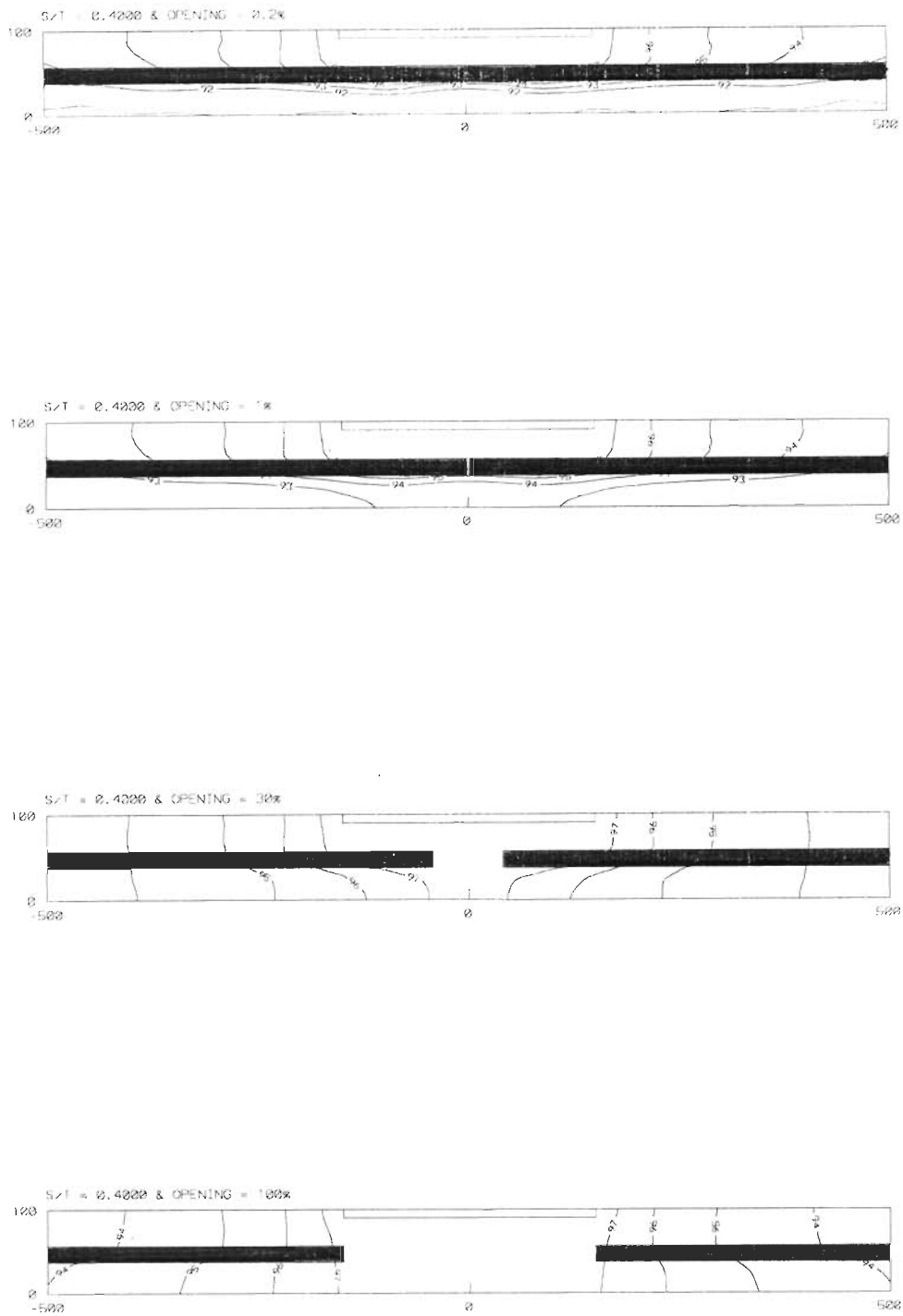


Fig. 6.7 Distribution of Hydraulic Potential (h) in the aquifer system when $S/T = 0.4000$ for Percentage Openings, $O_p = 0.2\%$, 1% , 30% and 100% .

SIMULATION OF FLOW IN MULTILAYERED AQUIFER SYSTEM WITH AND WITHOUT DISCONTINUITY

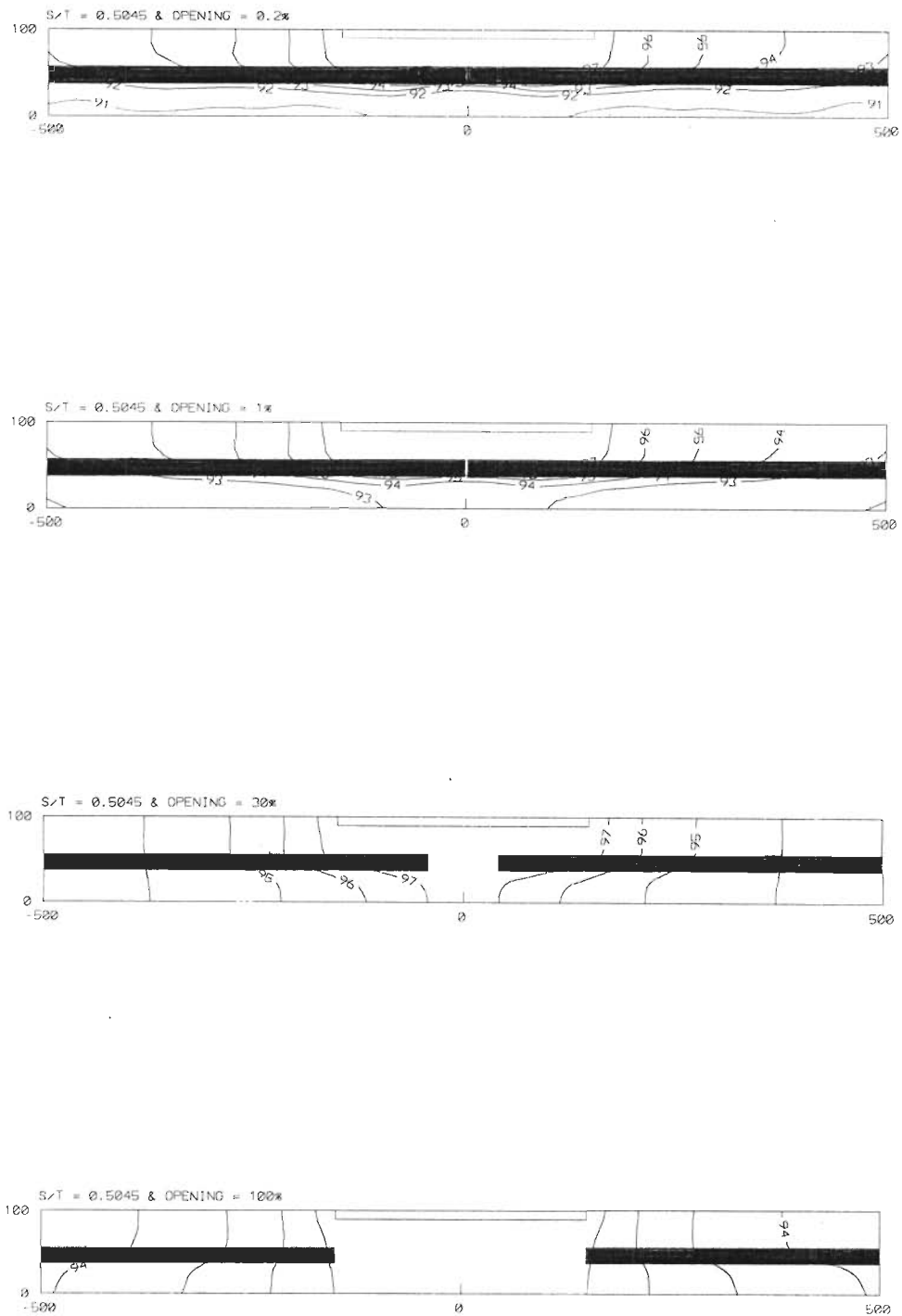


Fig. 6.8 Distribution of Hydraulic Potential (h) in the aquifer system when $S/T = 0.5045$ for Percentage Openings, $O_p = 0.2\%$, 1% , 30% and 100% .

when $S/T=0.0540, 0.2162, 0.4$ and 0.5045 , respectively. For smaller discontinuities, a definite groundwater flow down to the bottom aquifer is indicated by the cluster of potential lines. It can be seen that as the percentage opening (O_p) increases, the equipotentials are being more spread with larger slopes indicating more groundwater flow towards the boundaries.

Similarly, equipotential lines are drawn for $S/T = 0.0540, 0.2162, 0.40$ and 0.5045 with percentage openings, $O_p=30\%$ and 100% , respectively [Fig. 6.9 and Fig. 6.10]. Comparing the sequence of plots, it can be seen that with larger values of S/T the seepage to the bottom aquifer is also more.

Graphs have been constructed between the normalised distance, X/L and the normalised hydraulic head, $(h - H_b)/\Delta H$ for different S/T ratios as well as several percentage openings, O_p . Thus, Fig. 6.11 to Fig. 6.14 show normalised hydraulic potentials (h_n) in the top as well as in the bottom aquifers for percentage openings, $O_p=0.2\%, 1\%, 30\% \& 100\%$, respectively when $S/T = 0.0540$. It is clear that when the percentage opening, O_p is small [Fig. 6.11 and Fig. 6.12], the hydraulic potential in the bottom aquifer is smaller than that in the top aquifer. However, for a percentage opening, $O_p=30\%$ the potential in the bottom aquifer exceeds that of the top aquifer after a certain distance from the source [Fig. 6.13]. Further, the hydraulic potential is higher than that of the top aquifer throughout the system when the percentage opening (O_p) becomes 100% [Fig. 6.14].

Similar plots have been made for the case of a larger value of $S/T (= 0.5045)$ to demonstrate the influence of aquifer properties on the above aspects [vide Fig. 6.15, Fig. 6.16, Fig. 6.17 and Fig. 6.18]. Though the pattern appears the same, it can be seen that the exceedence of hydraulic potential in the bottom aquifer occurs even for the smaller percentage openings, O_p [Fig. 6.15 and Fig. 6.16].

Another interesting feature the analysis reveals is that in the top aquifer the hydraulic head distribution seems invariant with respect to percentage openings, O_p for a specific S/T value [Fig. 6.19]. Nevertheless, for larger values of S/T , the rate of change of head in the top aquifer is steeper. This indicates that as S/T value increases the distance of influence of the source decreases. However, in the bottom aquifer, for a given S/T value the hydraulic potential is rising with increased dimension of the discontinuities [Fig. 6.20 and Fig. 6.21]. Unlike the top aquifer, the percentage opening, O_p

SIMULATION OF FLOW IN MULTILAYERED AQUIFER SYSTEM WITH AND WITHOUT DISCONTINUITY

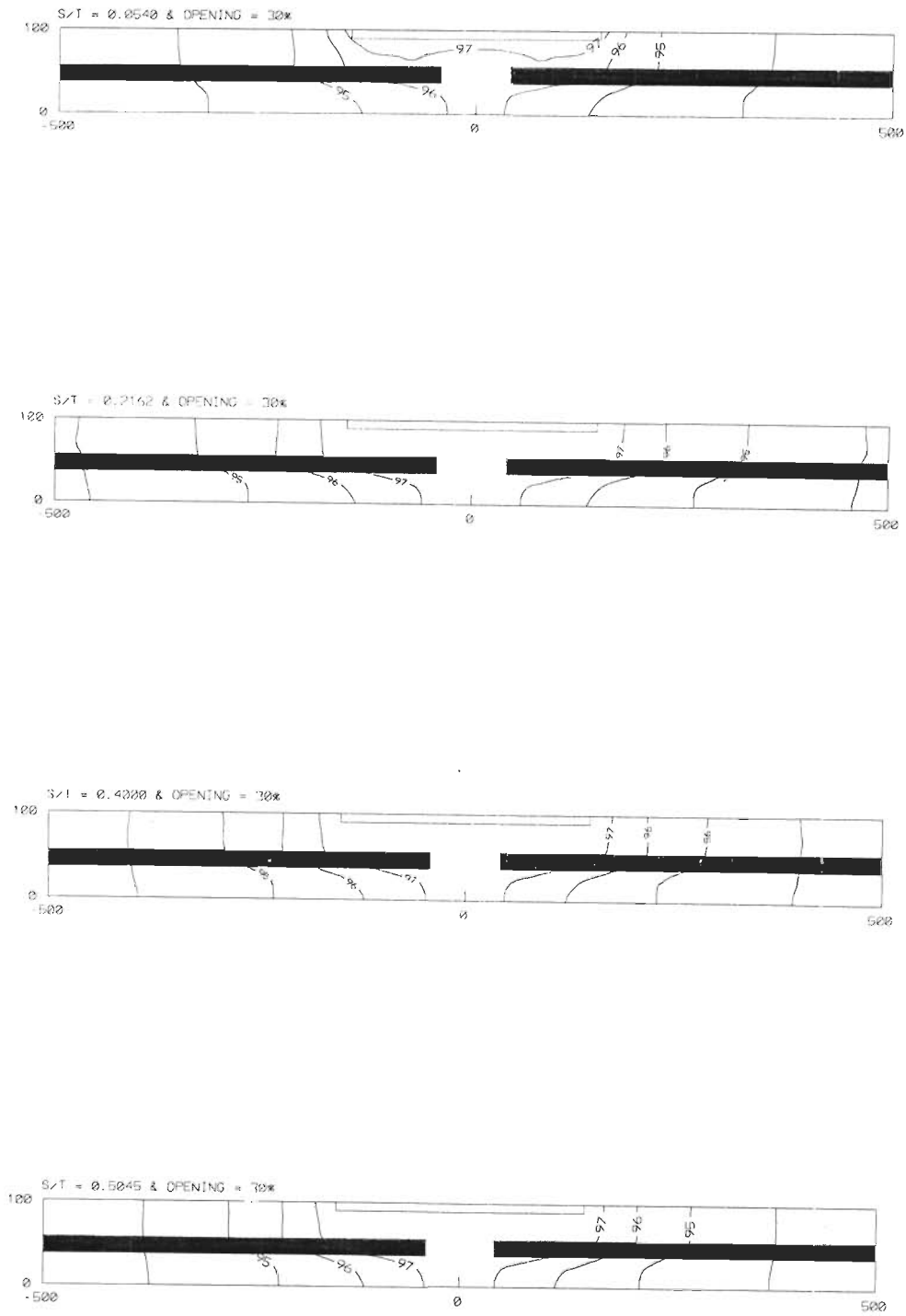


Fig. 6.9 Distribution of Hydraulic Potential (h) in the aquifer system when Percentage Opening, $O_p = 30\%$ for $S/T = 0.0540, 0.2162, 0.4000$ and 0.5045 .

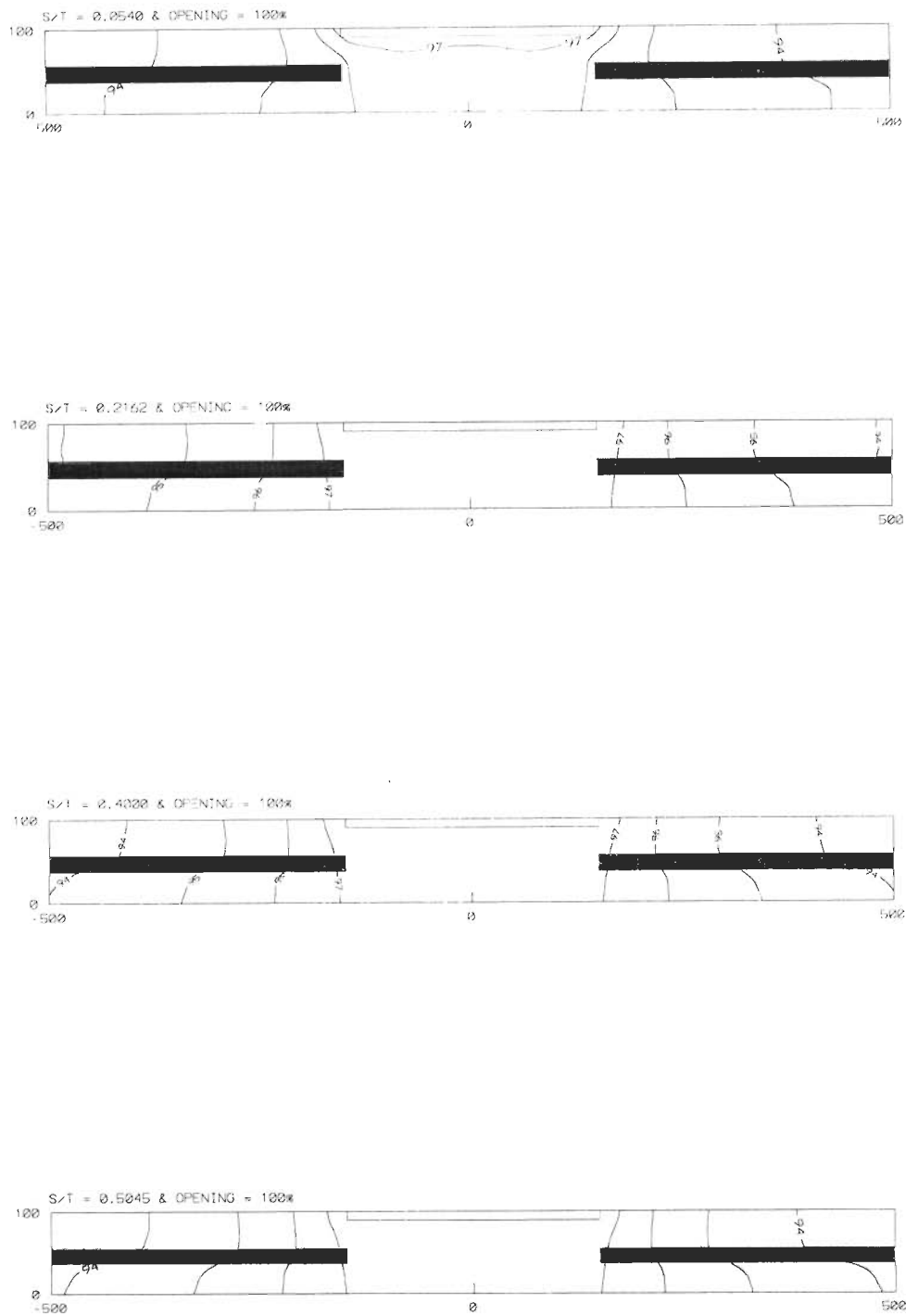


Fig. 6.10 Distribution of Hydraulic Potential (h) in the aquifer system when Percentage Opening, $O_p = 100\%$ for $S/T = 0.0540, 0.2162, 0.4000$ and 0.5045 .

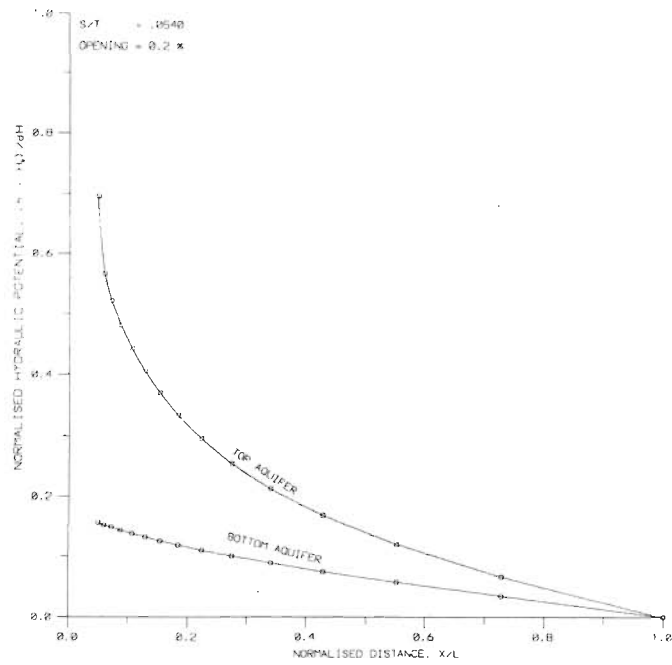


Fig. 6.11 Distribution of Normalised Hydraulic Potentials (h_n) between the Centre and the Boundary of the aquifer system (vertical section) when Percentage Opening, $O_p=0.2\%$ and $S/T=0.0540$.

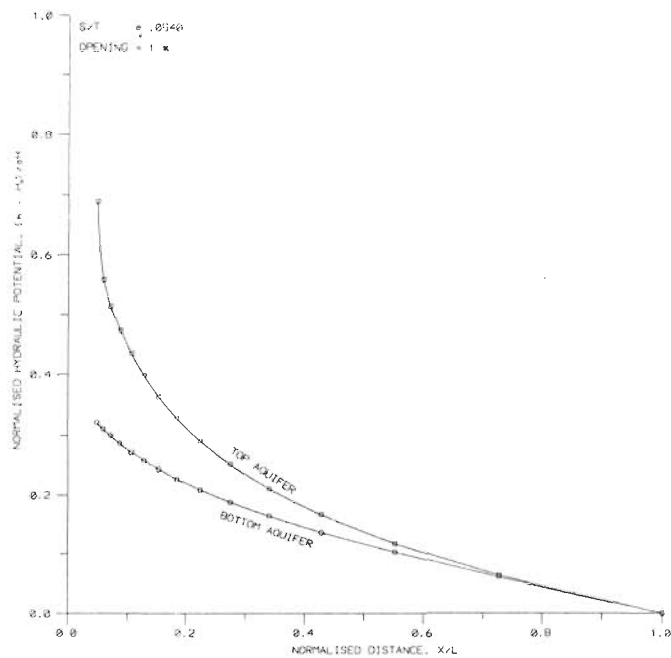


Fig. 6.12 Distribution of Normalised Hydraulic Potentials (h_n) between the Centre and the Boundary of the aquifer system (vertical section) when Percentage Opening, $O_p=1\%$ and $S/T=0.0540$.

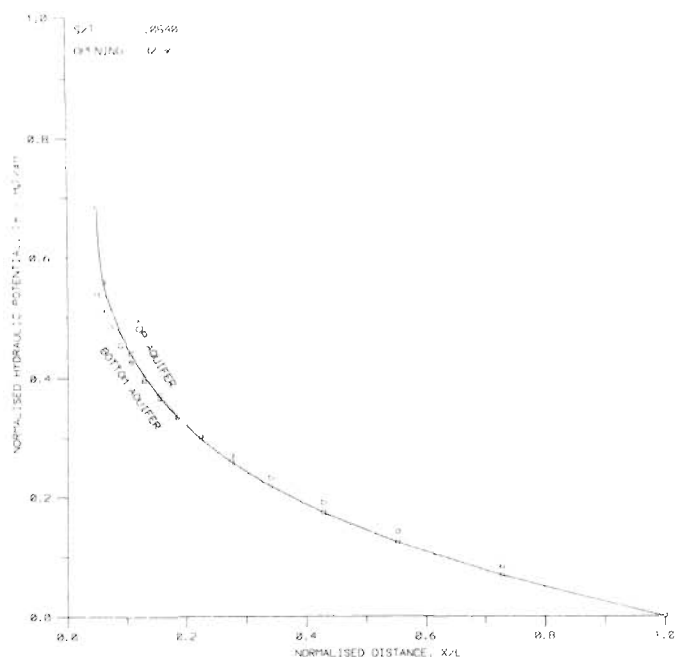


Fig. 6.13 Distribution of Normalised Hydraulic Potentials (h_n) between the Centre and the Boundary of the aquifer system (vertical section) when Percentage Opening, $O_p=30\%$ and $S/T=0.0540$.

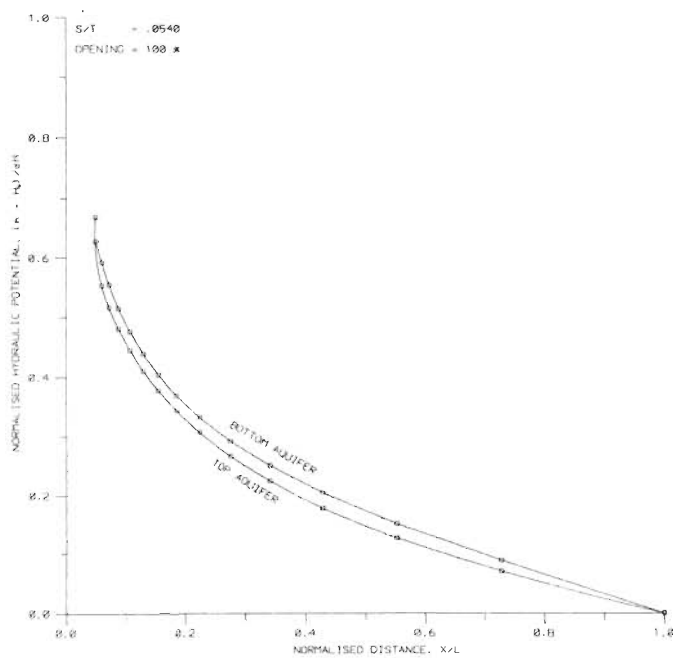


Fig. 6.14 Distribution of Normalised Hydraulic Potentials (h_n) between the Centre and the Boundary of the aquifer system (vertical section) when Percentage Opening, $O_p=100\%$ and $S/T=0.0540$.

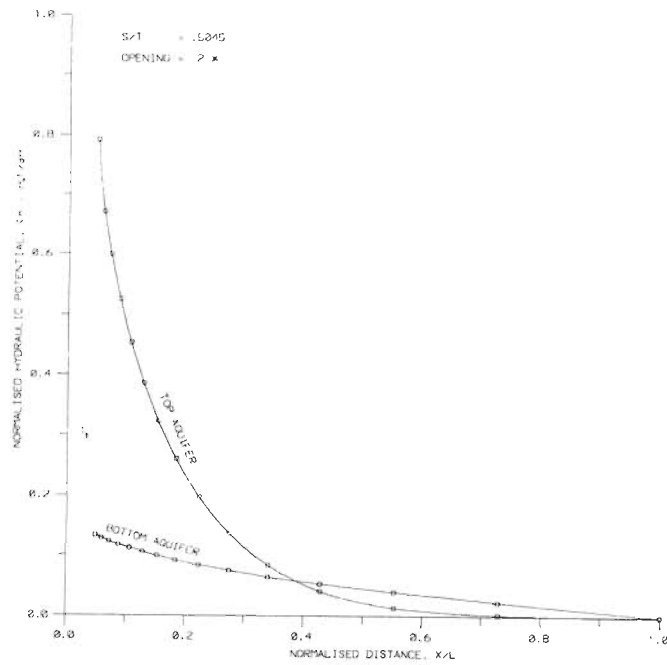


Fig. 6.15 Distribution of Normalised Hydraulic Potentials (h_n) between the Centre and the Boundary of the aquifer system (vertical section) when Percentage Opening, $O_p=0.2\%$ and $S/T=0.5045$.

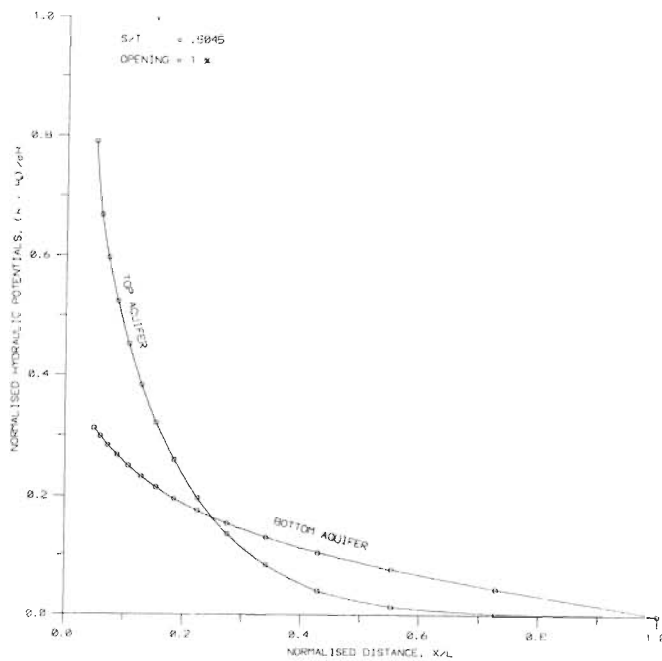


Fig. 6.16 Distribution of Normalised Hydraulic Potentials (h_n) between the Centre and the Boundary of the aquifer system (vertical section) when Percentage Opening, $O_p=1\%$ and $S/T=0.5045$.

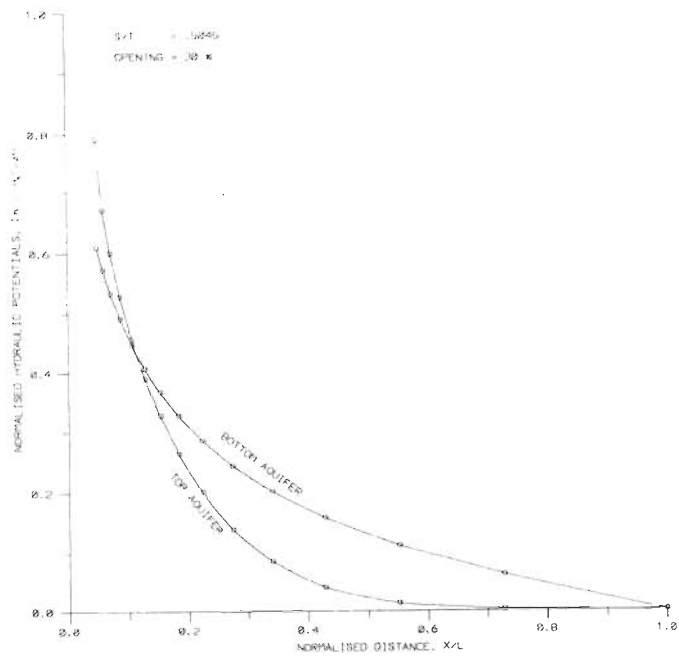


Fig. 6.17 Distribution of Normalised Hydraulic Potentials (h_n) between the Centre and the Boundary of the aquifer system (vertical section) when Percentage Opening, $O_p=30\%$ and $S/T=0.5045$.

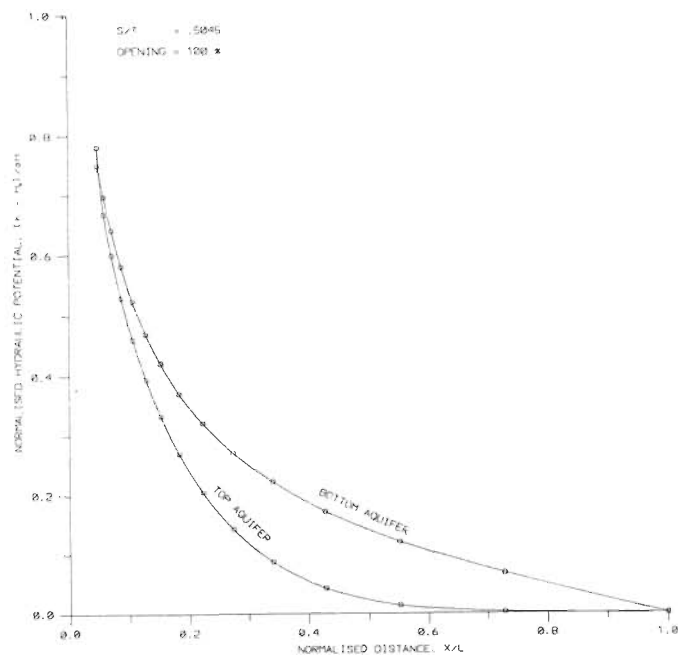


Fig. 6.18 Distribution of Normalised Hydraulic Potentials (h_n) between the Centre and the Boundary of the aquifer system (vertical section) when Percentage Opening, $O_p=100\%$ and $S/T=0.5045$.

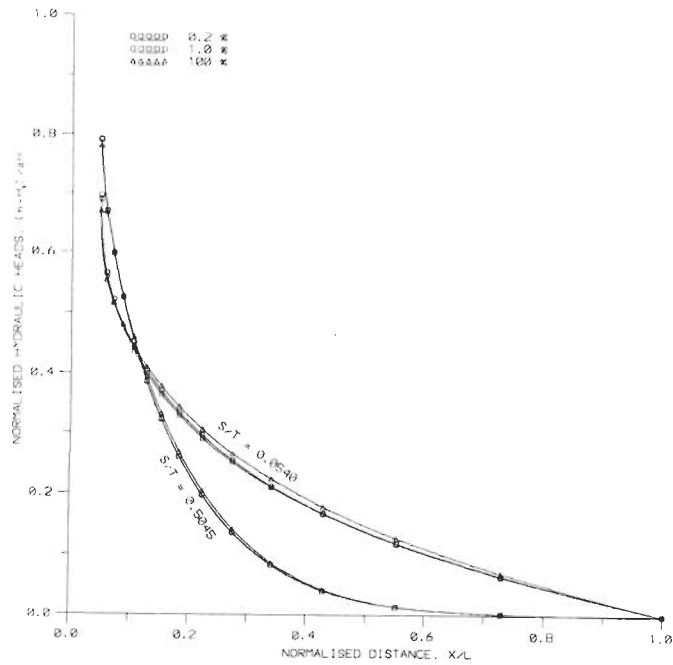


Fig. 6.19 Distribution of Normalised Hydraulic Potentials (h_n) in the top aquifer between the Centre and the Boundary of the aquifer system (vertical section) for different Percentage Openings (O_p) and S/T ratios.

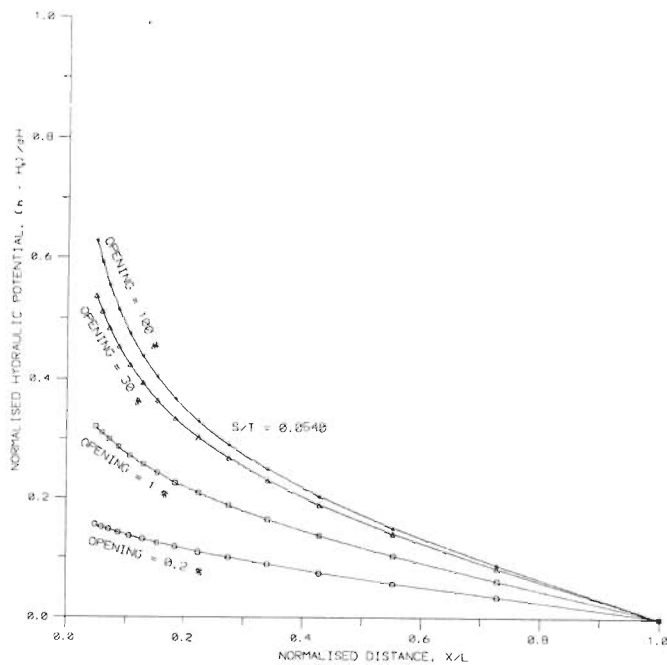


Fig. 6.20 Distribution of Normalised Hydraulic Potentials (h_n) in the bottom aquifer between the Centre and the Boundary of the aquifer system (vertical section) for S/T=0.0540 and Percentage Openings, $O_p = 0.2\%$, 1% , 30% and 100% .

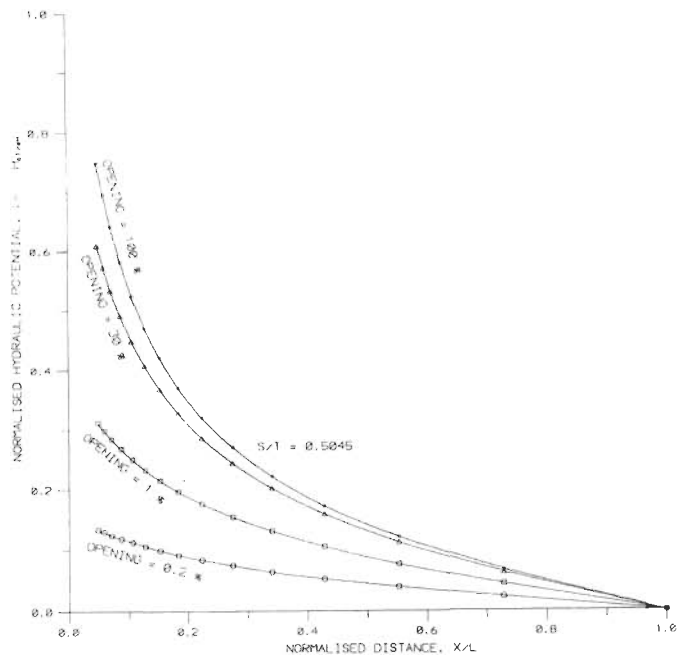


Fig. 6.21 Distribution of Normalised Hydraulic Potentials (h_n) in the bottom aquifer between the Centre and the Boundary of the aquifer system (vertical section) for $S/T=0.5045$ and Percentage Openings, $O_p = 0.2\%$, 1% , 30% and 100% .

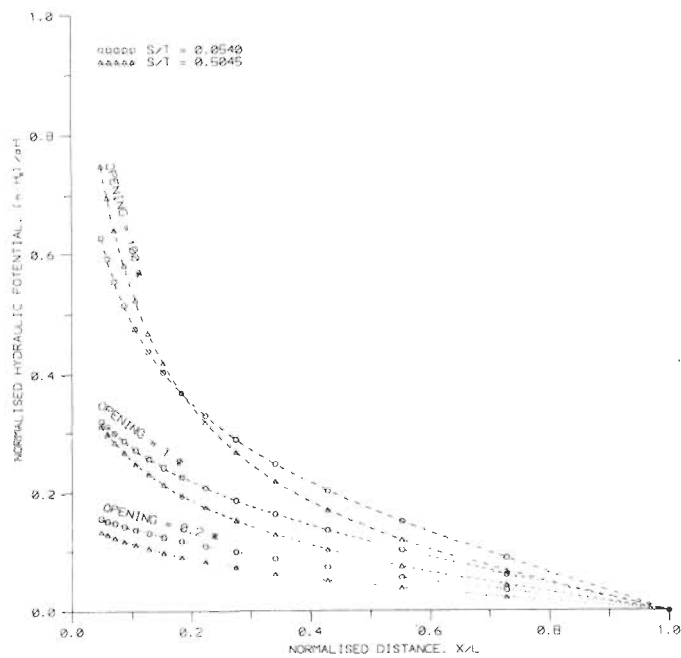


Fig. 6.22 Distribution of Normalised Hydraulic Potentials (h_n) in the bottom aquifer between the Centre and the Boundary of the aquifer system (vertical section) for several Percentage Openings (O_p) and S/T ratios.

also affects the distribution of the hydraulic potentials there; larger the discontinuity, steeper is the slope of hydraulic potential change [Fig. 6.22].

In view of the discussion preceded, it is clear that there exists some point, X_R on the X -axis between the source and the sink for which the hydraulic potential is the same for both the bottom as well as the top aquifers [vide Fig. 6.11 to Fig. 6.18]. With reference to this point, the bottom aquifer has a lower hydraulic potential towards the source-side and higher hydraulic potential towards the sink-side on comparison with that of the top aquifer. In other words, this is a point, X_R where reversal of hydraulic potential takes place between the top and bottom aquifers.

But for the existence of the flow barrier which separates the aquifer system into a top and a bottom aquifer, the direction of groundwater flow also would have been reversed. These points of reversal (X_R) of hydraulic potential vary with the degree of discontinuity (O_p) in the aquitard as well as the ratio S/T , as discernible from the graphs. Fig. 6.23 displays the reversal points, X_R for hydraulic potentials for different percentage openings (O_p) in the case of one small and one large S/T value. For a specified discontinuity, it is observed that the reversal points (X_R) are comparatively closer to the source when the aquifer system is assigned with a larger S/T value. However, when the discontinuity is sufficiently large (say, 80% and above) the sensitivity with respect to S/T ratio is apparently vanished [Fig. 6.23]. This point is further revealed in the difference curve of Fig. 6.24.

The quantities of seepage for both the top and bottom aquifers have been computed for several percentage openings, O_p as well as S/T values [Fig. 6.25]. The plot indicates that for the top aquifer the quantity of seepage is unaffected by the percentage openings (O_p). Nevertheless, the quantity of seepage to the top aquifer is found to be reduced with higher S/T values [Fig. 6.25]. Unlike the top aquifer, the seepage quantities admitted to the bottom aquifer is varying with percentage openings (O_p) as well as S/T ratio [Fig. 6.25]. Evidently, this variation is more pronounced when the percentage openings (O_p) are smaller.

The values of fractional seepage (F_{sb}) to the bottom aquifer (F_{sb}) are plotted against S/T ratios for selected percentage openings, O_p [Fig. 6.26]. The graphs indicate increased contribution to the bottom aquifer with increased dimension of the discontinuity (O_p) as well as for larger values of S/T

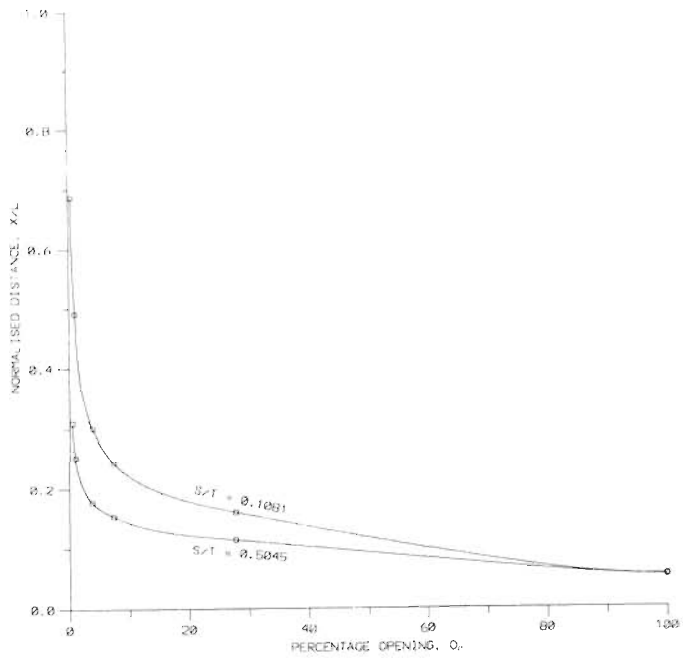


Fig. 6.23 Percentage Opening (O_p) versus Reversal Points (X_R) of hydraulic potentials (expressed in terms of Normalised Distance, X/L) for $S/T=0.1081$ and 0.5045 .

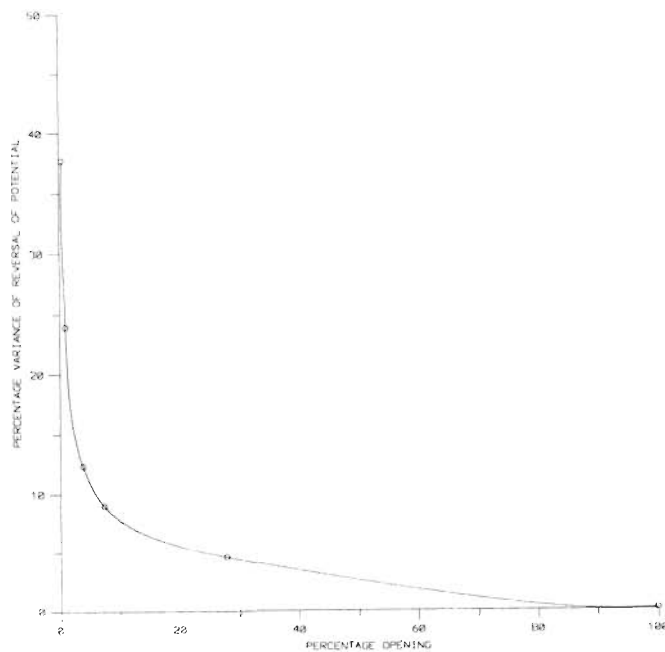


Fig. 6.24 Difference curve of Reversal Points (X_R) of hydraulic potentials (expressed as percentage variance) corresponding to $S/T = 0.0540$ and 0.5045 plotted against Percentage Opening (O_p).

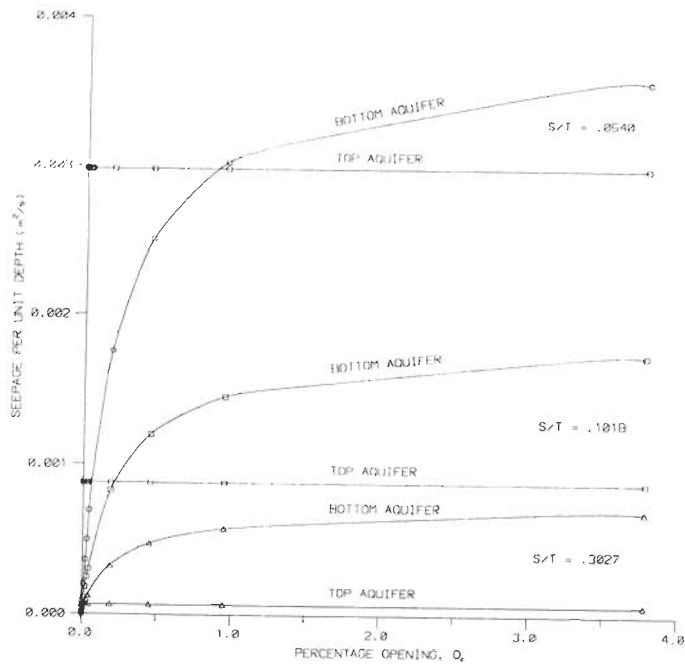


Fig. 6.25 Percentage Opening (O_p) versus specific seepage to the top as well as the bottom aquifer, respectively for several values of S/T ratio.

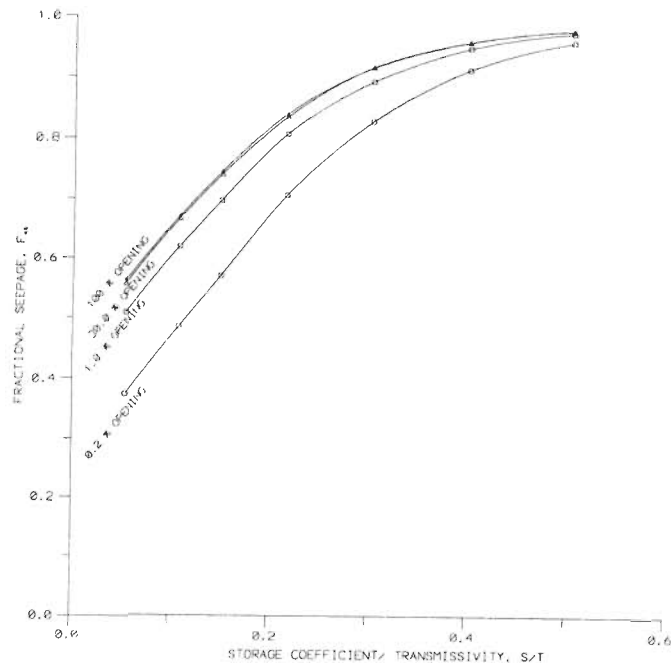


Fig. 6.26 S/T ratio versus Fractional Seepage, F_{sb} to the bottom aquifer for Percentage Openings, $O_p = 0.2\%$, 1% , 30% and 100% .

ratio. It is significant to note that even for a very small percentage opening (O_p) in the aquitard (say, 1%), the contribution of seepage to the bottom aquifer is remarkably high [Fig. 6.26]. Further, as the 100% discontinuity curve almost matches with that of 30% discontinuity, the quantities of fractional seepage (F_{sb}) to the bottom aquifer are nearly the same for percentage openings, $O_p=30\%$ and $O_p=100\%$. Thus, values of O_p greater than 30% do not seem to have contributing additionally to the fractional seepage (F_{sb}). In other words, a percentage opening (O_p) of just 30% (i.e., a discontinuity of only one-third the width of the source) in the flow-barrier can suffice optimum recharging of the underlying aquifer. This aspect may be of importance in the practice of artificial recharging by means of hydraulic connectors.

Also, from Fig. 6.26 it is clear that for larger values of S/T the relevance of O_p on fractional seepage (F_{sb}) diminishes. For instance, when $S/T=0.5$ fractional seepage, F_{sb} attains a maximum (nearly 1.0) irrespective of the dimension of the discontinuity. In short, there is optimum recharge taking place to the aquifer below the discontinuous aquitard for a large S/T ratio even when the dimension of the discontinuity is very small.

It is fascinating to note that even a very small discontinuous zone (a percentage opening like $O_p=0.2\%$) in an aquitard can induce substantial quantities of seepage down to the bottom aquifer for the range of S/T ratios used. On the other hand, replenishment of an aquifer below a flow-barrier can be accomplished through an artificially created minute discontinuity, as in the case of hydraulic connectors.

6.6.2 EFFECT OF LOCATION OF THE DISCONTINUITY IN THE AQUITARD ON RECHARGING

Four sets of cases have been designed and simulation of groundwater flow/ hydraulic potentials (h) in the aquifer system has been carried out to study how the location of the discontinuity in the aquitard influences the seepage from the source to the aquifer system. The aquitard is positioned approximately in the middle of the aquifer system. Investigations comprise of several combinations of the percentage opening (O_p) and its location at different points on the aquitard. Sensitivity of the results with regard to different aquifer parameter combinations has also

examined. Following are the aspects dealt with in this section:

- (i) Effect of shifting of the discontinuity (along the X-axis, in terms of X/L values) on the recharging of the aquifer system, for a specific value of the S/T ratio, for a certain position of the aquitard and for several percentage openings (O_p).
- (ii) Effect of shifting of the discontinuity on the recharging of the aquifer system for the case of a small percentage opening (O_p), for a certain position of the aquitard and for several values of the S/T ratio (i.e., for different aquifer parameter combinations).
- (iii) Effect of moving a large discontinuity close to the sink on the recharging of the aquifer system, for a fixed position of the aquitard and for several values of S/T ratio.
- (iv) Effect of shifting of a specified discontinuity to several X/L points on the recharging of the aquifer system, for a certain position of the aquitard.

6.6.2.1 Effect of Shifting of the Discontinuity on Recharge for a Specified Value of S/T Ratio and Several Percentage Openings

The effect of shifting of the aquitard discontinuity on the recharging of the aquifer system has been analysed for several percentage shifts (M_p) of the discontinuity with the position of the aquitard at a depth of about $D/2$. The set of cases studied is illustrated in the Table-6.2.

Table 6.2 Matrix table of various cases with the position of the aquitard at 0.53 and $S/T=0.1081$

Percentage Opening (O_p)	Percentage Shift (M_p) of Opening from the centre										
	0	10	20	30	40	50	60	70	80	90	100
5	✓	✓	✓	✓	✓	✓	✓	✓	✓	✓	✓
15	✓	✓	✓	✓	✓	✓	✓	✓	✓	✓	✓
25	✓	✓	✓	✓	✓	✓	✓	✓	✓	✓	✓
35	✓	✓	✓	✓	✓	✓	✓	✓	✓	✓	✓
45	✓	✓	✓	✓	✓	✓	✓	✓	✓	✓	✓

The percentage shifts (M_p) of the discontinuity in these cases have been restricted to the half-width of the source (i.e., the shift is between $X/L=0$ and $X/L=0.04$). Thus, a shift, $M_p=100\%$ of the

discontinuity implies that the discontinuity being located at a distance equal to $w/2$ (half-width of the source) from the centre. Cases pertaining to shifting of discontinuity to larger extent being discussed under separate sections.

The distribution of hydraulic potential, h (as equipotential lines) in the aquifer system for three locations of the discontinuity beneath the source is shown in Fig. 6.27. The vertical sections of the aquifer system displayed are for the cases with the percentage opening (O_p) equals 5%. Since the aquitard is of very low permeability, groundwater flow is to take place mainly through the discontinuity only. As such, the change in the distribution of hydraulic potentials can be noticed as the discontinuity shifts. Apparently, the discontinuity in the aquitard attracts flow towards it and transmits down to the bottom aquifer.

The equipotential lines in the aquifer system as seen in Fig. 6.28 is obtained when discontinuities of different dimensions have been located midway between the centre and edge of the source ($M_p=50\%$). The dimensions of the discontinuity vary between 5% and 45%. Comparison of equipotentials in the bottom aquifer reveals that the hydraulic potential in the aquifer builds up with widening of the discontinuity as there will be reduced resistance to groundwater flow with wider discontinuity. Therefore, seepage of water down to the bottom aquifer is more for a larger discontinuity even when it is located away from the centre.

The above observations are further elaborated using Fig. 6.29, Fig. 6.30 and Fig. 6.31. These graphs show the normalised values of hydraulic potential for the bottom aquifer plotted against the normalised distance (X/L) for three discontinuities with their different locations respectively. When the dimension of the discontinuity increases, the hydraulic potentials ^{are} also found to be raising. Another feature evident from the plots is the reduction in the hydraulic potentials, especially the peak values, as the discontinuity shifts away from the centre. Consequently, reduction of groundwater flow to the bottom aquifer can be expected with shifting of the discontinuity. It may, therefore, be concluded that to effect optimum seepage down to the bottom aquifer, the discontinuity, irrespective of its dimension, should be located centrally below the source. Comparison of hydraulic potentials obtained with percentage openings, $O_p=5\%$, 25% and 45% at two locations of the aquitard ($X/L=0$ and $X/L=0.1081$) confirms the fact that hydraulic potentials in the bottom aquifer is higher for a

SIMULATION OF FLOW IN MULTILAYERED AQUIFER SYSTEM WITH AND WITHOUT DISCONTINUITY

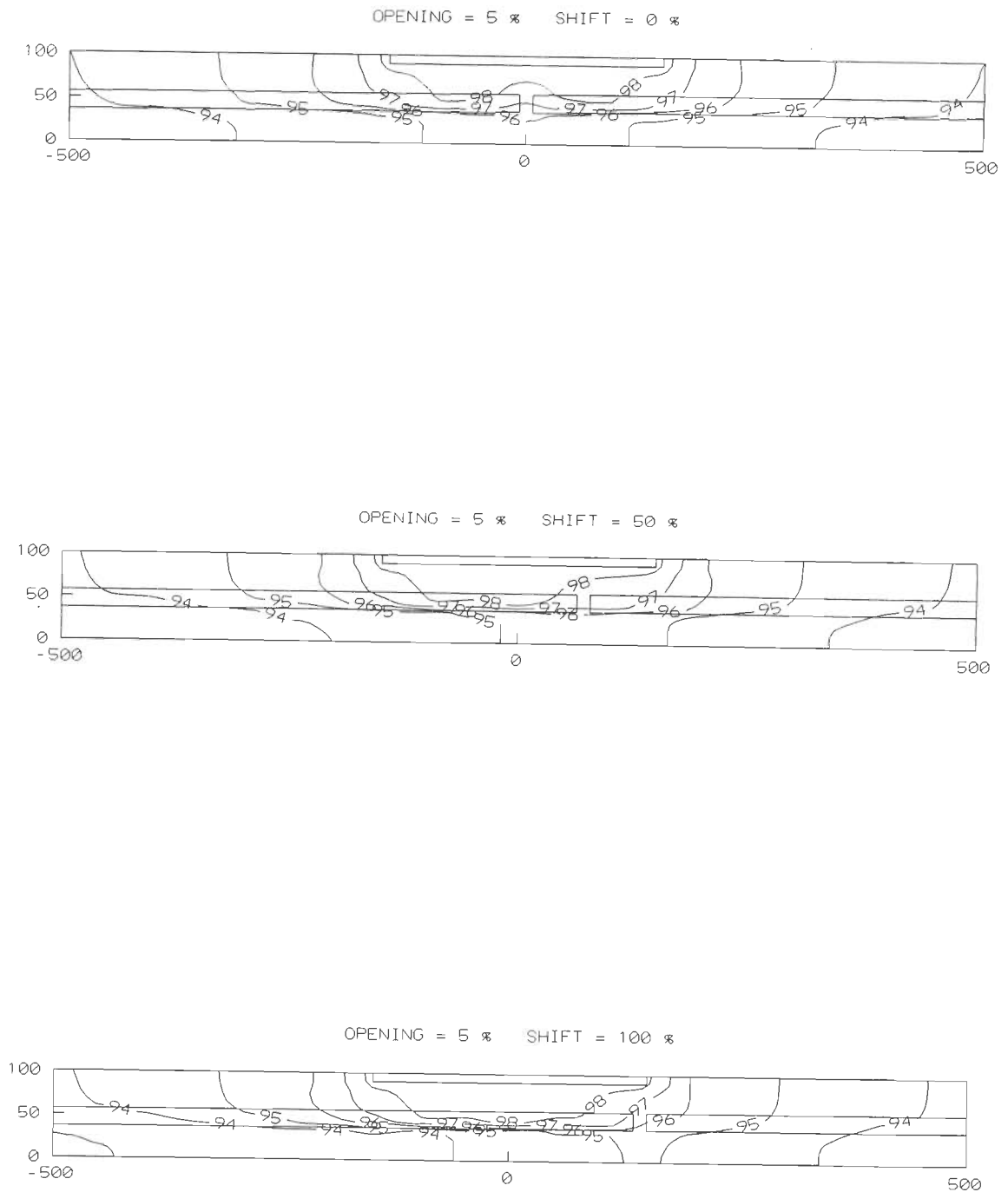


Fig. 6.27 Distribution of hydraulic potentials (h) in the aquifer system for three locations (Shift, $M_p=0\%$, 50% and 100%) with Percentage Opening, $O_p=5\%$ when the discontinuous Aquitard Position, $P_d=0.53$.

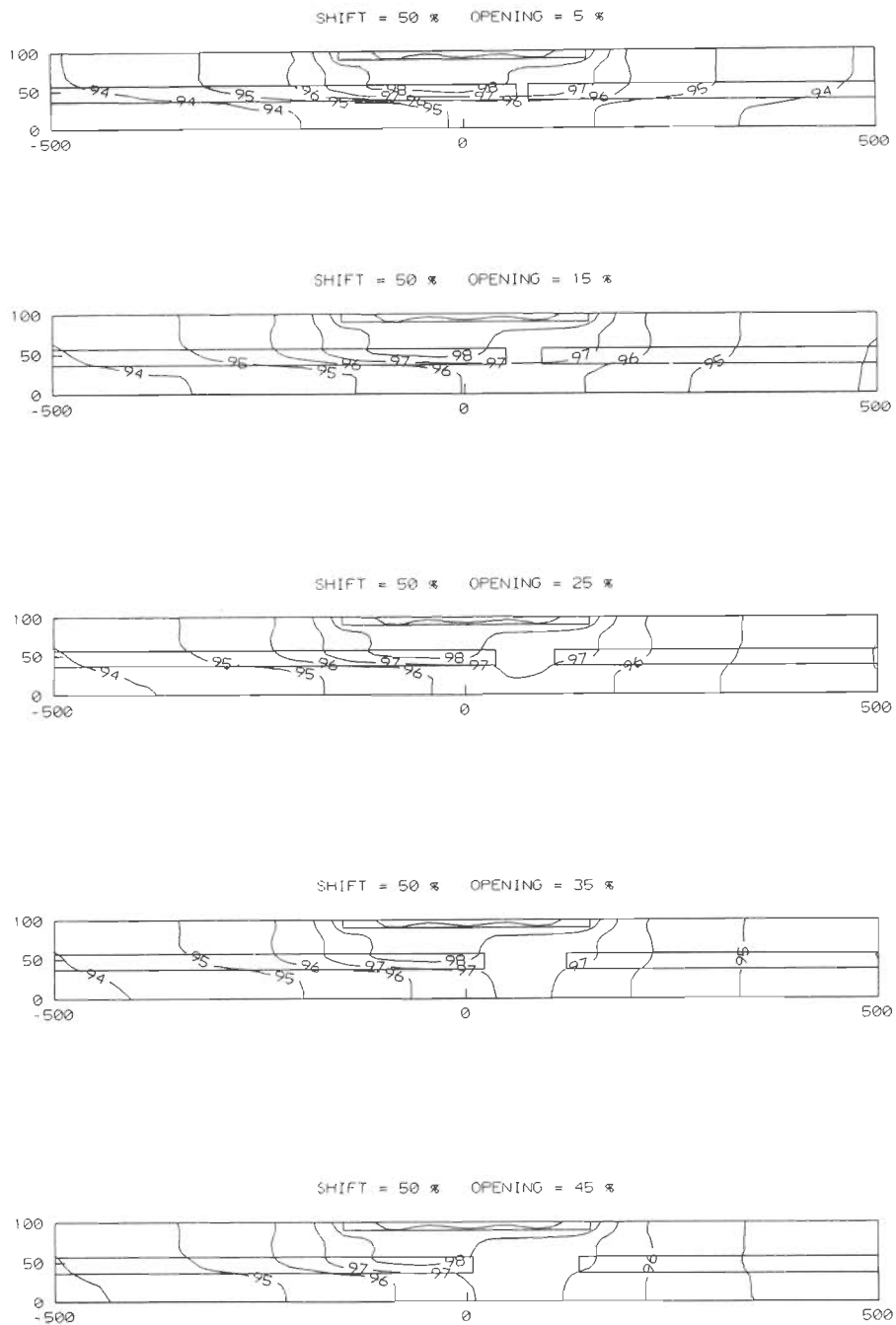


Fig. 6.28 Distribution of hydraulic potentials (h) in the aquifer system for several Percentage Openings (O_p) with the aquitard discontinuity located mid-way between the centre and the fringe of the source (Shift, $M_p=50\%$) when the discontinuous Aquitard Position, $P_d=0.53$.

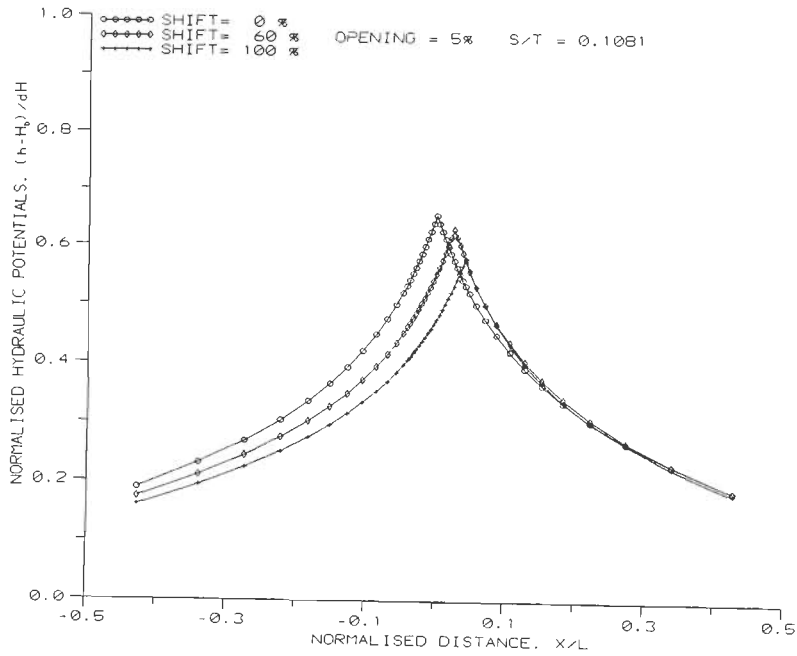


Fig. 6.29 Normalised Distance (X/L) versus Normalised Hydraulic Potentials (h_n) in the bottom aquifer for three locations (M_p) of the aquitard discontinuity (Percentage Opening, $O_p=5\%$) below the source.

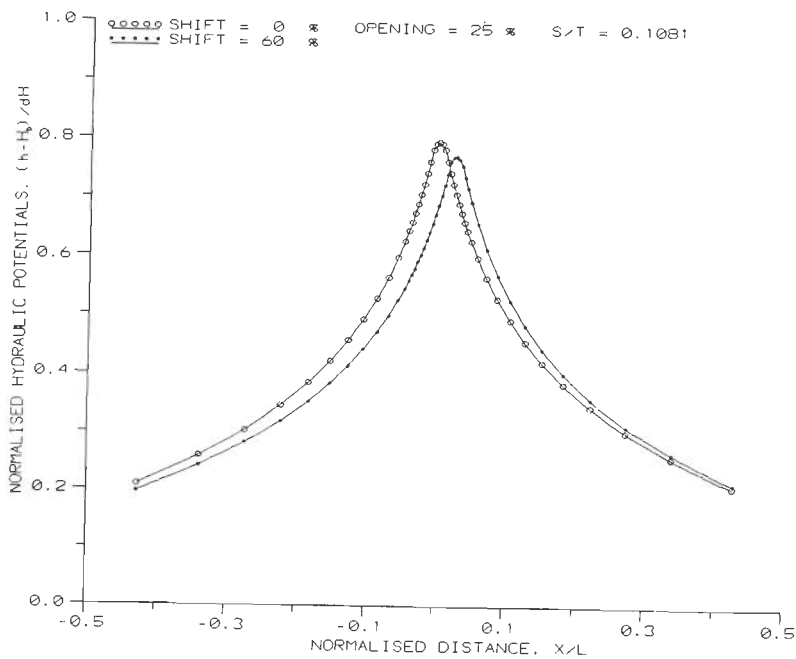


Fig. 6.30 Normalised Distance (X/L) versus Normalised Hydraulic Potentials (h_n) in the bottom aquifer for two locations (M_p) of the aquitard discontinuity (Percentage Opening, $O_p=25\%$) below the source.

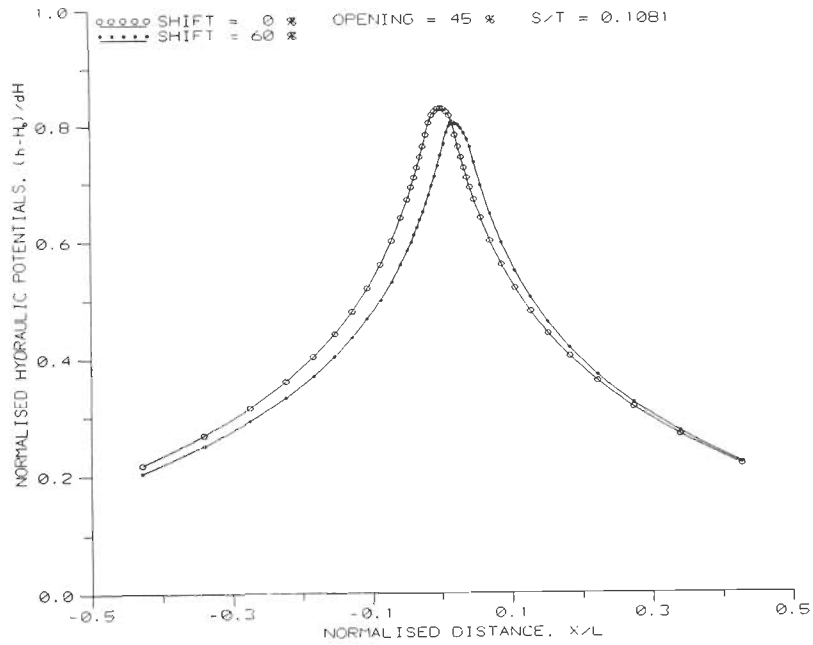


Fig. 6.31 Normalised Distance (X/L) versus Normalised Hydraulic Potentials (h_n) in the bottom aquifer for two locations (M_p) of the aquitard discontinuity (Percentage Opening, $O_p=45\%$) below the source.

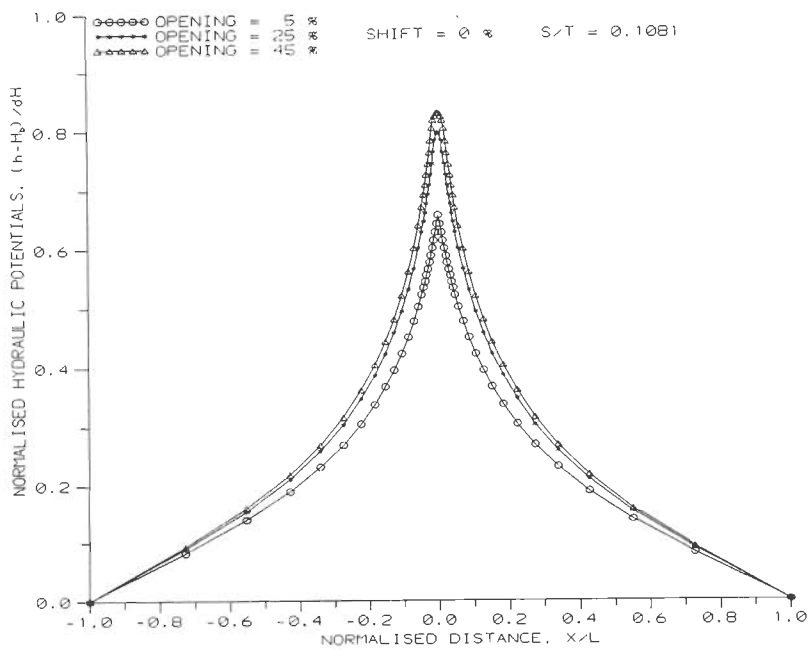


Fig. 6.32 Normalised Distance (X/L) versus Normalised Hydraulic Potentials (h_n) in the bottom aquifer for different Percentage Openings (O_p) with a Shift, $M_p=0\%$ and $S/T = 0.1081$.

larger discontinuity in spite its location [Fig. 6.32 and Fig. 6.33]. Though the pattern appears to be similar in these two plots, the peak is shifted towards the location of the discontinuity in Fig.6.33.

The nature of hydraulic potentials in the bottom aquifer vis-a-vis the location of the discontinuity can be understood from Fig. 6.34 for several percentage openings (O_p). The peak values of hydraulic potentials corresponding to different locations of the discontinuity are plotted therein for several dimensions of the discontinuity. Reduction in the peak potential values is evident in all the cases regardless of the dimension of discontinuity, as the discontinuity moves away from the centre of the aquifer system. However, as discussed earlier, higher hydraulic potentials are registered with larger dimension of the discontinuity. Moreover, the peak values of normalised hydraulic potential (h_n) plotted against the percentage openings (O_p) as shown in Fig. 6.35 verify these observations.

The drop in the hydraulic potentials as the discontinuity shifts away from the centre is depicted in Fig. 6.36. The normalised hydraulic potentials (h_n) just below the discontinuity at its shifted locations and that at $X/L=0$ are compared for two cases with different percentage openings (O_p). The difference between the hydraulic potentials at these two points (at the centre and at the discontinuity) gradually increases as the discontinuity shifts away form the centre. This is expected as the transmission of groundwater flow down to the bottom aquifer is predominantly through the discontinuous zone only.

The effectiveness of recharging of the bottom aquifer against various locations of the discontinuity has also been evaluated. The fractional seepage (F_{sb}) to the bottom aquifer has been computed for various cases with different percentage openings (O_p) and percentage shifts (M_p) for the purpose. Locations of the discontinuity (M_p) versus fractional seepage (F_{sb}) shown in Fig. 6.37 reveals the nature of seepage to the bottom aquifer. Reduction in fractional seepage (F_{sb}) with shifting of the discontinuity away from the centre is clear. Further, there is quantitative increment in fractional seepage (F_{sb}) for a larger discontinuity.

From the discussions it is obvious that when the discontinuity, irrespective of its dimension, is shifted away from the centre there ought to be a reduction of groundwater flow taking place down

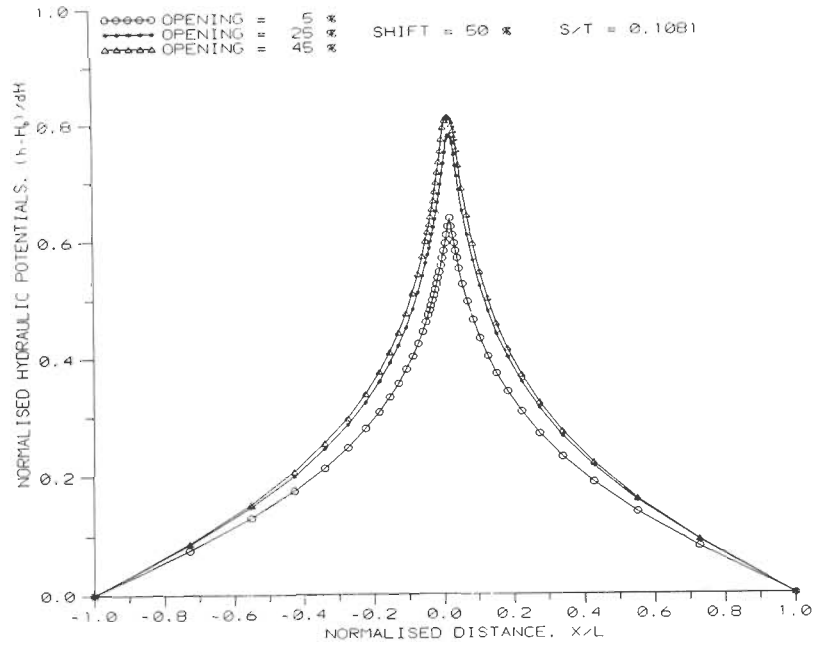


Fig. 6.33 Normalised Distance (X/L) versus Normalised Hydraulic Potentials (h_n) in the bottom aquifer for different Percentage Openings (O_p) with a Shift, $M_p = 50\%$ and $S/T = 0.1081$.

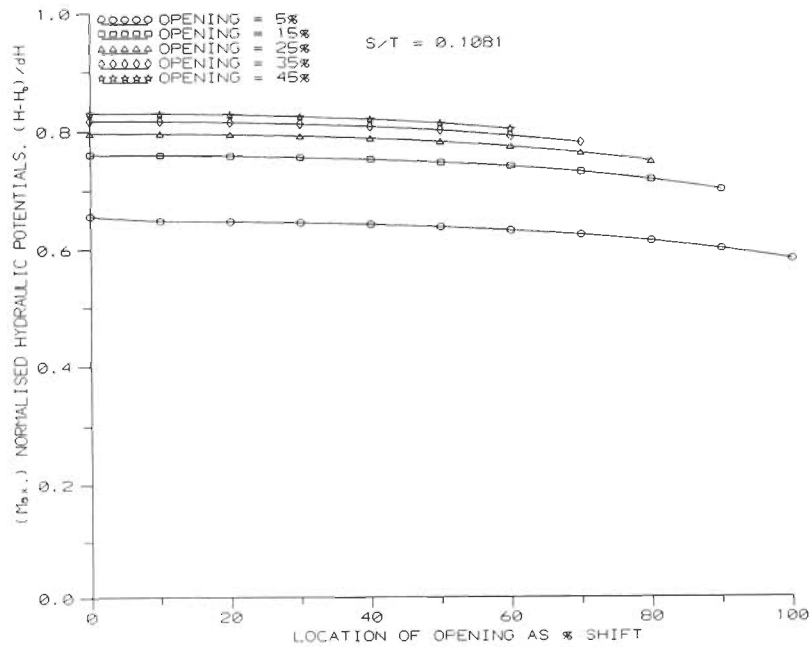
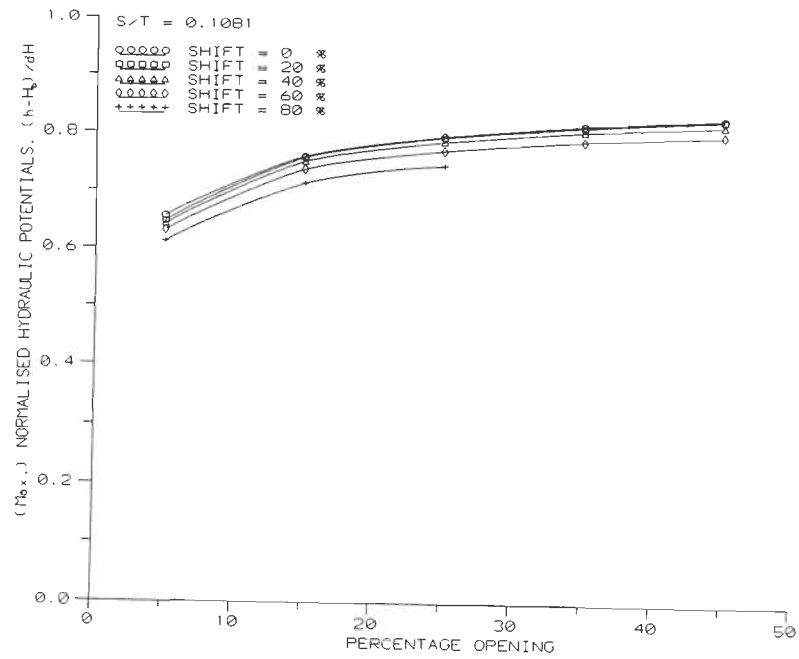


Fig. 6.34 Location (M_p) of the aquitard discontinuity below the source versus maximum values of Normalised Hydraulic Potentials (h_n -max) in the bottom aquifer for several Percentage Openings (O_p).



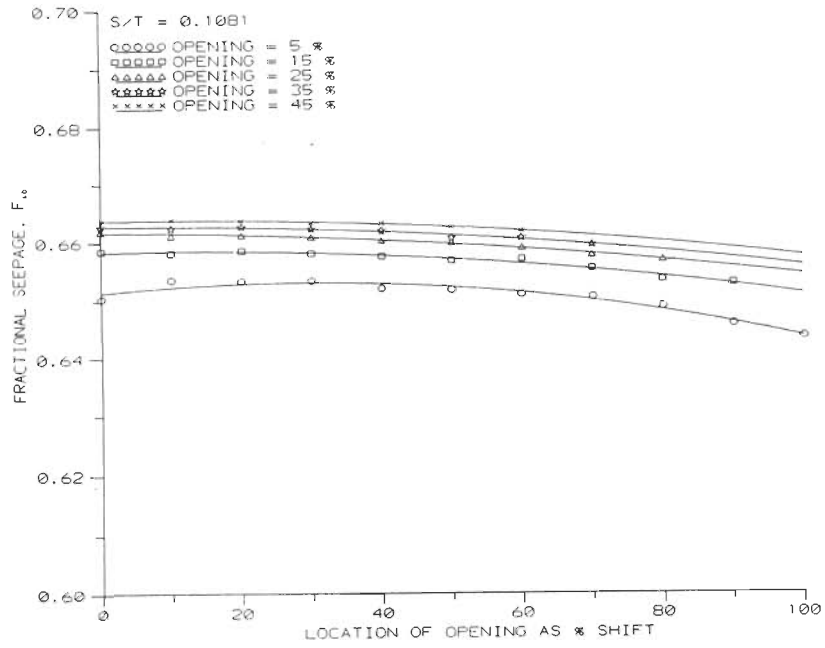


Fig. 6.37 Location (M_p) of the aquitard discontinuity below the source versus Fractional Seepage (F_{sb}) to the bottom aquifer for several Percentage Openings (O_p) when $S/T=0.1081$.

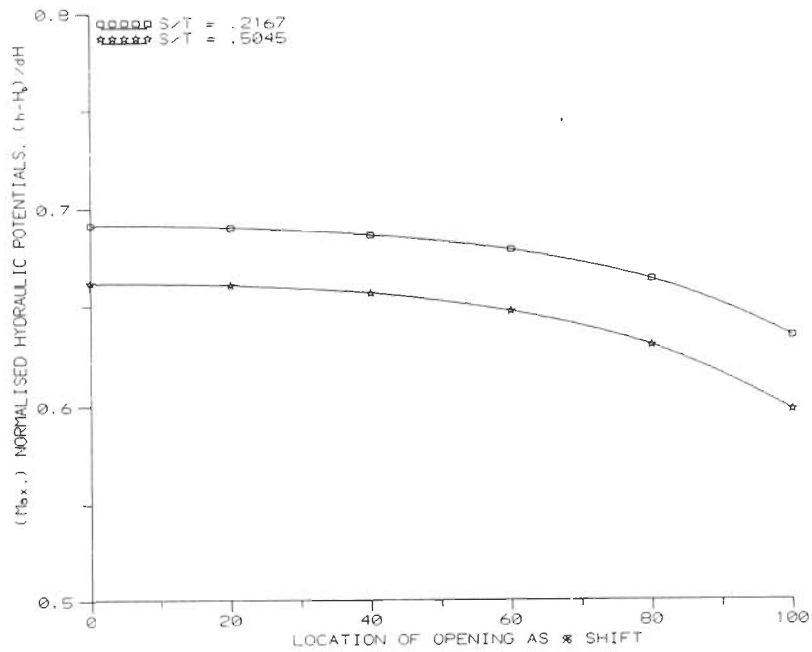


Fig. 6.38 Location (M_p) of the aquitard discontinuity below the source versus maximum values of Normalised Hydraulic Potentials (h_n -max) in the bottom aquifer for two S/T ratios with Percentage Opening, $O_p=5\%$.

to the bottom aquifer. Thus, for attaining optimum recharging of the bottom aquifer the opening (discontinuity) must be centrally located below the source. *the source should be located right above the aquitard discontinuity.*

6.6.2.2 Effect of Shifting of the Discontinuity on Recharge for a Specified Discontinuity of the Aquitard and Several Values of the S/T Ratio

The effect of shifting of a small discontinuity ($O_p=5\%$) on the recharging of the aquifer system having distinct parameter values has been analysed. The sensitivity with respect to the aquifer parameters is looked into. The inventory of cases examined with different S/T ratios and percentage shifts (M_p) of the discontinuity is presented in the Table-6.3.

Table 6.3 Matrix table of various cases simulated with position of the aquitard at $P_d=0.53$ and Percentage Opening, $O_p=5\%$.

Aquitard S/T Ratio	Percentage Shift (M_p) of Opening from the centre					
	0	20	40	60	80	100
0.1081	✓	✓	✓	✓	✓	✓
0.2162	✓	✓	✓	✓	✓	✓
0.3027	✓	✓	✓	✓	✓	✓
0.4000	✓	✓	✓	✓	✓	✓
0.5045	✓	✓	✓	✓	✓	✓

A few representative cases have been selected from this list for discussion. Locations of the discontinuity versus normalised hydraulic potentials (h_n) in the bottom aquifer is plotted in Fig. 6.38 for two S/T ratios of the aquifer. It may be noticed that the normalised hydraulic potential (h_n) in the bottom aquifer is higher at all the locations of the discontinuity for the small S/T ratio. This suggests that a specific aquifer system may develop higher hydraulic potentials due to recharging when the storage coefficient value is low and/ or the hydraulic conductivity is high while all other factors remaining the same.

Fig. 6.39 depicts S/T ratio versus fractional seepage (F_{sb}) for two locations of the discontinuity, one below the centre and the other below the periphery of the source. The fractional seepage (F_{sb}) to the bottom aquifer is high for an aquifer system with a large S/T value. Hence, for a given set-up, an aquifer system with large S/T ratio may transmit higher fractions of the total discharge to the bottom aquifer irrespective of the location of the discontinuity. However, it has been noticed that only the fraction of the total discharge which being transmitted to the bottom aquifer is high for a large S/T ratio, whereas the total discharge from the aquifer system is in fact quantitatively smaller for a large S/T ratio. *Can some reason be attributed to this phenomenon*

6.6.2.3 Effect of Shifting of the Discontinuity on Recharge for a Specified Position of the Aquitard and Several Values of the S/T Ratio

The previous analyses (of Sections-6.6.2.1 and 6.6.2.2) have been pertaining to cases where the locations of the discontinuity confined within the extent of the source. Consequently, the dimension of the discontinuity could never exceed 50% of the source width in those cases. However, in this section a generalised simulation analysis has been presented with complete coverage of the aquifer system using a larger dimension of the discontinuity and its locations anywhere between the centre of the aquifer system (source) and the boundary (sink). Table-6.4 shows the cases studied with two locations of the discontinuity, one at the centre and the other far away from the centre, for different parameters aquifer systems.

Table 6.4 Matrix table of various cases studied with position of the aquitard at $P_d=0.53$ and Percentage Opening, $O_p=117\%$

X/L	S/T Ratio				
	0.1081	0.2162	0.3027	0.4000	0.5045
0.00	✓	✓	✓	✓	✓
0.43	✓	✓	✓	✓	✓

Two locations of the discontinuity, one in the middle of the aquitard and the other at a distance approximately half way between the centre and the boundary of the aquifer system, have been considered for evaluating ^{the} effect of location of the discontinuity on the recharging. The

*↓
aquifer recharge*

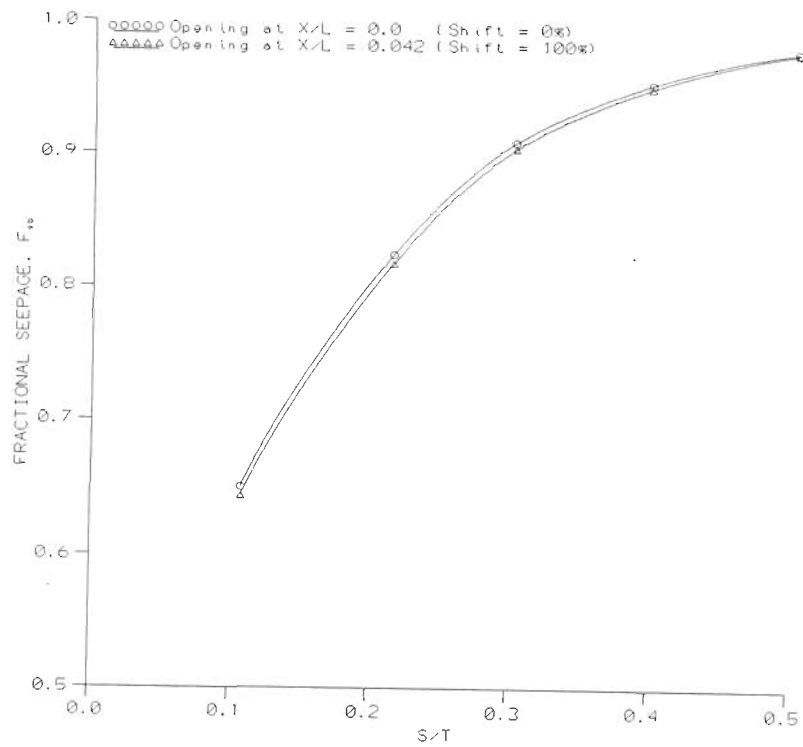


Fig. 6.39 S/T ratio versus Fractional Seepage (F_{sb}) to the bottom aquifer for two locations (Shift, $M_p=0\%$ and 100%) of the aquitard discontinuity with $O_p=5\%$.

equipotentials in the aquifer system with locations of the discontinuity at $X/L = 0$ and at $X/L = 0.43$, respectively are shown in Fig. 6.40 for two representative S/T ratios. When the discontinuity is located at the centre of the aquitard, the equipotential lines are well distributed in the bottom aquifer. However, as the discontinuous zone shifted away from the source and located at a large distance ($X/L = 0.43$), the potential distribution in the bottom aquifer is sparse or even absent. This indicates that the flow of water down to the bottom aquifer is meagre or non-existent when the discontinuity is located about mid-way between the centre and the boundary.

When the discontinuity is centrally located, the normalised distance (X/L) versus normalised hydraulic potential (h_n) in the bottom aquifer for several S/T ratios is given in Fig. 6.41. This graph may be compared with the one shown in Fig. 6.42 for which the discontinuity is located half way between the source and the boundary of the aquifer system. Higher hydraulic potential is observed for smaller S/T values when the discontinuity is far away from the source. Though higher hydraulic potentials are observed for smaller S/T values when the discontinuity is located at the centre, a reverse trend can be noticed in a small region below the source. This can be attributed to the stagnation of groundwater flow in the vicinity of the source by virtue of the assigned aquifer parameters.

Fig. 6.43 superimposes the hydraulic potentials for the two locations of the discontinuity at $X/L = 0$ and $X/L = 0.43$. It follows that the hydraulic potential in the bottom aquifer is much lower when the discontinuity is located at $X/L = 0.43$. On the sensitivity of hydraulic potentials with regard to the aquifer parameters, it is noticed that the hydraulic potential build-up in the bottom aquifer is weaker for an aquifer system with large S/T value corroborating the distributional pattern of hydraulic potentials discussed already.

Further, the fractional seepage (F_{sb}) to the bottom aquifer is maximum when the discontinuity is located at the centre (below the source) compared to any other location. Also, irrespective of the location of the discontinuity, the fractional seepage (F_{sb}) is found to be higher for an aquifer system with high S/T value. These facts are illustrated in Fig. 6.44 wherein fractional seepage (F_{sb}) for two locations of the discontinuity is plotted against the S/T ratios. Therefore, in the case of an aquifer system with a small S/T ratio, more of the groundwater flow may be discharged through the top

SIMULATION OF FLOW IN MULTILAYERED AQUIFER SYSTEM WITH AND WITHOUT DISCONTINUITY

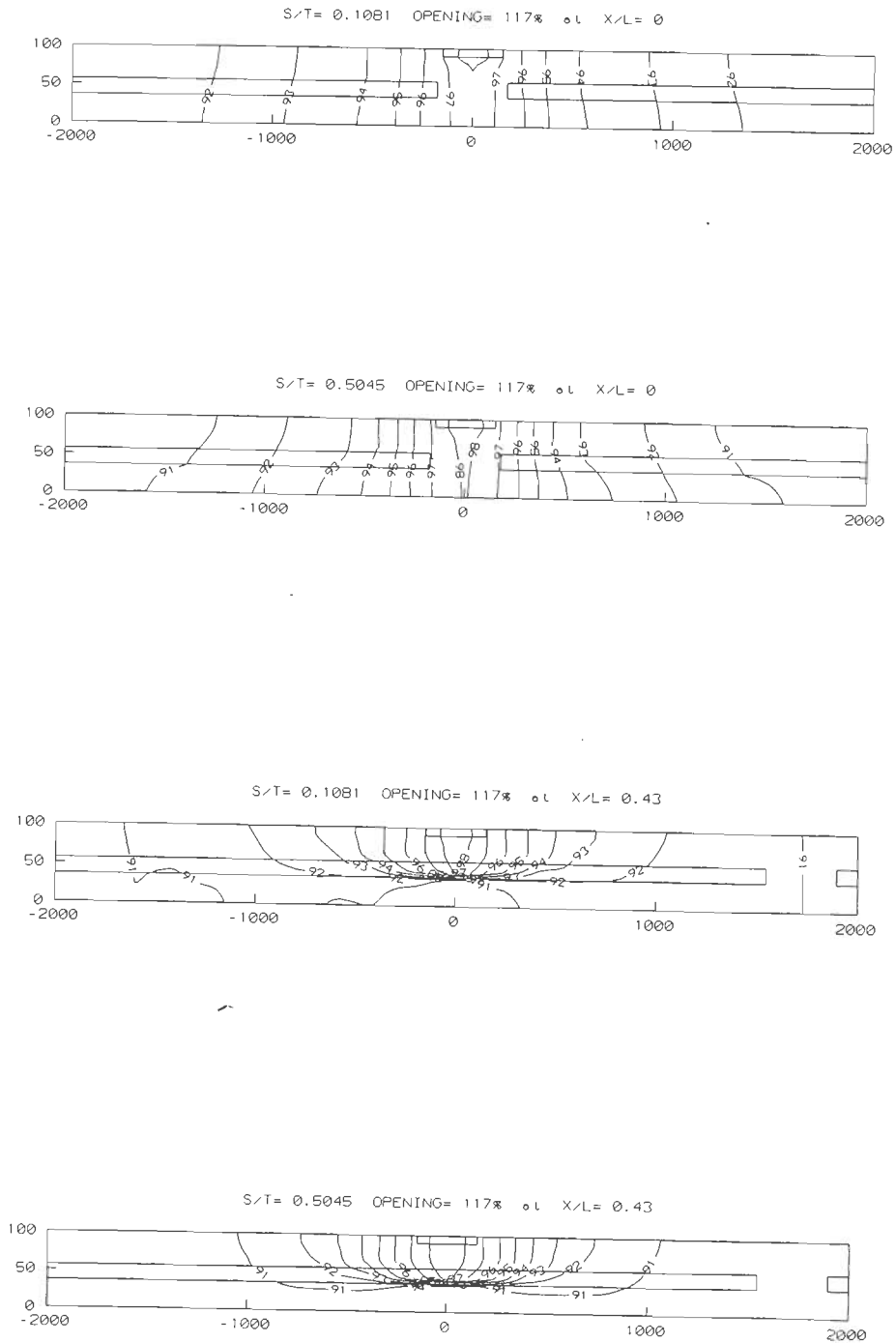


Fig. 6.40 Distribution of hydraulic potentials (h) in the aquifer system with the aquitard discontinuity located at $X/L=0$ and $X/L=0.43$ in the aquitard for $S/T=0.1081$ and $S/T=0.5045$ when the discontinuous Aquitard Position, $P_d=0.53$.

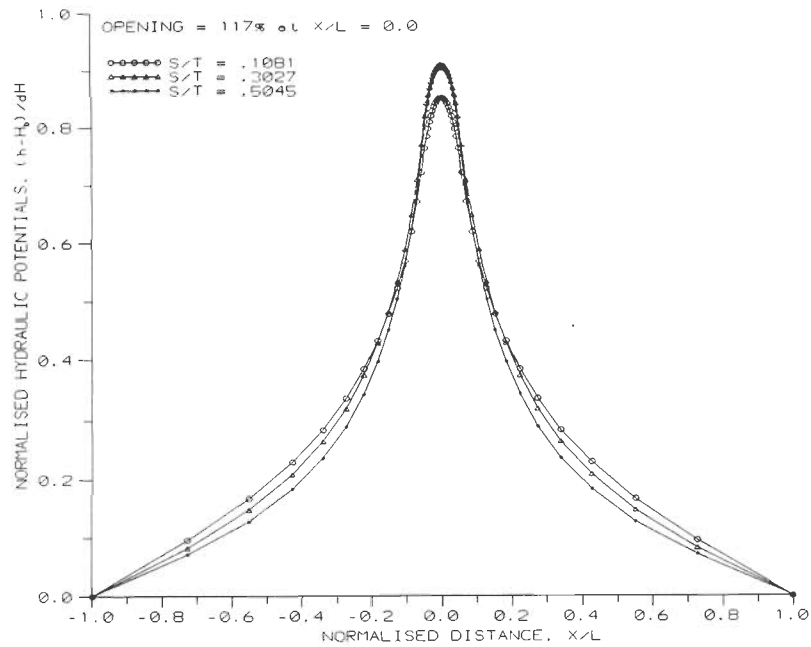


Fig. 6.41 Normalised Distance (X/L) versus Normalised Hydraulic Potentials (h_n) in the bottom aquifer for different S/T ratios when the aquitard discontinuity ($O_p = 117\%$) is located at $X/L = 0$.

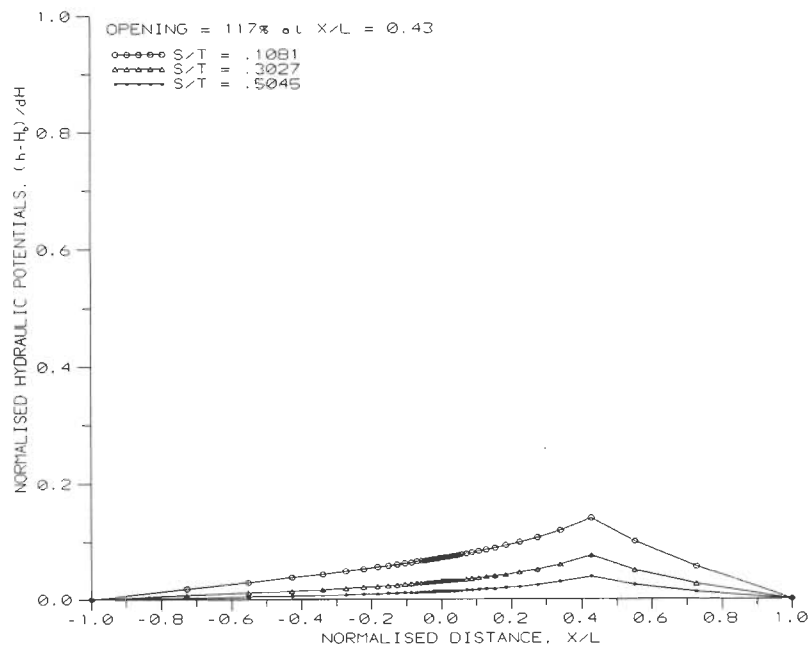


Fig. 6.42 Normalised Distance (X/L) versus Normalised Hydraulic Potentials (h_n) in the bottom aquifer for different S/T ratios when the aquitard discontinuity ($O_p = 117\%$) is located at $X/L = 0.43$.

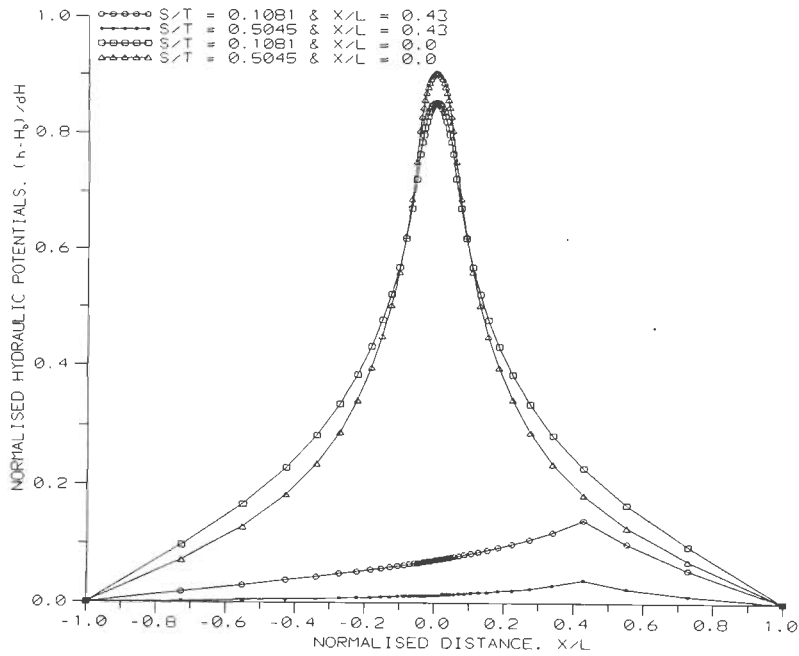


Fig. 6.43 Normalised Distance (X/L) versus Normalised Hydraulic Potentials (h_n) in the bottom aquifer for two S/T ratios when the aquitard discontinuity ($O_p = 117\%$) is located at $X/L = 0$ and $X/L = 0.43$.

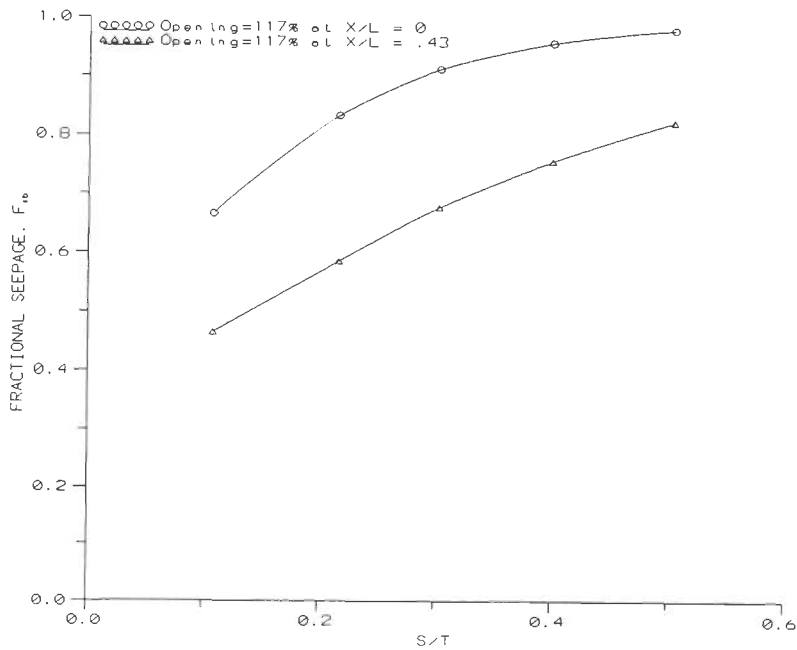


Fig. 6.44 S/T ratio versus Fractional Seepage (F_{sb}) to the bottom aquifer when the aquitard discontinuity ($O_p = 117\%$) is located at $X/L = 0$ and $X/L = 0.43$, respectively.

aquifer without contributing towards the recharging of the bottom aquifer. This conforms with the observations made in the previous Sections.

However, from a plot of maximum values of normalised hydraulic potential (h_n) in the bottom aquifer for different S/T ratios [Fig. 6.45], it may be seen that there is a reduction in the maximum value of the hydraulic potential for large S/T ratios. This is more pronounced when the discontinuity is located away from the source. Therefore, for an aquifer system with low hydraulic diffusivity (T/S) the discharge would also be less even though the fractional seepage (F_{sb}) is more. Besides, the recharging of the bottom aquifer is found to be very less, regardless of the aquifer parameters, when the discontinuity is located at normalised distance, $X/L > 0.5$.

6.6.2.4 Effect of Shifting of the Discontinuity to Several X/L Points on Recharge for a Specific Position of the Aquitard

The simulation studies carried out in this section have been formulated with uniform model grids of the aquifer system so as to enable the discontinuity of the aquitard to be located successively at regular intervals. The dimension of the discontinuity for the various cases has been fixed to be equal to the width of the water body ($O_p=100\%$). Table-6.5 gives the cases simulated with several locations of the discontinuity between the centre and the boundary of the aquifer system for a given aquifer set-up. This helps to provide a continuous scenario for analysing the effect of the location of the discontinuity on the recharging of the aquifer system.

Table 6.5 Matrix table of various cases studied with position of the aquitard at $P_d=0.53$ and Percentage Opening, $O_p=100\%$.

X/L	0.00	0.15	0.30	0.45	0.60	0.75	0.90
$S/T=0.1081$	✓	✓	✓	✓	✓	✓	✓

The distribution of hydraulic potentials (h) when the discontinuity being located progressively towards the boundary at three locations, $X/L=0$, $X/L=0.15$ and $X/L=0.30$, respectively is presented [Fig. 6.46]. The distribution patterns of the hydraulic potentials are different for different locations of the discontinuity. Fading of the hydraulic potential field in the bottom aquifer

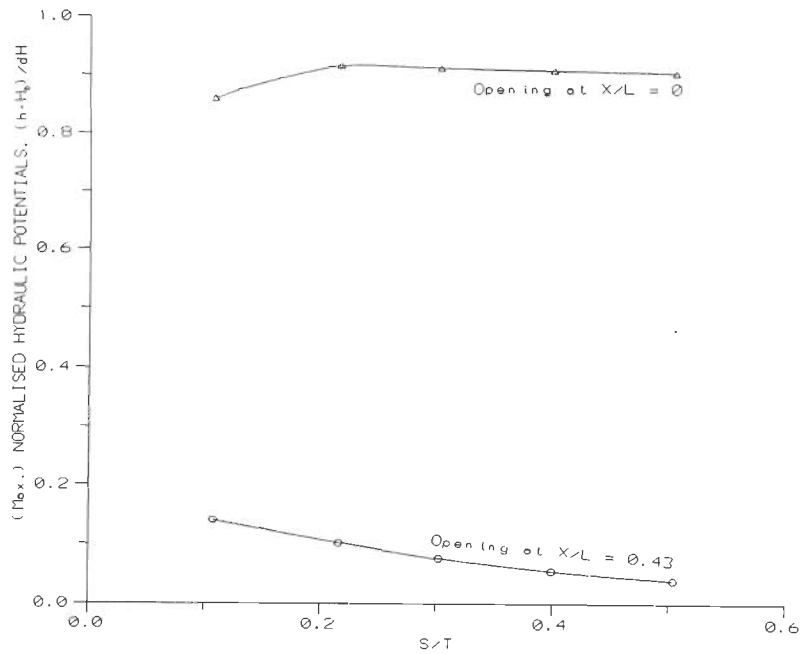


Fig. 6.45 S/T ratio versus maximum values of Normalised Hydraulic Potentials (h_n -max) in the bottom aquifer when the aquitard discontinuity ($O_p=117\%$) is located at $X/L=0$ and $X/L=0.43$.

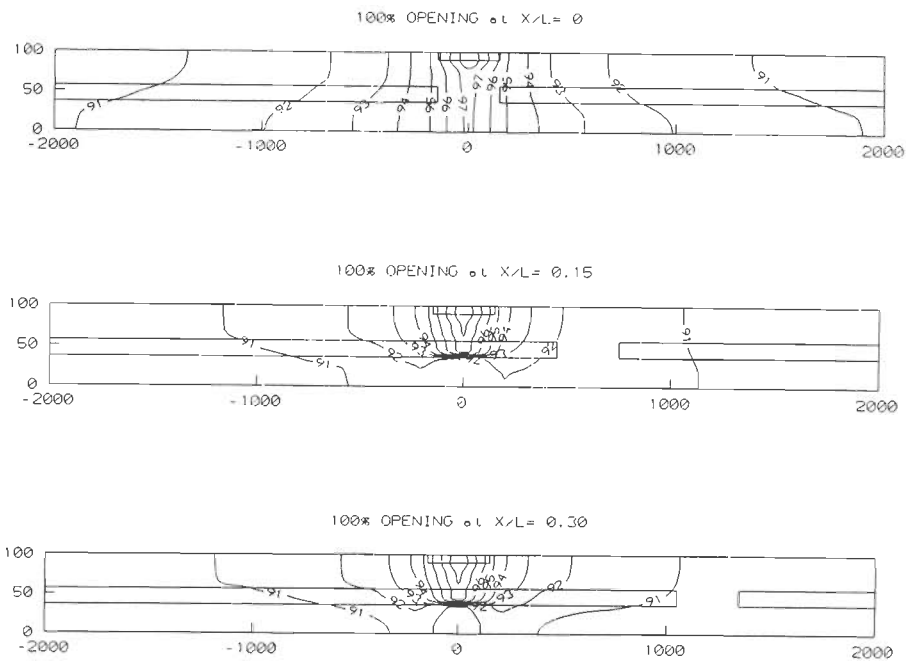


Fig. 6.46 Distribution of hydraulic potentials (h) in the aquifer system for three locations (at $X/L=0$, 0.15 and 0.30) of the aquitard discontinuity ($O_p=100\%$) when the discontinuous Aquitard Position, $P_d=0.53$.

can be noticed as the discontinuity moves away from the source. However, the distribution of hydraulic potentials in the top aquifer is apparently less susceptible to the location of the discontinuity as evident from Fig. 6.47, wherein the hydraulic heads for the three locations of the discontinuity are plotted. Normalised distance (X/L) versus normalised hydraulic potential (h_n) in the bottom aquifer for several locations of the discontinuity is shown in Fig. 6.48. The hydraulic potential in the bottom aquifer influenced by the shifting of location of the discontinuity is quite clear. It can be noticed that when the discontinuity is placed at half way between the centre and the boundary of the system, the hydraulic potential in the bottom aquifer is considerably low suggesting the inadequacy of the discontinuity to transmit water to the bottom aquifer. Thus, locating the discontinuity beyond a normalised distance, $X/L=0.5$ has no significance, as observed earlier.

The maximum values of normalised hydraulic potentials (h_n) for various locations of the discontinuity is also plotted [Fig. 6.49]. A near-exponentially decreasing pattern emerges as the discontinuity moves away from the source. More than 50% reduction in the maximum value of the hydraulic potential, compared to that corresponding to the location of the discontinuity at $X/L=0$, is observed even when the discontinuity is shifted to a point at $X/L=0.1$. Further, the maximum value of hydraulic potential corresponding to the location of the discontinuity at $X/L=0.5$ is found to be much smaller. This supports the fact that the discontinuity located at farther points are not efficient in transmitting water to the bottom aquifer. The fractional seepage (F_{sb}) values corresponding to various locations of the discontinuity also show a diminishing contribution associated with the shifting of the discontinuity away from the centre [Fig. 6.50]. The fractional seepage (F_{sb}) reduces to half of its value (corresponding to that at $X/L=0$) when the discontinuity is shifted to $X/L=0.5$.

The preceding discussions reveals that the hydraulic potentials in the bottom aquifer as well as the fractional seepage (F_{sb}) tends to reduce as the discontinuity in the aquitard shifts towards the boundary. Hence, in the context of artificial recharging, a recharging pond or percolation tank needs to be located accordingly to effect optimum recharging of an underlying aquifer.

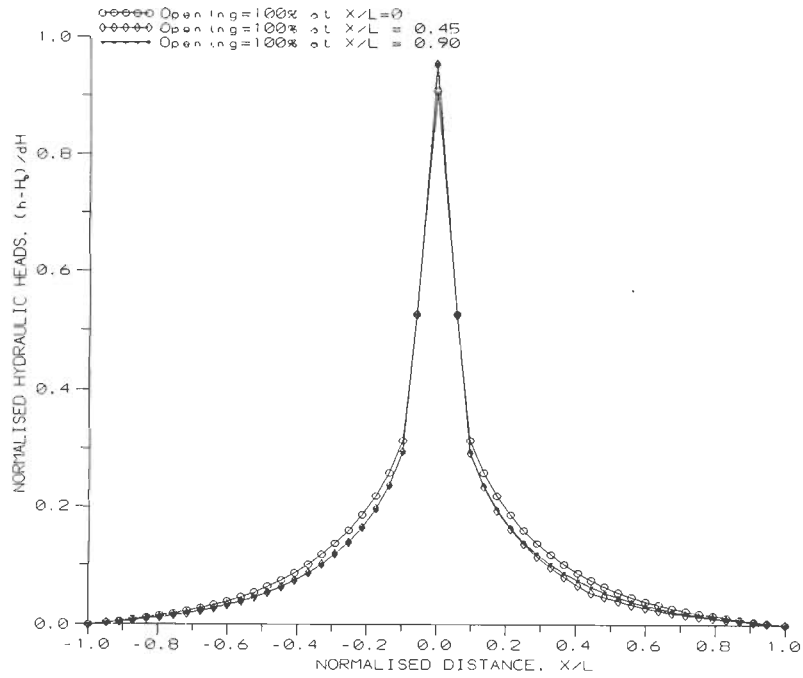


Fig. 6.47 Normalised Distance (X/L) versus Normalised Hydraulic Heads (h_n) in the top aquifer when the aquitard discontinuity ($O_p = 100\%$) is located at different X/L points.

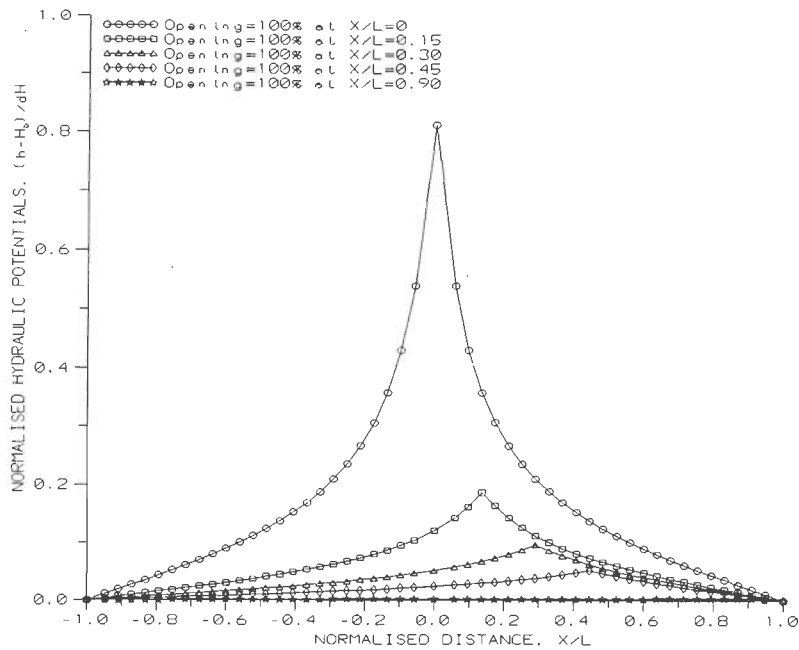


Fig. 6.48 Normalised Distance (X/L) versus Normalised Hydraulic Potentials (h_n) in the bottom aquifer when the aquitard discontinuity ($O_p = 100\%$) is located at different X/L points.

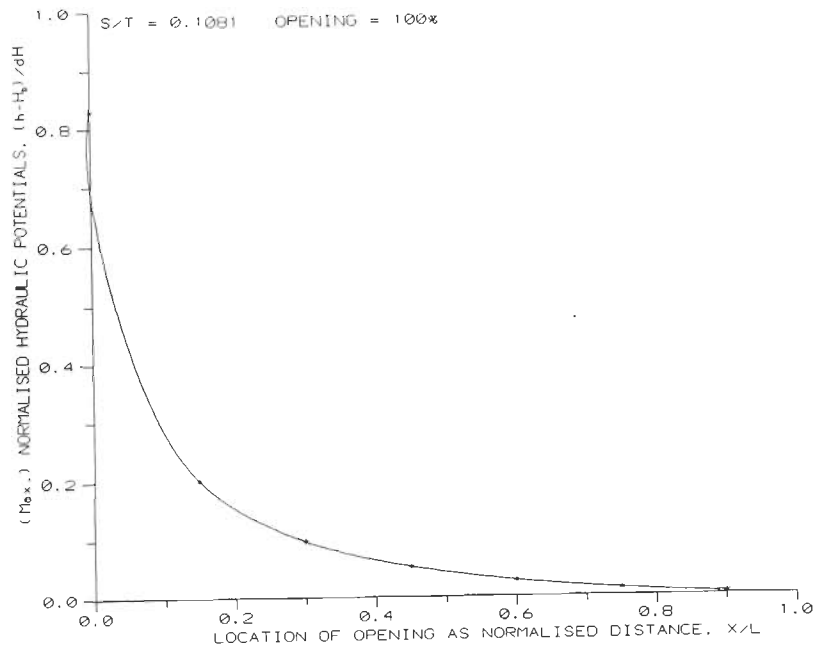


Fig. 6.49 Location (M_p) of the aquitard discontinuity (in terms of Normalised Distance, X/L) versus maximum values of Normalised Hydraulic Potentials (h_n) in the bottom aquifer when Percentage Opening, $O_p = 100\%$.

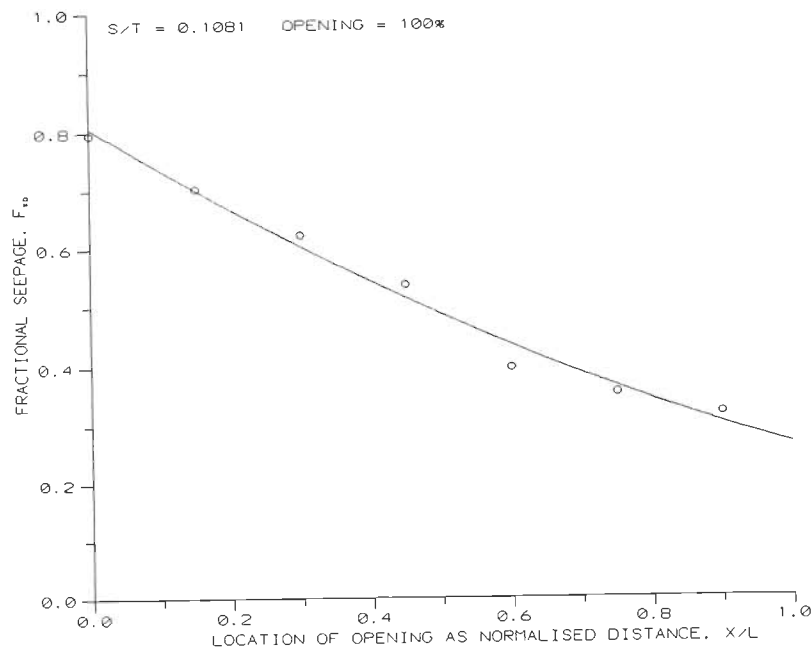


Fig. 6.50 Location (M_p) of the aquitard discontinuity (in terms of Normalised Distance, X/L) versus Fractional Seepage (F_{sb}) to the bottom aquifer when Percentage Opening, $O_p = 100\%$.

6.6.3 EFFECT OF DEPTH-WISE POSITIONING OF THE DISCONTINUOUS AQUITARD ON RECHARGING

The effect of the location of the aquitard discontinuity on the recharging of the aquifer system has been discussed in the preceding sections for a fixed position of the aquitard at a depth of about $D/2$. The effect of depth-wise positioning of the discontinuous aquitard in the porous medium on the recharging of the aquifer system is analysed in this section. The location of the discontinuity (of 5%) is fixed at $X/L=0$. The discontinuous aquitard is placed at several depths without disturbing the general setup of the aquifer system. The position of the aquitard is indicated by the positioning depth, P_d (ratio of the depth of the aquitard to the total depth of the aquifer system). By this convention, positioning depth, $P_d=0.5$ implies that the aquitard is exactly placed in the middle of the aquifer system.

6.6.3.1 Effect of Positioning of the Aquitard on the Recharge for Several Depth-wise Positions and Values of S/T Ratio

Several cases formulated with a combination of S/T ratios and positioning depths (P_d) for a specific discontinuity at the centre of the aquitard are given in the Table-6.6.

Table 6.6 Matrix table of various cases studied with different positions of the aquitard for Percentage Opening, $O_p=5\%$.

S/T Ratio	Position of the Aquitard (P_d)						
	0.68	0.63	0.58	0.53	0.48	0.43	0.38
0.1081	✓	✓	✓	✓	✓	✓	✓
0.2162	✓	✓	✓	✓	✓	✓	✓
0.3027	✓	✓	✓	✓	✓	✓	✓
0.4000	✓	✓	✓	✓	✓	✓	✓
0.5045	✓	✓	✓	✓	✓	✓	✓

The distribution of hydraulic potentials (h) in the vertical section for several S/T ratios of the aquifer system for a positioning depth, $P_d=0.53$ is presented [Fig. 6.51]. Also, the equipotentials in the aquifer system for several positions of the discontinuous aquitard is depicted in Fig. 6.52.

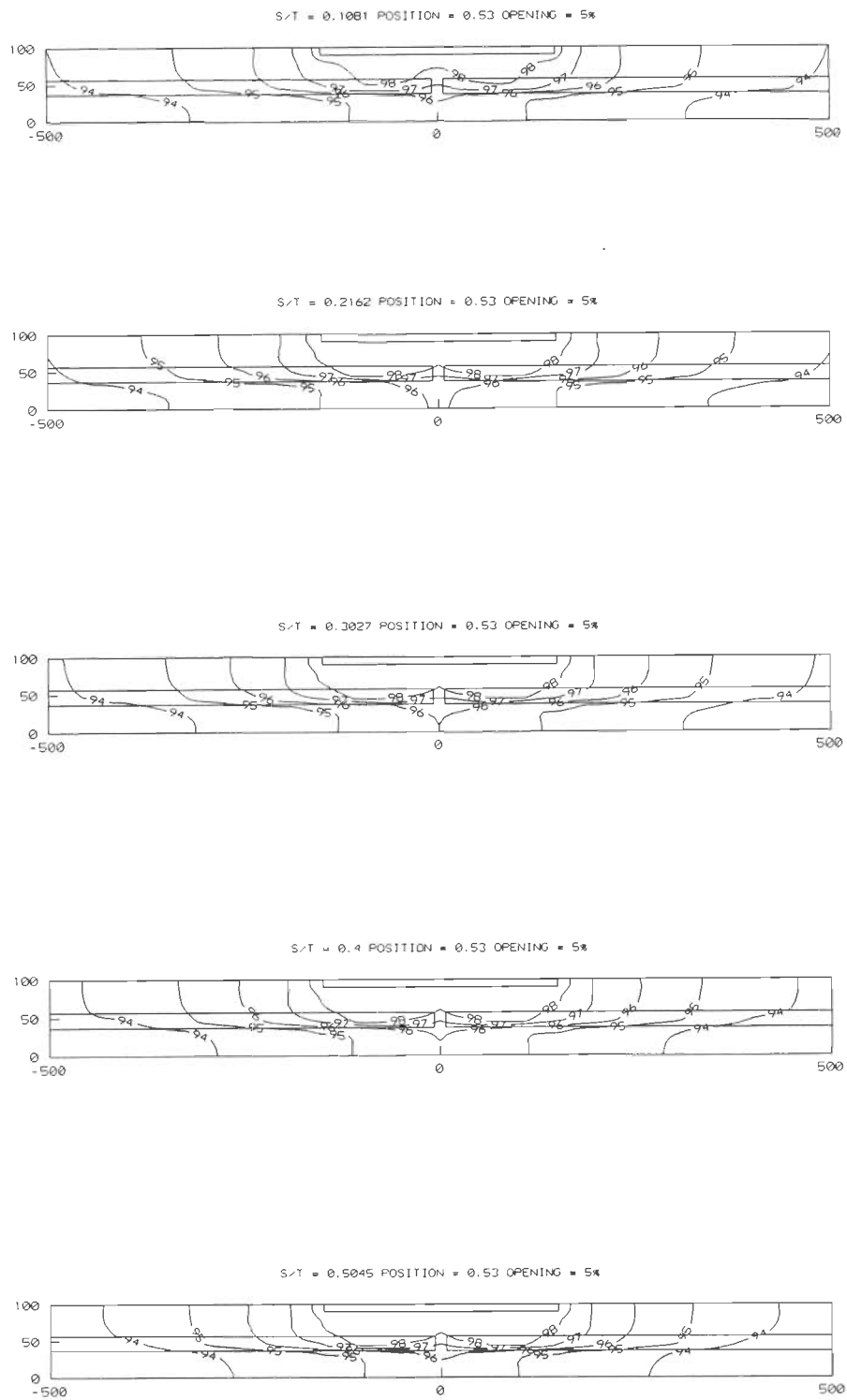


Fig. 6.51 Distribution of hydraulic potentials (h) in the aquifer system for several S/T ratios for a Percentage Opening, $O_p=5\%$ when the discontinuous Aquitard Position, $P_d=0.53$.

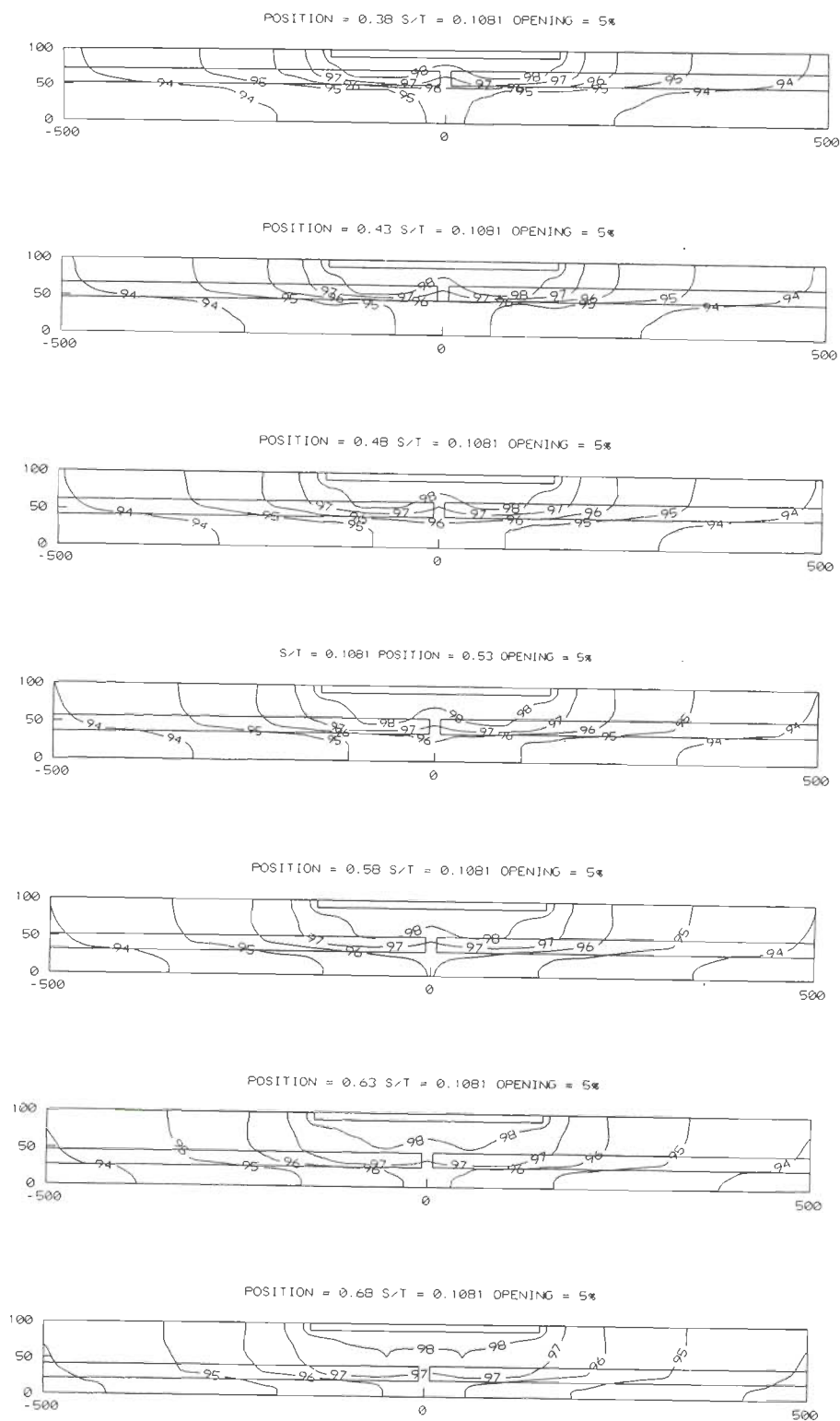


Fig. 6.52 Distribution of hydraulic potentials (h) for several Aquitard Positions (P_d) when $S/T=0.1081$ and Percentage Opening, $O_p=5\%$.

Apparently, the hydraulic potentials in the bottom aquifer tend to increase when the discontinuous aquitard is positioned nearer to the lower boundary.

The normalised hydraulic potentials (h_n) in the top and bottom aquifer, respectively have been plotted for selected positioning depths (P_d) of the discontinuous aquitard [Fig. 6.53 and Fig. 6.54]. It is observed that the hydraulic head/ potential is on the rise with increasing positioning depth (P_d) of the aquitard. Positioning of the discontinuous aquitard deeper in the aquifer system is associated with deepening of the top aquifer as the overall setup has been preserved. Now, a thicker top aquifer can receive more seepage from the source to build up higher hydraulic heads. This, in turn, may result in increased recharging of the bottom aquifer thereby raising the hydraulic potential there.

The sensitivity of hydraulic heads/ potentials with regard to aquifer parameters has also been elaborated [Fig. 6.55 and Fig. 6.56]. Higher hydraulic heads/ potentials (for top as well as bottom aquifer) are observed in the case of aquifer systems with smaller S/T ratios.

Further, the behaviour of maximum values of normalised hydraulic potential (h_n) in the bottom aquifer has been examined vis-a-vis the positioning depths (P_d) of the discontinuous aquitard [Fig. 6.57]. The linearly increasing trend of the graph suggests that the hydraulic potential in the bottom aquifer builds-up as the discontinuous aquitard moves closer to the lower boundary. However, the fractional seepage (F_{sb}) exhibited a reverse trend [Fig. 6.58]; it reduces with increased positioning depths (P_d) of the aquitard. This suits to the logic as the bottom aquifer becomes thinner with increased positioning depths (P_d) of the aquitard resulting in reduced holding capacity, thereby limiting the fractional seepage (F_{sb}). The sensitivity of fractional seepage (F_{sb}) with respect to aquifer parameters can be judged from Fig. 6.59.

The analysis shows that the behaviour of hydraulic heads/ potentials in the top/ bottom aquifer is identical. The hydraulic potentials are found to be higher when the discontinuous aquitard is closer to the impermeable lower boundary (i.e., when the top aquifer is thicker than the bottom aquifer). However, the fractional seepage, F_{sb} (fraction of the total seepage from the source that reaches the bottom aquifer) decreases for larger positioning depths (P_d).

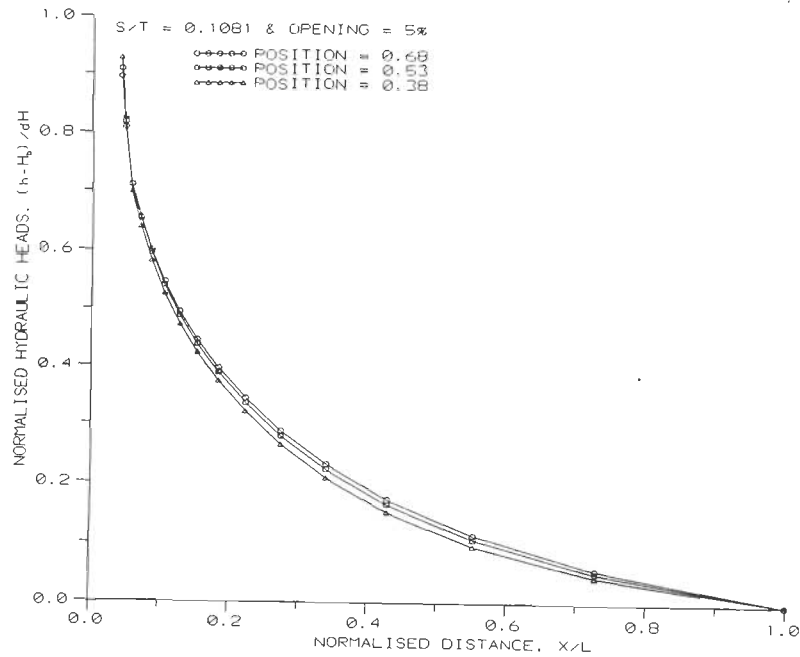


Fig. 6.53 Normalised Distance (X/L) versus Normalised Hydraulic Heads (h_n) in the top aquifer for different Aquitard Positions (P_d) when $S/T=0.1081$ and Percentage Opening, $O_p=5\%$.

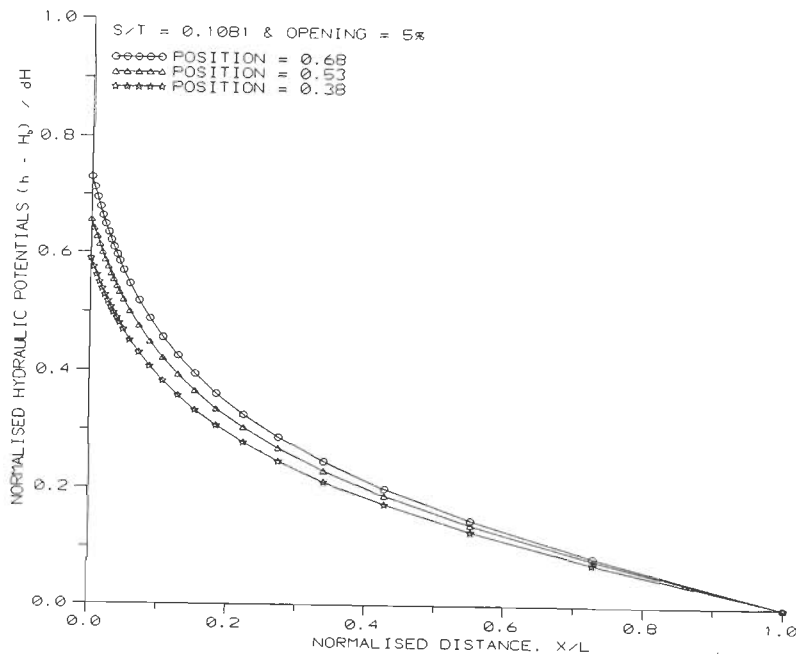


Fig. 6.54 Normalised Distance (X/L) versus Normalised Hydraulic Potentials (h_n) in the bottom aquifer for different Aquitard Positions (P_d) when $S/T=0.1081$ and Percentage Opening, $O_p=5\%$.

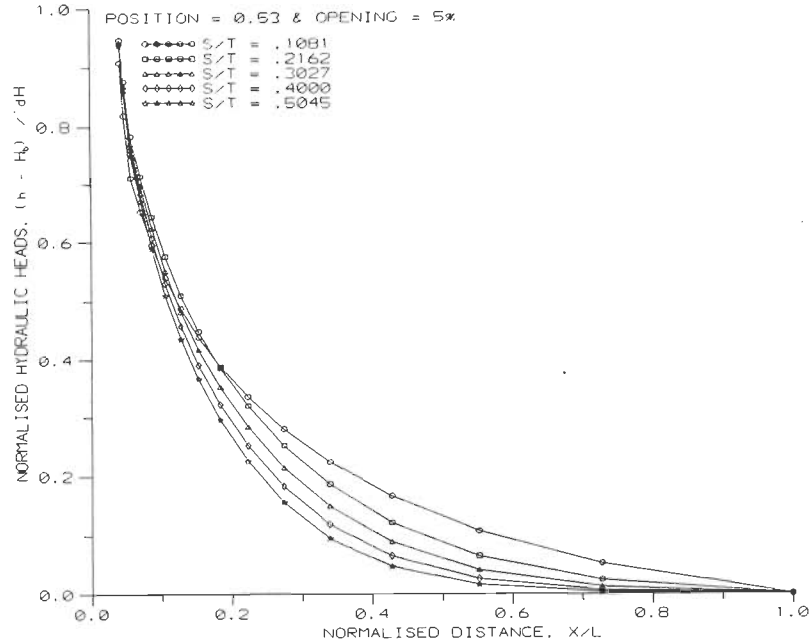


Fig. 6.55 Normalised Distance (X/L) versus Normalised Hydraulic Heads (h_n) in the top aquifer for several S/T ratios when the Aquitard Position, $P_d=0.53$ and Percentage Opening, $O_p=5\%$.

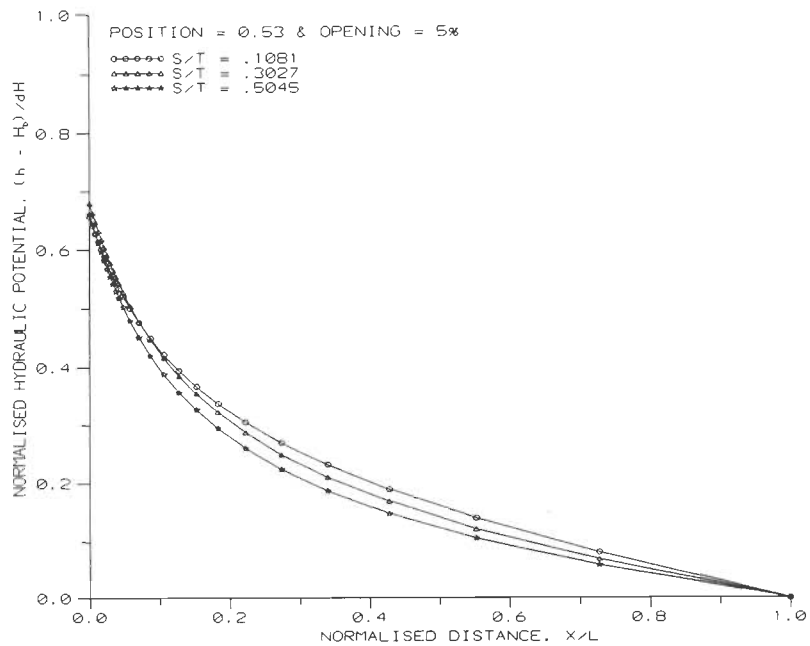


Fig. 6.56 Normalised Distance (X/L) versus Normalised Hydraulic Potentials (h_n) in the bottom aquifer for different S/T ratios when the Aquitard Position, $P_d=0.53$ and Percentage Opening, $O_p=5\%$.

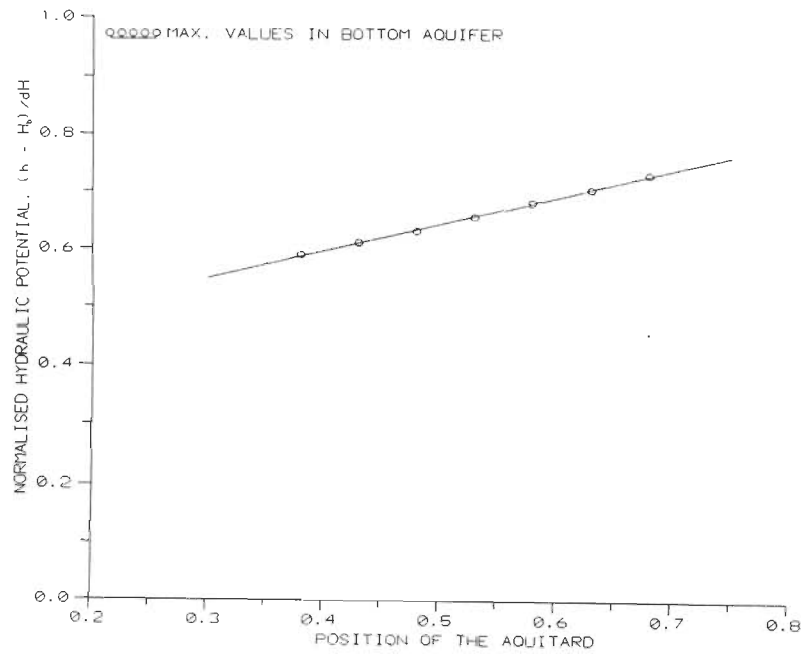


Fig. 6.57 Aquitard Position (P_d) versus maximum values of Normalised Hydraulic Potentials (h_n -max) in the bottom aquifer for a Percentage Opening, $O_p = 5\%$.

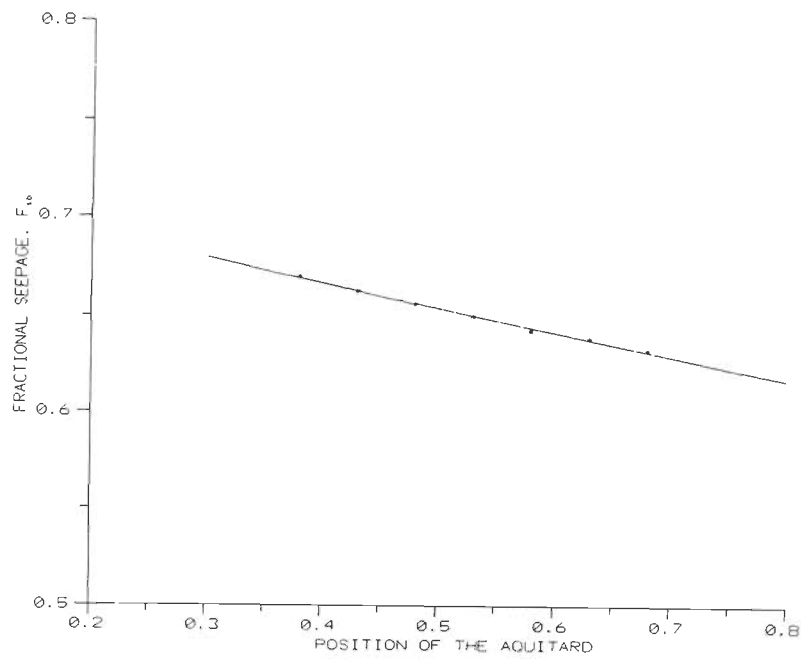


Fig. 6.58 Aquitard Position (P_d) versus Fractional Seepage (F_{sb}) to the bottom aquifer for a Percentage Opening, $O_p = 5\%$.

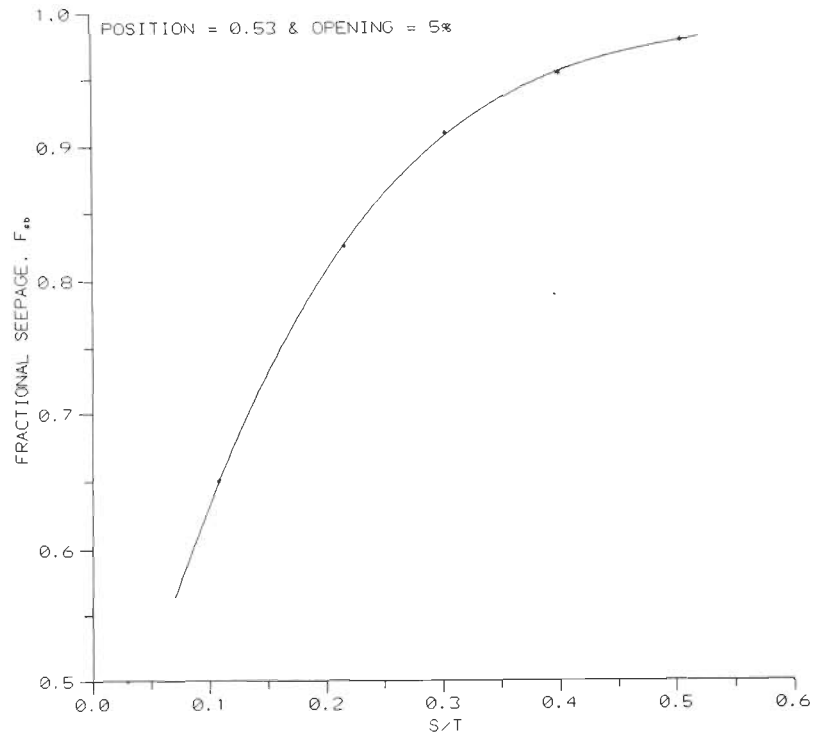


Fig. 6.59 S/T ratio versus Fractional Seepage (F_{sb}) to the bottom aquifer for the Aquitard Position, $P_d=0.53$ and a Percentage Opening, $O_p=5\%$.

6.7 RESULTS

The preceding analyses dwell on the recharging characteristics/ due to a surface water source, of an aquifer-aquitard-aquifer system in which the aquitard is discontinuous. The simulation studies pertain to the effect of the following aspects on the recharging of the aquifer system:

- (i) Dimension of the aquitard discontinuity in a centrally positioned aquitard,
- (ii) Location of the discontinuity in the aquitard with respect to the source, and
- (iii) Depth-wise position of the discontinuous aquitard in the aquifer system.

The important findings/ results from these investigations *are summarised* have been enumerated in the following sections:

6.7.1 DIMENSION OF THE AQUITARD DISCONTINUITY

Results from the analysis on the effect of dimension of the aquitard discontinuity in a centrally positioned aquitard on the recharging of the aquifer system are:

- (i) The fractional seepage, F_{sb} is found to be invariant to changes in storage coefficient or hydraulic conductivity values for a constant ratio of S/T .
- (ii) For the aquifer above the discontinuous aquitard, the aquitard discontinuity influences the head distribution only in the vicinity of the source.
- (iii) For the aquifer below the discontinuous aquitard, the head distribution (thereby recharge) is influenced by the aquitard discontinuity and is sensitive to S/T ratio.
- (iv) Even for a very small percentage opening (O_p), it is observed that the contribution of seepage to the bottom aquifer (responsible for its recharge) is significantly high. Further, the recharging of the bottom aquifer is facilitated with large ratios of S/T .

6.7.2 HORIZONTAL LOCATION OF THE AQUITARD DISCONTINUITY

Investigation on the effect of the location of the aquitard discontinuity on the recharging of the aquifer system has yielded results relevant to artificial recharge practices.

- i) The hydraulic potential in the aquifer below the discontinuous aquitard (bottom aquifer) tends to reduce as the aquitard discontinuity shifts away from the source. The maximum seepage to the bottom aquifer occurs when the aquitard discontinuity, irrespective of its dimension, is located centrally below the recharging source.
- ii) The maximum hydraulic potential in the bottom aquifer is always directly below the discontinuity, even when the aquitard discontinuity is shifted away from the source.
- iii) The fractional seepage, F_{sb} to the bottom aquifer gets reduced with the shifting of the aquitard discontinuity. *from the centre of the source.*
- iv) For a given location of the aquitard discontinuity, the extent of influence on recharging of the aquifer system is found to be high for smaller discontinuities. For larger aquitard discontinuities the influence of their location on recharging tends to reduce.

6.7.3 POSITIONING DEPTH OF THE DISCONTINUOUS AQUITARD

The cases analysed with several depth-wise positions of the discontinuous aquitard reveal that the positioning of the aquitard within aquifer system has a regulatory role on the recharging of the bottom aquifer. It is found that:

- i) When the discontinuous aquitard is positioned nearer to the source, the hydraulic potential field in the top and bottom aquifers is less effective compared to that for a deeper position of the aquitard.
- ii) Though the aquifer system has developed higher potentials with the discontinuous aquitard positioned closer to the impermeable boundary (implying a reduced thickness of the bottom aquifer), the fractional seepage (F_{sb}) to the bottom aquifer is found to be reduced quantitatively.

- ① Too many ^{extra} commas (,) are found in the thesis.
- ② Too many slashes (/) are used, which normally should be avoided.

SUMMARY AND CONCLUSIONS

7.1 GENERAL

Studies have been carried out on the hydraulic responses of recharging due to surface water sources in multilayered as well as anisotropic aquifer systems in the backdrop of artificial recharge practices. Analytical and numerical methods have been employed in performing the studies presented in the thesis. Based on the advances made in the theory of geoelectrical sounding, analytical models have been developed and validated for aquifer simulation in multilayered/homogeneous anisotropic aquifer systems. Further, numerical simulation analyses have been performed with the application of MODFLOW in the case of an aquifer-aquitard-aquifer system to infer useful results. The important contributions ^{and} conclusions ^{from} of these studies are enlisted below.

7.2 SUMMARY OF RESULTS AND CONCLUSIONS

1. Analytical solutions have been developed for the computation of steady-state hydraulic potentials and streamlines, due to surface water sources, in multilayered aquifer systems.
2. Using the developed analytical solutions, computational algorithms for the hydraulic potentials and streamlines have been devised for the case of a three-layered aquifer system (3LPNT- for the case of a point source, 3LLIN- for the case of a finite length line source and 3LARL- for the case of an areal source).
3. A generalised computational algorithm for the hydraulic potentials and streamlines due to a point source has also been devised in the case of a multilayered aquifer system (NLPNT).

4. The working of the developed models has been demonstrated with numerical examples. Also, a validation of the developed models has been performed using MODFLOW.
5. The developed analytical models require fewer input data and are computationally very efficient. For instance, a five layer aquifer system simulated with $41 \times 41 \times 25$ grid points using the analytical algorithm NLPNT was found to be about twenty five times faster than that of a corresponding MODFLOW simulation with the same number of grid points when executed on a 32-bit Pentium (300MHz) Personal Computer.
6. Analytical solutions have been developed for computing the hydraulic potentials due to a point source and that due to a finite-length line source in a homogeneous anisotropic aquifer systems with dipping beds. Computational algorithms, HANI-P (for the case of a point source) and HANI-L (for the case of a finite-length line source) have been devised using the developed analytical solutions to enable demonstration of these models. Besides, the validity of the developed analytical expressions has been verified for isotropic assumptions.
7. Following conclusions are deduced from the analyses concerning the recharging of an aquifer-aquitard-aquifer system:
 - a) When the depth-wise position of the continuous aquitard in the aquifer system is at a depth greater than three times its thickness, the influence of the aquitard on the recharging of the aquifer system is found to be insignificant.
 - b) For a constant ratio of storage coefficient and transmissivity (S/T), the fractional seepage (fraction of the total seepage from the source contributed to the top aquifer as well as the bottom aquifer) is found to be invariant with changes in either storage coefficient or hydraulic conductivity.
 - c) For the aquifer below the discontinuous aquitard, the head distribution is governed by the S/T ratio as well as the dimension of the aquitard discontinuity.
 - d) Even for a very small percentage opening (of the aquitard), the quantitative contribution of seepage to the bottom aquifer (responsible for its recharging) is found

to be quite significant. For instance, a 1% opening can contribute nearly as much as that of a 30% opening. 77

- e) The maximum hydraulic potential in the aquifer below the discontinuous aquitard is found to be directly below the discontinuity, and need not be below the source. Further, optimum recharging of the bottom aquifer occurs when the aquitard discontinuity is located centrally below the recharging source.
- f) For a given location of the aquitard discontinuity, the extent of influence on recharging is found to be high for smaller discontinuities; as the discontinuity becomes larger the influence of its horizontal location on the recharging tends to reduce.
- g) When the aquitard is positioned (depth-wise) nearer to the source, the recharging of the aquifer system is found to be reduced compared to that for a deeper position of the aquitard.

change
is
suggested
in
page 147

7.3 FURTHER PERSPECTIVES

In continuation to the present effort, the following topics constitute future work:

1. Formulation of analytical solutions for the case of buried sources in multilayered aquifer systems.
2. Formulation of analytical solution for stream function in the case of an anisotropic aquifer system
3. Formulation of analytical solutions for a three-dimensional anisotropic aquifer system with an arbitrary orientation of the finite-length line source.

REFERENCES

1. Allam, A.R., Amer, A.M., Attia, F.A.R., and Sherif, M.M., Numerical simulation of artificial recharge of groundwater through spreading basins, *ICID Journal* 47(1), 19-29, 1998.
2. Anderman, E.R., Hill, M.C., and Poeter, E. P., Two-dimensional advective transport in ground-water flow parameter estimation, *Ground Water* 34(6), 1001-1009, 1996.
3. Anderson, M.P. and Cheng, X., Long and short term transience in gw/lake system in Wisconsin, USA, *J. Hydrol.* 145, 1-18, 1993.
4. Anderson, M.P. and Woessner W.W., *Applied groundwater modelling- Simulation of flow and advective transport*, Academic Press, London, 1991.
5. Balek, J. and Bursik, M., Groundwater recharge processes in sedimentary structures of the Czech Cretaceous basin, *J. Hydrol.* 111(1-4), 225-234, 1989.
6. Bakker, M. and Strack, O.D.L., Capturezone delineation in two dimensional ground water flow models, *Water Resour. Res.* 32(5), 1309-1315, 1996.
7. Bakker, M., Simulating groundwater flow in multi-aquifer systems with analytical and numerical Dupuit-models, *J. Hydrol.* 222, 55-64, 1999.
8. Barlow, P.M. and Moench, A.F., Analytical solutions and computer programmes are hydraulic interction of stream-aquifer systems, *USGS Open File Report* 98-415A, 1998.
9. Barua, G. and Tiwari, K.N., Analytical solutions of seepage into ditches from ponded fields, *J. Irrigation and Drainage Engg.* 121(6), 396-404, 1995.
10. Barua, G. and Tiwari, K.N., Theories of ditch drainage in layered anisotropic soil, *J. Irrigation and Drainage Engg.* 122(6), 321-330, 1996.
11. Bear, J., *Dynamics of fluids in porous media*, Elsevier Scientific Publishing Co., New York, 1972.
12. Beckers, J. and Frind, E.O., Simulating groundwater flow and runoff for the Oro Moraine aquifer system, Part 1. Model formulation and conceptual analysis, *J. Hydrol.* 229, 265-280, 2000.
13. Bhattacharya, P.K. and Patra, H.P., *Direct Current Geoelectric sounding-principles and interpretation*, Elsevier Scientific Publishing Co., Amsterdam, 1968.

14. Bobba, A. G., Bukata, R. P. and Jerome, J. H., Digitally processed satellite data as a tool in detecting potential groundwater flow systems, *J. Hydrol.* 131(1-4), 25-62, 1992.
15. Boehmer, W.K. and Boonstra, J., Analysis of drawdown in the country rock of composite dike aquifers, *J. Hydrol.* 94, 199-214, 1987.
16. Born, S.M., Smith, S.A. and Stephenson, D.A., Hydrology of glacial-terrain lakes, with management and planning applications, *J. Hydrol.* 43, 7-43, 1979.
17. Bouwer, H., Back, J.T. and Oliver, J.M., Predicting infiltration and groundwater mounds for artificial recharge, *J. Hydrologic Engg.* 4(4), 350-357, 1999.
18. Bradley, C., Transient modelling of water-table variation in a floodplain wetland, Narborough Bog, Leicestershire, *J. Hydrol.* 185, 87-114, 1996.
19. Bredehoeft, J.D., Cooper Jr., H.H. and Papadopoulos, I.S., Inertial and storage effects in well aquifer systems, an analog investigation, *Water Resour. Res.* 2, 697-707, 1966.
20. Brown, R.F. and Signor, D.C., Groundwater recharge, *Water Resour. Bull.* 8(1), 132-149, 1972.
21. Bruch Jr., J.C., Seepage streams out of canal and ditches overlying shallow water tables, *J. Hydrol.* 41, 31-41, 1979.
22. Bruker, S.M. and Haitjema, H.M., Modelling steady state conjunctive groundwater and surface water flow with analytic elements, *Water Resour. Res.* 32(9), 2725-2732, 1996.
23. Charbeneau, R.J. and Street, R.L., Modelling groundwater flow fields containing point singularities: Streamlines, traverse times, and breakthrough curves, *Water Resour. Res.* 15(6), 1445-1450, 1979.
24. Cheng, X. and Anderson, M. P., Numerical simulation of groundwater interaction with lakes allowing for fluctuating lake levels, *Ground Water* 31(6), 929-933, 1993.
25. Cherkauer, D.S. and Nader, D.C., Distribution of groundwater seepage to large surface water bodies: the effect of hydraulic heterogeneities, *J. Hydrol.* 109, 151-165, 1989.
26. Cherkauer, D.S. and Zvibleman, Hydraulic connection between Lake Michigan and a shallow groundwater aquifer, *Ground Water* 19(4), 376-381, 1981.
27. Christian, J.T., Flow nets by the finite element method, *Ground Water* 18 (2), 178-181, 1980.

REFERENCES

28. Connell, L.D., Jayatilaka, C. and Bailey, M., A quasi-analytical solution for groundwater movement in hillslopes, *J. Hydrol.* 204, 108-123, 1998.
29. Crowe, A.S. and Schwarts, F.W., Simulation of lake-watershed systems; 1. Description and sensitivity analysis of the model, *J. Hydrol.* 52, 71-105, 1981.
30. Dane, J.H. and Molz, F.J., Physical measurements in subsurface hydrology, *Reviews of Geophysics (Supplement)*, 270-279, 1991.
31. Daniels, J.J., Interpretation of buried electrodes resistivity data using a layered earth model, *Geophysics* 43(5), 988-1001, 1978.
32. Dwight, H.B., *Tables of integrals and other mathematical data* (4th Edition, in Russian), The Macmillan Company, New York, 1961
33. Eldho, T.I. and Rao, B.V., Estimation of canal seepage in a layered porous media using boundary element method, *Proceedings of New Delhi Symposium on Subsurface-water Hydrology* (Ed. by Singh, V.P. and Kumar, B), Kluwer Academics Publ., The Netherlands, 91-100, 1996.
34. Eshleman, K.N., Pollard, J.S. and O'brien, A.K., Interaction between ground water and surface water in a Virginia Coastal Plain Watershed: 1. Hydrological flowpaths, *Hydrological Processes* 8, 389-410, 1994.
35. Evans, D.G. and Raffensperger, J.P., On the stream function for variable density groundwater flow, *Water Resour. Res.* 28(8), 2141-2145, 1992.
36. Finsterle, S. and Pruess, K., Solving the estimation-identification problem in two-phase flow modeling, *Water Resour. Res.* 31(4), 913-924, 1995.
37. Fitts, C.R., Modelling three dimensional flow about ellipsoidal inhomogeneities with application to flow to a gravel packed well and flow through lens-shaped inhomogeneities, *Water Resour. Res.* 27(5), 815-824, 1991.
38. Fitts, C.R. and Strack, O.D.L., Analytic solutions for unconfined groundwater flow over a stepped base, *J. Hydrol.* 177, 65-76, 1996.
39. Fogg, G.E. and Senger, R.K., Automatic generation of flownets with conventional groundwater modelling algorithms, *Ground Water* 23(3), 336-344, 1985.

40. Freeze, R.A. and Cherry, J.A., *Ground Water*, Prentice-Hall, Englewood Cliffs, New York, 1979.
41. Frind, E.O. and Matanga, G.B., The dual formulation of flow of contaminant transport modelling, 1. Review of theory and accuracy aspects, *Water Resour. Res.* 21, 159-169, 1985.
42. Genereux, D. and Bandopadhyay, I., Numerical investigation of lake bed seepage patterns: effects of porous medium and lake properties, *J. Hydrol.* 241, 286-303, 2001.
43. Gjerde, K.M. and Tyvand, P.A., Anisotropy as a limit of layering- the decay of a disturbed free surface in a porous medium, *J. Hydrol.* 94, 267-288, 1987.
44. Grundl, T. and Delwiche, J., Water quality response to the partial casing of a well, *Ground Water* 30(1), 45-49, 1992.
45. Haitjema, H.M., Modelling three dimensional flow in confined aquifers by superposition of both two and three dimensional analytic functions, *Water Resour. Res.* 21(10), 1557-1566, 1985.
46. Haitjema, H.M. and Kraemer, S.R., A new analytic function for modelling partially penetrating wells, *Water Resour. Res.* 24(5), 683-690, 1988.
47. Haitjema, H.M., *Analytic element modelling of groundwater flow*, Academic Press, New York, 1995.
48. Haitjema, H.M. and Kelson, V.A., Using the stream function for flow governed by Poisson's equation, *J. Hydrol.* 187, 367-386, 1996.
49. Hamming, R.W., *Numerical methods for scientists and engineers*, McGraw Hill, New York, 1962.
50. Hantush, M.S., Flow of ground water in relatively thick leaky aquifers, *Water Resour. Res.* 3(2), 583-590, 1967a.
51. Hantush, M.S., Flow to wells in aquifers separated by a semi-pervious layer, *J. Geophys. Res.* 72(6), 1709-1720, 1967b.
52. Harr, M.E., *Ground water and Seepage*, Mc Graw Hill, New York, 1962.
53. Hemker, C.J., Steady groundwater flow in leaky multiple aquifer systems, *J. Hydrol.* 72, 355-374, 1984.

REFERENCES

54. Hemker, C.J., Transient well flow in vertically heterogeneous aquifers, *J. Hydrol.* 225, 1-18, 1999a.
55. Hemker, C.J., Transient well flow in layered aquifer systems: the uniform well-face drawdown solution, *J. Hydrol.* 225, 19-44, 1999b.
56. Hemker, C.J. and Maas, C., Unsteady flow to wells in layered and fissured aquifer systems, *J. Hydrol.* 90, 231-249, 1987.
57. Herrera, I., Theory of multiple leaky aquifers, *Water Resour. Res.* 6(1), 185-193, 1970.
58. Holder, A.W., Bedient, P.B. and Dawson, C.N., FLOTRAN, a three dimensional groundwater model, with comparisons to analytical solutions and other models, *Adv. Water Resour.* 23, 517-530, 2000.
59. Hubert, M.K., The theory of ground water motion, *J. Geology* 48(8:I), 785-944, 1940.
60. Hunt, B., Flow to a well in a multiaquifer system, *Water Resour. Res.* 21(11), 1637-1641, 1985.
61. Isiorho, S.A., Matisaff, G. and Wehn, K.S., Seepage relationships between lake Chad and the Chad aquifers, *Ground Water* 34(5), 819-826, 1996.
62. James, L.D., NSF research in hydrologic sciences, *J. Hydrol.* 172, 3-14, 1995.
63. Kacimov, A.R., Three dimensional groundwater flow to a lake: an explicit analytical solution, *J. Hydrol.* 240, 80-89, 2000.
64. Khader, M. H. A., A study on flow towards a three-layer aquifer system, *Hydrology and Water Resources Symposium*, Adelaide, 1980.
65. Koefoed, O., *Geosounding Principles: Vol.1*, Elsevier Scientific Publishing Co., Amsterdam, 1979.
66. Konikow, L.F. and Mercer, J.W., Groundwater flow and transport modelling, *J. Hydrol.* 100, 379-409, 1988.
67. Konikow, L.F. and Bredehoeft, J.D., Groundwater models cannot be validated, *Adv. Water Resour.* 15, 75-83, 1992.

68. Krabbenhoft, D.P., Bowser, C.J., Anderson, M.P. and Valley, J.W., Estimating ground water exchange with lakes: 1. The stable isotope mass balance method, *Water Resour. Res.* 26(10), 2445-2453, 1990a.
69. Krabbenhoft, D.P., Anderson, M.P. and Bowser, C.J., Estimating ground water exchange with lakes: 2. Calibration of a 3-Dimensional, solute transport model to a stable isotope plume, *Water Resour. Res.* 26(10), 2455-2462, 1990b.
70. Lafe, O.E., Liggett, J.A. and Liu, P.L.F., BIEM solutions to combinations of leaky, layered, confined, unconfined, non-isotropic aquifers, *Water Resour. Res.* 17(5), 1431-1444, 1981.
71. Lal, A.M.W., Numerical errors in groundwater and overland flow models, *Water Resour. Res.* 36(5), 1237-1247, 2000.
72. La Venue, M., Andrews, R. W. and Rama Rao, B. S., Groundwater travel time uncertainty analysis using sensitivity derivatives, *Water Resour. Res.* 25(7), 1551-1566, 1989.
73. Leake, S.A., Lawson, P.W., Lilly, M.R. and Claar, D.V., Assignment of boundary conditions in embedded groundwater flow models, *Ground Water* 36(4), 621-625, 1998.
74. Lee, T.M., Effects of nearshore recharge on groundwater interactions with a lake in mantled karst terrain, *Water Resour. Res.* 36(8), 2167-2182, 2000.
75. Lei, S., An analytical solution for steady flow into a tunnel, *Ground Water* 37(1), 23-26, 1999.
76. Lopez, D.L. and Smith, L., Fluid flow in fault zones: Analysis of the interplay of convective circulation and topographically driven groundwater flow, *Water Resour. Res.* 31(6), 1489-1503, 1995.
77. Luther, K. and Haitjema, H.M., Approximate analytic solutions to 3D unconfined groundwater flow within regional 2D models, *J. Hydrol.* 229, 101-117, 2000.
78. Maas, C., Groundwater flow to a well in a layered porous medium 1. Steady flow, *Water Resour. Res.* 23(8), 1675-1681, 1987a.
79. Maas, C., Groundwater flow to a well in a layered porous medium 2. Nonsteady multiple aquifer flow, *Water Resour. Res.* 23(8), 1683-1688, 1987b.
80. Marcus, H. and Evenson, D.E., Directional permeability in anisotropic porous media, *Univ. of California, Berkeley, Water Resour. Centre Contrib.* 31, 1961.

REFERENCES

81. Marcus., H., The permeability of a sample of an anisotropic porous medium, *J. Geophys. Res.* 67(13), 5215-5225, 1962.
82. Marinelli, F. and Niccoli, W.L., Simple analytical equations for estimating ground water inflow to a mine pit, *Ground Water* 38(2), 311-314, 2000. ✓
83. Marsily, G.D., Ledoux, E., Levassor, A., Poitrial, D. and Salem, A., Modelling of large multilayered aquifer systems: Theory and applications, *J. Hydrol.* 36, 1-34, 1978.
84. Martin, P.J. and Frind, E.O., Modelling a complex multi-aquifer system: The Waterloo moraine, *Ground Water* 36(4), 679-690, 1998.
85. Matanga, G.B., Pseudo potential functions in construction of flow nets for contaminant transport modelling, *Water Resour. Res.* 24(4), 553-560, 1988.
86. Matanga, G.B., Stream functions in three dimensional groundwater flow, *Water Resour. Res.* 29(9), 3125-3133, 1993.
87. Mazáč, O., Kelly, W.E. and Landa, I., A hydrogeophysical model for relations between electrical and hydraulic properties of aquifers, *J. Hydrol.* 79, 1-19, 1985.
88. Mc Bride, M.S. and Pfankuch, H.O., The distribution of seepage within lakes, *USGS J. Res.* 3(5), 595-612, 1975.
89. Mc Donald, M. G. and Harbaugh, A. W., A modular three dimensional finite difference groundwater flow model, USGS National Centre, Reston, Virginia, USA , 1984.
90. Meigs, L.C. and Bahr, J.M., Three dimensional ground water flow near narrow surface water bodies, *Water Resour. Res.* 31(12), 3299-3307, 1995.
91. Mishra, G.C., Confined and unconfined flows through anisotropic media, Ph.D. Thesis, Department of Civil and Hydraulic Engineering, Indian Institute of Science, Bangalore, India, 1972.
92. Moench, A.F. and Barlow, P.M., Aquifer response to stream-stage and recharge variations, 1. analytical step-response functions, *J. Hydrol.* 230, 192-210, 2000.
93. Morrison, N., Introduction to sequential smoothing and prediction, Mc Graw-Hill Book Co., New York, 1969.

94. Munter, J.A. and Anderson, M.P., The use of groundwater flow models for estimating lake seepage rates, *Ground Water* 19(6), 608-616, 1982.
95. Nachiappan, R.P., Surface water and groundwater interaction studies using isotope techniques, a PhD thesis, Deptt. of Earth Sciences, University of Roorkee, India, 2000.
96. Naff, R.L., Radial flow in heterogeneous porous media: an analysis of specific discharge, *Water Resour. Res.* 27(3), 307-316, 1991.
97. Narasimhan, T.N., Hydraulic characterisation of aquifers, reservoir rocks, and soils: A history of ideas, *Water Resour. Res.* 34(1), 33-46, 1998.
98. Neuman, S.P. and Witherspoon, P.A., Theory of Flow in a Confined 2-aquifer system, *Water Resour. Res.* 5(4), 803-816, 1969a.
99. Neuman, S.P. and Witherspoon, P.A., Applicability of current theories to flow in leaky aquifers, *Water Resour. Res.* 5(4), 817-829, 1969b.
100. Nield, S. P. and Townley, L.R. and Barr, A.D., A frame-work for quantitative analysis of surface water groundwater interaction: flow geometry in a vertical section, *Water Resour. Res.* 30(8), 2461-2475, 1994.
101. Nieuwenhuizen, R., Zijl, W. and Veldhuizen, M.V., Flow pattern analysis for a well defined by point sinks, *Transport in Porous Media* 21, 209-223, 1995.
102. Niwas, S. and Israil, M., Computations of apparent resistivity using an exponential approximation of kernel functions, *Geophysics* 51(8), 1594-1602, 1986.
103. Nobes, D.C., Troubled waters: Environmental applications of electrical and electromagnetic methods, *Proceedings of XII EM Induction Workshop*, 1994.
104. Nutbrown, D.A., A model study of the effects of artificial recharge, *J. Hydrol.* 31, 57-65, 1976.
105. Osiensky, J.L. and Donaldson, P.R., Electrical flow through an aquifer for contaminant source leak detection and delineation of plume evolution, *J. Hydrol.* 169, 243-263, 1995.
106. Osiensky, J.L. and Williams, R.E., A two dimensional MODFLOW numerical approximation of mise-a-la-masse electrical flow through porous media, *Ground Water* 34(4), 727-733, 1996.
107. Ostfeld, A., Muzaffar, E. and Lansley, K.E., Analytical groundwater flow solutions for channel-aquifer interaction, *J. Irrigation and Drainage Engg.* 125(4), 196-202, 1999.

REFERENCES

108. Papadopoulos, I.S., Nonsteady flow to a well in an infinite anisotropic aquifer, Proceedings of Symposium, IASH, 21-30, 1965.
109. Parasnis, D.S., Theory and practice of electric potential and resistivity prospecting using linear current electrodes, *Geoexploration* 3(1), 3-69, 1965.
110. Parasnis, D.S., Three dimensional electric mise-a-la-masse survey of an irregular lead-zinc-copper deposit in central Sweden, *Geophys. Prospecting* 15(3), 407-437, 1967.
111. Patra, H.P. and Nath, S.K., *Schlumberger Geoelectric Sounding in Groundwater (Principles, Interpretation and Application)*, Oxford & IBH Publishing Co., New Delhi, 1999.
112. Pfankuch, H.O. and Winter, T.C., Effect of anisotropy and groundwater system geometry on seepage through lakebeds:1. Analog and dimensional analysis, *J. Hydrol.* 75, 213-237, 1984.
113. Polubarinova-Kochina, P.Ya., *Theory of groundwater movement*, Princeton Univ. Press, Princeton, New Jersey, 1962.
114. Popov, O.V. and Sokolov, B.L., Quantitative assessment of interaction between surface water and groundwater, Proceedings of Budapest Symposium on Conjunctive Water Use, IAHS Publ. 156, 71-75, 1986.
115. Prasad, S.N. and Romkens, M. J. M., An integral solution of groundwater recharge, Proceedings of Budapest Symposium on Conjunctive Water Use, IAHS Publ. 156, 61-69, 1986.
116. Prickett, T. A., Modelling techniques for groundwater evaluation, *Adv. Hydroscience* 10, Academic Press, New York, 1-143, 1975.
117. Pucci Jr., A. A. and Pope, D. A., Simulated effects of development on regional ground water/surface water interactions in the northern coastal plain of New Jersey, *J. Hydrol.* 167, 241-262, 1995.
118. Pujari, P.R., Stabilised analytic Signal algorithm in 2D and 3D resistivity data analysis, a Ph D thesis, Deptt. of Earth Sciences, University of Roorkee, India, 1998.
119. Rabbani, M.G. and Warner, J.W., A finite element linked model for analysis of solute transport in 3-D space of multilayer subsurface systems, *J. Hydrol.* 199, 163-182, 1997.
120. Rai, S.N. and Singh, R.N., Two-dimensional modelling of water table fluctuation in response to localised transient recharge, *J. Hydrol.* 167, 67-174, 1995.

121. Ranganna, G., Lokesh, K.N., Gajendragad, M.R., Chandrakant, G., Harshendra, K., Ars, A.K. and Kori, M.M., Studies on infiltration characteristics in soils of Pavanje River basin of DK district, *Hydrology J. of IAH*, Vol. XIV(1), 33-40, 1991.
122. Rao, N.H. and Sarma, P.B.S., Recharge from rectangular areas to finite aquifers, *J. Hydrol.* 53, 269-275, 1981.
123. Rastogi, A.K. and Pandey, S.N., Modelling of artificial recharge basins of different shapes and effect on underlying aquifer system, *J. Hydrologic Engg.* 3(1), 62-68, 1998.
124. Reynolds, J. W. and Spruill, R. K., Ground-water flow simulation for management of a regulated aquifer system: A case study in the North Carolina Coastal Plain, *Ground Water* 33(5), 741-748, 1995.
125. Rushton, K.R., Surface water- ground water interactions in irrigation schemes, *Proceedings of Budapest Symposium on Conjunctive Water Use*, IAHS Publ. 156, 17-27, 1986.
126. Rushton, K.R. and Redshaw, S.C., *Seepage and Ground Water Flow*, John Wiley and Sons, 1979.
127. Rushton, K.R. and Tiwari, S.C., Mathematical modelling of a multilayered alluvial aquifer, *J. Institution of Engineers (I)*, EV 70, 47-54, 1989.
128. Sacks, L.A., Herman, J.S., Konokow, L.F. and Vela, A.L., Seasonal dynamics of gw-lake interaction at Donana park, Spain, *J. Hydrol.* 136, 123-154, 1992.
129. Sahuquillo, A., Quantitative characterization of the interaction between ground water and surface water, *Proceedings of Budapest Symposium on Conjunctive Water Use*, IAHS Publ. 156, 3-16, 1986a.
130. Sahuquillo, A. and Andreu, J., Quantitative analysis of the interaction between groundwater and surface water by the eigen values method, *Proceedings of Budapest Symposium on Conjunctive Water Use*, IAHS Publ. 156, 51-60, 1986b.
131. Scheidegger, A.E., *The physics of flow through porous media*, Macmillan Co., New York, 1957.
132. Seiler, K.P. and Lindner, W., Near-surface and deep groundwaters, *J. Hydrol.* 165, 33-44, 1995.
133. Sekhar, M., Kumar, M.S. and Sridharan, K., Parameter estimation in anisotropic leaky aquifer system, *J. Hydrol.* 163, 373-391, 1994.

REFERENCES

134. Senger, R.K. and Fogg, G.E., Stream functions and equivalent fresh water heads for modelling regional flow of variable density groundwater: 1. Review of theory and verification, *Water Resour. Res.* 26(9), 2089-2096, 1990.
135. Singh, S.B., Personal communications, National Geophysical Research Institute, Hyderabad, India, 1998.
136. Singh, V. P., *Elementary Hydrology*, Prentice-Hall Inc., N.J., USA, 1992.
137. Skibitzke, H.E., The use of analogue computers for studies in groundwater hydrology, *J. Inst. Water Engg.* 17, 216-230, 1963.
138. Smiles, D.E. and Knight, J. H., The transient water table beneath a leaking canal, *J. Hydrol.* 44, 149-162, 1979.
139. Sokol, D., Position and fluctuations of water level in wells perforated in more than one aquifer, *J. Geophys. Res.* 68(4), 1079-1080, 1963.
140. Sondhi, S. K., Rao, N. H. and Sarma, P. B. S., Assessment of groundwater potential for conjunctive water use in a large irrigation project in India, *J. Hydrol.* 107(1-4), 283-295, 1989.
141. Sophocleous, M. and Perkins, S.P., Calibrated models as management tools for stream aquifer systems: the case of Central Kansas, USA, *J. Hydrol.* 152, 31-56, 1993.
142. Sridharan, K., Sathyanarayana, D. and Reddy, A. S., Analysis of flow near a dug well in an unconfined aquifer, *J. Hydrol.* 119(1-4), 89-103, 1990a.
143. Sridharan, K., Sekhar, M. and Mohan Kumar, M. S., Analysis of an aquifer-water table aquitard system, *J. Hydrol.* 114(1-2), 175-189, 1990b.
144. Srinivas, A., Venkateswara Rao, B. and Gurunadha Rao, V.V.S., Groundwater flow model in a granitic water shed, In: *Proc. of Int. Geol. Cong. Beijing*, Vol.3, 300, 1996.
145. Srinivas, A., Venkateswara Rao, B. and Gurunadha Rao, V.V.S., Recharge process and aquifer models of a small watershed, *Hydrological Sci. J.* 44(5), 681-692, 1999.
146. Stolwijk, N.H.M., Zijl, W. and Boekelman, R., The penetration depth in modelling natural ground water flow, *J. Hydrol.* 185, 171-182, 1996.

147. Strack, O. D. L. and Haitjema, H.M., Modeling double aquifer flow using a comprehensive potential and distributed singularities. 1 Solution for homogeneous permeability, *Water Resour. Res.* 17(5), 1535-1549, 1981a.
148. Strack, O. D. L. and Haitjema, H.M., Modeling double aquifer flow using a comprehensive potential and distributed singularities: 2 Solution for inhomogeneous permeabilities, *Water Resour. Res.* 17(5), 1551-1560, 1981b.
149. Strack, O. D. L., *Groundwater Mechanics*, Prentice Hall, Englewood, New Jersey, 1989.
150. Strack, O.D.L., Principles of the analytic element method, *J. Hydrol.* 226, 128-138, 1999.
151. Su, N., Formula for computation of time varying recharge of ground water, *J. Hydrol.* 160, 123-135, 1994.
152. Swain, E. D., Implementation and use of direct-flow connections in a coupled groundwater and surface water model, *Ground Water* 32(1), 139-144, 1994.
153. Townley, L.R. and Trefry, M.G., Surface water-groundwater interaction near shallow circular lakes: Flow geometry in three dimensions, *Water Resour. Res.* 36(4), 935-949, 2000.
154. Townley, L. R. and Davidson, M. R., Definition of a capture zone for shallow water table lakes, *J. Hydrol.* 104, 53-76, 1988.
155. Tyvand, P.A., Decay of a disturbed free surface in a layered porous medium, *J. Hydrol.* 71, 377-382, 1984.
156. Tyvand, P.A., Decay of a disturbed free surface in an anisotropic porous medium, *J. Hydrol.* 83, 367-371, 1986.
157. Ursino, N., Gimmi, T. and Fluhler, H., Combined effects of heterogeneity, anisotropy, and saturation on steady state flow and transport: A laboratory sand tank experiment, *Water Resour. Res.* 37(2), 201-208, 2001.
158. Ursino, N., Roth, K., Gimmi, T. and Flühler, H., Upscaling of anisotropy in unsaturated Miller-similar porous media, *Water Resour. Res.* 36(2), 421-430, 2000.
159. Van der Veer, P., Exact solutions for two dimensional ground water flow in a semiconfined aquifer, *J. Hydrol.* 156(1-4), 91-99, 1994.

REFERENCES

160. Verhoest, N.E.C. and Troch, P.A., Some analytical solutions of the linearised Boussinesq equation with recharge for a sloping aquifer, *Water Resour. Res.* 36(3), 793-800, 2000.
161. Walton, W.C., *Groundwater Resources Evaluation*, McGraw-Hill, New York, 1970.
162. Walton, W. C., Progress in analytical groundwater modeling, *J. Hydrol.* 43, 149-159, 1979.
163. Warner, J.W., Molden, D., Chehata, M. and Sunada, D.K., Mathematical analysis of artificial recharge from basins, *Water Resour. Bull.* 25(2), 401-411, 1989.
164. Watson, G.N., *A Treatise on the Theory of Bessel's Functions*, Cambridge University Press, London, 1980.
165. Wikramaratna, R.S., An analytical solution for the effects of abstraction from multiple layered confined aquifer with no cross flow, *Water Resour. Res.* 20(8), 1067-1074, 1984.
166. Winter, T.C., *Numerical simulation analysis of the interaction of lakes and groundwater*, USGS Professional Paper 1001, USA, 1976.
167. Winter, T.C., Numerical simulation of steady state three dimensional ground water flow near lakes, *Water Resour. Res.* 14, 245-254, 1978.
168. Winter, T.C., Uncertainties in estimating the water balance of lakes, *Water Resour. Bull.* 17(1), 82-115, 1981.
169. Winter, T.C., The interaction of lakes with variably saturated porous media, *Water Resour. Res.* 19(5), 1203 -1218, 1983.
170. Winter, T.C., Recent advances in understanding the interaction of groundwater and surface water, *Rev. Geophys.* 33, 1995.
171. Winter, T.C., Relation of streams, lakes and wetlands to groundwater flow systems. *Hydrogeol. J.* 7, 28-45, 1999.
172. Winter, T.C. and Pfannkuch, H.O., Effect of anisotropy and ground water system geometry on seepage through lakebeds: 2. Numerical simulation analysis, *J. Hydrol.* 75, 239-253, 1984.
173. Workman, S.R., Serrano, S.E. and Liberty, K., Development and application of an analytical model of stream/ aquifer interaction, *J. Hydrol.* 200, 149-163, 1997.

174. Wright, C.E., Surface water and ground water interaction, International Hydrology Programme Rreport, UNESCO, 1980.
175. Yates, S.R., An analytical solution to saturated flow in a finite stratified aquifer, *Ground Water* 26(2), 199-206, 1988.
176. Yu, F.-X. and Singh, V. P., Modeling 3D ground-water flow by modified finite-element method, *ASCE Journal of Irrigation and Drainage Engineering* 120(5), 892-909, 1994.
177. Zijl, W., Numerical simulations based on stream functions and velocities in three-dimensional groundwater flow, *J. Hydrol.* 85, 349-365, 1986.
178. Zohdy, A.A.R., Eaton, G.P. and Mabey, D.R., Application of surface geophysics to groundwater investigations, *Techniques of Water Resources Investigations, USGS Book 2: D1*, 1974.

APPENDIX

LIST OF PUBLICATIONS RELEVANT TO THE THESIS

1. Jose, M.K. and Seethapathi, P.V., Influence of aquitard on the flow regime in a multi-layer aquifer system with a recharging source, J. Applied Hydrology, 10(3&4), 1997.
2. Jose, M.K. and Seethapathi, P.V., Influence of a discontinuous flow-barrier on the seepage from a surface water body, Environment Management (Vol. 1), Elsevier Science Publishing Co., Amsterdam, 641-648, 1998a.
3. Jose, M.K. and Seethapathi, P.V., Influence of an opening in a confining layer on recharging of an underlying aquifer, Proceedings of National Seminar on Artificial Recharge of Groundwater, Central Ground Water Board, New Delhi, India, i/9-i/19, 1998b.
4. Jose, M.K., Effect of Anisotropy on Seepage from a Water Body, Technical Report TR(BR5/98-99), National Institute of Hydrology, Roorkee, India, 1999
5. Jose, M.K. and Sastry, R.G.S., Computation of Aquifer potentials in a layered porous medium: An analytical model, In Proc. of National Seminar on "Water and land Management including CAD", Guwahati, India, November 2001.
6. Sastry, R.G.S. and Jose, M.K., Recharging in an anisotropic aquifer system with inclined soil bedding planes, In Proc. of National Seminar on "Water and land Management including CAD", Guwahati, India, November 2001.
7. Jose, M.K. and Sastry, R.G.S., Analytical Determination of Steady-state Hydraulic Head and Stream Lines in a 3-layered Aquifer System, Water Resour. Res., (WR-752, under revision) *when submitted*
8. Jose, M.K. and Sastry, R.G.S., A Semi-analytical Procedure for the Computation of Hydraulic Heads and Streamlines in Multilayered Aquifer Systems, J. Hydrol., (HYDROL 1702, under revision) *when submitted should be indicated.*

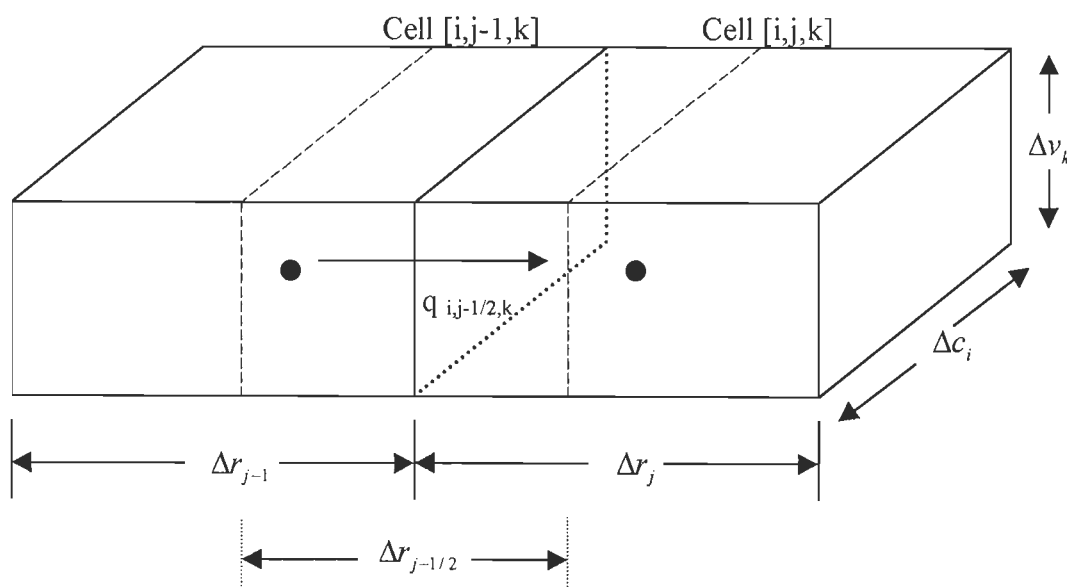
CORRIGENDUM

Page No.	Line No.	Printed in the thesis as:	Corrected, and may be read as:
i	4	...the hydraulic properties, flow parameters of the porous medium and...	<i>...the hydraulic properties, parameters of the flow domain and...</i>
i	9	...groundwater models can be of great use.	<i>...groundwater models can be of significant value from a practical point of view.</i>
i	13	...developing new analytical approaches...	<i>...developing better analytical approaches...</i>
i	16	...analytical models render faster techniques to simulate flow...	<i>...analytical models are computationally faster to simulate flow...</i>
1	2	...in the form of ice, and does not...	<i>...in the form of ice does not...</i>
2	1	...hydraulic connectors; among these, ...	<i>...hydraulic connectors. Among these, ...</i>
2	4	...the expected recharging rates, the hydraulic response...	<i>... expected recharging rates, hydraulic response...</i>
2	19	...and extractions for the aquifer...	<i>...and extractions from the aquifer...</i>
3	1	... studies, generalised methodologies/ results on...	<i>... studies; generalised methodologies and discussion on results on...</i>
3	2	So, it has been...	<i>Therefore it has been...</i>
3	4	...flow in the context of...	<i>...flow involving the...</i>
3	8	Further, they offer...	<i>Further, these models offer...</i>
3	16	So, here attempts are made towards the...	<i>Therefore attempts are made in the present study towards the...</i>
4	14, 15	...aquifer system by use of analytical methods as well as numerical modelling techniques, leading to valuable results.	<i>...aquifer system using analytical methods as well as numerical modelling techniques.</i>
5	2	These studies covered: ...	<i>These studies involve:...</i>
5	7	...each chapter being devoted to a particular...	<i>...each chapter covers a particular...</i>
5	22	It deals with a study on the recharging in an aquifer-....	<i>It deals with recharge to the aquifer-...</i>
5	25, 26	Investigations on the recharging in an aquifer-aquitard-aquifer system with a discontinuous aquitard is presented.	<i>Recharge investigations on an aquifer-aquitard-aquifer system with a discontinuous aquitard are presented.</i>

6	4	...further perspectives for future investigations in continuation to the present effort are given...	...further perspectives for future investigations are given...
7	2	However, this necessitates a sound background of...	However, this necessitates an adequate background of...
35	11	...in the RZ-plane [vide Fig. 3.2]...	...in the RZ-plane [Fig. 3.2]...
37	Table 3.1	K_1 (m ³ /s) K_2 (m ³ /s) K_3 (m ³ /s)	K_1 (m/s) K_2 (m/s) K_3 (m/s)
43	Table 3.2	K_1 (m ² /s) K_2 (m ² /s) K_3 (m ² /s)	K_1 (m/s) K_2 (m/s) K_3 (m/s)
66	Eqn. (4.1)	$q_x = -K \frac{\partial \phi}{\partial x}$	$q_x = -K_x \frac{\partial \phi}{\partial x}$
66	7/ 8	...the hydraulic gradient due to change in hydraulic potential,...	...the hydraulic gradient that causes the flow,...
79	2	$\Phi(y, z) = \frac{Q_L}{2\pi K_m} \left[\sinh^{-1} \left(\frac{B_z - G_z}{\beta z} \right) + \left(\frac{B_z + G_z}{\beta z} \right) \right]$	$\Phi(y, z) = \frac{Q_L}{2\pi K_m} \left[\sinh^{-1} \left(\frac{B_z - G_z}{\beta z} \right) + \sinh^{-1} \left(\frac{B_z + G_z}{\beta z} \right) \right]$
100	24	...of the water body presumed to have...	...of the water body is presumed to have...
101	4	...consisting of 50 time-steps has been chosen...	...consisting of 50 time-steps ($\Delta t = 10$ days) has been chosen...
101	12	The following general assumptions hold good for the simulation of hydraulic potentials and groundwater flow...	Following assumptions are considered for the conceptual model to compute the hydraulic potentials simulating groundwater flow...
105	15	...flow due to potential build-up above compared to that...	...flow due to potential build-up above it compared to that...
138	16	Therefore, seepage of water down to the bottom...	Therefore, seepage to the bottom...
138	21	...the hydraulic potentials also found to be raising.	...the hydraulic potentials are also found to be rising.
138	25	...optimum seepage down to the bottom aquifer,...	...optimum seepage to the bottom aquifer,...
147	1, 2	Thus, for attaining optimum recharging of the bottom aquifer the opening (discontinuity) must be centrally located below the source.	Thus, for attaining optimum recharging of the bottom aquifer the source should be located right above the aquitard discontinuity.
148	22, 23	...the aquifer system, have been considered for evaluating effect of location of the discontinuity on the recharging.	...the aquifer system have been considered for evaluating the effect of location of the discontinuity on the aquifer recharge.
159	4	...has been discussed, in the preceding sections, for a...	...has been discussed in the preceding sections for a...

167	2	...characteristics, due to a surface water source, of an...	...characteristics due to a surface water source of an...
167	8	...these investigations have been enumerated in the...	...these investigations are summarised in the...
168	11	...of the aquitard discontinuity.	...of the aquitard discontinuity from the centre of the source.
169	1	...the hydraulic responses of...	...the hydraulic response of...
169	8	...contributions/ conclusions of these studies...	...contributions and conclusions from these studies...
170	9	...point source and that due to a finite-length...	...point source and a finite-length...
171	1	For instance, a 1% opening can contribute nearly as much as that of a 30% opening.	For instance, an opening of 1% can contribute nearly as much seepage as that for an opening of 30%.
171	5,6	Further, optimum recharging of the bottom aquifer occurs when the aquitard discontinuity is located centrally below the recharging source.	Further, optimum recharging of the bottom aquifer occurs when the recharging source is located right above the aquitard discontinuity.

Figure with reference to Section "5.3.2 MODEL DESCRIPTION" on Page: 96



Flow into the grid cell [i,j,k] from cell [i,j-1,k] with reference to the MODFLOW discretisation convention (after McDonald and Harbaugh, 1984).

Index of notations of the parameters used in the analysis of the cases of continuous aquitard (Chapter: 5, page: 104) and discontinuous aquitard (Chapter: 6, page: 115 &116)

Parameter/ Notation	Description of the term
D	Depth to the lower boundary of the aquifer system
H_s	Hydraulic head in the source
H_b	Hydraulic head in the boundary
d_u	Thickness of upper aquifer
d_m	Thickness of aquitard
d_b	Thickness of bottom aquifer
h_u	Hydraulic potential in the upper aquifer
h_m	Hydraulic potential in the aquitard
h_b	Hydraulic potential in the bottom aquifer
q_{au}	Average discharge per unit width in upper aquifer
q_{ab}	Average discharge per unit width in bottom aquifer
q_{uu}	Seepage per unit thickness of the upper aquifer
q_{ub}	Seepage per unit thickness of the bottom aquifer
l_d	Length of the aquitard discontinuity in the X direction
X_d	Distance of the location of the discontinuity from the centre
$AFHR = h_u / h_b$	Aquifer head ratio
$AFTR = d_u / d_b$	Aquifer thickness ratio
$ATDR = d_u / d_m$	Aquitard depth ratio
$ATHR = h_u / h_m$	Aquitard head ratio
$DISR = q_{au} / q_{ab}$	Discharge ratio
$F_{sb} = q_{ub} / (q_{uu} + q_{ub})$	Fractional Seepage
$\Delta H = H_s - H_b$	Head Causing Flow
H	Hydraulic Potential
X/L	Normalised Distance
$h_n = (h - H_b) / \Delta H$	Normalised Hydraulic Potential
$O_p = (l_d * 100) / 2w \%$	Percentage Opening
$M_p = (X_d * 100) / 2w \%$	Percentage Shift
$P_d = d_u / D$	Positioning Depth
X_R	Reversal Point (distance at which $h_u = h_b$)
S/T	Ratio of Storage Coefficient to Transmissivity

Typical parameter index for the MODFLOW simulations for the case of Discontinuous Aquitard described in Chapter 6 (w.r.t. Page: 114)

Parameter	Description	Value
d_u	Thickness of top aquifer	43 m
d_m	Thickness of aquitard	20 m
d_b	Thickness of bottom aquifer	37 m
K_T	Hydraulic conductivity for top aquifer	2.5E-4 m/s
K_M	Hydraulic conductivity for aquitard	2.5E-10 m/s
K_B	Hydraulic conductivity for bottom aquifer	2.5E-4 m/s
L	Half-width of the aquifer system	4000m
D	Depth to the lower boundary of the aquifer system	100 m
w	Half-width of the source body	150 m
H_b	Head in the boundary	90 m
h_0	Initial head	90 m
ΔH	Head Causing Flow	9 m
S_y	Specific yield	0.15
S	Storage coefficient	1E-9 (for aquitard), 1E-3 (bottom aquifer)
T	Transmissivity	1.08E-2 ((for top aquifer), 5E-9(for aquitard, 9.25E-3 (for bottom aquifer)
i,j, k	Model Grid	51 rows x 51 cols. X 10 layers